COPY NUMBER 9

LICENSING REPORT

for

MAINE YANKEE ATOMIC POWER COMPANY

HIGH DENSITY SPENT FUEL POOL RERACKING PROJECT

by

BRAND UTILITY SERVICES, INC.

with

STONE & WEBSTER ENGINEERING CORPORATION
GENERAL DYNAMICS / ELECTRIC BOAT DIVISION
YANKEE ATOMIC ELECTRIC COMPANY

REVISION 0
JANUARY 1993

EXECUTIVE SUMMARY

This document is in support of a license amendment request to increase the fuel storage capacity of the Maine Yankee spent fuel pool from 1476 to 2019 spent fuel assemblies. This capacity increase is required to provide spent fuel storage space through the duration of the current operating license.

The increased spent fuel storage capacity will be provided by installing new, high-density spent fuel racks in the spent fuel pool. These new racks are similar to other licensed designs and provide for conventional storage of spent fuel in a single tier, rectilinear array of free-standing modules that is compatible with existing fuel handling equipment, procedures, and techniques at Maine Yankee. The new racks are configured in a two-region arrangement.

Region I consists of 228 storage locations and utilizes a standard flux trap design. The Region I racks will accommodate fuel with an initial enrichment of up to 4.5 $^{w}/_{o}$ U^{235} and with no exposure or burnup restrictions.

Region II consists of 1791 storage locations and is an arrangement of modules of rectangular box cells connected on their corners. Region II accommodates fuel with a reactivity equivalent to an enrichment of 4.5 $^{w}/_{o}$ U^{235} that has 30 GWD/MTU burnup. Both regions utilize BORAL™ as a neutron absorber. The new racks include full-size BORAL™ surveillance test samples that will be periodically removed and tested to confirm the integrity of the BORAL™ over the design life of the racks.

The new, high-density storage racks are constructed of 304L stainless steel and are designed in accordance with the guidance of Sections 9.1.2 and 3.8.4 of NUREG-0800, Regulatory Guides 1.29 and 1.92, and the 1978 NRC position paper on spent fuel storage applications. All design, material procurement, fabrication, and installation activities are performed in compliance with 10CFR50, Appendix B, Quality Assurance requirements.

The new, high-density racks are designed to Seismic Category I requirements. Seismic response of the fuel racks accounts for the nonlinearities inherent in free standing racks: fuel-to-rack gaps; rack-to-rack gaps; rack-to-wall gaps; rack tipping and/or sliding; large displacements; and submergence considerations of hydrodynamic coupling, fluid-structure interaction, and entrained and virtual mass. Design analysis of the racks is performed in a sequence of stages from a static load assessment of the fuel support baseplate of a single isolated cell through a full 3-D finite element structural analysis of a complete rack module with various spent fuel loadings to a finite element analysis of representations of the entire rack array in the spent fuel pool. All analyses are performed using the ANSYS® finite element computer code, which has been successfully used to license other high density spent fuel racks. The rack analysis demonstrates that the racks are stable under dynamic conditions, and stress levels for all load combinations are within the criteria of Section 3.8.4 of NUREG-0800.

The effect of the new racks on the fuel building structure has been analyzed and determined to be within the original Seismic Category I design requirements. Moment, axial, and shear capacities of the critical region of the foundation slab were evaluated for structural integrity. The local punching shear and bearing capacities in the vicinity of the rack support feet as well as the hydrodynamic loads on the spent fuel pool walls caused by the fuel racks during seismic events were also evaluated.

Analyses have been performed that demonstrate that the thermal-hydraulic characteristics of the new rack design, coupled with the arrangement within the spent fuel pool, allow sufficient cooling for each assembly under normal and postulated accident conditions. The maximum heat load with the increased pool capacity will not exceed the existing design heat load of the spent fuel pool cooling system. Thermal-hydraulic analyses have been performed that demonstrate that local boiling will not occur anywhere in the pool, and that local pin cooling will be adequate under the maximum heat load conditions. These analyses incorporate a 2-D approach using the RETRAN computer code, a method that has previously been utilized for licensing high density fuel storage racks and that has been proven to be conservative relative to a 3-D approach. Results of analyses of postulated partial and complete loss of spent fuel pool circulation and/or cooling scenarios are within the current licensing basis.

Criticality analyses of the new spent fuel storage racks show that the maximum calculated K_{eff}, including margins for uncertainty in the calculation method and mechanical tolerances, is less than 0.95 with a 95% probability at a 95% confidence level. A validated combination of criticality safety methods based on the KENO-V.a, CASMO-3, PDQ-7, and SIMULATE-3 computer codes has been used. These codes have been used to license other high density spent fuel racks. The criticality analyses included the postulated accidents of a dropped fuel assembly on top of the racks, an assembly inadvertently placed adjacent to the outside of a rack module, and a misplaced unirradiated assembly into Region II.

The design basis fuel handling accident in the fuel building is the drop of a spent fuel assembly in the spent fuel pool. Since the reracking causes no change in the fuel design and the new racks withstand this accident without damage to the stored fuel, the fuel handling accident analyses in the current licensing basis are unchanged by the reracking. The current Maine Yankee technical specifications do not allow spent fuel shipping cask movement over the spent fuel pool, so the consequences of a dropped cask are not analyzed. The reracking will cause no changes in the radiation zones within the Fuel Building.

The new, high-density spent fuel racks will be fabricated by the General Dynamics/Electric Boat Division manufacturing facility. Computer numerically controlled (CNC) punch presses will be used to accurately cut and punch the stainless steel plate, and a CNC brake will form the rack structural members. Gas metal arc welding, utilizing ASME certified procedures and welders, will be used to assemble the rack modules. Full-height prototypes of both Region I and II modules have been fabricated, inspected, and tested to demonstrate successful design implementation and fabrication.

The new racks will be installed and leveled remotely. Stored fuel will be shuffled so that no racks will be moved that contain stored fuel. Racks will be lifted a maximum of 12 in. off the spent fuel pool floor while moving to or from the cask handling pit, where racks are removed from and placed in the pool. The installation sequence will maintain a safe load path at all times, and will utilize a temporary heavy lift system designed and qualified to NUREG-0612 criteria. Comprehensive radiological controls will be implemented to ensure personnel doses are as low as reasonably achievable (ALARA). A combination of extensive preplanning, training, radiological surveys, radiochemical analyses, and an extensive contamination control protocol will provide a basis for implementation of the Maine Yankee ALARA policy. The total occupational exposure for the reracking operation is estimated to be 4 to 6 man-rem. Individual exposures will be well within NRC limits as controlled by the Maine Yankee Radiation Protection Program. The existing racks will be hydrolazed, dried, and then packaged and shipped offsite for disposal.

The design, material procurement, fabrication, and installation of the new, high-density racks are governed by a Management Plan for Project Quality that meets or exceeds the quality assurance requirements of 10CFR50, Appendix B, as well as those requirements imposed by specified codes and standards. Maine Yankee has approved the vendors and conducts its own performance-related surveillances to verify proper implementation of the quality assurance program of the vendors.

An environmental assessment has been performed and demonstrates that the proposed spent fuel capacity increase will result in no significant impact on the environment. The storage of spent fuel at Maine Yankee is an interim condition until a Federal repository is established to accept spent fuel assemblies. The currently available alternatives (i.e., spent fuel storage in new, high-density racks in the existing spent fuel pool, fuel rod consolidation in the existing racks, construction of a new spent fuel pool, and dry cask storage) were evaluated for environmental impact, operational time constraints, technical feasibility, and overall cost. The evaluation determined that the use of new, two-region, high-density spent fuel storage racks has no significant environmental impact in meeting the required need for the expanded spent fuel storage capacity. Use of this approach will not result in any irreversible commitments of land, water, or air resources.

MAINE YANKEE ATOMIC POWER COMPANY

TABLE OF CONTENTS

Section	Title	Page
	EXECUTIVE SUMMARY	ES-1
1.0	INTRODUCTION	1-1
2.0	FUEL RACK PHYSICAL DESCRIPTION	2-1
2.1	GENERAL	2-1
2.2	FUEL STORAGE CELL	2-4
2.3	REGION I RACKS	2-6
2.4	REGION II RACKS	2-7
2.5	SUPPORT FOOT ASSEMBLY	2-8
2.6	APPLICABLE CODES, STANDARDS, AND SPECIFICATIONS	2-9
2.7	RACK MATERIALS	2-12
2.7.1	General	2-12
2.7.2	BORAL™ Neutron Absorber	2-12
2.7.3	Materials Compatibility	2-13
3.0	FUEL RACK ANALYSIS	3-1
3.1	LOADS AND LOADING COMBINATIONS	3-1
3.2	DESIGN AND ANALYSIS PROCEDURES	3-4
3.2.1	Analytical Approach	3-5
3.2.2	Linear Structural Models	3-6
3.2.3	Nonlinear Dynamic Models	3-11
3.2.4	Modeling Details	3-16
3.2.5	Bounding Analysis Cases	3-24
3.3	ACCEPTANCE CRITERIA	3-27
3.4	RESULTS	3-29
3.5	REFERENCES	3-34
4.0	FUEL BUILDING	4-1
4.1	DESCRIPTION	4-1
4.2	STRUCTURAL ANALYSIS	4-2
4.2.1	Description	4-2
4.2.2	Building Analysis	4-2
4.2.3	Pool Wall Gamma Heating	4-5
4.3	SYSTEMS ANALYSIS	4-6
4.3.1	HVAC Performance	4-6
4.3.2	Fuel Pool Cooling System	4-6
4.4	REFERENCES	4-8

TABLE OF CONTENTS

Section	Title	Page
5.0	THERMAL-HYDRAULIC CONSIDERATIONS	5-1
5.1	GENERAL DESCRIPTION	5-1
5.2	SPENT FUEL POOL DECAY HEAT LOAD	5-3
5.2.1	Spent Fuel Pool Decay Heat Load Calculation	5-3
5.2.2	Normal Refueling Core Discharge Scenario	5-4
5.2.3	Full Core Discharge Scenario	5-4
5.2.4	Summary/Conclusions	5-5
5.3	FUEL ASSEMBLY/PIN COOLING ANALYSIS	5-6
5.3.1	Limiting Fuel Cell Location Evaluation	5-7
5.3.2	RETRAN Fuel Cell Model Description	5-7
5.3.3	Cell Exit Coolant Temperature Results	5-9
5.3.4	Fuel Pin Temperatures	5-9
5.3.5	Flux Trap Cooling	5-11
5.3.6	Blocked Cell Analysis	5-11
5.4	LOSS OF FORCED POOL CIRCULATION	5-12
5.4.1	Loss of One Spent Fuel Pool Cooling Pump	5-12
5.4.2	Loss of All Forced Circulation Cooling Flow/Total Loss of Spent Fuel Pool Cooling	5-13
5.4.3	Alternative Methods for Cooling and Makeup	5-13
5.5	REFERENCES	5-15
6.0	NUCLEAR SAFETY	6-1
6.1	CRITICALITY ANALYSIS	6-1
6.1.1	Description	6-1
6.1.2	Methodology	6-2
6.1.3	Fuel Storage Cells	6-3
6.1.4	Analyses and Tolerances	6-4
6.2	ACCIDENT SITUATIONS	6-9
6.2.1	Dropped Assembly	6-9
6.2.2	Assembly Adjacent to Racks	6-9
6.2.3	Assembly in Corner of Racks	6-9
6.2.4	Misplaced Assembly	6-10
6.2.5	Accident Analysis Results	6-10
6.3	OTHER SITUATIONS ANALYZED	6-11
6.3.1	Effects of Pool Temperature	6-11
6.3.2	Region I to Region II Interface	6-11
6.4	REFERENCES	6-12

TABLE OF CONTENTS

Section	Title	Page
7.0	RADIOLOGICAL SAFETY	7-1
7.1	EFFECT OF RERACKING ON NORMAL OPERATIONS AND ACCIDENT EVALUATIONS	7-1
7.1.1	Fuel Assembly Accidents	7-1
7.1.2	Fuel Building Radiation Zones	7-1
7.1.3	Annual Radioactive Waste Generation	7-2
7.1.4	Airborne Activity	7-2
7.1.5	Radiation Doses	7-3
7.2	RADIATION PROTECTION DURING RERACKING OPERATIONS	7-5
7.2.1	Introduction	7-5
7.2.2	Spent Fuel Pool Radiological Characterization	7-5
7.2.3	ALARA Program	7-7
7.2.4	Training	7-9
7.2.5	Work Controls	7-9
7.2.6	Radiation and Contamination Surveys	7-9
7.2.7	Contamination Control	7-9
7.2.8	Decontamination Efforts	7-10
7.2.9	Radwaste Generation/Disposal During Reracking	7-10
7.2.10	Anticipated Radiation Exposure During Reracking	7-10
8.0	FUEL RACK FABRICATION	8-1
8.1	REGION I RACK MODULE	8-2
8.2	REGION II RACK MODULE	8-3
8.3	FABRICATION AND CONSTRUCTION PRACTICES	8-4
8.4	FABRICATION AND CONSTRUCTION MATERIALS	8-5
9.0	INSTALLATION AND REMOVAL OPERATIONS	9-1
9.1	LIFTING AND POSITIONING OF RACKS	9-3
9.2	RACK MOVEMENT SCENARIO	9-6
9.3	INSTALLATION AND TEST DEVICES	9-8
9.4	SAFETY PRECAUTIONS	9-9
9.5	EXISTING RACK DISPOSAL	9-11
9.5.1	Packaging and Shipping	9-11
9.5.2	Unloading and Staging	9-11
9.5.3	Cutting and Dismantling	9-11
9.5.4	Decontamination	9-11
9.5.5	Surveying of Materials After Cleaning	9-11
9.5.6	Final Disposal	9-12

MAINE YANKEE ATOMIC POWER COMPANY

TABLE OF CONTENTS

Section	Title	Page
10.0	ACCIDENT ANALYSIS	10-1
11.0	IN-SERVICE SURVEILLANCE PROGRAM	11-1
11.1	GENERAL	11-1
11.2	BORAL™ PANEL TESTING	11-1
11.2.1	Description	11-1
11.2.2	Benchmark Data	11-1
11.2.3	Testing	11-2
11.2.4	Acceptance Criteria	11-3
12.0	QUALITY ASSURANCE	12-1
12.1	BRAND UTILITY SERVICES, INC.	12-2
12.2	STONE & WEBSTER ENGINEERING CORPORATION	12-3
12.2.1	Nuclear Quality Assurance Program	12-3
12.2.2	Project Quality Assurance Plan	12-3
12.2.3	Surveillances	12-3
12.3	GENERAL DYNAMICS/ELECTRIC BOAT DIVISION	12-4
12.3.1	Quality Assurance Program Implementation	12-4
12.3.2	Inspection	12-5
12.4	YANKEE ATOMIC ELECTRIC COMPANY	12-6
13.0	ENVIRONMENTAL ASSESSMENT	13-1
13.1	NEED FOR INCREASED STORAGE CAPACITY	13-1
13.2	ALTERNATIVES	13-2
13.3	RESOURCES COMMITTED	13-6
13.4	REFERENCES	13-7
APPENDIX A	ANSYS® DESCRIPTION AND BENCHMARKING	

MAINE YANKEE ATOMIC POWER COMPANY

LIST OF TABLES

Table	Title
1-1	Maine Yankee Spent Fuel Discharge Data
3-1	Load Combinations and Acceptance Limits
3-2	Fuel Mechanical Design Parameters
3-3	Single Rack Analyses Results
3-4	Allowable Stress Limits
3-5	Maximum Stress Results Summary High Density Spent Fuel Racks
5-1	Maine Yankee Spent Fuel Pool Cooling System Parameters
5-2	Maine Yankee Spent Fuel Pool Assembly Inventory
5-3	Projected Required Decay Times for Full Core Discharge
5-4	Cell Cooling/Pin Cooling Model Parameters
5-5	Assembly Cooling Analysis Results
5-6	Heat Exchanger Conditions - Loss of One Fuel Pool Cooling Pump
5-7	Complete Loss of Forced Circulation/Cooling Results
6-1	Nominal Dimensions and Tolerance
6-2	Fuel Assembly Nominal Design Specifications
6-3	Summary of Criticality Analyses
6-4	Axial Burnup/Moderator History Effects
6-5	Summary of Accident Analyses

LIST OF TABLES

Table	Title
6-6	Effect of Temperature on Reactivity
7-1	Estimated Radiation Doses for Construction Activities

LIST OF FIGURES

Figure	Title
1-1	Existing Spent Fuel Pool Arrangement
1-2	Proposed Spent Fuel Pool Arrangement
2-1	Region I Configuration
2-2	Region II Configuration
2-3	Basic Fuel Storage Cell
2-4	Typical Region I Rack Module
2-5	Typical Region II Rack Module
2-6	Support Foot Assembly
3-1	X Axis - Ground Response Spectra
3-2	Y Axis - Ground Response Spectra
3-3	Z Axis - Ground Response Spectra
3-4	SSE Displacement Time History
3-5	1/2 SSE Displacement Time History
3-6	Single Rack Dynamic Model
3-7	Fuel Storage Cell Base
3-8	Axial Buckling Model
3-9	Lateral Buckling Model
3-10	Region I Subassembly

LIST OF FIGURES

Figure	Title
3-11	Region I Subassembly Support Foot
3-12	Region II Subassembly
3-13	Region II Detailed Structural Model
3-14	Diagonal Loading Model
3-15	Row Loading Models
3-16	Multiple Rack Model
3-17	Proposed Maine Yankee Spent Fuel Pool Layout
3-18	Region I Rack Reaction Loads
3-19	Region II Rack Reaction Loads
3-20	Region I Single Foot Reaction Load (X-Direction)
3-21	Region I Single Foot Reaction Load (Y-Direction)
3-22	Region I Single Foot Reaction Load (Z-Direction)
3-23	Region I Fuel Reaction Loads
3-24	Region II Fuel Reaction Loads
3-25	Region I Individual Support Foot Uplift
3-26	Region I Individual Support Foot Slip
3-27	Region II Individual Foot Uplift
3-28	Region II Individual Foot Slip
3-29	Fuel Motion Within Storage Cell

MAINE YANKEE ATOMIC POWER COMPANY

LIST OF FIGURES

Figure	Title
3-30	Total Fuel Impact on Storage Cell Walls
3-31	Region II Rack X-Direction Displacement With Rack-Rack Hydrodynamic Coupling
3-32	Region II Rack Z-Direction Displacement With Rack-Rack Hydrodynamic Coupling
3-33	Region II Rack Rotation With Rack-Rack Hydrodynamic Coupling
3-34	Region II Rack X-Direction Displacement With No Rack-Rack Hydrodynamic Coupling
3-35	Region II Rack Z-Direction Displacement With No Rack-Rack Hydrodynamic Coupling
3-36	Region II Rack Rotation With No Rack-Rack Hydrodynamic Coupling
3-37	Multiple Rack Analysis Module A and B Displacement
3-38	Multiple Rack Analysis Module C and D Displacement
5-1	Spent Fuel Pool Loading Schedules
5-2	Proposed Maine Yankee Spent Fuel Pool Layout
5-3	Spent Fuel Pool Flow Limiting Locations
5-4	RETRAN02 MOD5 Spent Fuel Pool 2-D Cell Model
5-5	Limiting Fuel Cell Axial Profile
5-6	Fuel Pin Cross-Sectional Conduction Model
6-1	Basic Fuel Storage Cell

MAINE YANKEE ATOMIC POWER COMPANY

LIST OF FIGURES

Figure	Title
6-2	Region I Configuration
6-3	Region II Configuration
6-4	Region I CASMO-3/KENO-V.a Comparison
6-5	Region II CASMO-3/KENO-V.a Comparison
6-6	Maine Yankee Spent Fuel Pool Assembly Placement Limitations
8-1	Typical Region I Rack Module
8-2	Typical Region II Rack Module
9-1	Existing Spent Fuel Pool Arrangement
9-2	Proposed Spent Fuel Pool Arrangement
9-3	Temporary Heavy Lift System
9-4	Temporary Gantry Crane
9-5	Drag Test Module
9-6	Up-Ending Fixture
9-7	Lifting Fixture
9-8	Fuel Rack Height Adjustment Tool
12-1	Quality Assurance Organization
12-2	Fabrication QA Program Documentation

1.0 INTRODUCTION

Maine Yankee Atomic Power Station (Maine Yankee) is a pressurized water reactor facility owned and operated by the Maine Yankee Atomic Power Co. (MYAPCO) of Augusta, Maine. The plant is located in Wiscasset, Maine on the Back River. Maine Yankee received its construction permit from the Atomic Energy Commission in October 1968 and its operating license in September 1972. The station began commercial operation in December 1972.

Maine Yankee is a single unit, three-loop Combustion Engineering nuclear steam supply system with the reactor core consisting of 217 fuel assemblies. The spent fuel is stored in the spent fuel storage pool within the fuel building, which is founded on bedrock. The spent fuel storage pool is a conventional spent fuel pool lined with stainless steel. Currently, the plant has capacity to store 1476 spent fuel assemblies in a single region rack configuration, as shown on Figure 1-1. As of the date of this report, there are 1058 assemblies stored in the pool.

Table 1-1 provides the spent fuel storage inventory to date and that planned for the immediate future through Cycle 15 operation. The spent fuel storage pool with the existing racks will be unable to accommodate the fuel planned to be discharged after the 1999 refueling. The unavailability of a high-level waste repository and lack of assurance that the Federal Government will take possession of the spent fuel by the date that the spent fuel pool is full necessitate the reracking of the pool.

The reracking of the spent fuel pool is scheduled for 1995, at which time sufficient capacity will exist in the existing racks to shuffle the fuel, remove these racks, and install new racks while maintaining a safe load and transport path.

This license amendment application addresses the reracking of the spent fuel pool to provide 2019 storage locations in a two-region arrangement. Region I consists of 228 locations, and Region II consists of 1791 locations. Region I is designed to accept fresh fuel with up to 4.5 $^{w}/_{o}$ U^{235} enrichment, and Region II is designed to accept spent fuel with a maximum reactivity equivalent of the same enrichment and a burnup of 30 GWD/MTU. The proposed spent fuel pool arrangement is shown on Figure 1-2.

The proposed new racks are a single tier, rectilinear array of free-standing modules. The racks utilize previously licensed concepts and do not introduce any new design concepts, fabrication techniques, installation methods, or operating philosophies. They are intended to be installed and utilized at the plant without relaxation of existing operational limitations and restrictions. The top elevation of the new racks will be the same as that of the existing racks. The rack structure is of austenitic stainless steel, all-welded construction. The basic component of both Region I and Region II racks is a square tube (or cell) with neutron absorber material in the form of BORAL™ strips applied to the exterior walls and covered by a protective sheathing. The cells are 9.085-in. wide. The cell size has been selected to accommodate bowed or twisted spent fuel assemblies with clearance. For the Region I racks, the cells are spaced at 10.5-in. centers, and fuel is stored in the cells. The spacing between cells is used as a flux trap for fast neutron thermalization. For the Region II racks, the cells are spaced 9.085 in. apart on alternating rows within a single rack. Although the new racks are on a smaller center-to-center distance than the existing racks, the clearance between stored fuel and the cell wall is greater in the new racks than in the existing racks. The fuel is stored in both the cells and in the "virtual cells" formed between the cells. The cells are connected on their corners.

The racks are designed and fabricated in accordance with ASME Section III, Subsection NF, 1989 Edition and Addenda up to and including 1991. Design, material procurement, and fabrication conform with the requirements of 10CFR50, Appendix B.

A team consisting of Brand Utility Services, Inc., General Dynamics/Electric Boat Division, Stone & Webster Engineering Corporation, and Yankee Atomic Electric Company is conducting the design, fabrication, and installation of the racks.

This report documents that the design complies with all applicable NRC requirements. The new racks are analyzed to demonstrate the adequacy of the structural, thermal-hydraulic, and criticality characteristics. These analyses show that the new racks are consistent with the current licensing basis for Maine Yankee. The rack configuration maintains a maximum K_{eff} of 0.95 under all postulated conditions, protects the stored fuel during all design basis events, provides adequate cooling of the stored fuel, maintains the maximum decay heat load in the pool within the existing design value, maintains adequacy of the fuel pool structure, and causes no increase in the probability or consequences of accidents.

TABLE 1-1

MAINE YANKEE SPENT FUEL DISCHARGE DATA

Cycle No.	Discharge Date	Batch No.	No. Assy	Wt. Assy KgU	Enrichment $^{w}/_{o}$ U^{235} In	Out	Exposure MWD/MTU
1	6/74	0100010	12	393.96	2.024	1.110	10652
		0101010	56	358.27	2.408	1.366	11912
		0102010	2	394.71	2.947	2.288	6522
		0103010	1	368.00	2.950	1.951	10470
		0104010	1	358.46	2.953	1.960	10359
1A	5/75	0100011	57	393.96	2.024	0.827	15686
		0101011	24	358.27	2.408	1.108	15995
		0102011	22	394.71	2.947	2.109	8565
		0103011	35	368.00	2.950	1.731	13329
		0104011	7	358.46	2.953	1.618	14884
		0110011	2	395.46	2.368	2.079	2769
		0111011	2	395.28	1.945	1.506	4316
		0112011	2	386.43	1.945	1.448	5058
		0113011	1	380.05	2.006	1.511	5150
2(1)	4/77	0200020	69	389.67	1.950	0.681	18042
		0201020	1	353.69	2.519	0.971	20434
3	7/78	0110030	12	395.28	1.945	0.774	15850
		0111030	53	386.43	1.945	0.761	16220
		0200030	12	35[illegible]	2.519	0.583	29424
		0201030	28	389.14	2.896	1.027	24409

TABLE 1-1 (CONT)

MAINE YANKEE SPENT FUEL DISCHARGE DATA

Cycle No.	Discharge Date	Batch No.	No. Assy	Wt. Assy KgU	Enrichment $^w/_o$ U^{235} In	Out	Exposure MWD/MTU
		0202030	12	372.16	2.896	0.818	28841
		0203030	16	363.27	2.896	0.797	29262
4	1/80	0200040	61	353.69	2.519	0.573	29696
		0201040	12	389.14	2.896	0.657	33193
5	5/81	0200050	1	353.69	2.519	0.632	28070
		0300050	16	388.81	2.741	0.611	31944
		0301050	16	380.29	2.740	0.555	33524
		0302050	40	387.76	3.036	0.795	31460
6	9/82	0200060	1	353.69	2.519	0.605	28812
		0400060	48	388.81	3.035	0.776	31912
		0401060	24	378.88	3.033	0.642	35404
7	3/84	0200070	1	353.69	2.519	0.546	30476
		0500070	48	381.48	3.003	0.720	32725
		0501070	4	372.85	3.003	0.528	38235
		0502070	20	363.99	3.003	0.635	34872
8	8/85	0200080	1	353.69	2.519	0.500	31865
		0600080	48	380.83	3.002	0.620	35508
		0601080	4	371.75	3.002	0.525	38342
		0602080	20	363.16	3.002	0.607	35684
9	3/87	0200090	1	353.69	2.519	0.441	33819

TABLE 1-1 (CONT)

MAINE YANKEE SPENT FUEL DISCHARGE DATA

Cycle No.	Discharge Date	Batch No.	No. Assy	Wt. Assy KgU	Enrichment $^{w}/_{o}$ U^{235} In	Out	Exposure MWD/MTU
		0700090	8	379.49	3.288	0.628	39684
		0701090	12	[illegible]1.06	3.288	0.558	41717
		0702090	40	362.45	3.288	0.761	35805
		0703090	4	354.18	3.288	0.538	41988
		0800090	2	361.57	3.302	0.923	31993
10	10/88	0200100	1	353.69	2.519	0.446	33676
		0800100	8	378.93	3.301	0.820	34514
		0801100	28	370.05	3.303	0.642	39154
		0802100	28	361.57	3.302	0.623	39543
11	4/90	0700110	8	379.49	3.288	0.741	36536
		0800110	1	361.57	3.302	0.429	46045
		0900110	4	388.18	3.307	0.599	40182
		0901110	24	378.37	3.303	0.544	41780
		0902110	36	370.08	3.302	0.603	39726
12	2/92	0800120	1	361.57	3.302	0.940	47079
		1000120	20	389.33	3.502	0.704	39598
		1001120	20	379.86	3.501	0.518	45285
		1002120	16	371.22	3.499	0.585	42939
		1100120	4	380.58	3.693	0.955	34230
13[2]	8/93	0800130	1	361.57	3.302	0.430	45158

TABLE 1-1 (CONT)

MAINE YANKEE SPENT FUEL DISCHARGE DATA

Cycle No.	Discharge Date	Batch No.	No. Assy	Wt. Assy KgU	Enrichment $^{w}/_{o}$ U^{235} In	Out	Exposure MWD/MTU
		1000130	8	371.22	3.499	0.555	43850
		1100130	28	390.71	3.690	0.699	42639
		1101130	32	380.58	3.693	0.637	44288
		1102130	8	372.79	3.695	0.466	49755
14[2]	3/95	0800140	1	361.57	3.302	0.452	44387
		1000140	8	389.33	3.502	0.707	39523
		1200140	28	390.58	3.684	0.744	41368
		1201140	12	382.22	3.682	0.544	47268
		1202140	20	374.06	3.681	0.479	49337
15[2]	9/96	0800150	1	361.57	3.302	0.492	43058
		1200150	8	390.58	3.684	0.771	40619
		1300150	12	390.63	3.702	0.644	44131
		1301150	28	381.29	3.700	0.673	43231
		1302150	20	372.29	3.703	0.527	47651

[1] Assemblies EF045 and part of EF046, both from Cycle 2, were placed in consolidated form in March 1992 as part of a fuel consolidation test program. This program was approved by the NRC in a June 16, 1982, letter from the NRC to MYAPCO. This consolidated assembly is the only completed consolidation effort at Maine Yankee.

[2] Projected fuel discharge.

MAINE YANKEE ATOMIC POWER COMPANY

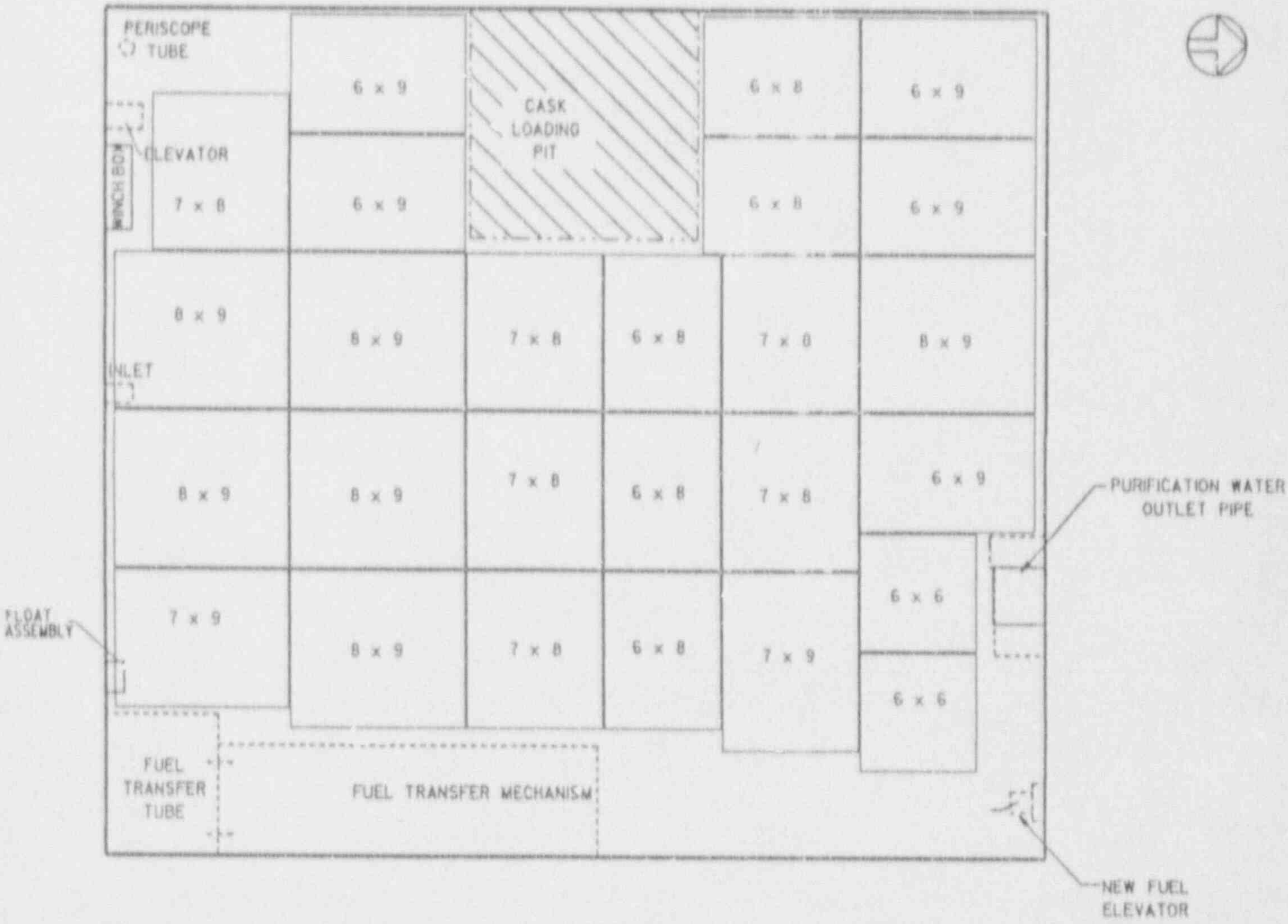

FIGURE 1-1
EXISTING SPENT FUEL POOL ARRANGEMENT

MAINE YANKEE ATOMIC POWER COMPANY

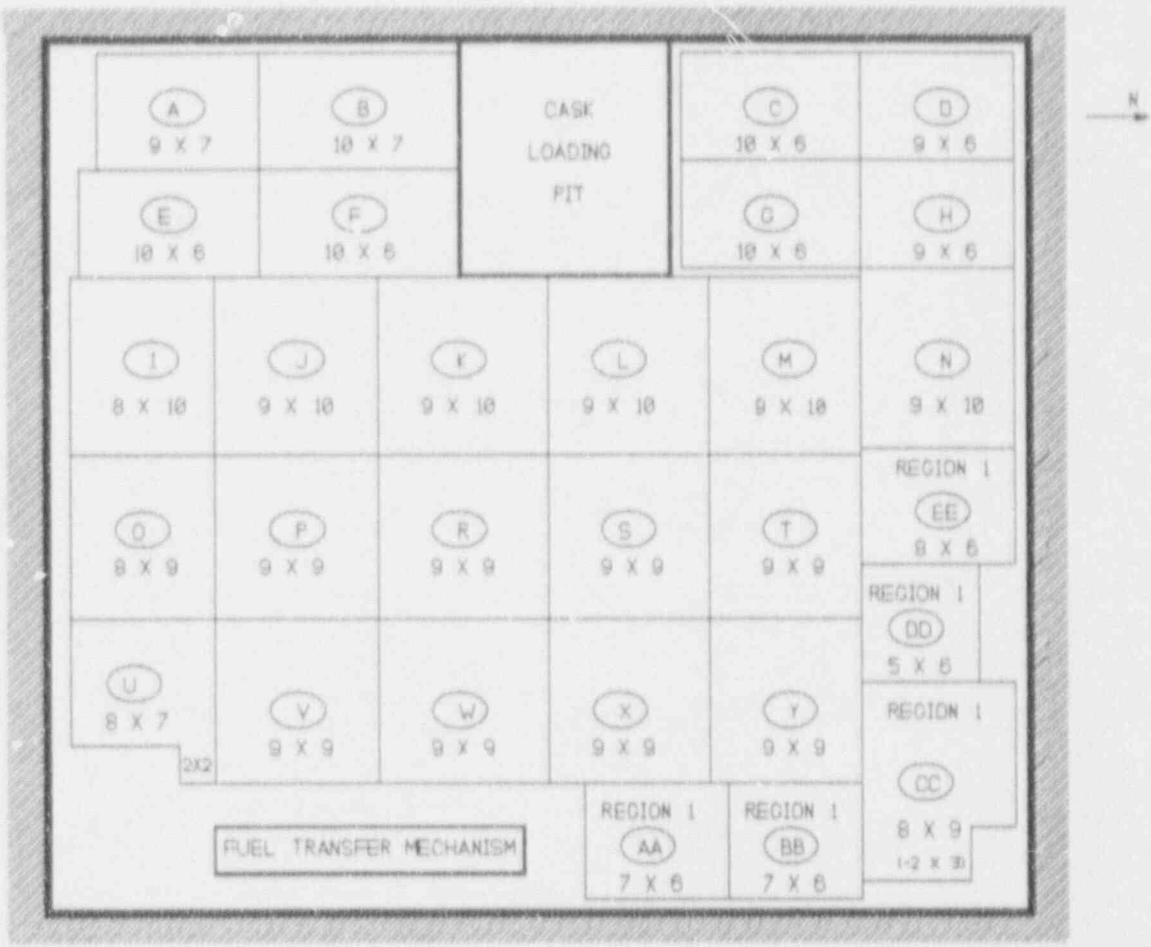

FIGURE 1-2
PROPOSED SPENT FUEL POOL ARRANGEMENT

2.0 FUEL RACK PHYSICAL DESCRIPTION

2.1 GENERAL

The high density spent fuel storage racks provide for conventional storage of spent nuclear fuel in a single tier, rectilinear storage array that is compatible with existing fuel handling equipment, procedures, and techniques at Maine Yankee. The design of the spent fuel storage racks allows for the most efficient utilization of available fuel storage areas within the fuel pool. This fuel storage array is an optimized arrangement of fuel racks utilizing a conventional storage cell pitch that is consistent with currently accepted fuel rack design, analysis, and fabrication practices. The design concept of the high density spent fuel storage racks does not require any fabrication techniques or processes which have not been utilized in rack concepts previously licensed for similar applications.

Two distinct rack configurations are provided to maximize the total storage capacity within the confines of the fuel pool and are arranged in two regions as shown on Figure 1-2. The spent fuel racks will be assembled in modules to fill the Maine Yankee storage pool, providing the maximum number of storage locations. There will be the following rack modules for Region I and Region II.

Module Cell Configurations

Region I

Quantity	Module Size
2	7 x 6
1	8 x 6
1	8 x 9 (less 2 x 3)
1	5 x 6

Module Cell Configurations (Cont)

Region II

Quantity	Module Size
4	6 x 10
1	7 x 10
1	7 x 8 (plus 2 x 2)
1	7 x 9
2	9 x 6
1	8 x 10
5	9 x 10
8	9 x 9
1	9 x 8

The Region I rack configuration is shown on Figure 2-1. They are of the flux trap design with layers of neutron absorber, water, and neutron absorber between every fuel storage location as is similar to the currently installed racks. The fuel storage cells are composed of square tubes with neutron absorber sheets attached on all four exterior cell sides. This rack design is able to accommodate spent fuel with an initial enrichment of up to 4.5 $^{w}/_{o}$ U^{235} with no burnup or exposure restrictions. A complete full core discharge can be accommodated in the spent fuel pool with the use of Region I. The Region I racks provide a larger fuel center-to-center pitch and a larger amount of active neutron absorber than found in the higher storage density portion of the pool. A total of 228 Region I fuel storage locations is provided in 5 rack modules.

The Region II rack configuration is shown on Figure 2-2. These high density storage racks consist of modular arrays of square box cells connected on their corners. Spent fuel is inserted into the boxes as well as into the spaces diagonal to the boxes such as on a checkerboard. These spaces are called "virtual cells." These Region II racks provide maximum fuel storage density within the pool, and make up the majority of the rack modules provided. The Region II racks accommodate spent fuel assemblies with a reactivity equivalent of an initial enrichment of up to 4.5 $^{w}/_{o}$ U^{235} and a burnup of 30 GWD/MTU. A total of 1791 Region II fuel storage locations is provided in 24 rack modules.

The basic structure of the fuel racks is formed by vertical cells tied together into modules that are free-standing assemblies. The rack modules are of various sizes in order to maximize utilization of the available pool area. The sole contact with the building structure is through the rack support foot assemblies which rest on the pool floor. There is no requirement for tensile holddown or lateral shear restraint at the pool floor, between rack modules, or to the pool walls to maintain rack stability under the design loading conditions. Rack support feet are adjustable to allow for rack leveling at the time of installation and do not bear directly on any welded seams in the liner floor. Adjustment provisions of the support feet are accessed from above through a storage cell, and are actuated by long-handled tooling. This avoids the need for in-pool presence of installation personnel.

The height of the high-density fuel rack structure and the location of the stored fuel are maintained at the same elevation as currently provided by the existing spent fuel storage racks, ensuring compatibility with existing fuel handling equipment, procedures, and techniques at Maine Yankee.

All materials used in the construction of the fuel racks are compatible with the service environment within the fuel pool, all interfacing surfaces of stored fuel, and the pool liner. All storage rack surfaces contacting the fuel assemblies are free of sharp corners, edges, or weld beads that could damage the fuel assembly. The high-density fuel storage racks have a design life of 40 years.

2.2 FUEL STORAGE CELL

The basic component of the high density storage racks is the fuel storage cell, shown on Figure 2-3. This cell is used in both the Region I and Region II rack assemblies, with minor differences between both to accommodate the structural differences in the two rack module configurations.

The fuel storage cell is fabricated from 14-gage (0.0747-in. thick; ASTM A240 Type 304L stainless steel sheet. The cell is 9.085-in. square, outside dimension, and 168-in. long. Each cell is formed by continuously welding two formed angles together at what become diagonal corners of the cell. Use of Type 304L stainless steel enhances weldability as well as maintaining compatibility with the service environment.

A fixed neutron absorber, in the form of BORAL™, is placed on the outside surfaces of the cell. The BORAL™ is both located and contained in place by a 24-gage (0.032-in. thick) ASTM A240 Type 304L stainless steel cover. The cover is intermittently welded to the cell by 1/2-in. long welds, 6 in. on center around the periphery of the cover. The top end of the cover is tapered into the cell wall to eliminate abrupt edges. While completely covering the neutron absorber material panel and protecting it from mechanical damage, the cover does not seal the neutron absorber off from the pool environment. In the event of BORAL™ offgassing, the cover provides for unrestricted vent paths top and bottom.

BORAL™ is a neutron absorber product form found in many NRC licensed high-density fuel storage rack applications. The BORAL™ neutron absorber has been in use in the Maine Yankee spent fuel pool since 1975. For this application, the BORAL™ panel is 7.75-in. wide x 140-in. long, centered on the face of the cell and located at a bottom elevation 3 in. above the fuel support surface within the rack. This ensures coverage of the active fuel zone for all stored fuel assemblies in the Maine Yankee spent fuel pool. The BORAL™ provides a minimum areal density of Boron 10 atoms of 0.020 gm/cm^2. The number of cell faces provided with BORAL™ panels is dependent on the rack configuration and the specific location of the particular cell within the stored fuel array. Adjacent fuel storage locations in the Region I array are separated by two neutron absorbing panels and a water gap; adjacent fuel storage locations in the Region II array are separated by a single neutron absorber panel; and interfacing surfaces between Regions are separated by two neutron absorber panels and a water gap equivalent to the distance between rack modules. No neutron absorber is provided on the outer periphery of Region II which faces fuel pool walls or open volumes, such as the cask handling area and fuel transfer canal.

The upper and lower edges of the Region II fuel storage cells are notched to accommodate the interlocking structure of the rack configuration. The Region I cells are square at each end. Upper edges of the Region II fuel storage cell that are not incorporated into the configuration-specific structure are provided with cleats fabricated out of the same material as the cell itself. The cleats project approximately 1/2-in. down from the top edge and serve to stiffen the top of the cell. The upper portion of the Region I modules have lead-in angles and the storage cells are welded to the upper grid structure. All protruding edges are tapered and welded.

Vent holes are provided in each face of the fuel storage cell (Figure 2-3). These provide flow paths to ensure sufficient flow under all conditions. The fuel support surface within each fuel storage location is provided by a 1/4-in. thick baseplate, which also serves to form the base structure of the rack modules. Coolant flow into each cell is provided by a central 4-in. diameter hole in the baseplate.

2.3 REGION I RACKS

The fuel storage cells in a Region I rack are located in a square array, 10.5 in. on center, as shown on Figure 2-1. The rack module is formed by welding fuel storage cells to upper and lower structural frames which position and retain the cells at the desired pitch. The top opening of each fuel storage location is flared outward to provide lead-in guidance during fuel handling operations.

The upper and lower frames are rectilinear grids of formed tubular shapes fashioned from the same 0.25-in. material as the rack base. The tubular cross section is 2.5-in. deep by 1.415-in. wide, outside dimension. The fuel storage cell lead-in guides are integral with the upper frame, and the lower frame is integral with the rack base. The tubular sections are fillet welded all around to each other at each grid intersection. Each fuel storage cell is fillet welded on all four sides to both the upper and lower frame. The resultant structure is a space frame of vertical cells bounded top and bottom by rigid membranes. Wrapper strips around the top and bottom periphery of each module project beyond the outer neutron absorber cover surfaces for mechanical protection. Figure 2-4 shows a typical Region I rack module.

These Region I racks are similar to the existing Maine Yankee racks. The existing racks utilize cells in a square array spaced 10.25 in. on center with lead-in surfaces at the top. The existing racks utilize BORAL™. The individual cells are welded together at top and bottom to form grids and are of welded stainless steel construction.

2.4 REGION II RACKS

Region II racks provide maximum density fuel storage with a center-to-center pitch of 9.085 in., as shown on Figure 2-2. The rack module is formed by corner-to-corner welding of fuel storage cells on a diagonal stagger in both directions. The result is a honeycomb structure of fuel storage cells where every other opening is formed by the outside surfaces of the interconnected cells. These "virtual cells" are bounded by the BORAL™ covers on each side. On the outer rows of each rack module, the open side of the virtual cells is closed by a formed channel of the same thickness and material as the basic fuel cell.

As the cell pitch of the array is equal to the nominal outside dimension of the fuel storage tubes, the vertical leg of the 1/4-in. thick angle at the base of the rack is shared by adjacent rows of cells. Welding each angle to its neighboring angle results in a solid 1/4-in. thick base across the entire rack module, stiffened by 1/4-in. thick gussets (the vertical legs of the angles) across the width of the rack.

At the top of the rack, parallel to the base angles, the fuel storage cells are welded to and positioned by 3/16-in. thick by 5-in. deep flat bars. As with the base angles, each top bar is integral with adjacent rows of cells. The cleats, which span the full width of the cell on the two remaining top edges, are welded to the opposing flat bars forming a rigid frame around each cell opening, as well as for the entire rack module.

Each fuel storage cell is welded to the base angles on all four sides and to each adjacent storage cell for a vertical distance of 6 in. continuously, and then intermittently for the height of the rack to provide shear connection within the module. As with the Region I rack configuration, the top and bottom peripheries of the module are wrapped with integrally welded strips that tie the module together as well as protect the outer neutron absorber covers.

The end result is a lightweight yet very rigid construction, capable of safely supporting the stored fuel under all loading conditions with a minimum of steel and the optimum use of neutron absorber. Every adjacent pair of fuel storage cells throughout the array in the Region II areas of the fuel pool is separated by a single neutron absorber slab. Cell surfaces on the outer periphery of the array which face the pool walls or open spaces such as the cask loading pit do not require neutron absorber, since no fuel can be stored outside the rack module. Figure 2-5 shows a typical Region II rack module.

2.5 SUPPORT FOOT ASSEMBLY

The support foot assembly, shown on Figure 2-6, is common to both rack geometries. It is centered under a fuel storage cell and attached to the base of the rack by a cruciform arrangement of 1/2-in. thick stiffener bars. These bars extend out under adjacent storage cells and transfer the load from the cells to the supporting foot. In this manner, the support foot on a Region II rack is directly supporting the weight of nine fuel storage locations. This effectively eliminates the necessity for a monolithic rack base structure. Support feet are also located directly under the corner fuel storage location of certain rack modules with appropriate stiffener bar arrangements that interface and share load with inner support feet.

The support foot assembly is designed to allow sufficient cooling flow past the assembly to the stored fuel.

The support foot is threaded to allow for ± 1-in. vertical adjustment at installation for leveling the racks. The adjustment is affected by rotating the threaded foot with a long-handled tool which fits into a socket provided in the foot.

The support foot assembly also functions as the load pick-up point during handling for transport and/or installation.

2.6 APPLICABLE CODES, STANDARDS AND SPECIFICATIONS

Spent fuel storage racks do not fall under the jurisdiction of any design code. However, design and analysis activities for the high density fuel storage racks do comply with various design standards and applicable NRC requirements and guidelines which apply to specific facets of the fuel rack design:

- The philosophy of the high density fuel rack design is in compliance with 1967 interim General Design Criteria 66, 67, 68, and 69 and is consistent with 1971 10CFR50 Appendix A, General Design Criteria 61 and 62, and with the NRC Standard Review Plan, NUREG-0800, Section 9.1.2;

- Mechanical design and analysis procedures, loading combinations, and allowable stress criteria are in accordance with SRP 3.8.4;

- Seismic categorization and analyses are in accordance with NRC Regulatory Guides (RGs) 1.29 and 1.92;

- Physical and chemical characteristics for material selection criteria are in accordance with ASME III, Subsection NF requirements for Class 3 components.

The high-density spent fuel storage racks for Maine Yankee are classified as nuclear safety-related Seismic Category I components in accordance with RG 1.29, and all design activities are performed in compliance with 10CFR50, Appendix B, Quality Assurance Program requirements.

A complete list of codes, standards, and regulatory documents used for the design and analysis of the Maine Yankee high density spent fuel storage racks follows:

American National Standards Institute

ANSI N18.2	1973	Nuclear Safety Criteria for the Design of Stationary Pressurized Water Reactor Plants
ANSI N45.2.9	1974	Requirements for Collection, Storage, and Maintenance of Quality Assurance Records for Nuclear Power Plants
ANSI N210	1976	Design Objectives for Light Water Reactor Spent Fuel Storage Facilities at Nuclear Power Stations

<u>American Institute of Steel Construction</u>

AISC	1980	Steel Construction Manual, Eighth Edition

<u>American Society of Mechanical Engineers</u>

ASME II		Section II - Material Specifications
ASME III		Section III - Nuclear Power Plant Components, Div. 1

<u>United States Nuclear Regulatory Commission</u>

Draft General Design Criteria for Nuclear Power Plants (1967 Interim Design Criteria)

GDC 66	Prevention of Fuel Storage Criticality
GDC 67	Fuel and Waste Storage Decay Heat
GDC 68	Fuel and Waste Storage Radiation Shielding
GDC 69	Protection Against Radioactive Release from Spent Fuel and Waste Storage

US NRC Division 1 Regulatory Guides - Power Reactors

RG 1.29	1978	Seismic Design Classification, Rev. 3
RG 1.124	1978	Design Limits and Loading Combinations for Class 1 Linear Type Component Supports
RG 1.44	1973	Control of the Use of Sensitized Stainless Steel
RG 1.92	1976	Combination of Modes and Spatial Components in Seismic Response Analysis

Division 3 Regulatory Guides - Fuels and Materials Facilities

RG 3.41	1977	Validation of Calculational Methods for Nuclear Criticality Safety

Division of Technical Information (USAEC)

TID 7024	1963	Nuclear Reactors and Earthquakes

Standard Review Plans for Nuclear Power Plants (NUREG-0800)

SRP 3.8.4	1981	Other Seismic Category I Structures, Rev. 1
SRP 9.1.2	1981	Spent Fuel Storage (Auxiliary Systems), Rev. 3
NRC Position Paper	1978	"Review and Acceptance of Spent Fuel Storage and Handling Applications"; NRC Letter to Power Reactor Licensees from B. K. Grimes, and 1979 Letter of Modifications and Corrections

2.7 RACK MATERIALS

2.7.1 General

The spent fuel storage racks will be fabricated from 304L stainless steel. All material will be procured in accordance with ASME requirements. All material will be purchased and controlled in accordance with the approved 10CFR50 Appendix B Quality Assurance Program discussed in Chapter 12.

All materials used in the construction of the fuel racks are compatible with the service environment within the fuel pool, and all interfacing surfaces of stored fuel and the pool liner.

2.7.2 BORAL™ Neutron Absorber

The length and placement of the BORAL™ neutron absorber material will accommodate all fuel designs used and anticipated for Maine Yankee. The BORAL™ material is an aluminum clad, aluminum and boron carbide sintered material. The BORAL™ is covered with a thin sheet of 304L stainless steel for physical protection as well as to define and restrict the BORAL™ location. The protective stainless steel sheet is open to the BORAL™ and intermittently welded to the cell along its length to allow hydrogen gas, generated through the oxidation of aluminum, to escape. The BORAL™ neutron absorber material will be manufactured under the control and surveillance of a Quality Assurance/Quality Control Program that meets the requirements of 10CFR50, Appendix B. The boron carbide material will conform to ASTM C 750-80 nuclear grade type III. Special attention will be paid to the maintenance of the boron carbide in a dry condition during fabrication. Sample checks for moisture will be made periodically during production. The aluminum cladding will meet the requirements of ASTM B-209, "Standard Specification for Aluminum Alloy Sheet and Plate."

The final BORAL™ sheets will have surfaces free of any visual anomalies and meet the following specifications:

Boron-10 Areal Density:	0.020 grams per cm^2, minimum
Strip Width:	7.75 $\pm$ 0.0625 in.
Strip Thickness:	0.075 $\pm$ 0.004 in.
Strip Length:	140 $\pm$ 0.0625 in.

An inservice surveillance program will provide confirmation that the BORAL™ in the spent fuel racks is stable and will function over the life of the racks. This is accomplished through an accelerated test of the ability of BORAL™ to withstand high energy radiation in the spent fuel pool for the lifetime of the racks. Chapter 11 describes this program in detail.

2.7.3 Materials Compatibility

BORAL™ is the only dissimilar metal in the new racks. The galvanic corrosion that will take place will form a protective oxide coating on the aluminum to prevent further corrosion. Abrasion of the oxide layer by fuel assembly movement is prevented by the protective sheathing. No galvanic insulator is necessary under these conditions.

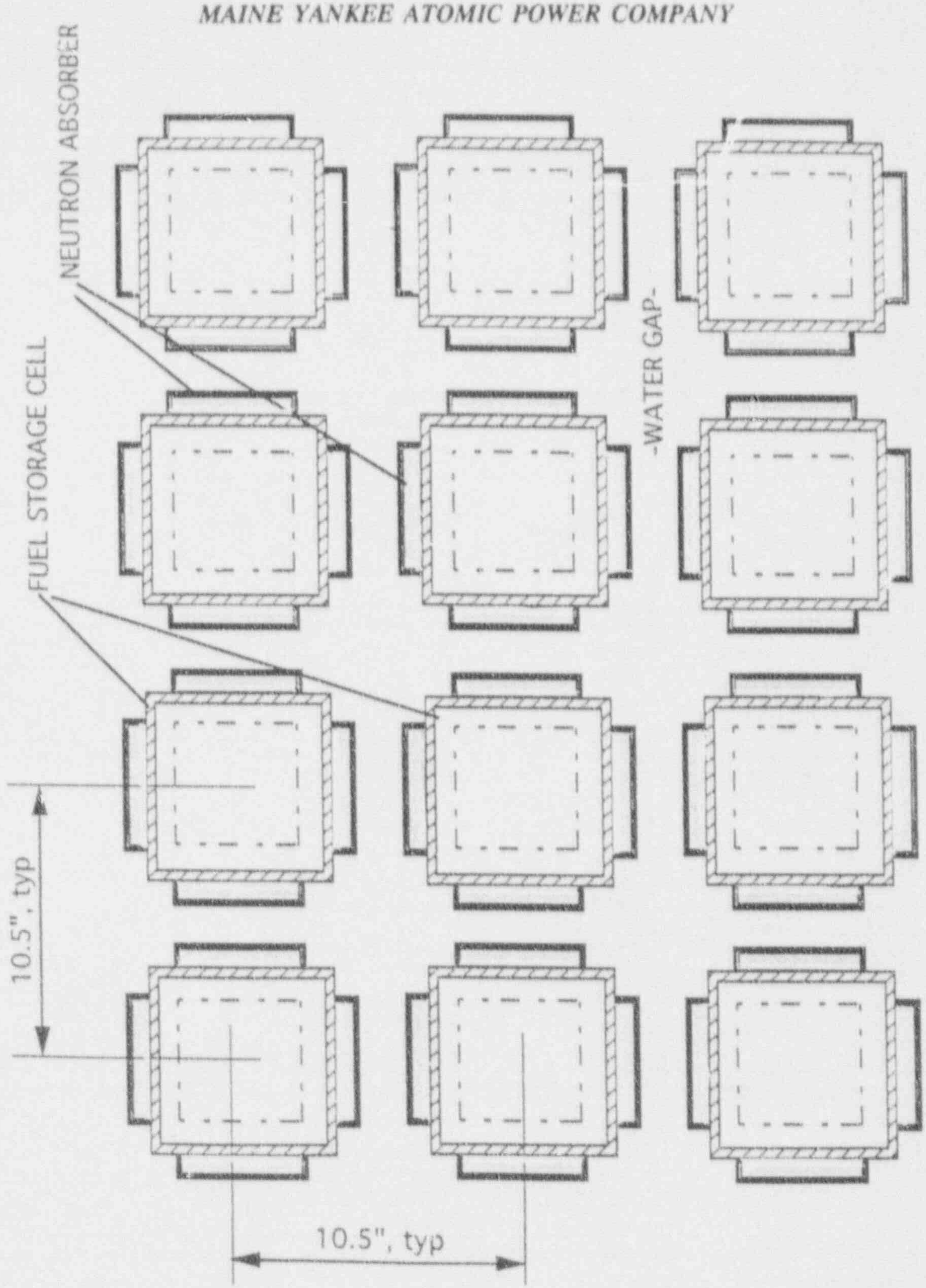

FIGURE 2-1
REGION I CONFIGURATION

MAINE YANKEE ATOMIC POWER COMPANY

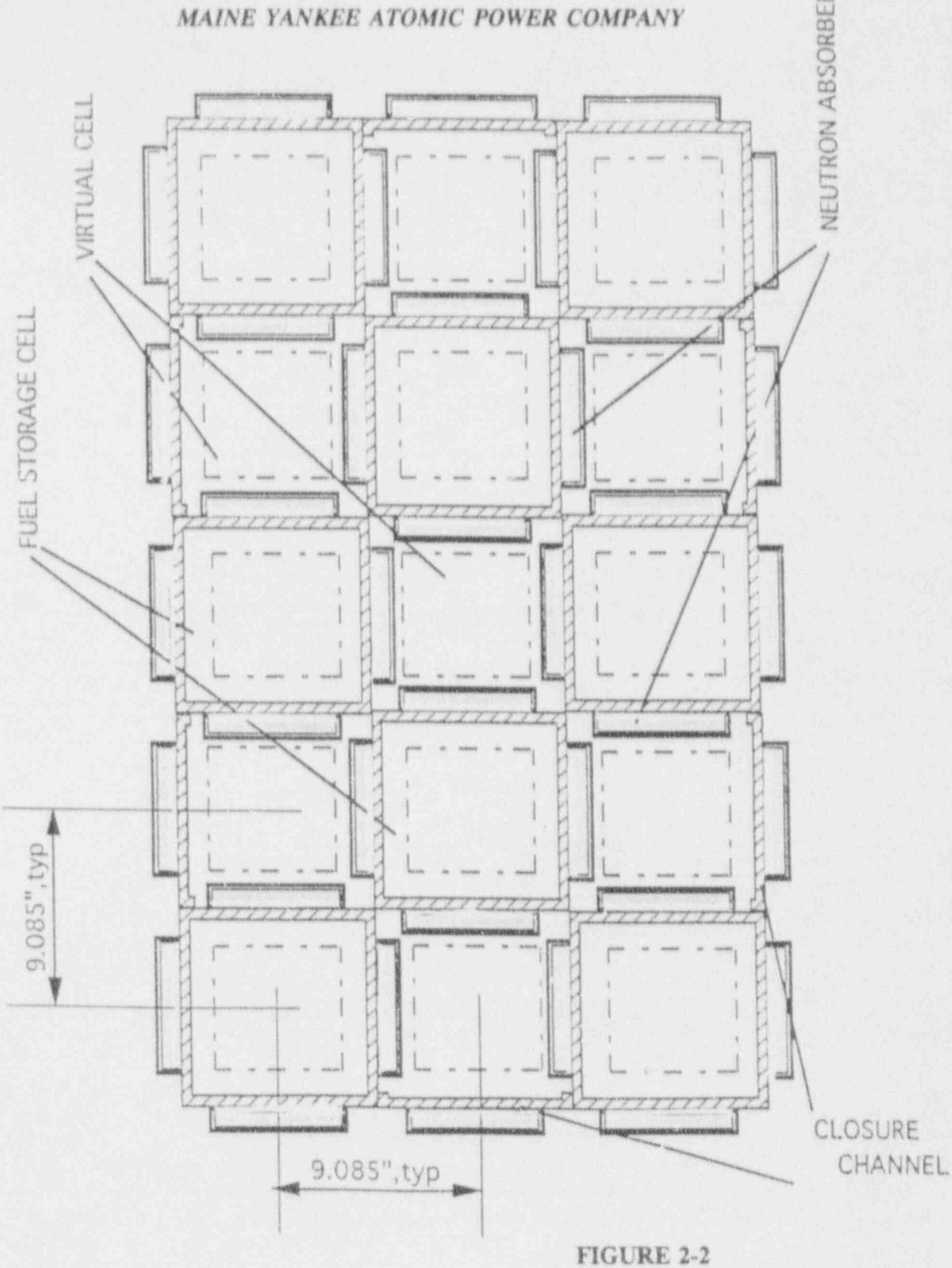

FIGURE 2-2
REGION II CONFIGURATION

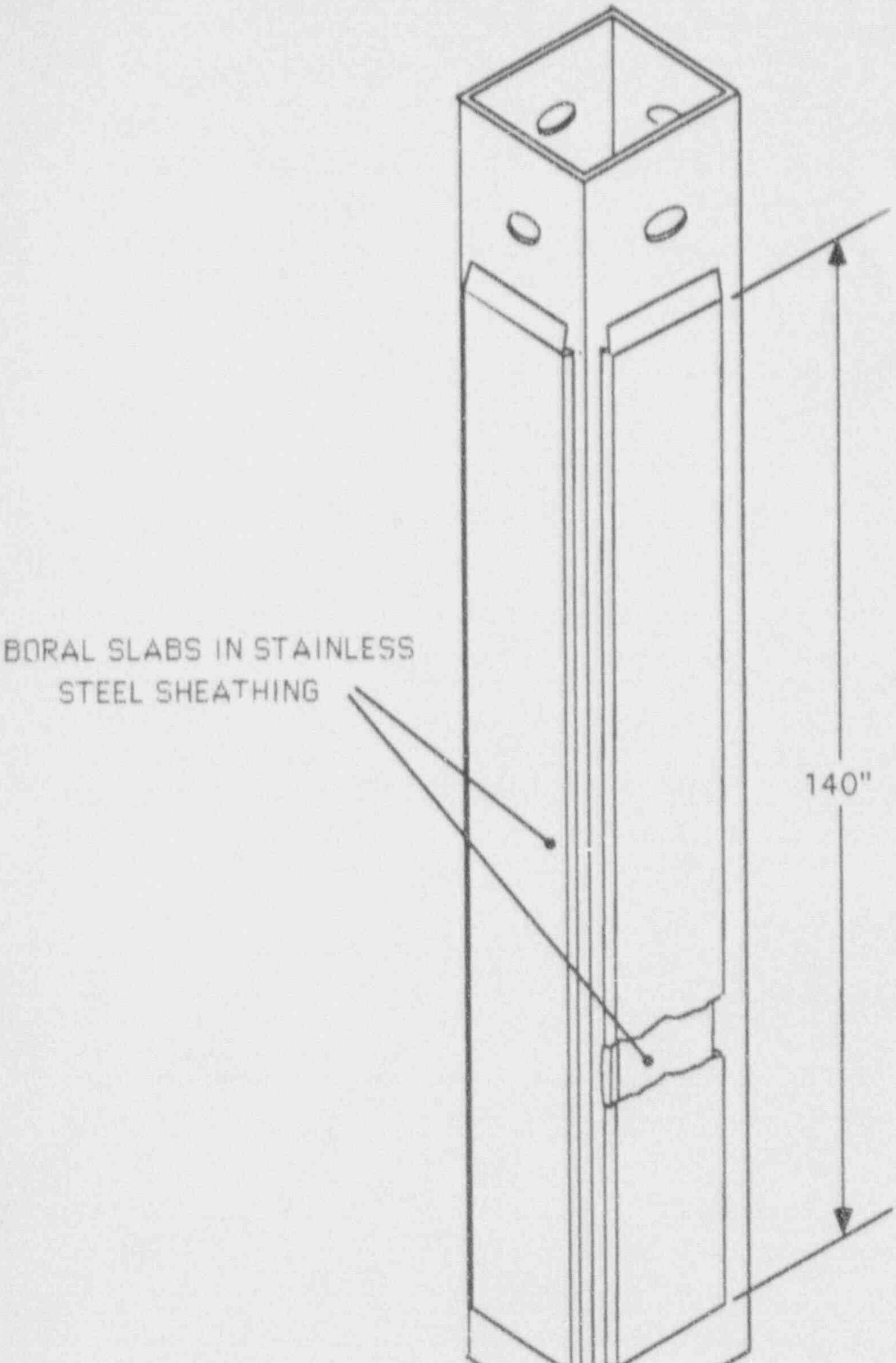

FIGURE 2-3
BASIC FUEL STORAGE CELL

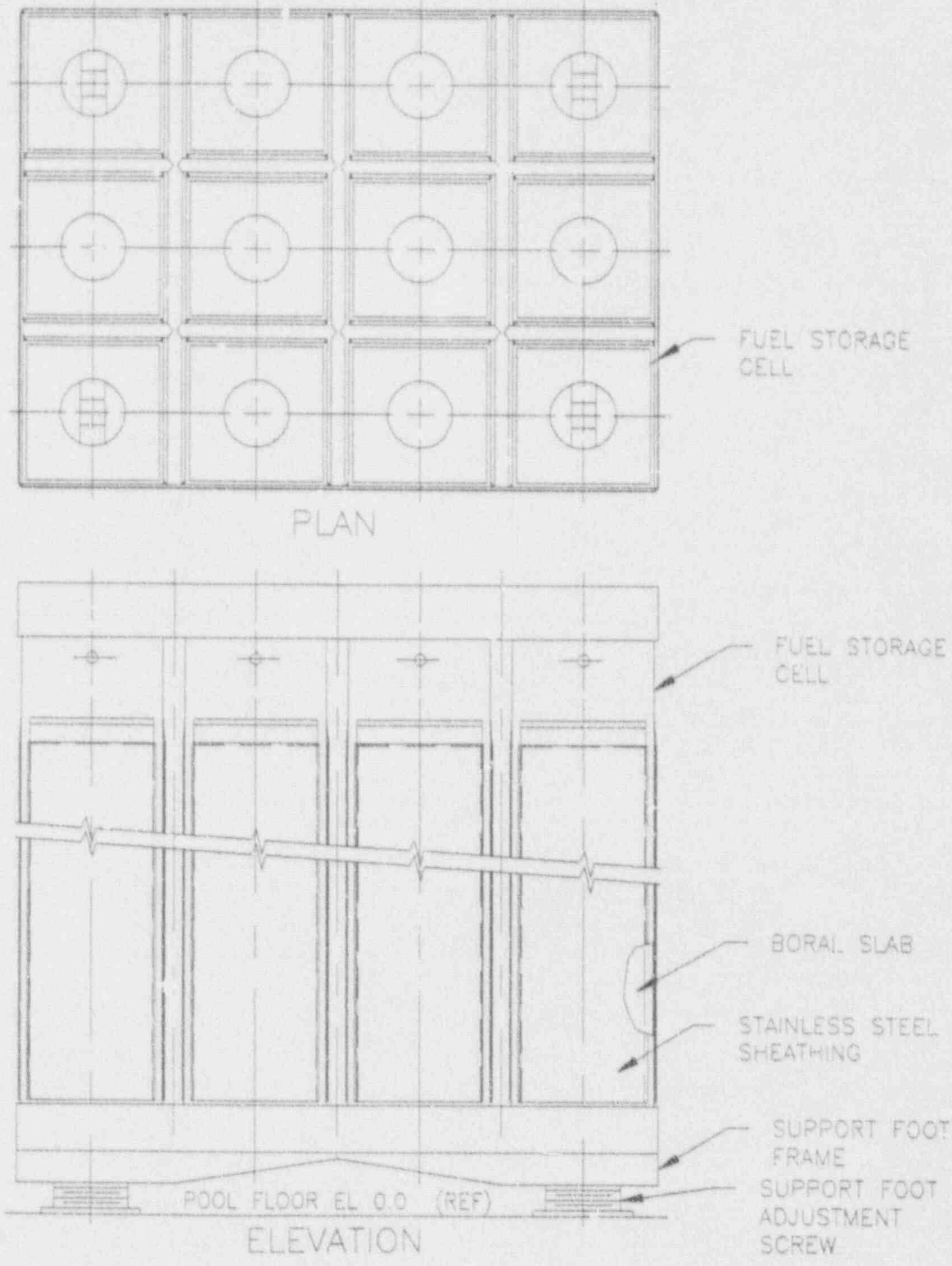

FIGURE 2-4
TYPICAL REGION I RACK MODULE

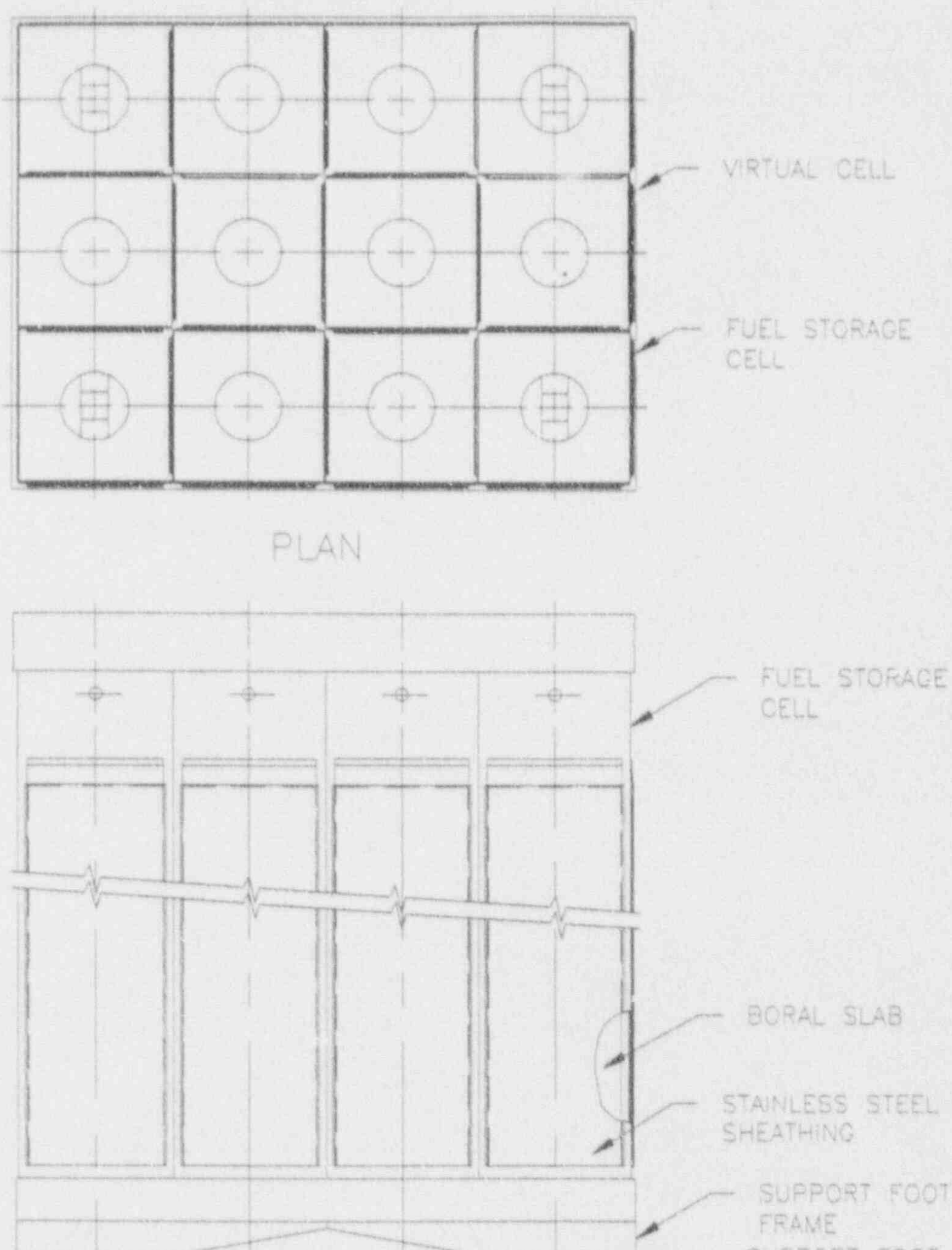

FIGURE 2-5
TYPICAL REGION II RACK MODULE

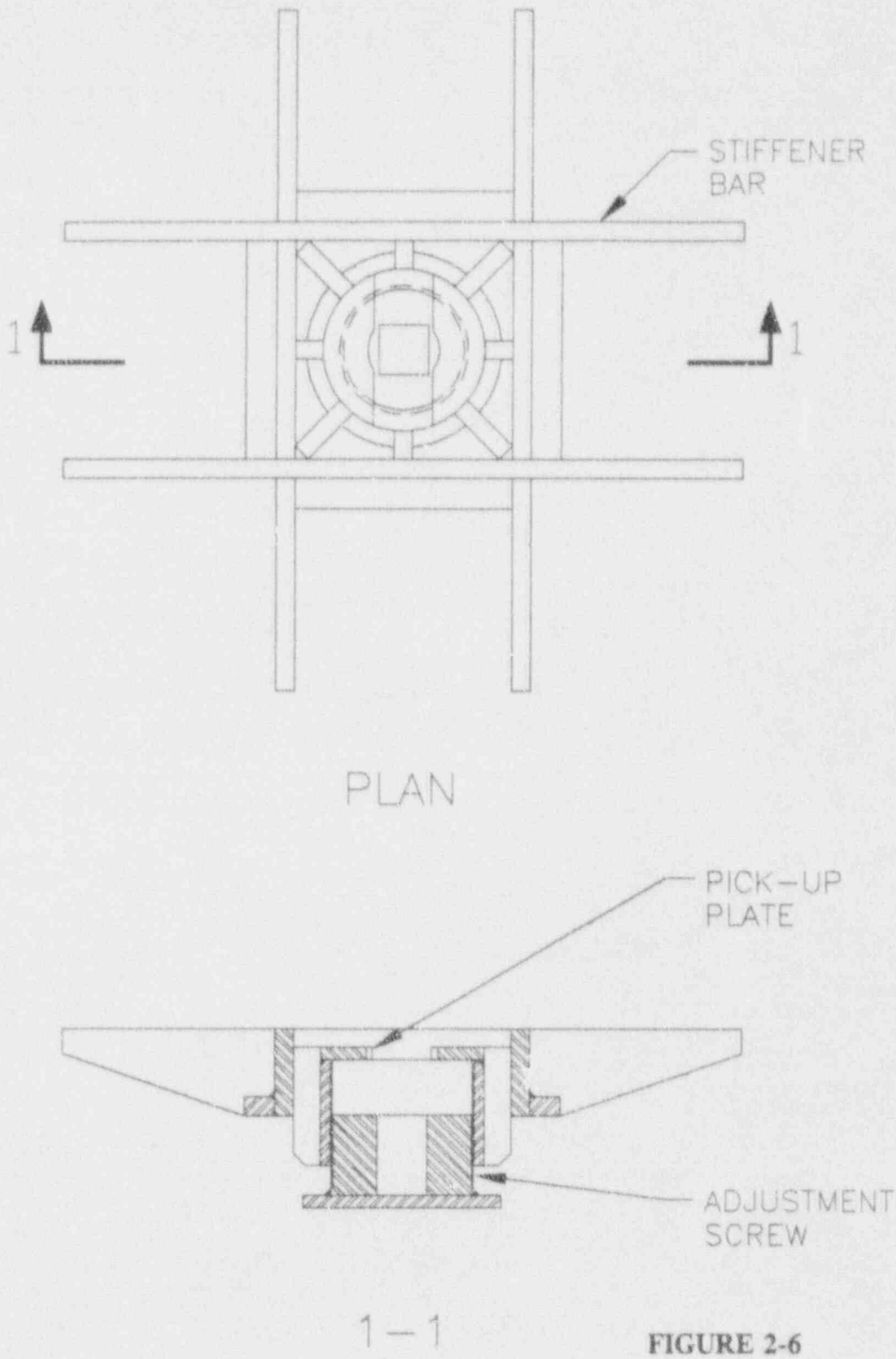

FIGURE 2-6
SUPPORT FOOT ASSEMBLY

3.0 FUEL RACK ANALYSIS

This section describes the structural analysis of the Maine Yankee high density spent fuel storage racks, which includes the evaluation of seismic loading and accounts for submergence effects. The discussion is presented in four subsections: Loads and Loading Combinations; Design and Analysis Procedures; Acceptance Criteria; and Results.

3.1 LOADS AND LOADING COMBINATIONS

The high density spent fuel storage racks are designed for the following loads in accordance with SRP 3.8.4, Appendix D, as defined in Table 3-1.

Dead Load : D

The weight of the individual rack module. Rack weights are based on a stainless steel weight density of 0.286 lb/in.^{3}, and a BORAL™ density of 0.091 lb/in.^{3}. BORAL™ is the only non-stainless steel material in the high density spent fuel storage racks.

Live Load : L

The weight of a stored fuel assembly is 1280 lb, or 1360 lb with a stored Control Element Assembly (CEA), as defined in Table 3-2.

L includes up to a total of 85 CEAs stored with fuel assemblies with up to a total of 24 CEAs stored with fuel assemblies in rack modules D, H, and N for Region II. This reflects storage in accordance with Maine Yankee operational procedures. However, for ease of computation, individual Region I and Region II rack modules are conservatively evaluated assuming that all stored fuel assemblies contain a CEA.

The design of Region II high-density fuel rack modules also accommodates storage of fuel with an equivalent weight of up to two times that of conventional fuel assemblies.

Thermal Effects : T_o and T_a

T_o for both Region I and Region II is defined as the existing licensed maximum pool bulk temperature of 154°F, under plant normal and shutdown conditions.

T_a for both Region I and Region II is defined as a ΔT = 100°F imposed on a pool bulk temperature of 100°F in any one fuel storage location. The heated fuel storage cell is taken at an interior rack location, surrounded by empty locations at the ambient pool temperature. This condition conservatively is the maximum thermal difference across the rack structure and represents the insertion of a freshly discharged fuel assembly. The temperature increase is taken as increasing linearly from coolant inlet to coolant outlet. T_a is evaluated for all Region I and Region II rack modules.

Grapple Snag Loads : P_f

P_f is the upward force on a rack module caused by the postulated jamming of a fuel assembly during removal from a fuel storage location; equal to 2000 lb.

Accidental Load Drop : F_d

F_d is the equivalent force on a rack module due to an impacting dropped object. This condition envelops the full spectrum of postulated fuel handling accidents and dropped objects which may enter the spent fuel pool. For Maine Yankee this condition is bounded by:

- 3.75 ft-K impact energy due to a 2500 lb object (submerged weight) with a 8.4- x 8.4-in. square cross section, at any location at the top surface of the installed rack array;

- 35.1 ft-K impact energy due to a 2500 lb object (submerged weight) with a 8.4- x 8.4-in. square cross section, on the fuel support surface in any one fuel storage location within the installed rack array.

Seismic Load : E and E'

Seismic loads are the same for both Region I and Region II, where E' represents the Design Basis Earthquake (SSE), and E represents the Operating Basis Earthquake (1/2 SSE).

In accordance with the USNRC letter to Maine Yankee (Ref. 3-5), dated March 26, 1987, a ground response spectrum obtained using the 50th percentile amplification factors in NUREG/CR-0098, and a peak acceleration of 0.18g, is acceptable as the Design Basis Earthquake for all new systems and their associated structures and components for the Maine Yankee plant.

Figures 3-1, 3-2, and 3-3 define the Maine Yankee X, Y, and Z direction 0.18g NUREG/CR-0098 ground response spectra which are applicable to the Maine Yankee fuel building. These spectra are based on Maine Yankee site characteristics of compression wave velocity between 13,000 to 15,000 fps, and shear wave velocity of 7000 fps. Seismic input to the fuel rack dynamic analyses for E' is the acceleration time-history input data corresponding to the ground response spectra, as presented on Figures 3-4 and 3-5. Seismic loading E is taken as 50% of the E' acceleration time-history inputs.

The acceleration time-history data is converted to displacement time-histories for input to the ANSYS® program, which is used for the rack structural analysis. Integration of the acceleration records to obtain displacements is performed by Stone & Webster computer program INTBSL (ST-307, Baseline Correction and Integration). Input to ST-307 is an equal time interval acceleration time history. The program integrates the acceleration data and performs a parabolic baseline correction to eliminate the potential for drift in the output data. Output from ST-307 are baseline corrected acceleration, velocity, and displacement time-histories.

3.2 DESIGN AND ANALYSIS PROCEDURES

The primary function of the high density spent fuel storage racks is to maintain stored fuel in a subcritical array while protecting it from mechanical damage. Local rack deformation under uplift or impact loads is considered permissible to the extent that subcriticality of the array is maintained and resultant damage to stored fuel is minimized. Under combinations of deadload, thermal and seismic conditions, resultant stresses are limited to levels which ensure positive margins on acceptance limits.

Structural adequacy of the designs is demonstrated by comparison of calculated stress levels within the fuel rack against the specified design limits. Dimensional stability is demonstrated by comparison of calculated displacements and rotations of the rack modules against the established inter-rack and rack-to-structure clearances. Results of these comparisons verify positive margins against rack overturning and impact interactions. It is concluded that the Region I and Region II high density fuel rack modules are structurally adequate for their intended function.

The fuel racks are designed to accommodate the fuel described in Table 3-2.[1] Storage cell dimensions are compatible with the maximum distortions historically encountered with this fuel at Maine Yankee to preclude binding during fuel handling and storage operations. The Region I and Region II fuel racks are compatible with fuel handling equipment and procedures at the Maine Yankee plant. Fuel is stored within the racks in a vertical orientation, and at the same elevation as previously licensed fuel storage systems at the plant.

The high density fuel storage racks are designed to Seismic Category I requirements. Seismic response of the fuel racks accounts for the nonlinearities inherent in free standing high-density fuel storage racks: fuel-to-rack gaps; rack-to-rack gaps; rack-to-wall gaps; rack tipping and/or sliding; large displacements; and submergence considerations of hydrodynamic coupling, fluid-structure interaction, and entrained and virtual masses.

A 3-D nonlinear transient seismic analysis of the high density fuel racks is performed utilizing displacement time history data obtained from integration of acceleration time histories for three orthogonal simultaneous earthquake directions. Figure 3-6 depicts a typical mathematical model, showing the fuel-rack-structure interfaces, gaps, and fluid coupling elements.

---

[1]Region II racks are also designed to accommodate fuel with an equivalent weight of up to two times that of conventional fuel.

For these nonlinear analyses, elastic properties are calculated treating the module as a composite beam, accounting for the aspect ratios of the different rack module sizes, and the honeycomb-like structure of the Region II racks. Fuel element mass and stiffness properties are derived from published fuel assembly dimensional data and specific as-built characteristics.

Nonlinear properties for impact springs and elemental damping values include local rack flexibilities and fuel rod beam flexibility calculated from cladding thickness using conventional strength of materials relationships.

Rack stability is assured under dynamic displacements, and addresses all fuel loading conditions, i.e., completely full, completely empty, or an intermediate amount of stored fuel, whether random or ordered. Rack module stability against overturning and the possibility of rack-to-rack and rack-to-wall impacts are evaluated for a bounding range of friction coefficients. Coherent and dissimilar behavior of adjacent racks and pool structures is addressed.

Fluid motion due to free surface effects (fuel pool slosh) is accounted for in accordance with TID-7024 (Ref. 3-1).

Basic structural analysis of individual fuel storage cells and composite rack modules is performed in accordance with ASME III, Subsection NF.

3.2.1 Analytical Approach

Design analysis of the high-density spent fuel storage racks is performed in a sequence of stages leading from static load assessment of the fuel support baseplate of a single, isolated fuel storage cell; through a full 3-D finite element structural model of a complete rack module with support structure; up to 3-D nonlinear dynamic models representing multiple fuel racks within the fuel pool. Governing element and nodal forces are extracted from the dynamic analyses and utilized to evaluate stresses, including weld joint stresses and localized stress distributions in the 3-D structural models, using manual calculations where appropriate.

Each stage incorporates modeling data developed in previous steps of the analysis. As Region I and Region II configurations utilize common elements (e.g., fuel storage cell), modeling data is also shared by the load and stress analyses of both rack types.

Analyses of the Region I and Region II high density spent fuel storage racks are performed in the sequence described in the following sections. All computer aided analyses are done using the ANSYS® finite element code, as described in Appendix A.

3.2.2 Linear Structural Models

Fuel Storage Cell Base

A 3-D finite element representation of the fuel support baseplate and interfacing vertical walls of a single fuel storage cell is examined. Figure 3-7 depicts the plate elements, boundary conditions (fixity), and applied loads. This model addresses stresses and deformations in the fuel support base and lower portions of the cell walls due to vertical loads from fuel deadweight and (equivalent static) vertical seismic loadings.

Invoking symmetry, 1/4 of the base of the (nominal) 9- x 9-in. cell is modeled, consisting of:

- A base plate, 1/4-in. thick (horizontal leg of the base angle) with a central 4-in. diameter coolant flow hole;

- A 1/4-in. thick stiffener (vertical leg of the base angle), 2 1/2-in. high, along one edge of the base;

- A 14-gage stiffener, 2 1/2-in. high, along the second edge, representing the lower extremity of the fuel storage cell walls.

This model geometry represents the Region II configuration which bounds the Region I configuration for this evaluation. The Region I base consists of a tubular frame on all four sides of the fuel cell, supported on the module baseplate. In addition, the Region II rack configuration is also evaluated for the heavier equivalent fuel assembly (up to two times the weight of conventional fuel).

Boundary conditions are:

- Symmetry along the two "cuts" which separate the 1/4 section from the base of a single fuel storage cell;

- Vertical and rotational fixity along the top of the 14-gage stiffener;
- Rotational constraint of the base around the cell edges when the adjacent cells are also loaded.

The model consists entirely of ANSYS® STIF63 elastic quadrilateral shell elements.

The analysis is a static deadweight evaluation. The loading is one quarter of the weight of an equivalent fuel assembly applied over an area representing the contact surface of the fuel assembly support foot.

Cell Buckling

Much of the high density storage rack module is made of metal formed into an array of square tubes. Since the thickness of the material is small compared to the other dimensions, there is a potential for the allowable stress in compression to be governed by buckling. The basic model of the fuel storage cell is evaluated for buckling along its axis as well as across the width of a face. Again, the analysis invokes symmetry so only a portion of the cell is modeled.

For axial compression, buckling will not occur at either end of the cell, as the upper end is minimally stressed and the lower end is supported by connection to relatively thick members, which inhibits local buckling. Thus, the analysis investigates mid-span buckling, and the model uses a clamped boundary at the bottom. As the analysis uses a uniform compression load along the length of the model, the top end is also considered clamped in order to avoid boundary-induced buckling. The model length is long enough for the midspan to be reasonably unaffected by the end conditions (i.e., essentially infinite).

The ANSYS® finite element model contains the following (Figure 3-8):

- Quarter-symmetry section of cell,
- BORAL™ cover plate on outer surface of cell (this item is conservatively ignored in the rack structural analysis),
- Attachment between cover plate and cell at 6-in. intervals, representing intermittent welds,

- Symmetry boundary conditions along the two "cuts" which define the quadrant,
- Rotational, axial, and lateral fixity at the fixed end,
- Rotational and lateral fixity at the loaded end.

For compression across the cell width a 1/2 symmetry model 1-in. wide represents a portion of the cell, well removed from the reinforcement provided by the lower rack structure, and provides the proper stiffnesses at the cell corners (Figure 3-9). Symmetry boundary conditions are at all "cuts," although tension in the cell axial direction is released. Vertical constraint is provided at one corner, and the compressive load is applied at the other corner.

In both models, all elements are ANSYS® STIF63 quadrilateral shell elements.

An iterative large displacement solution evaluated for several values of load is used to develop critical buckling loads for the cell in both directions. This approach is preferred over an eigenvalue buckling solution by the authors of ANSYS® since it accounts for imperfections, and loading directions conform to the buckled shape. As the solution is iterated for a given load, it converges below the critical buckling load and diverges above it. The load intermediate between convergent and divergent solutions is established as the critical buckling load.

The allowable stress in the cell axial direction (vertical) is not buckling limited, but the stress due to loads applied across the cell width is. However, stresses in this direction are generally low and are accommodated within the allowable.

Rack Module Subassembly and Detailed Structural Models

Elements of the basic fuel storage cell base model and the buckling model are incorporated into a full height model of an interconnected array of fuel storage cells, including adjustable support foot assemblies. Quarter-symmetry models for both Region I and Region II configurations are generated with ANSYS® STIF63 quadrilateral shell elements. Primarily, the models are used for static load analyses to establish the number and location of support feet.

The 14-gage fuel storage cells are 9.085-in. square tubular sections with neutron absorber panel assemblies on all four sides. The cells are modeled with cross-sectional properties based upon the fuel storage cell cross section, with no consideration of the structural properties of the neutron absorber sheath. However, the mass of each neutron absorber panel and sheath is distributed along the height of the fuel storage cell. Therefore, the dynamic response of the rack module is based upon section properties that include the neutron absorber panel mass; and the stress analysis is based on section properties that do not include any strength or stiffness contribution of the neutron absorber panel sheath, thereby producing a conservative analysis.

The integrated assembly of the Region II fuel storage cells is stiff in the vertical direction due to the relatively great depth of the structural section of the rack modules and the shear connection between adjacent tubes. By comparison, the bottom plate is compliant, as vertical loads are acting out-of-plane. Thus, the fuel loading in cells which are not directly supported by a foot assembly is transmitted in vertical tension into the array of cells. Near each support foot, the load from distant cells is transmitted down through the cell walls to the foot. Here the loads are from multiple cells and the stresses are greatest.

A Region I subassembly of a 1/4 model of an 8 x 6 module is shown on Figure 3-10. It consists of a 4 x 3 array of fuel storage cells 10.5 in. on center, connected together by upper and lower gridwork frames, founded on a 1/4-in. baseplate. As they offer no benefit regarding strength or stiffness of the rack structure, the fuel cell lead-in members are not included. A view of the underside of the model (Figure 3-11) shows the support foot assembly detail, including stiffener gussets that extend beneath adjacent cells.

The rack quadrant is modeled with the following characteristics:

- 14-gage material thickness forms the walls of the cells;
- 1/4-in. thick material forms the 1.41-in. x 2.75-in. gridwork frames at the top and bottom of the rack;
- The base is 1/4-in. thick ;
- A 1/2-in. thick foot assembly extends beneath the perimeter of several adjacent cells;
- The center of the foot assembly is 3/4-in. thick and includes radial spokes and a central hub.

A Region II subassembly 1/4 model of a 9 x 9 rack module is shown on Figure 3-12. Using symmetry, one quadrant of the rack is modeled with the following characteristics:

- 14-gage material thickness forms the walls of the cells;
- 3/16-in. thick material forms a 1-D grid 5-in. deep at the top of the rack, and a 2 1/2-in. band along one edge at the bottom;
- The base is 1/4-in. thick ;
- A 1/2-in. thick foot assembly extends beneath the perimeter of several adjacent cells, similar to Region I as shown on Figure 3-11;
- The center of the foot assembly is 3/4-in. thick and includes radial spokes and a central hub.

Boundary conditions for the models are as follows:

- Symmetry along the two "cuts" defining the rack quadrant, applying symmetry as appropriate for the loading direction.
- Constraint in the vertical direction at the four lower corners of the storage cell representing the hub into which the rack foot is threaded.

The intermittent welds providing shear connection between fuel storage cells in the Region II configuration are treated as continuous connections in the models, with element sizes on the order of the weld spacing. Manual analysis of weld stresses accounts for the differences between continuous and intermittent welds. The design allowables for this weld configuration have been established based on test results (Ref. 3-4).

Each model is statically evaluated for vertical and lateral loads to establish the number and location of feet required to assure that acceptable stresses will be realized during the detailed design analysis. These static loads are meant to represent deadweight, vertical seismic loads, and lateral seismic loads, respectively. The loads primarily result from the fuel weight since the weight of the racks is small by comparison. In these analyses, forces are applied as follows:

- A downward pressure load on the bottom plate.

- A lateral pressure load on the cell walls.

Static Analysis

Once the above evaluations have resolved design features, the selected configuration is analyzed in detail for all loads and load combinations. Analytical models developed in the process of design development are fundamental to this analysis.

Each subassembly model is individually evaluated for Dead Load, D, and Live Load, L, to develop stresses for input to the load combinations shown in Table 3-1.

The same models are also used for analysis of thermal loading conditions, T_o and T_a, for input to detailed analyses of the load combinations.

Figure 3-13 shows the detailed 3-D finite element model of a full 9 x 10 Region II rack module. This detailed structural model accurately represents the physical characteristics of the rack structure.

3.2.3 Nonlinear Dynamic Models

Single Rack

The single rack nonlinear dynamic model is a simplified 3-D model composed of an equivalent rack structural model and additional elements to account for the fuel assembly, fuel-to-storage cell gaps, hydrodynamic masses, and fluid coupling elements for Region I and Region II configurations.

The equivalent properties from the structural model are as follows:

- Fuel storage cells are represented as 3-D beam elements with effective stiffness and mass properties.

- Storage cell to foot connectivity is provided by beams having the same stiffness as the detailed rack model. These stiffnesses are established by imposing distributed unit loads on the detailed model.

- Support foot with vertical and lateral stiffnesses and the nonlinear capabilities of sliding behavior, with friction, and one-way gaps allowing vertical lift and contact impact.

The simplified model is verified by performing static and modal analyses on the detailed and simplified models and comparing results (deflections, natural frequencies, and mode shapes), in air and submerged.

The fuel assemblies are represented by a combination of 3-D beam elements. The beam elements have properties of stiffness, area, and mass, factored by the number of fuel assemblies represented in the analytical model (dependent on the rack size and percentage of cells loaded). The fundamental bending frequency is the same as for a single fuel bundle. Connection between the base of the fuel and the rack supporting surfaces uses a 3-D sliding gap element allowing lift-off and contact impact. The stiffness is based on the stiffness of the fuel bundle base assembly and the local stiffness of the rack bottom plate.

Lateral fuel impact stiffnesses are computed considering the local and global stiffnesses of the fuel bundle grids and the local stiffness of the fuel rack cell wall. Only the latter stiffness is considered at the contact points between the cell and the upper and lower fuel bundle end plates. To minimize the number of elements, contact is modeled at only several grid locations and the impact stiffness is taken as a multiple of the computed value. Fuel-to-rack gaps are modeled by four 3-D gap elements at each impact elevation, each having the appropriate stiffness.

Hydrodynamic coupling between the fuel assembly and cell is modeled using the approach of R. J. Fritz (Ref. 3-2), as implemented by the ANSYS® STIF38 dynamic fluid coupling element. (The general subject of coupling is addressed further in Section 3.2.4, Modeling Details.) As the fuel assembly is an open array of rods, flow around the rods and through the array is the condition that produces the governing hydrodynamic mass, which is calculated based on the kinetic energy of the fluid. The hydrodynamic mass elements are modeled at eight locations along the length of the fuel with values proportional to the effective fuel length at each location.

The hydrodynamic mass between the fuel rack and the pool wall and between rack modules for out-of-phase rack motion is also modeled by the STIF38 element. These hydrodynamic mass elements are coupled to the rack centerline at the same elevations where the fuel-to-rack fluid coupling elements are located. The values of hydrodynamic mass for the fuel rack module are based on potential flow theory, assuming free flow into the volumes above and below the rack and through the Region I storage cell array, again using the method of Fritz. A single fluid coupling element is connected between the rack and the floor. Dummy masses are lumped on the simplified model to (1) represent the rotary inertia of the entrained water if the rack rotates about a vertical axis, and (2) represent the vertical mass of the entrained water. The multiple rack model is verified to ensure that the combination of dummy masses and fluid coupling elements is such that the proper reactions are developed for a static load applied in any one of the three orthogonal directions. Thus the foot loads are compatible with the rack weight, and the fluid coupling loads are compatible with the water mass.

Partial Fuel Loading Models

Nonlinear models for partial fuel loading are created for three loading geometries: full load to one side of a diagonal and full load on one-half of the rack, providing maximum eccentricity across the narrow dimension, and empty rack loadings. These models are used to address specific types of rack motion. The diagonal loading model (Figure 3-14) addresses fuel loading eccentricity shifting the center of gravity toward one support foot and producing torsional rotation. The row loading models (Figure 3-15) address fuel loading on one side of the rack module causing the rack to rock up on one side with a tipping motion. The empty rack model is used to calculate the motion of an empty rack. Displacement results of these models and the full rack model are used to determine the rack combination resulting in the maximum relative motions, and to envelope the random placement of fuel in the rack.

Finite element details in the fuel storage cell structure and fuel assembly models are the same as those used in the full rack model, but with stiffness and mass properties equivalent to the number of cells or fuel assemblies in the particular loading configuration. Hydrodynamic coupling elements that represent the rack to pool wall interaction are the same in all models.

Weak Fluid Coupling

While most analyses consider the response of a single rack hydrodynamically coupled to the surrounding pool structure or other racks, the effect of no coupling is also investigated. This analysis uses the existing single rack model, assuming no hydrodynamic mass term. This is physically equivalent to having the rack in the middle of a very large pool such that rack motion does not impart significant kinetic energy to the surrounding fluid. As such, the analysis represents an extreme limiting condition.

Nonlinear Multiple Rack Model

Analyses of single rack modules incorporate specific assumptions which lead to conservative results concerning their structural response: all stored fuel assemblies are taken as vibrating coherently, maximizing reactions and/or impacts due to fuel motion; adjacent rack modules are taken as vibrating out of phase, maximizing the potential for rack-to-rack impacts; variations in fuel loading, friction, and boundary conditions (from small gaps to essentially infinite spacing) bound maximum rack displacements. However, fluid coupling between adjacent objects establishes that the force on one at any given time is dependent upon the relative acceleration of the other. Therefore, single rack analyses cannot persuasively account for the potential interactions between adjacent racks and building structure (pool walls) as they are affected by hydrodynamic coupling phenomena. Although spent fuel racks have historically been qualified as individual units, consideration of the coupling and potential interaction between multiple racks in a pool indicates the following potential differences from single rack evaluations:

- Total rack movement due to slipping between the rack feet and pool liner is potentially greater in the multiple rack analyses.

- The motion of adjacent racks tends to be in-phase, even though a fundamental assumption of the single rack analyses is out-of-phase motion.

To address potential nonconservatisms of a single rack analysis, additional analyses are performed for multiple rack configurations under design basis seismic events within the Maine Yankee spent fuel pool. Due to the number of racks in the model, each is represented by a simplified geometry, but the model retains all of the features required to adequately explore multi-rack phenomena (see Figure 3-16):

- The effects of disparate rack dimensions.

- The effects of varying fuel loading amounts and distributions.

- The effects of different fluid gaps between rack modules.

- The effects of significantly different fluid gaps between rack modules and pool walls.

These analyses investigate the response of a multiple rack array in the Maine Yankee fuel pool under SSE conditions for the two limiting conditions of friction between rack and liner: $\mu = 0.2$ and $\mu = 0.8$. The evaluation is limited to a section of the pool rather than the entire pool and its contents, but adequately addresses the range of conditions found in the pool. The region of the pool selected for analysis contains four different size rack modules and a wide variation in the water filled clearances between racks and between racks and pool walls. To further assure that the widest potential range of responses is exhibited by the racks in the model, the placement of fuel in the racks is carefully chosen to encourage dissimilar behavior.

To make the nonlinear time-history analysis practicable, the analysis considers a section through the pool containing four Region II racks: Racks A, B, C, and D. See Figure 3-17. The selected section through the pool contains the full range of fluid spacings and, since the widest rack spacing (across the cask loading pit) and the narrowest spacing (0.5 in.) are included, this section also has regions with relatively weak and relatively strong fluid coupling. Generous clearances at the ends of the pool also enhance the potential for large rack motion.

The analysis is a full 3-D dynamic analysis; forces in out-of-plane directions contribute to slipping of the rack feet and rack tipping. In essence, the racks are considered to be in a long, narrow pool defined by a wall artificially induced on the east side.

To maximize the variabilities in the model and demonstrate that there is no structural need for administrative controls on the placement of fuel in the racks, a wide variation in fuel placement is assumed. This includes a full rack, an empty rack, and two racks with the fuel clustered at a corner and end, respectively. This maximizes the potential for dissimilar rack motions, and the latter cases promote rack tipping and rotation, representing a condition worse than any likely to be encountered in practice.

The heaviest rack (10 x 7) is considered full; the lightest rack (9 x 6), is empty; and the 10 x 6 rack is considered 20% full with all of the fuel concentrated at the end of the rack nearest the cask laydown area to maximize the potential for rotation and for tipping towards the open space. On the premise that a light rack is more likely to be jostled around in an earthquake when the adjacent rack is full, the 9 x 7 rack is considered relatively empty: 10 cells in one corner are considered loaded, maximizing the chance for rack rotation about the vertical axis.

3.2.4 Modeling Details

Rack Models

For the nonlinear dynamic rack models for both the single and multiple rack analyses, the shell structures of the rack modules are modeled as simplified figures utilizing a series of ANSYS® STIF4 elastic beam elements (see Figure 3-6). Symmetric modes such as "breathing" modes and certain diagonal shear modes of the shell structure have low participation factors for seismic loading, and are thus ignored. Each rack is modeled by a stick figure containing a vertical multi-element beam having the bending and shear properties of the array of cells that make up the rack. These members represent bending, shear, and twisting in the rack module assembly.

The rack support feet are modeled as ANSYS® STIF52 sliding/gap elements, and are free to slide (with a prescribed coefficient of friction) and to lift off the floor. The support beams that connect the feet to the vertical beam contain the mass of the rack base (i.e., the feet and 1/4-in. thick base plate), are ANSYS® STIF4 elements, and are assigned a stiffness derived from applying unit loads to the detailed structural model of a typical rack module. For computational purposes in the multiple rack analysis, the six to eight support feet on each rack are represented by four support points, one under the center of each of the four corner cells of the rack. Thus, each foot in the multiple rack model represents 1 1/2 to 2 actual support feet, with stiffness properties assigned accordingly.

For convenience, rack dimensions are based on the nominal centerline spacing between fuel bundles times the number of cells. This is precise for certain applications (e.g., foot location) and represents the midplane of the sheet metal when referring to a cell wall.

Fuel Models

All fuel bundles in a rack are assumed to move in unison and are represented by a single massive bundle having the same natural frequencies as a single bundle. This assumption causes all bundles to impact simultaneously, conservatively maximizing the potential for the racks to tip and slide.

The fuel is represented by a single multi-element beam in each rack having the mass and stiffness properties of the total number and placement of fuel bundles in the rack. The fuel is free to rattle about in the rack. It is supported at its bottom with a sliding/gap element so that sliding, with friction, and lift-off is possible. The coefficient of friction is taken as the same as between the rack and pool liner since, in all cases, the mating surfaces are of the same materials. In the vertical direction, a fluid coupling element accounts for the buoyancy force on the fuel and the vertical water mass on the rack.

The fuel bundle used for the Region II analyses is an equivalent bundle modeled to envelope the existing conventional and consolidated fuel bundles, as well as possible future bundles. Detailed modeling is based on the geometry of the existing consolidated bundle with the mass of an assumed "double-weight" fuel.

The fuel bundle is modeled using ANSYS® STIF4 elastic beam and STIF21 generalized mass elements. Based on the fuel bundle and rack geometries, it is anticipated that the upper portion of the fuel assembly will impact the cell walls most frequently, and the upper portion of the bundle is modeled with more detail. The lower portion of the bundle is considered less critical, and a more generalized model is used.

The fuel is laterally coupled to the fuel racks with gap elements and fluid coupling elements at eight elevations for the single rack models, and at two elevations for the multiple rack model. The four gap elements (±X and ±Z directions) at each elevation have the prescribed upper bound gap, an impact stiffness, and impact damping. The actual locations for fuel bundle contact with the rack cell walls is more distributed than used in the analysis, so the impact properties are ratioed accordingly. When closed, the gap elements have a stiffness representing the lateral stiffness of the spacer grids connecting the rods in the fuel bundle plus the local stiffness of the storage cell wall. The gap is the largest possible, representing unbowed fuel.

The fluid coupling element at each elevation provides buoyancy for lateral accelerations in both horizontal directions and also includes a coefficient that accounts for the enhanced local kinetic energy of the fluid which, for continuity, must pass between the fuel bundle rods much more rapidly than the bundle moves across the cell. This is based on the theory as presented by R. J. Fritz (Ref. 3-2) and is implemented by the ANSYS® STIF38 fluid coupling element. These elements also contain the mass of the undisplaced fluid in the cells in the coordinate directions for which they are active.

For rack modules assumed to contain eccentric fuel loadings, the beam model representing the fuel is located at the center of gravity of the distribution of fuel and water. Stiff beam elements connect these locations back to the centerline of the rack. In the multiple rack analysis, another set of stiff beams extends in the opposite direction from the centerline and supports mass elements representing the water in the unoccupied cells. These masses are only effective in the horizontal directions.

For rack rotation about a vertical axis, the multi-cellular structure imparts a similar motion to the entrained water. This inertia is added as lumped rotary masses at the centerline of the rack. For the partially filled rack modules, the value of this mass is adjusted to account for the rotary inertia inherent in the offset water masses.

The structural characteristics of the existing consolidated fuel bundle are used in the Region II rack modules. The fuel model density is conservatively enhanced to give a fuel bundle weight of 2600 lb, the upper limit considered for fuel consolidation. Fuel loading in the Region I rack modules is based on conventional fuel, with a stored CEA. Region I racks are also evaluated for a nominal single consolidated fuel assembly.

In all cases, the fuel is assumed to be preferentially centered within the fuel storage cell as an initial condition. Low stiffness dummy elements are utilized in the models to maintain this geometry in stable static equilibrium. This preferred orientation maximizes the impact loads of the fuel within the rack as all fuel is taken as vibrating coherently: fuel impact with the rack thus represents all stored bundles impacting simultaneously in the same direction. In reality, fuel position within each individual storage location is apt to be randomly distributed across a rack module. From this initial condition, the population of stored fuel will actually tend to behave chaotically rather than coherently when subjected to the statistically independent three directions of seismic time-history input.

Damping

There are several types of damping in the dynamic response of a nonlinear structure such as a high-density fuel storage rack: structural damping, fluid damping, and impact damping.

Structural damping values used for the seismic analysis of the fuel rack module are 2% for operating basis earthquake (OBE) and 4% for design basis earthquake

(DBE). These values are in accordance with RG 1.61 for welded steel structures and Maine Yankee licensing commitments.

Beta (i.e., stiffness) damping is assigned to the structural elements. A value of 4% in the range of 18 to 33Hz is assigned to the models for the DBE and 2% for the OBE. As Beta damping is frequency dependent, this conservatively results in negligible damping at the low frequencies that are dominant for the submerged rack modules.

Fluid damping was conservatively ignored in these analyses.

Impact damping is caused by the small amount of local plastic deformation which takes place in an impact. The two types of locations in the rack array that have impact are the fuel grid to storage cell wall, and the rack support foot to liner floor. The interface between the fuel and its vertical support does not exhibit any impact behavior as the fuel never loses vertical contact with the rack (see Section 3.4). Impact damping is conservatively ignored at the interface of the rack support foot and the liner floor. A 10% damping is taken for fuel impacts with the storage cell walls to account for the Coulomb (friction) losses exhibited by the flexing of fuel spacer grids, and the resultant flexing and sliding of the fuel rods through the grids.

Fluid Coupling

The effect of water on the dynamic response of a submerged structure is significant and is included in the modeling. Effects include the mass of entrained fluid (which is forced to participate in any motion), buoyancy effects, and hydrodynamic mass. The latter term occurs in confined regions where water must be squeezed through relatively narrow regions at high accelerations to permit the relative motion of two adjacent bodies. This causes the bodies to be coupled.

The hydrodynamic mass between the fuel assembly and the cell walls is based on the fuel rod array size and cell dimensions using the technique of potential flow and kinetic energy. Due to the open structure of the fuel bundle, the flow occurs through the bundle between the individual rods. In a similar manner, the hydrodynamic mass between the rack and pool wall is computed assuming that, as the gap closes, fluid flows out equally into the fluid volumes above and below the racks.

The racks are coupled to each other and to the pool by fluid coupling elements of the same type used to couple the fuel to the racks. The values are adjusted to account for the actual water mass and squeeze film masses in the pool. Although not inherent in the theory of Fritz, the ANSYS® implementation of the fluid coupling element has two directions of action which, while applicable for single bodies immersed in a fluid-filled container such as a fuel bundle in a cell, is not suitable when many bodies are immersed or where three directions are involved. Therefore, for the multiple rack analysis, the ANSYS® STIF38 element is treated as a 1-D element by coupling one degree of freedom to the desired structural nodes and coupling the other direction to a grounded node.[2] At each location, a separate element is required for each coordinate direction. The STIF38 elements have the following properties:

M_1 The mass of the water displaced by the introduction of a solid object. This provides a buoyancy force on the submerged object.

M_2 The mass of water within an outer enclosure before the introduction of a solid object.

M_H The squeeze film coefficient. This is a mass multiplier based on the principal that, as two submerged objects are brought together, the water must flow out of the space between them. If the cross section of the flow path is small, the resulting fluid velocity may be much greater than the velocity of the solid objects, resulting in a high kinetic energy and effective mass.

[2]For the single rack models, the lateral STIF38 fluid coupling elements are employed as 2 degrees of freedom elements, and the vertical coupling as a 1 degree of freedom element.

Fluid coupling coefficients depend on the shape of the two bodies, their relative displacement, etc. Fritz gives data for M_H for various body shapes and arrangements, as well as the theory required to compute this value for any geometry. It is noted that the force caused by this mass depends only on the relative accelerations of the two bodies and the fluid. This force is a strong function of the interbody gap, reaching large values for very small gaps. This inertial coupling is called fluid coupling. It has an important effect in rack dynamics. The motion of the rack as well as the lateral motion of a fuel assembly inside the storage location encounters this effect.

Fluid coupling elements have fixed values computed at the nominal rack separations. In reality, the hydrodynamic squeeze film coefficient increases as two racks come closer together. The effect of assuming constant gaps is conservative as the analysis shows racks coming closer together than may happen in reality. (Note: Since fluid flows around rods in a fuel bundle rather than being forced around a bluff body, this is not a limitation for fuel-to-rack coupling.)

All fluid coupling elements external to the racks pass through the rack vertical centerlines and offer no resistance to rotation about this axis. Rack rotations thus predicted by the analysis are conservatively high.

The vertical water mass is not inherently included in the above hydrodynamic elements and is included as separate lumped masses.

The "inner" node of the STIF38 element experiences a buoyancy force, and the "outer" node experiences a force proportional to the enclosed water mass, assuming no displacement by an enclosed object. Both nodes experience an additional equal and opposite reaction proportional to their relative acceleration. This force depends on the displaced water mass and a "squeeze film coefficient," which may be high if the space between objects is close, and the fluid must move laterally at great acceleration as it is displaced. These coefficients are established using the procedure which Fritz (Ref. 3-2) has presented.

Some submerged objects (the racks) contain water, and the mass of this water is separately included in the analytical model. If there is fuel in the racks, the fluid coupling elements between the rack and fuel provide the mass of the water remaining in the occupied cells. Where there is no fuel (the empty rack and the unoccupied cells), the water mass is represented by lumped masses. In the vertical direction, these masses are located at the bottom plate of the rack, which is where the force is applied if the rack were to be forced up or down. Laterally, these masses are located at two elevations, the quarter and three-quarter points along the height of the rack. The fluid masses are located at the centers of gravity of both the occupied and unoccupied cells. For the horizontal direction, the fluid coupling elements supporting the fuel have a mass, $M_2 - M_1$, accounting for the entrained water. In other cases (e.g., vertical direction or cells without fuel), this water mass is incorporated as a lumped mass. The difference between this mass and M_1 for the rack must equal the mass of the water actually displaced by the solid portions of the rack in order to obtain the correct buoyancy force.

Rack-to-rack and rack-to-pool fluid coupling is provided in all three directions and is also implemented with ANSYS® STIF38 fluid coupling elements. Special precautions are taken to separate the properties for each coordinate direction since the ANSYS® implementation of the Fritz method simultaneously produces forces in two orthogonal directions. STIF38 elements consider translational mass only, and STIF21 elements are used at the rack vertical beam nodes to account for the rotational mass of entrained water. These elements are given only torsional mass (ROTY), which are calculated based on the mass in each cell and its offset from the rack center.

Friction Coefficient

Since the fuel racks are free standing, the frictional resistance in the interface between the support feet and the pool floor is the only horizontal constraint. Thus, the value of friction coefficient must be accurately represented in a manner to conservatively calculate the displacements of the fuel rack and its potential for overturning. The response of the high density fuel racks is evaluated for the bounding range of coefficient of friction between 0.2 and 0.8 as suggested by Rabinowicz (Ref. 3-3). These bounding values are recognized as being beyond the 2-σ range defined in the referenced study.

The high friction factor case (μ = 0.8) is evaluated as the case where the rack module is exposed to the maximum amount of inertia of the building motion during a seismic event. This results in the largest loads imposed on the rack, including fuel impacts. The greater propensity for the rack feet to "stick" rather than slide maximizes the potential for rack tipping behavior and, consequently, for rotational displacements: rack tipping allows for pivoting about a single foot as the building structure displaces under the rack.

The low friction factor case (μ = 0.2) is evaluated as the case leading to maximum lateral displacements of a rack module, maximizing the potential of interactions with adjacent structures.

Both friction factor cases are evaluated and accounted for in the assessment of adequacy of the array of rack modules. Assessment of an intermediate or nominal friction factor represents a non-governing case, and is not addressed further.

Model Verification

The validity of the analytical models is verified in a series of preliminary analyses. First, the model geometry is verified, including connectivity and assignment of various parameters (element type, material, member properties, etc.).

Three static analyses are performed: 1) The model is stripped of the water and fuel and a deadweight analysis performed to assure that the support reactions are uniform and represent the weight of the racks in air; 2) Only the water elements are removed from the model, and another deadweight analysis is performed to ensure that the support reactions for each rack increase by the weight of the fuel, and are non-uniform in the racks with eccentrically placed fuel; and 3) The complete model is subjected to deadweight to verify that the support reactions decrease by the buoyant force. Static analyses of the complete model are also performed to verify that the fluid buoyancy terms are properly modeled in the lateral directions.

Modal analyses are performed for each of the models subjected to static analysis to review rack vibration modes (in air) and for overall behavior of the complete model.

The nonlinear analysis is performed by integration of the solution in discrete time steps. Due to the large number of iterations required, several iterations of the first second of response are performed with varying time steps to establish the longest time step producing a valid result.

Time History Analysis

The seismic analysis of the high density fuel storage racks is done by a 3-D nonlinear finite element time history analysis, inputting three simultaneous orthogonal displacement time histories to the rack model. The analysis was done using the ANSYS® finite element analysis code, which is a general purpose finite element code previously reviewed and approved by the NRC for structural dynamic application.

The analysis involves tracking the forces and motions in the system through approximately 20,000 time steps for the single rack models, and 33,000 time steps for the multiple rack model. At each iteration, the status of the nonlinear elements is checked for state changes (gaps opening/closing or surfaces slipping). If changes are occurring, the stiffness matrix is changed and another iteration is performed for the same point in time. These iterations are repeated until the state of the system converges. Then the solution proceeds to the next time point. An appropriate time step has been established for the single rack and the multiple rack models by performing multiple analyses of the initial seconds of the time-history record with varying time intervals to determine the time interval at which further reduction causes no significant change in calculated response.

3.2.5 Bounding Analysis Cases

The nonlinear models are analyzed for combinations of the following bounding cases:

- Seismic
  - Design Basis Earthquake
  - Operating Basis Earthquake
- Coefficient of Friction
  - $\mu = 0.2$
  - $\mu = 0.8$
- Rack Fill
  - Empty
  - Full
  - Fuel biased to one side, up to one-half full
  - Full to one side of diagonal
- Rack Size
  - Largest
  - Narrowest

The justification for the cases selected for analysis are as follows:

- The two seismic intensities must be evaluated to comply with SRP 3.8.4 and each has its own allowable stresses.

- The range in coefficient of friction is typically taken as bounding in fuel rack dynamic analysis for submerged stainless steel contact.

- The range of fuel loading in the rack is sufficient to cover the full range of weight (empty-to-full) as well as eccentric cases to maximize the potential for rotation and tipping.

- The range of rack size is intended to examine the heaviest rack and the one most likely to tip.

- Region I and Region II rack configurations have similar stiffness and fundamental frequency characteristics. As evidenced by the results obtained from the analysis, both configurations respond to seismic loading in a similar manner for similar fuel loading conditions.

- The cases are the conditions of maximum displacements (absolute and relative) and loads so that the limiting conditions are evaluated.

The results from these analyses include the fuel-to-cell impact loads, support foot loads, fuel rack structure internal loads and moments, rack displacements (support foot lift-off, fuel rack sliding), rack structural displacements, and fluid coupling loadings.

Since the seismic analysis is also conducted on a multiple rack model, the relative rack-to-rack displacements between racks at both the bottom and top of the racks as well as the absolute displacements at the bottom and top of the racks are obtained. The values of these results are the maximum values for the 20-second duration seismic event. This duration includes all of the limiting loads and displacements.

The maximum values of the loads and moments are used in the stress analysis of the rack structure, and the displacement results are used to show that separation margin against impact with an adjacent rack, or the pool wall, remains and that there is margin against overturning.

The following conservatisms are inherent in the analyses:

- Fluid damping is ignored.
- Friction coefficients of 0.2 minimum and 0.8 maximum are utilized.
- Hydrodynamic mass is based on constant gaps. In actuality, as the gap decreases, the hydrodynamic mass restoring force increases.
- Gaps between fuel and cell are maximized and produce the maximum impact forces.
- There is no rotational resistance from fluid coupling elements.

3.3 ACCEPTANCE CRITERIA

Acceptance criteria for the Maine Yankee high density spent fuel storage racks are as stated in SRP 3.8.4, Appendix D, for the Load Combination Method. The acceptance limits are based on ASME III Subsection NF, Class 3 limits for Service Levels A, B, and D; and functional capability of the fuel rack for load combinations including impact forces due to accidental load drops.

The structural elements which comprise the high-density spent fuel storage racks are Plate- and Shell-Type, as defined in paragraph NF-1212, and the allowable stress criteria of paragraph NF-3260, Table NF-3552(b)-1 and Appendix F of ASME III are applicable. The Level A and Level B allowable stresses for Class 3 Plate- and Shell-Type component supports designed by analysis are maximum normal (principal) stresses, as identified in paragraph NF-3250. In accordance with paragraph NF-3251.1, the basic allowables are:

primary membrane	$\sigma_1 \leq 1.0\ S$
membrane + bending	$\sigma_1 + \sigma_2 \leq 1.5\ S$
primary shear	$\tau_1 \leq 0.6\ S$

where S = allowable stress

Level D limits for design by analysis are based on primary stress intensities, as identified in paragraph F-1320. Stresses due to constraint of free end displacements or anchor point motions are conservatively considered as primary stresses. Peak stresses and thermal expansion stresses are secondary (self relieving), and not assessed for Level D limits. For elastic system analyses, these basic acceptance criteria as set forth in paragraph F-1332 are as follows:

primary membrane	$0.7\ S_u \geq P_m \leq 1.2\ S_y$ or $1.5\ S_m$
membrane + bending	$(P_m + P_b) \leq 1.5\ P_m$ limit
pure shear	$T \leq 0.42\ S_u$

Table NF-3552(b)-1 provides stress limit factors which are applied to the basic allowables of paragraph NF-3251.1. For Level A, the factor is K=1.0 for primary membrane, membrane plus bending , and shear allowables. For Level B, the factor is K=1.33 for primary membrane, membrane plus bending, and shear, with the further limitation of $\tau_1 \leq 0.42\ S_u$. No stress limit factors are applicable to Level D allowables.

In all cases, compressive stresses (membrane plus bending) are limited to one-half of the calculated critical buckling stress, with no factored increase.

Per Table NF-2121(a)-1, the appropriate material allowable and material property tables for A240 Type 304L are as listed in ASME III, Appendix A, Tables I.1-2, I.2-2, and I.7-2:

		100F	200F	300F
S	Allowable Stress	15.7 Ksi	15.7 Ksi	15.3 Ksi
S_m	Stress Intensity	16.7 Ksi	16.7 Ksi	16.7 Ksi
S_y	Yield Strength	25.0 Ksi	21.3 Ksi	19.1 Ksi
S_u	Tensile Strength	70.0 Ksi	66.2 Ksi	60.9 Ksi
E	Young's Modulus	28.3 E6 psi	27.6 E6 psi	27.0 E6 psi

The weld joint allowables of Subsection NF cannot be applied to the corner weld joint detail connecting the fuel storage cells in the Region II rack modules as it is not an ASME III recognized joint configuration for use in component supports. The design allowables for this weld configuration have therefore been established based on test results. The test results (Ref. 3-4) establish that the weld deposit is stronger than the specified minimum physical characteristics of the base metal, and the design allowables for the weld metal are conservatively set as equal to that of the parent metal.

The applicable stress limits for Level A, Level B, and Level D are listed in Table 3-4.

3.4 RESULTS

Results of the single rack dynamic analyses for the bounding case combinations identified in Section 3.2.3 produce the following conclusions. Representative plots of the conditions identified are provided in the figures:

- Uplift occurs at individual rack feet, but gross rack uplift never occurs. For the E' condition, Figures 3-18 and 3-19 depict the vertical reaction load for a Region I and Region II rack, respectively. Figures 3-20, 3-21, and 3-22 depict the X, Y, and Z reaction loads for an individual Region I support foot under E' conditions. It can be seen that, as the FY reaction goes to zero, so do the lateral reactions, at times reversing direction as the foot impacts back onto the liner floor.

- Stored fuel never lifts off of the storage cell support surface. Figures 3-23 and 3-24 depict the total fuel vertical reaction load in a fully loaded Region I and Region II rack, respectively, for the E' condition. It can be seen that the reaction loads oscillate about the total fuel weight, never going to a zero magnitude.

- Maximum uplift, and/or slip of an individual support foot occurs in a fully loaded rack, with the maximum friction coefficient condition. Figures 3-25 and 3-26 depict the magnitude of uplift and slip, respectively, for a single support foot on a fully loaded Region I rack for the E' condition with high friction factor. Figures 3-27 and 3-28 depict the same parameters, respectively, for a fully loaded Region II rack for the E' condition with high friction. It can be seen that total uplifts are on the order of small fractions of an inch, and are very short duration. Similarly, slip is limited to increments of small fractions of an inch, with a general trend in one direction.

- For the (D + L + E') loading condition, maximum support foot reactions occur in a fully loaded rack, with the maximum friction coefficient condition.

- For the (D + L + E) loading condition, maximum support foot reactions occur in a fully loaded rack, but at varying friction coefficient conditions.

- Fuel impact with the fuel storage cell walls is maximized by the high mass condition of a fully loaded rack, but does not vary by large factors, on a per cell basis, for the extremes of friction coefficients evaluated. Figure 3-29 depicts the motion of the fuel within a Region II rack storage cell for the E' condition as a function of the gap size to one wall of the cell. It can be seen that the fuel has an initial condition of being centered within the cell (≈ 0.3 in. gap) and oscillates within the confines of the cell, with the gap going from ≈0 to ≈0.6 in. Positions less than zero and at ≈0.61 in. indicate compression of the model impact spring elements on contact. Figure 3-30 depicts the durations and magnitude of the impacts on the cell walls. This represents the total fuel impact force for a full rack which, due to the conservatisms inherent in the analysis and the model, assumes totally coherent behavior of the stored fuel and simultaneous contact by all of the fuel.

- Free surface effects (pool slosh) are not a factor in the response of the Maine Yankee high density racks due to the depth of the installed array in the fuel pool.

The single rack analyses also confirm that, for rack separations on the order of that proposed for the Maine Yankee application, hydrodynamic coupling affects overall rack response. Figures 3-31, 3-32, and 3-33 depict the two lateral and the rotational displacements of a fully loaded Region II rack for the E' condition with $\mu = 0.8$, based on the nominal rack-to-rack gap within the installed pool array. Figures 3-34, 3-35, and 3-36 provide these parameters for the rack assuming that it is far removed from any adjacent structure (vertical hydrodynamic mass only; zero lateral hydrodynamic coupling terms). This latter case essentially treats the rack module as if it were submerged in an infinitely large pool, and represents a bounding rack displacement case for the scenario of a fully loaded rack surrounded by empty racks.

Table 3-3 lists the maximum reactions, forces, moments, and displacements for the single rack analyses for Region I and Region II racks.

The section of the Maine Yankee spent fuel pool analyzed for the interactions of a multiple rack array represents the whole pool installed array as it addresses the range of conditions found within the pool:

- The analysis is a full 3-D dynamic analysis utilizing the time history records for the SSE condition. Forces in out-of-plane directions contribute to rack rotation, slip and tipping.

- The analysis evaluates rack response at the upper and lower bound friction coefficients of $\mu = 0.2$ and $\mu = 0.8$.

- Multiple racks (four) are represented, each of a separate size, and arranged with respect to each other as they will be upon installation in the pool.

- Wide variations in percentage of occupied fuel storage locations and distribution of the fuel within the rack are provided for: the heaviest rack is considered full;

the lightest rack is empty; an intermediate rack is considered 20% full with all of the fuel concentrated at the end of the rack adjacent to the fuel cask laydown area to maximize the potential for rotation and tipping towards the open space; and, on the premise that a light rack is more likely to be jostled around in an earthquake when the adjacent rack is full, the remaining rack is eccentrically loaded with 10 fuel assemblies in one corner, maximizing the chance for rack rotation about the vertical axis.

- The full range of fluid separation gaps between racks, and rack to pool wall is represented from the nominal spacing between racks to the ≈ 10 ft gap across the cask loading pit.

- All fuel is taken as vibrating in phase within a rack to maximize effects due to fuel motion.

Results of the multiple rack dynamic analyses described in Section 3.2.3 produce the following conclusions, supportive of the conclusions drawn from the single rack dynamic analyses.

- The fuel rack modules behave essentially as rigid bodies.

- Uplift occurs at individual rack feet, but gross rack uplift never occurs. Maximum uplift occurs for the high friction coefficient cases, with the largest calculated uplift being less than 1/16 in.

- The bottom of the fuel rarely slides on the rack bottom plate, and the maximum slip is small. Stored fuel never lifts off the storage cell support surface.

- For loading cases where fuel is eccentrically placed in a rack, slipping of the rack support feet on the liner floor leads to rack rotation about its vertical axis. Evenly filled racks have little tendency to rotate. Although the hydrodynamic coupling elements are conservatively modeled so they do not resist rotational motion of the rack modules, total rotations are small, on the order of fractions of a degree.

- Slipping occurs with both low (μ = 0.2) and high (μ = 0.8) coefficients of friction. While time histories of the rack motions for these two extremes differ, the total slip motion is not necessarily greater for the lower friction condition.

- Rack motions due to sliding occur in numerous small increments. The total motion is small (less than 1/2 in.).

- Rack modules in close proximity tend to slide coherently, even if their fuel loadings are very different. Relative motions between closely spaced rack modules accumulate slowly as the integrated effect of slightly different amounts of slipping on the pool liner.

- Closely spaced rack modules tip in-phase due to fluid coupling, even if they have greatly differing masses due to differences in percentage of occupied storage locations. A large water gap between groups of rack modules permits each group to move independently of the other.

Therefore, adjacent rack modules do vibrate coherently due to the hydrodynamic coupling terms. Even the eccentricities biased into the models to foster out-of-phase behavior do not overcome this effect. Thus, within the installed rack array, rack modules tend to vibrate coherently, lessening the tendency for adjacent racks to impact. This is further enhanced by the single rack analysis results which show that maximum sliding and tipping displacements tend to be on the order of fractions of the installed gaps between racks.

Figures 3-37 and 3-38 depict the centerline motions of rack modules A, B, C, and D. It is seen that modules A and B, and C and D, respectively, are coupled together throughout the earthquake duration. Also plotted on the figures is the relative displacement for each of the sets of coupled racks. Again, it is seen that the racks never close the initial separation gaps between them, and that relative displacements are small.

It is concluded from the results of the single rack and multiple rack analyses that the Maine Yankee high-density spent fuel racks do not impact each other or the fuel pool walls during either the E or the E' seismic event. This applies for fuel loading conditions ranging from empty to full, including intermediate eccentric configurations. Additionally, total rack displacements within the pool are such that interactions with installed pool structures and areas reserved for operations other than fuel storage will not occur.

In reality, however, it is not considered possible to unequivocally conclude that there will be no impact between adjacent racks within the installed array during a design basis earthquake. The effects of slight variations in the as-installed locations and orientations of rack modules, coupled with their as-built geometries, are too complex to support that conclusion for the 1/2-in. initial gaps between racks. This is especially so for the Region I racks, which have less hydrodynamic coupling to their surroundings than the Region

II racks, and would possibly interact with each other (specifically rack modules AA, BB, and CC in a north-south direction) during an SSE. What interaction might occur, however, cannot be considered significant with respect to the intended function of the storage racks: the analyses demonstrate that adjacent racks never vibrate out of phase with each other, obviating the scenario of "head-on" impact in favor of oblique contact between surfaces generally moving in the same direction. Low energy transfers would be expected in such instances, with affected areas being highly localized. Structural integrity of the rack modules would be maintained, and general distortions of the dimensions of the storage array will not occur.

Table 3-5 presents a summary of the results of the stress analyses for the load combinations specified in Table 3-1. The maximum stress values are reported for a particular rack element, and the P_m, P_m+P_b, and T values are not necessarily concurrent at any one location within the rack structure. Only acceptance limits for Level A and Level D are tabulated, as the Level B limits are not governing. (Load combinations containing E for Level A and Level B Service Limits differ only in the thermal effects term. Therefore, in an assessment of primary stresses, the Level A limits are governing.)

Stress levels for the $(D+L+T_o+E)$ load combination are conservatively reported as stress intensity values, under the assumption, also conservative, of static loading conditions.

The appropriate allowable stress limits for all load conditions are met. Adequate margins against overturning are maintained under seismic loads, E and E'. The functional capability of the fuel racks is maintained under impact loading conditions.

It is concluded that the Maine Yankee high density spent fuel storage racks are adequate for their intended function and purpose.

3.5 REFERENCES

3-1 TID-7024, Nuclear Reactors and Earthquakes, US Atomic Energy Commission.

3-2 R. J. Fritz, "The Effects of Liquids on the Dynamic Motions of Immersed Solids," Transactions of the ASME, Journal of Engineering for Industry, February 1972, pp. 167-173.

3-3 E. Rabinowicz, "Friction Coefficients of Water-Lubricated Stainless Steel for a Spent Fuel Rack Facility," Massachusetts Institute of Technology, November 1976.

3-4 SWEC Maintenance Lab, Test Report MO2-93, "Maine Yankee - Testing of Fuel Rack Weld Joint Configurations."

3-5 USNRC letter to Maine Yankee, March 26, 1987.

MAINE YANKEE ATOMIC POWER COMPANY

TABLE 3-1

LOAD COMBINATIONS AND ACCEPTANCE LIMITS

Load Combination	Acceptance Limit
$D + L$	Level A Service Limits
$D + L + T_o$	
$D + L + T_o + E$	
$D + L + T_a + E$	Level B Service Limits
$D + L + T_o + P_f$	
$D + L + T_a + E'$	Level D Service Limits
$D + L + F_d$	The functional capability of the fuel racks should be demonstrated.

Where:

- D dead load (weight of rack)
- L live load (weight of fuel)
- T_o thermal effects and loads during normal operation or shutdown
- T_a thermal effects associated with the highest temperature abnormal condition
- E load of operating basis earthquake
- E' load of hypothetical earthquake
- P_f upward force caused by postulated stuck fuel assembly
- F_d force of an accidental load drop

TABLE 3-2

FUEL MECHANICAL DESIGN PARAMETERS

Conventional Fuel

Fuel Rod:

0.440 in	Outside Diameter
0.384 in.	Inside Diameter
0.028 in.	Cladding Thickness
0.3765 in.	Pellet Diameter
Zr - 4	Cladding Material
95.25% TD	Pellet Density
10.1072 g/cc	Stack Height Density, UO_2
4.5 $^w/_o$ U^{235}	Maximum Enrichment

CEA Guide Tube:

1.115 in.	Outside Diameter
1.035 in.	Inside Diameter
Zr - 4	Tube Material

Spacer Grid:

Leaf Spring	Grid Type
Zr - 4	Grid Material

TABLE 3-2 (CONT)

FUEL MECHANICAL DESIGN PARAMETERS

Fuel Assembly:

14 X 14	Fuel Rod Array, square
0.580 in.	Fuel Rod Pitch
176	Fuel Rods
5	CEA Guide Tubes
8	Spacer Grids
8.149 X 8.149 in.	Outside Dimensions, cross section
8.49 X 8.49 in.	Maximum envelope cross section
157 in.	Overall Length
1280 lb	Fuel Assembly Weight, dry
217	Fuel Assemblies in Core Load

CEA:

161 in.	Overall Length
80 lb	CEA Weight, dry
85	CEA in Core, total

MAINE YANKEE ATOMIC POWER COMPANY

TABLE 3-3

SINGLE RACK ANALYSES RESULTS

Single Rack Analyses: Maximum Reactions, Forces, Moments, Displacements

	Region I		Region II	
	OBE	DBE	OBE	DBE
Support Foot Reactions (lb):				
Single Foot Fx	5951	9771	8791	29090
Single Foot Fy	46570	24070	58670	92620
Single Foot Fz	17230	6187	7392	30630
Support Foot Displacements (in.):				
Uplift	0.0097	0.044	0.0073	0.0228
Slip	0.0377	0.123	0.0905	0.0129
Fuel Impact/Cell (lb):	488	811	324	594
Rack Internal Forces (lb):				
Total Rack Beam Fx	21540	35300	41710	97790
Total Rack Beam Fy	83320	139700	15860	40690
Total Rack Beam Fz	18710	39040	55350	95260
Rack Internal Moments (in.-K):				
Total Beam Mx	1542	1883	464	9099
Total Beam My	134	525	110	1140
Total Beam Mz	1814	1919	4325	8281

TABLE 3-4

ALLOWABLE STRESS LIMITS

	100° F	200° F	300° F
Service Level A			
Allowable Stress, S	15.7 Ksi	15.7 Ksi	15.3 Ksi
Primary Membrane, $\sigma_1 \leq 1.0S$	15.7 Ksi	15.7 Ksi	15.3 Ksi
Membrane + Bending, $\sigma_1 + \sigma_2 \leq 1.5S$	23.6 Ksi	23.6 Ksi	22.9 Ksi
Primary Shear, $\tau_1 \leq 0.6S$	9.42 Ksi	9.42 Ksi	9.18 Ksi
Service Level B			
Primary Membrane, $\sigma_1 \leq 1.33S$	20.88 Ksi	20.88 Ksi	20.35 Ksi
Membrane + Bending, $\sigma_1 + \sigma_2 \leq 2.0S$	31.32 Ksi	31.32 Ksi	30.52 Ksi
Primary Shear, $\tau_1 \leq 0.798S$	12.52 Ksi	12.52 Ksi	12.21 Ksi
Service Level D			
Primary Membrane, P $0.7S_u \geq P_m \leq 1.2S_y$	30.0 Ksi	25.56 Ksi	22.92 Ksi
Membrane + Bending, $(P_m + P_b) \leq 1.8S_y$	45.0 Ksi	38.34 Ksi	34.38 Ksi
Pure Shear, $T \leq 0.42S_u$	29.4 Ksi	27.8 Ksi	25.57 Ksi

TABLE 3-5

MAXIMUM STRESS RESULTS SUMMARY
HIGH DENSITY SPENT FUEL RACKS[1]

Rack Component	Loading Combination: $D + L + T_o + E$[2]								
	P_m (psi)		P_m Allowable	$P_m + P_b$ (psi)		$P_m + P_b$ (psi) Allowable	Max. Shear		Max. Shear Allowable
	Reg. I	Reg. II		Reg. I	Reg. II		Reg. I	Reg. II	
Support Foot	1823	3848	15700	7649	18800	23600	2697	6029	9420
Cell Base Plate	0	0	15700	21670	20241	23660	320	531	9420
Rack Base Structure	10660	15297	15700	10660	15528	23600	5330	7764	9420
Rack Hydrodynamic Pressure Loads	0	382	15700	14620	18244	23500	7310	9122	9420
Rack Cell	10760	15297	15700	10760	15528	23600	5380	7764	9420
Welds[3]	n/a	n/a	n/a	n/a	n/a	n/a	7570	5940	9420
Buckling	1330	1217	2680	n/a	n/a	n/a	n/a	n/a	n/a

n/a = Not Applicable

[1] Only the maximum stress is reported for any component.

[2] Only Level A acceptance limits are reported, as T_o induced stresses are secondary and are not evaluated in combination with D, L, and E.

[3] Welds in shear only.

TABLE 3-5 (CONT)

MAXIMUM STRESS RESULTS SUMMARY HIGH DENSITY SPENT FUEL RACKS[1]

Rack Component	Loading Combination: D + L + T_a + E'								
	P_m (psi)		P_m Allowable	$P_m + P_b$ (psi)		$P_m + P_b$ (psi) Allowable	Max. Shear		Max. Shear Allowable
	Reg. I	Reg. II		Reg. I	Reg. II		Reg. I	Reg. II	
Support Foot	4032	8671	27600	16257	41000	41400	5281	10449	28500
Cell Base Plate	0	0	27600	37900	27670	41400	560	725	28500
Rack Base Structure	14840	21989	27600	14840	22426	41400	7420	11231	28500
Rack Hydrodynamic Pressure Loads	0	952	27600	27680	31367	41400	13840	22729	28500
Rack Cell	1599	21989	27600	15900	22426	41400	7950	11231	28500
Welds[2]	n/a	n/a	n/a	n/a	n/a	n/a	11450	10260	28500
Buckling	1710	1777	2680	n/a	n/a	n/a	n/a	n/a	n/a

n/a = Not Applicable

[1] Only the maximum stress is reported for any component.

[2] Welds in shear only.

MAINE YANKEE ATOMIC POWER COMPANY

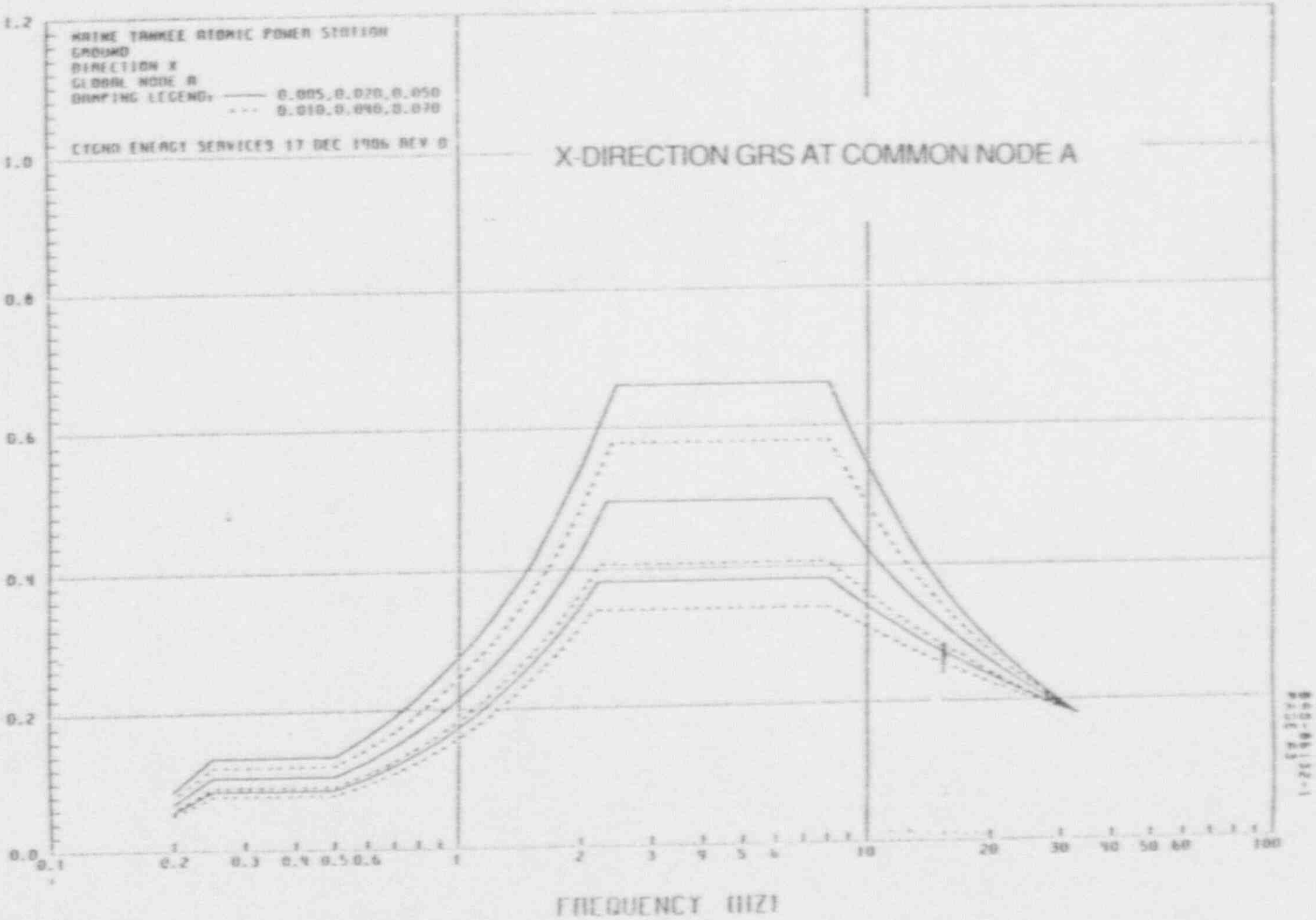

FIGURE 3-1
X AXIS -
GROUND RESPONSE SPECTRA

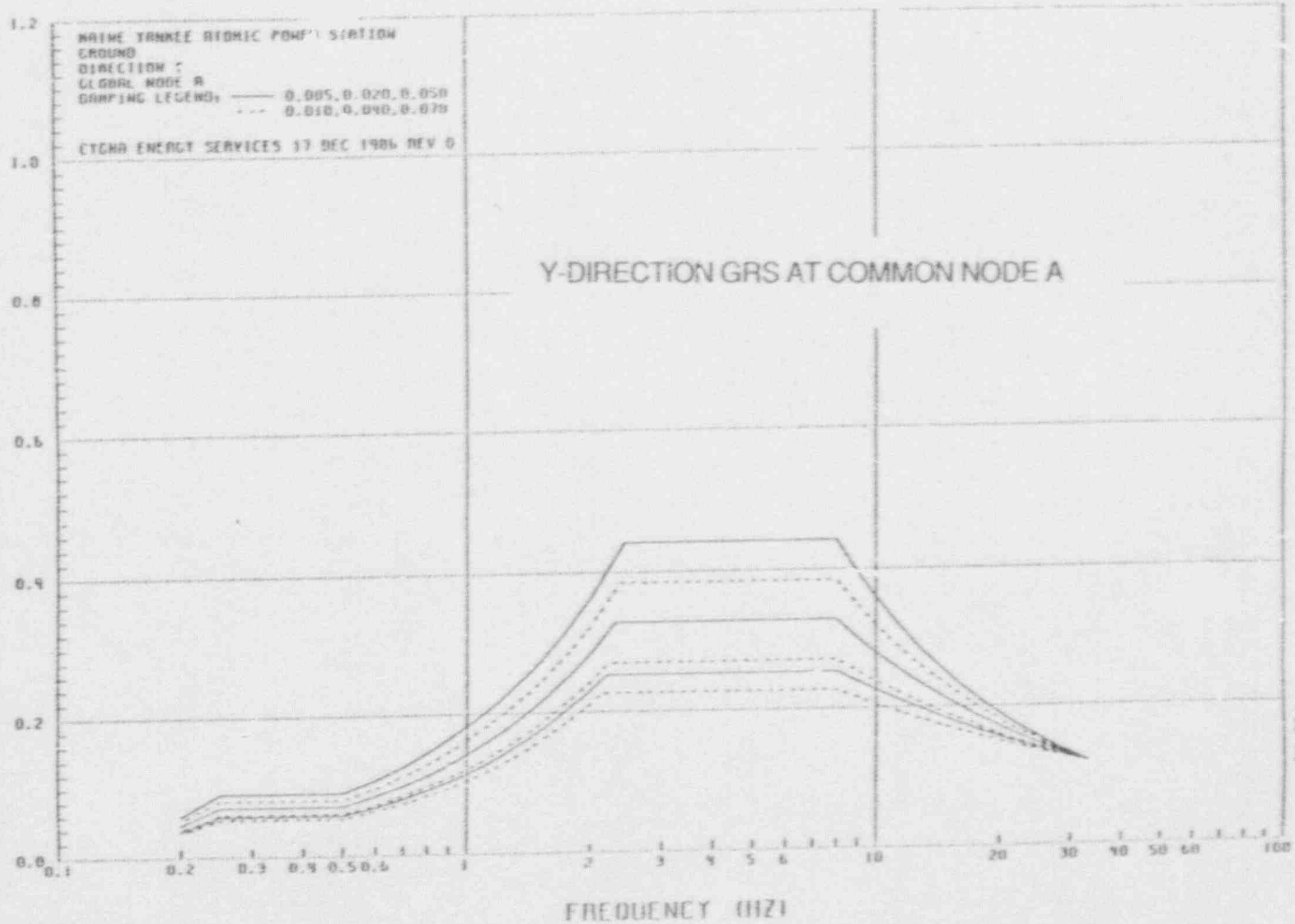

FIGURE 3-2
Y AXIS -
GROUND RESPONSE SPECTRA

MAINE YANKEE ATOMIC POWER COMPANY

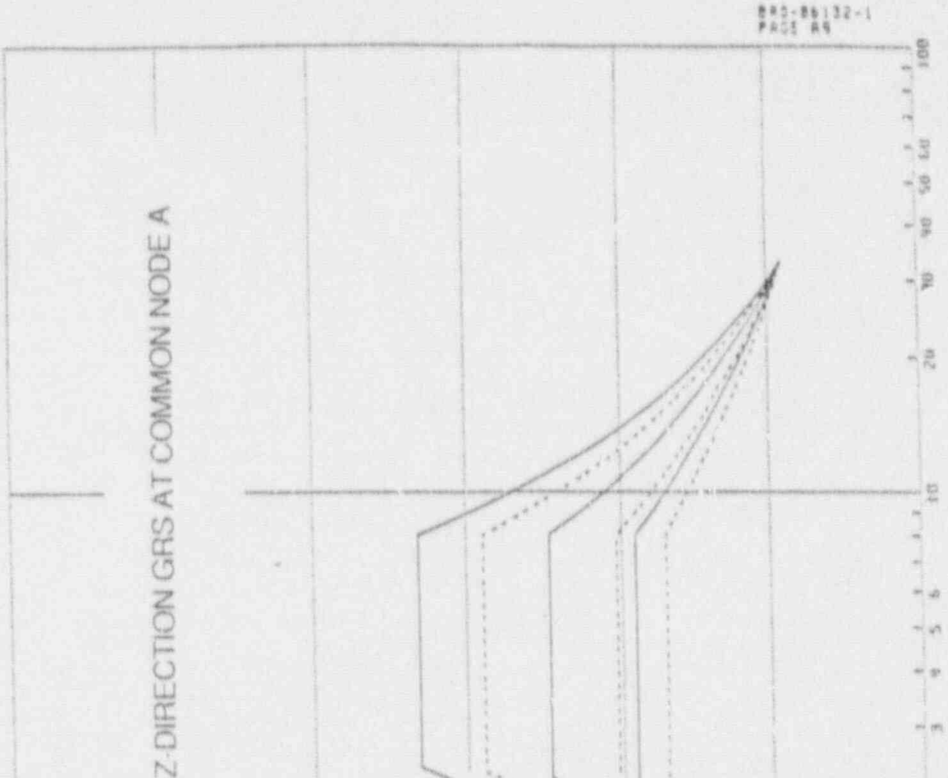

FIGURE 3-3
Z AXIS -
GROUND RESPONSE SPECTRA

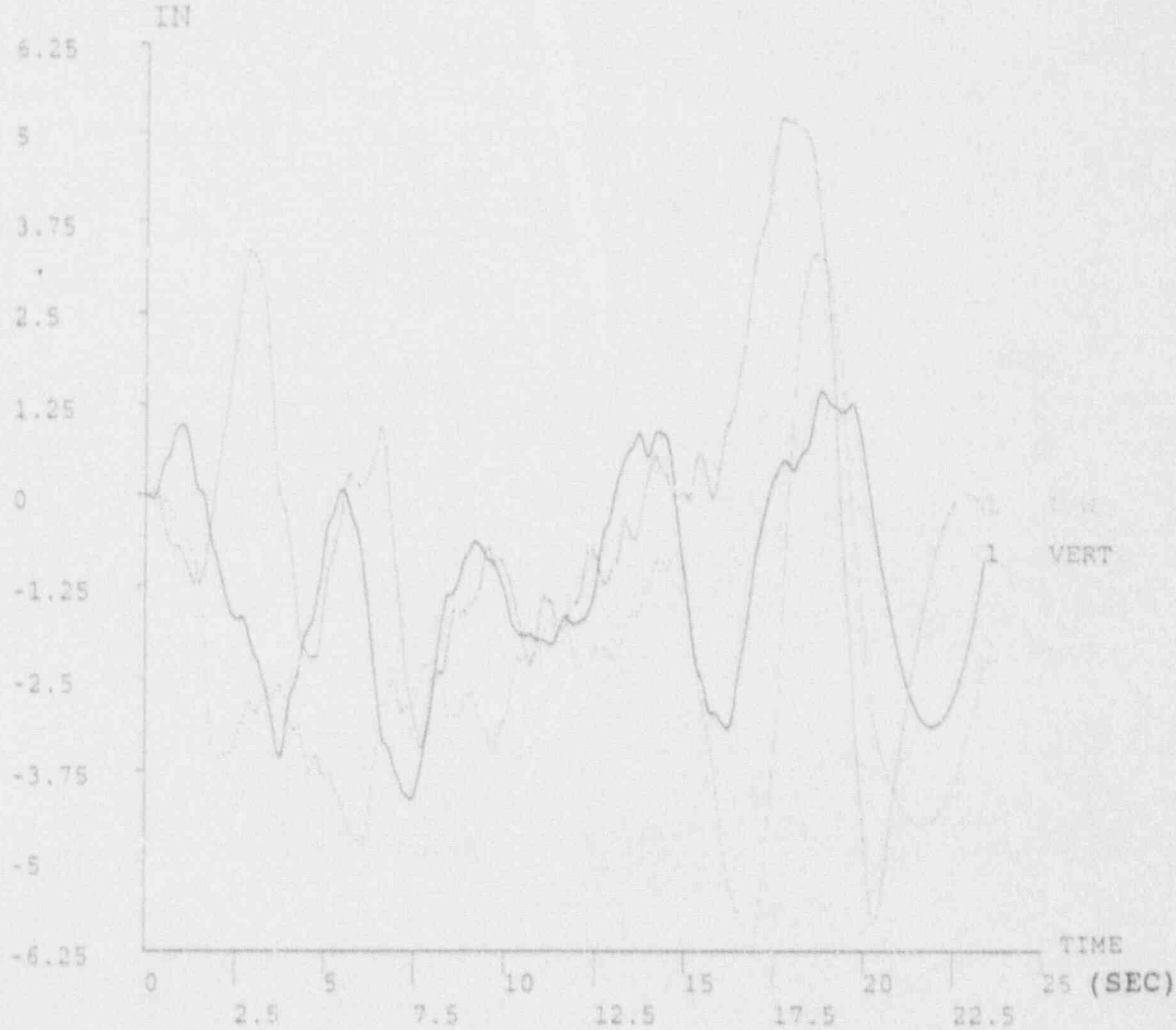

FIGURE 3-4
SSE DISPLACEMENT
TIME HISTORY

MAINE YANKEE ATOMIC POWER COMPANY

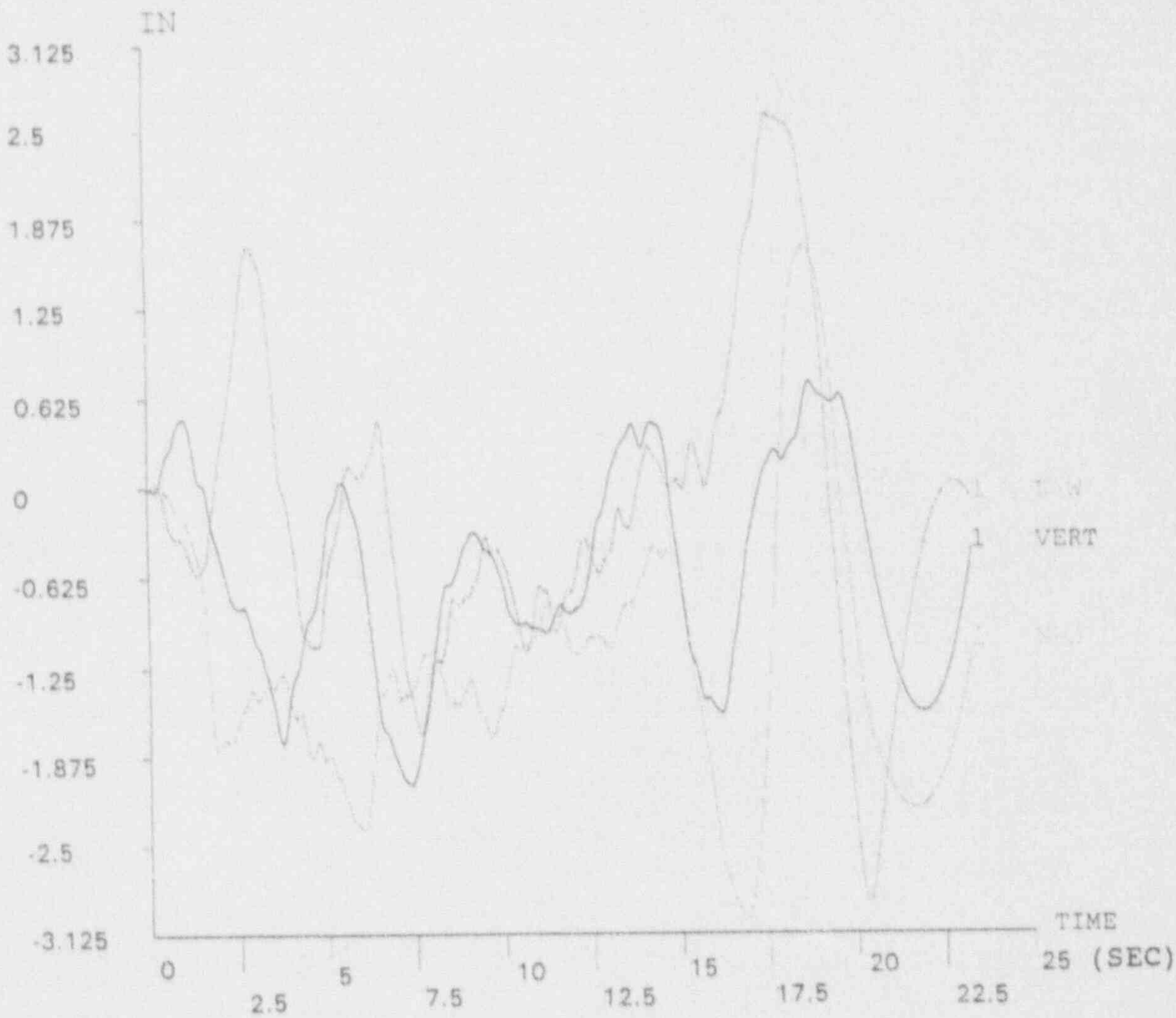

FIGURE 3-5
1/2 SSE DISPLACEMENT
TIME HISTORY

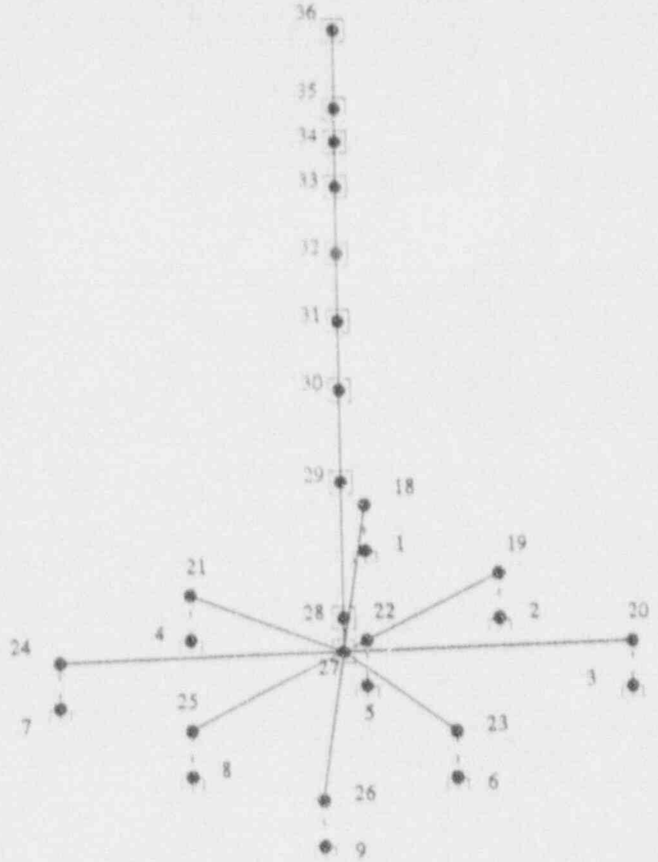

Stick Model - Rack Nodes

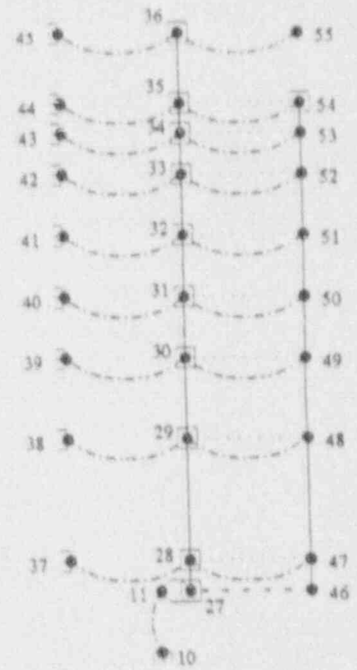

Rack, Fuel & Pool Details

Stick Model

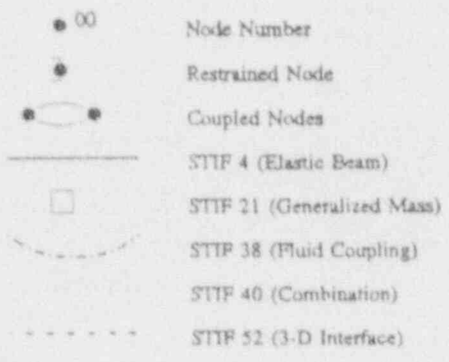

FIGURE 3-6
SINGLE RACK DYNAMIC MODEL

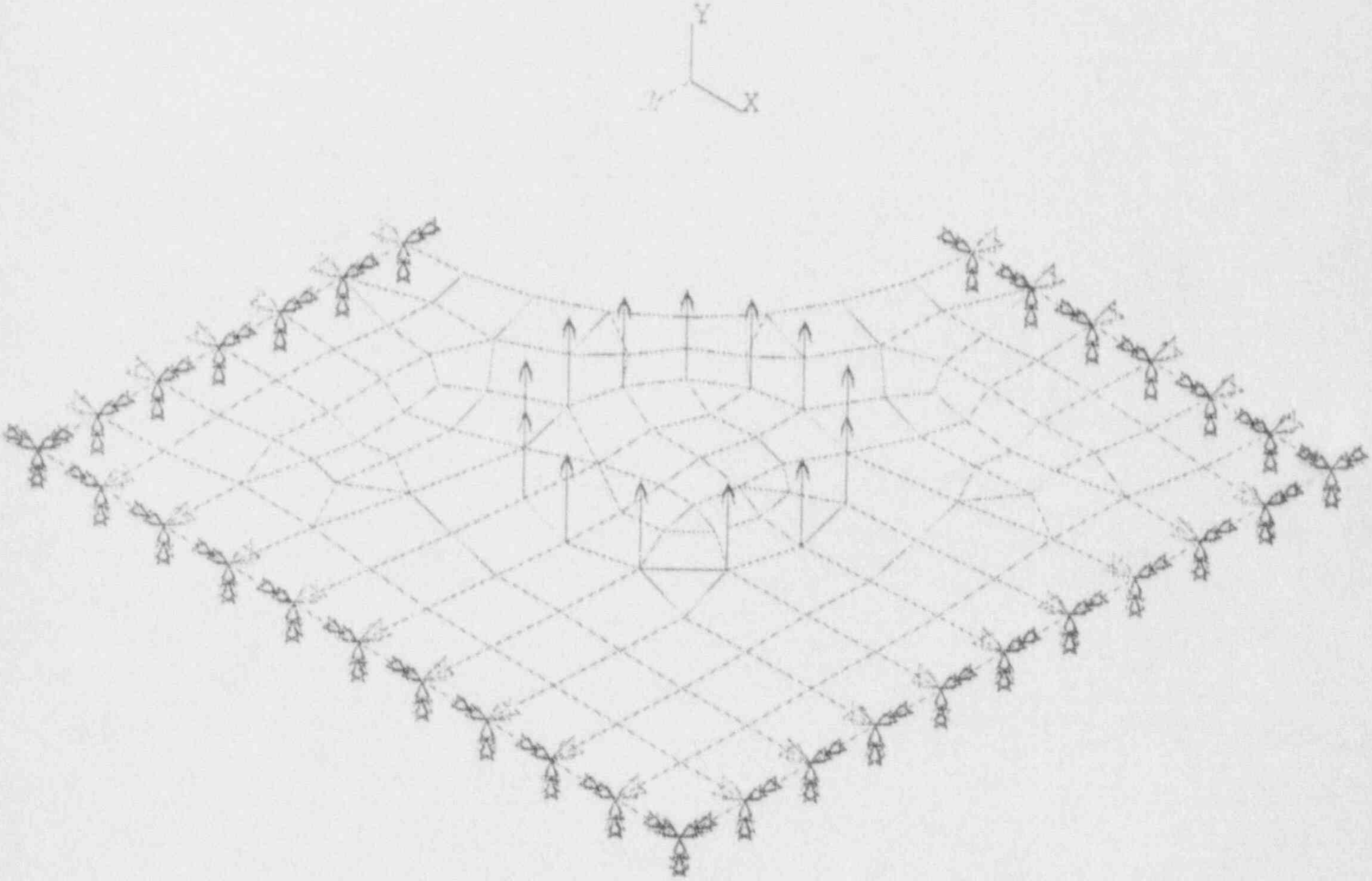

FIGURE 3-7
FUEL STORAGE CELL BASE

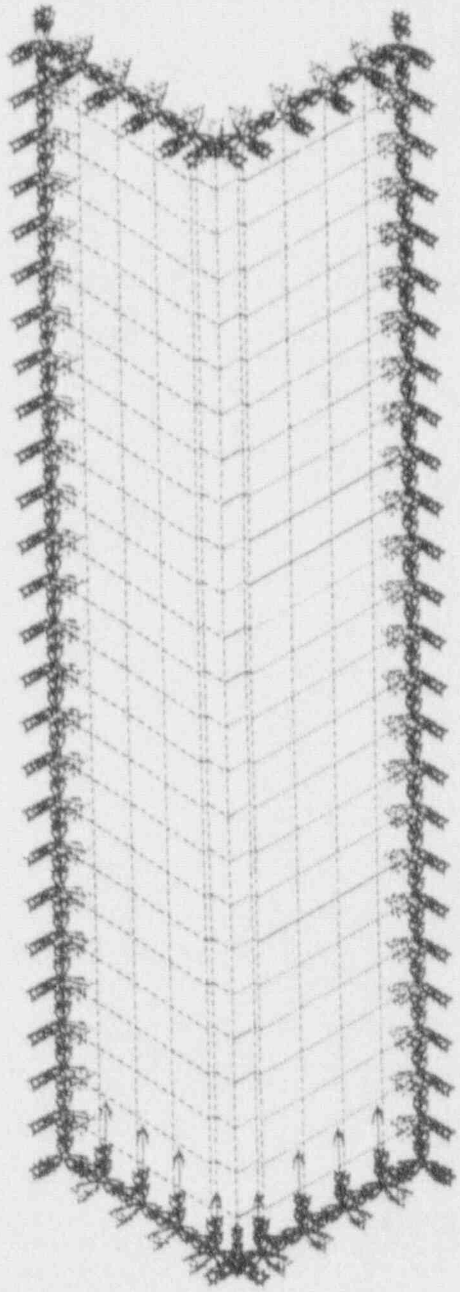

FIGURE 3-8
AXIAL BUCKLING MODEL

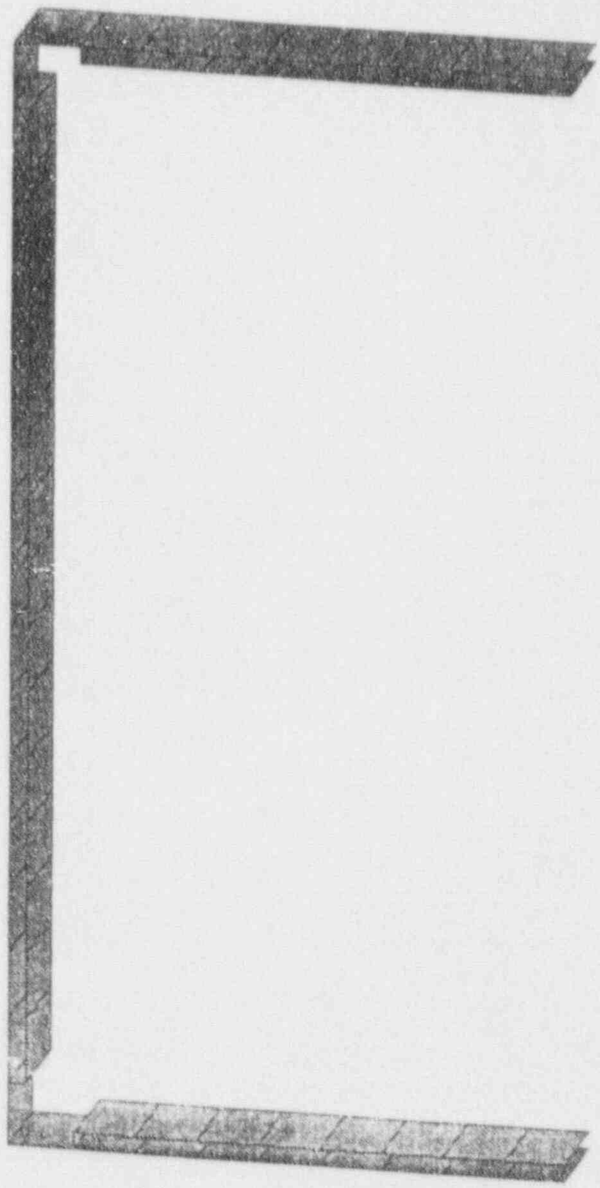

FIGURE 3-9
LATERAL BUCKLING MODEL

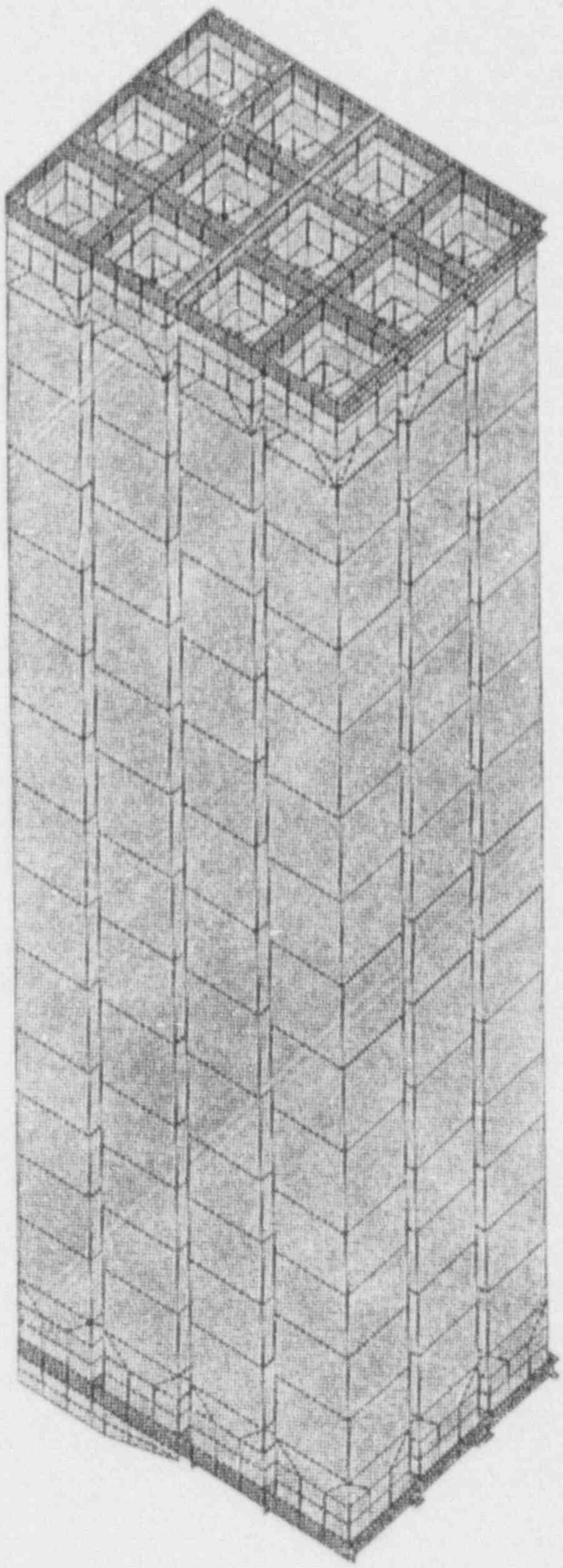

FIGURE 3-10
REGION I SUBASSEMBLY

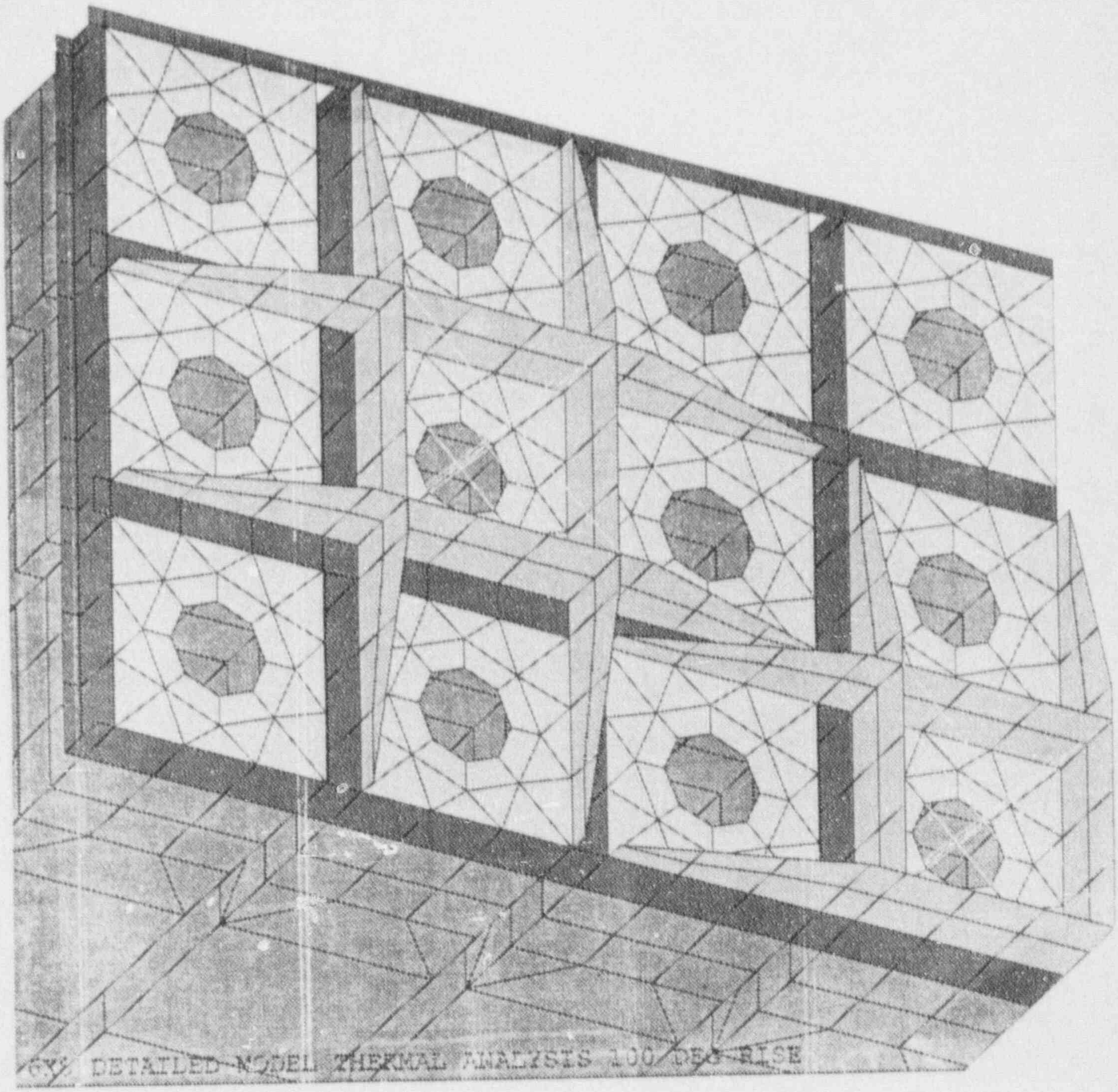

FIGURE 3-11
REGION I SUBASSEMBLY
SUPPORT FOOT

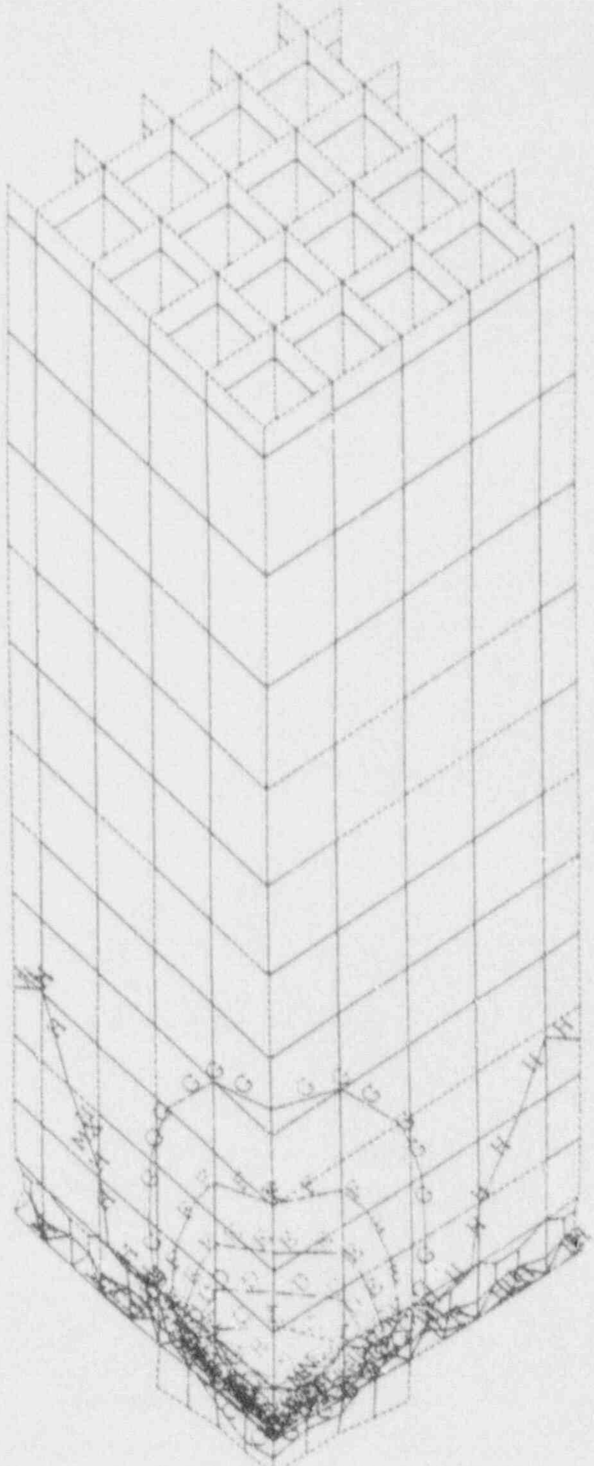

FIGURE 3-12
REGION II SUBASSEMBLY

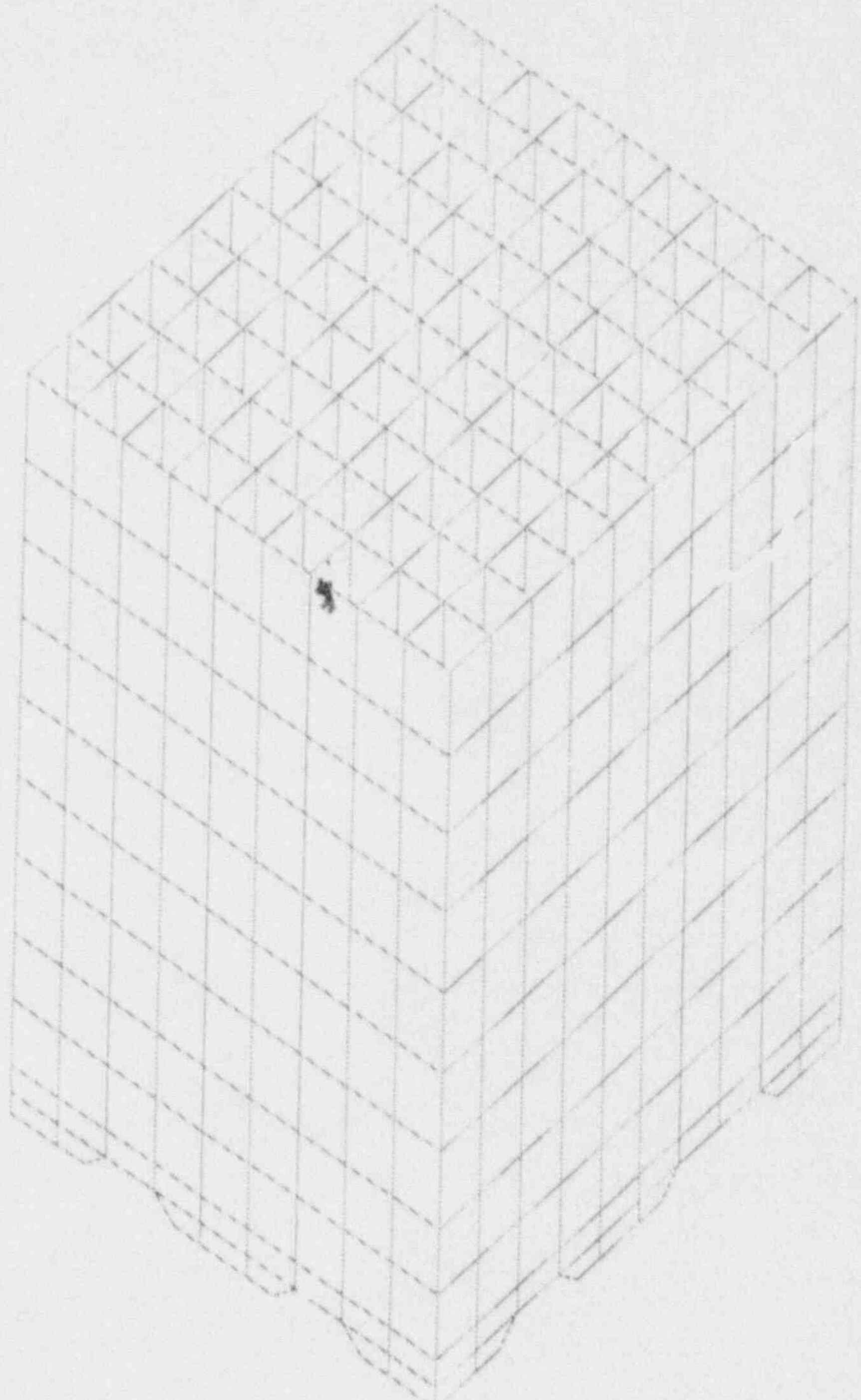

FIGURE 3-13
REGION II DETAILED
STRUCTURAL MODEL

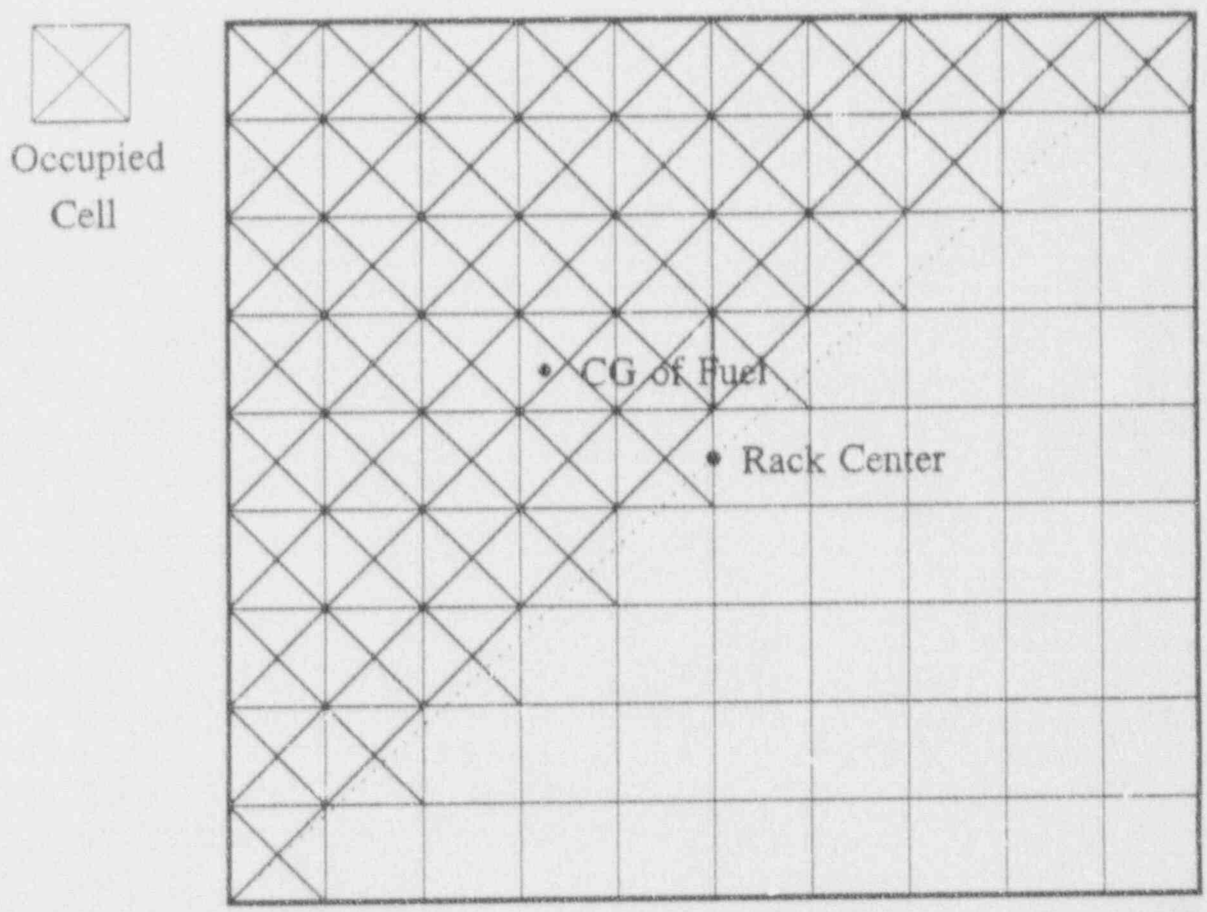

FIGURE 3-14
DIAGONAL LOADING MODEL

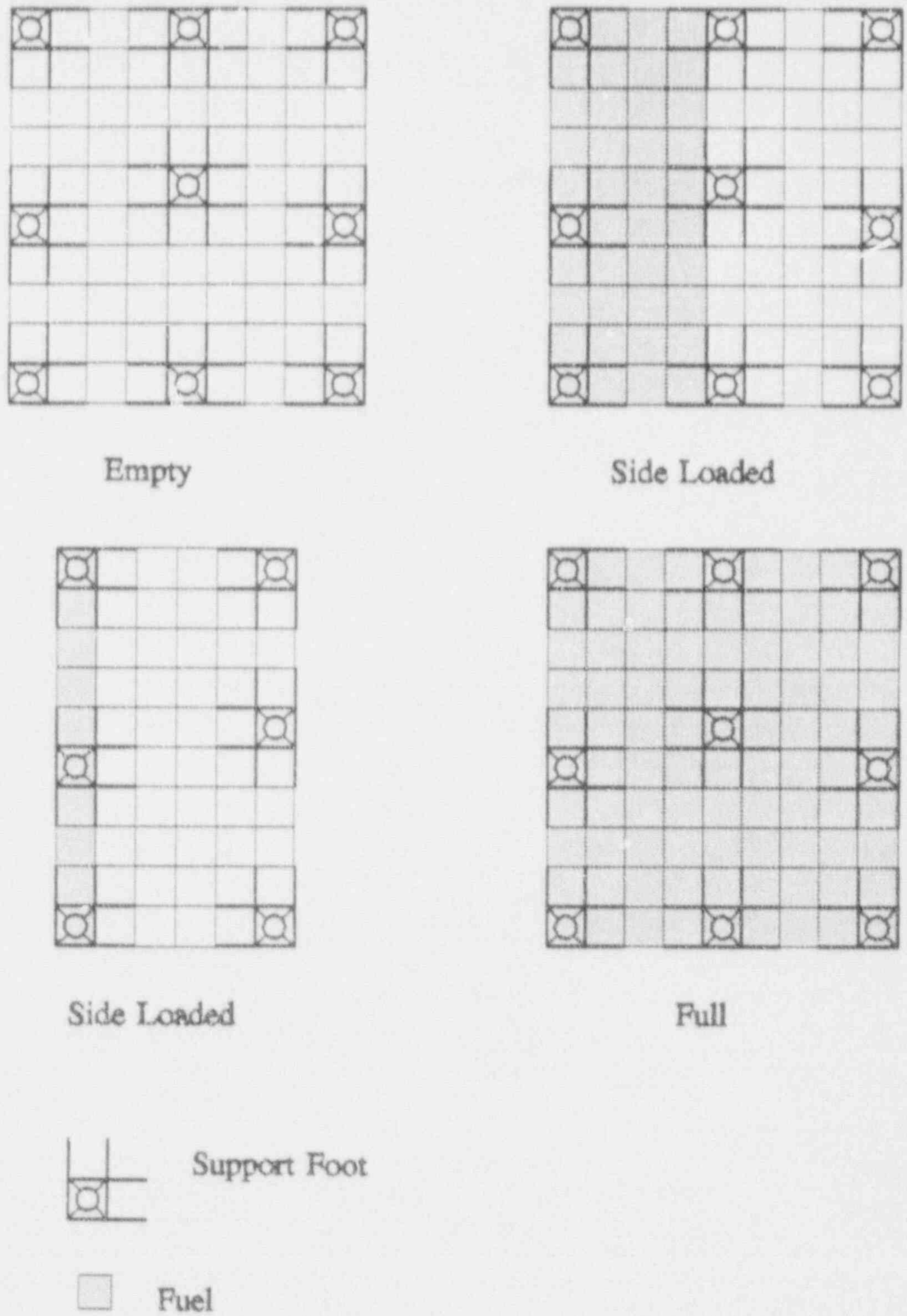

FIGURE 3-15
ROW LOADING MODELS

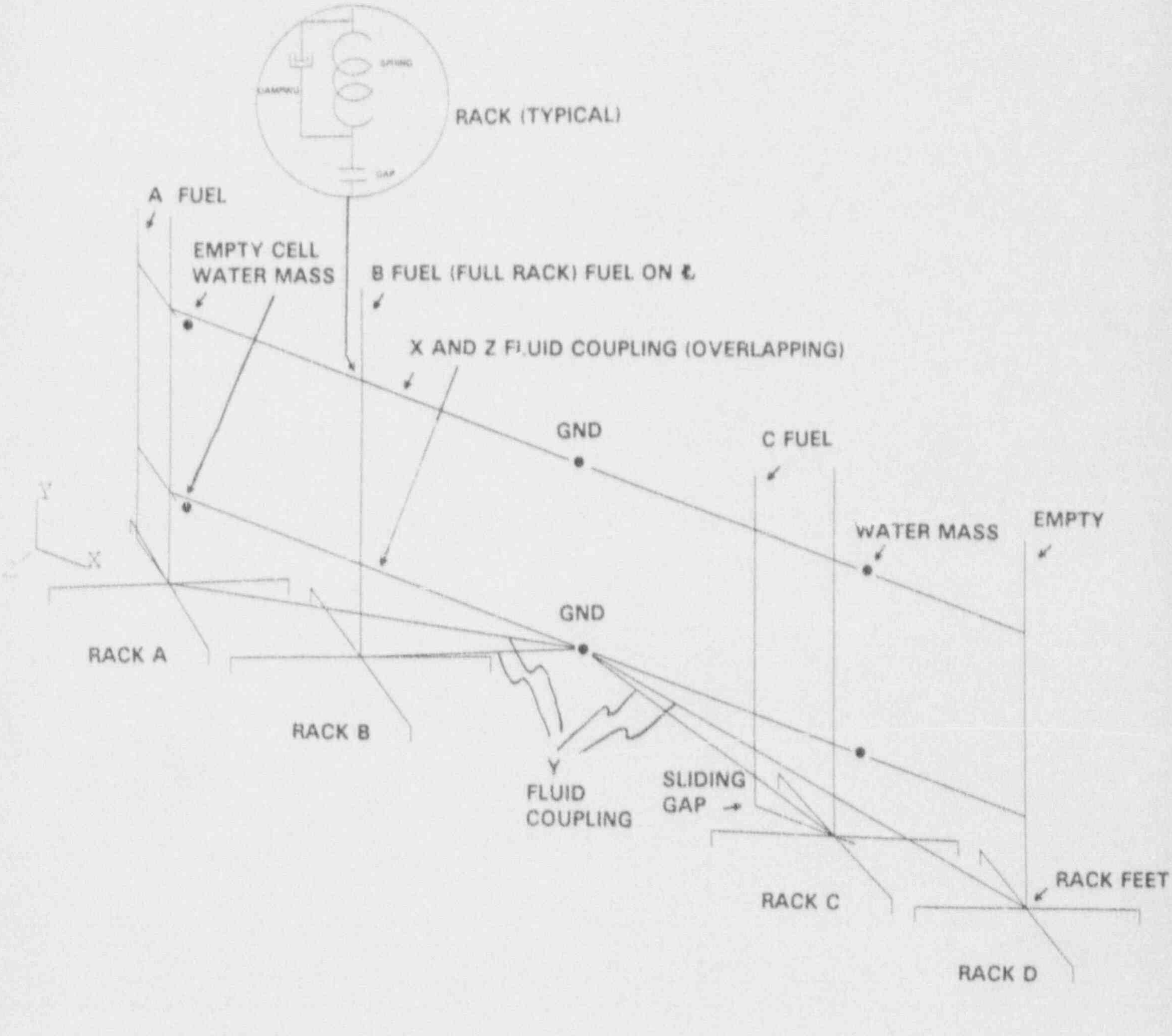

FIGURE 3-16
MULTIPLE RACK MODEL

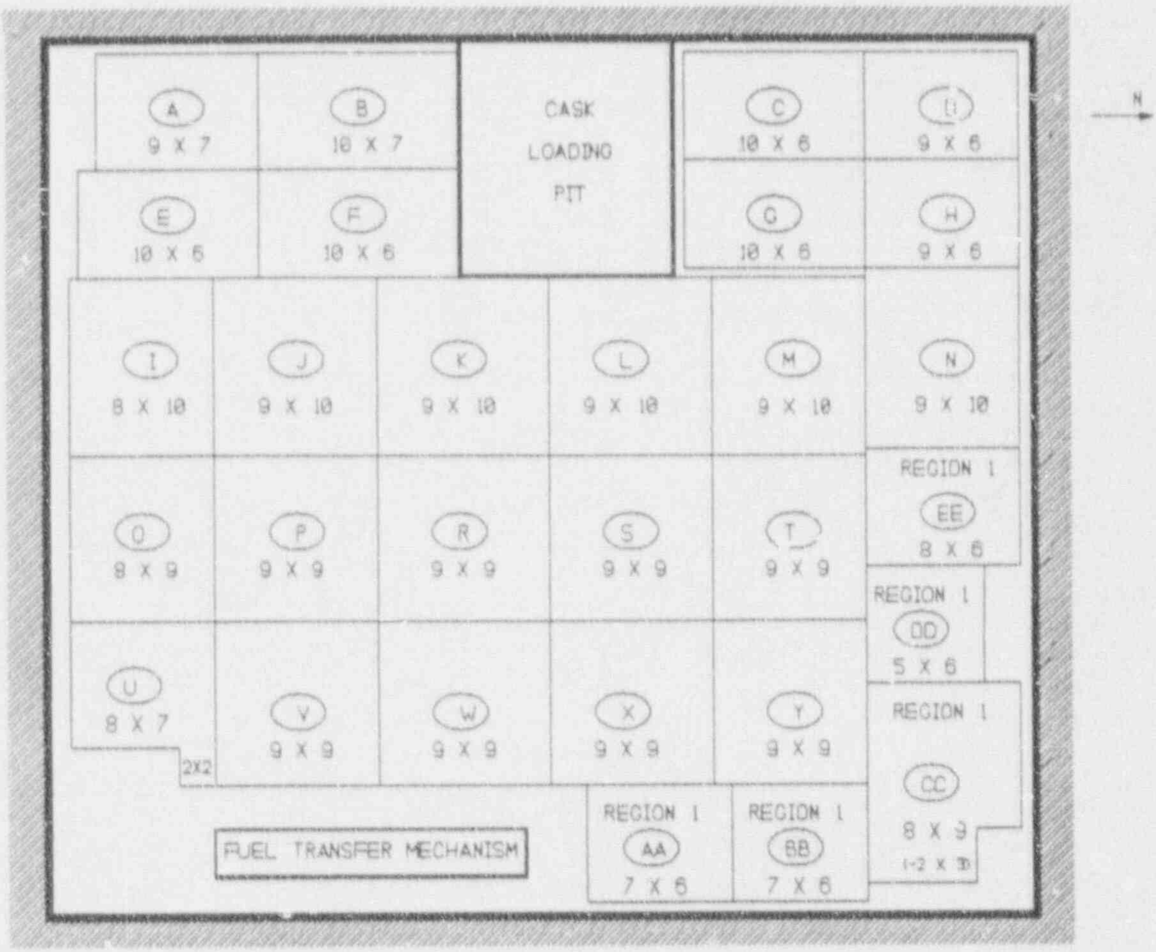

FIGURE 5-17
PROPOSED MAINE YANKEE
SPENT FUEL POOL LAYOUT

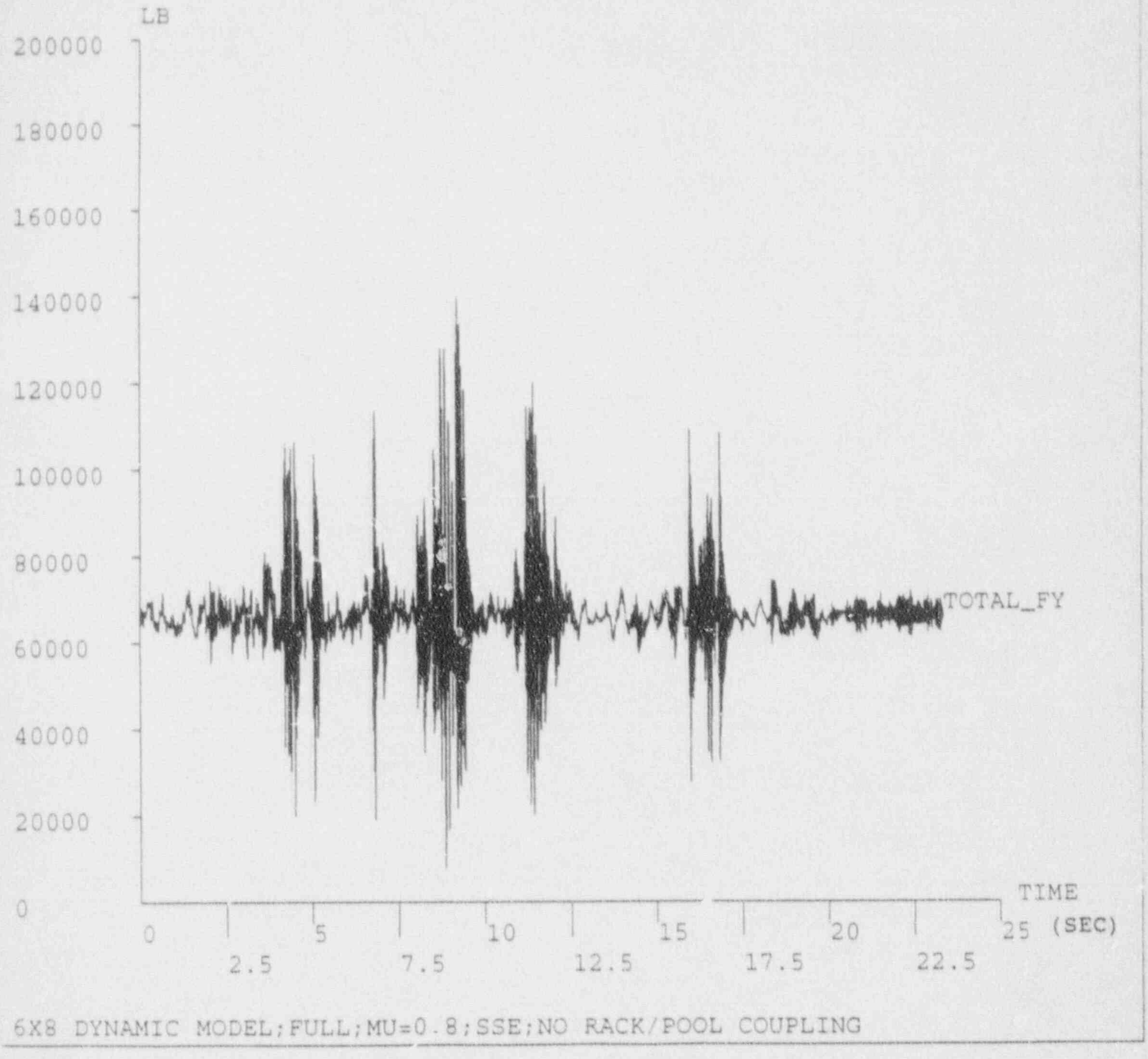

FIGURE 3-18
REGION I RACK
REACTION LOADS

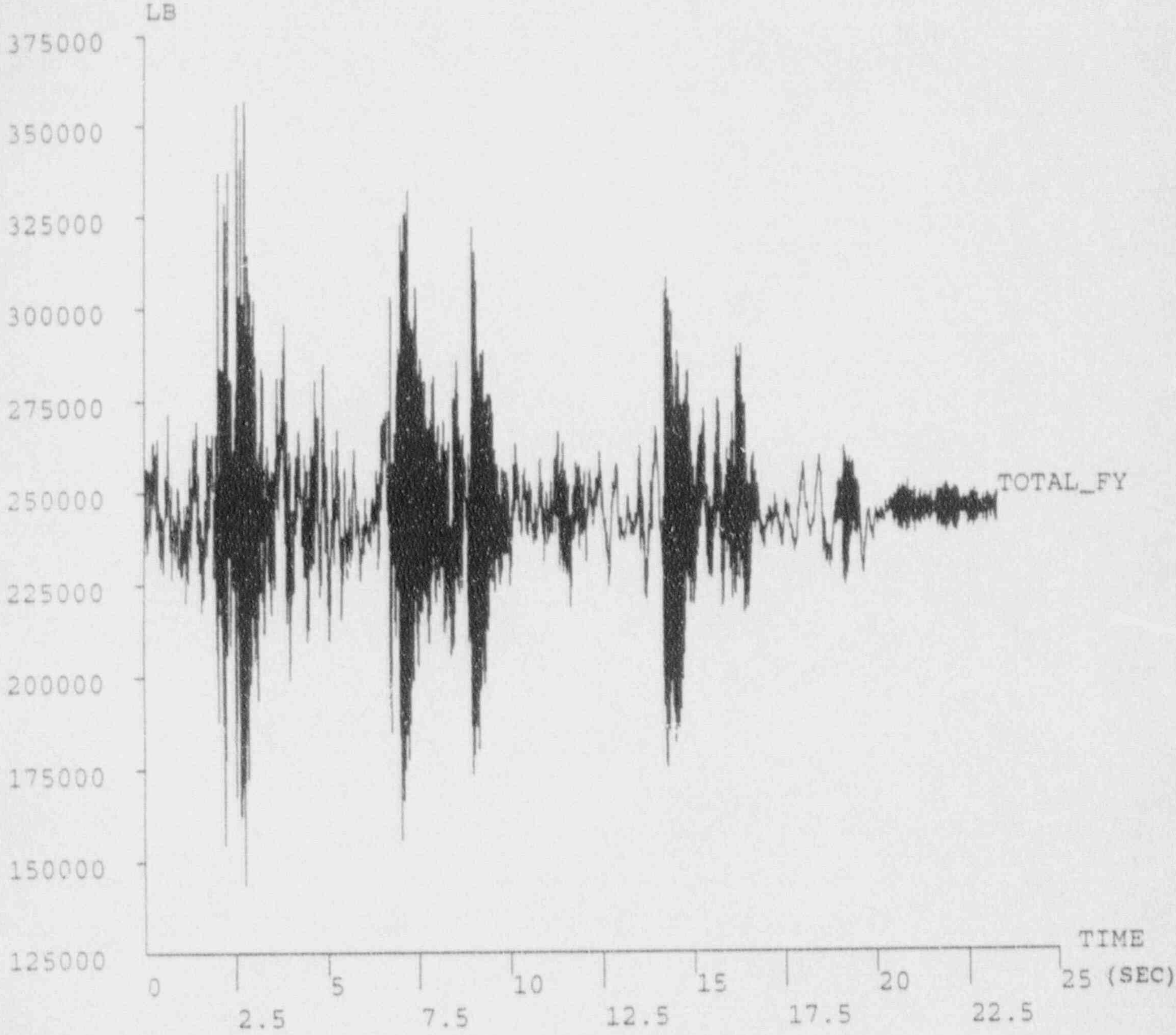

Full 9x10 Rack with DBE; mu=0.8 (no adjacent racks)

FIGURE 3-19
REGION II RACK
REACTION LOADS

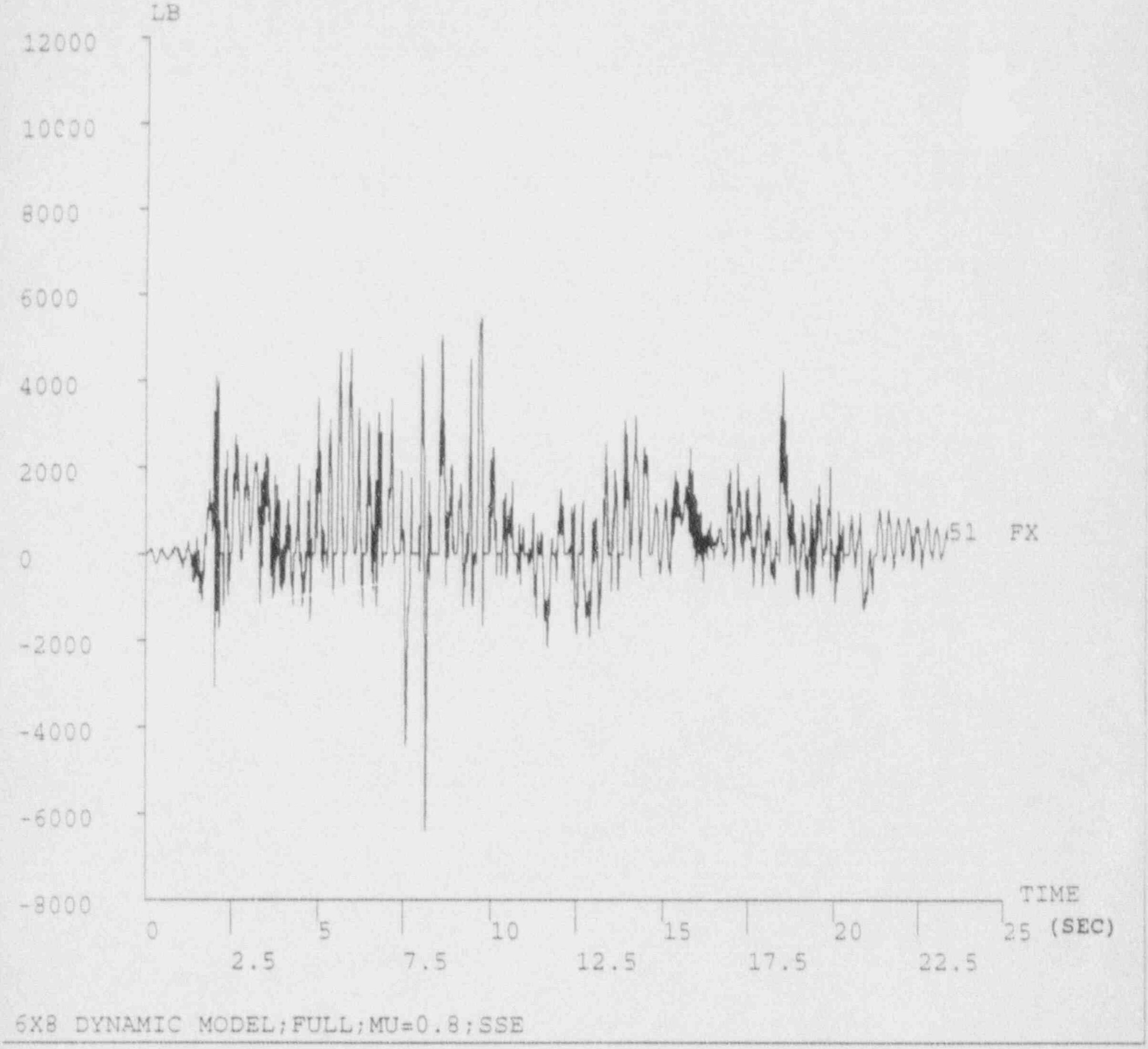

FIGURE 3-20
REGION I SINGLE FOOT
REACTION LOAD (X-DIRECTION)

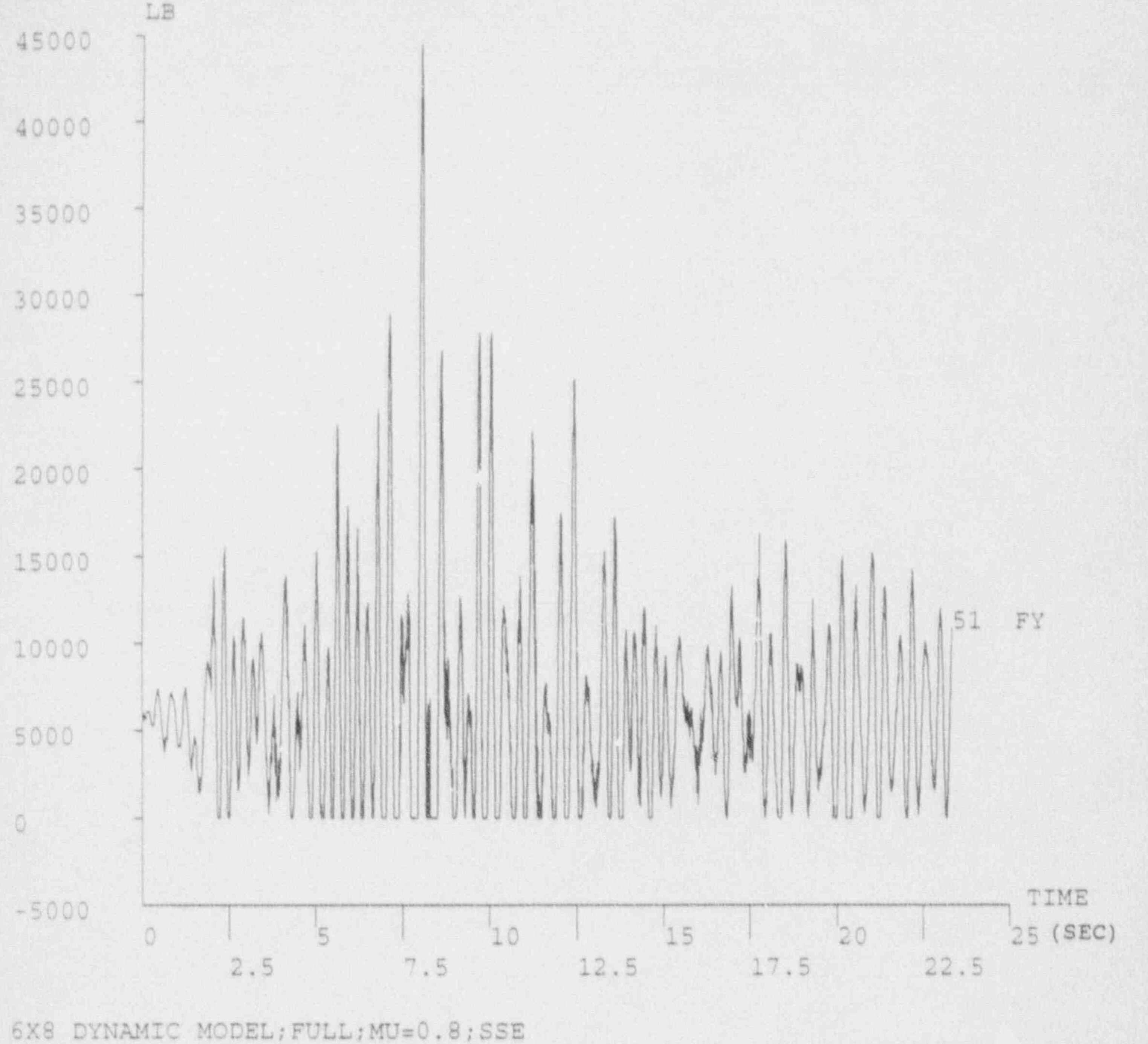

FIGURE 3-21
REGION I SINGLE FOOT
REACTION LOAD (Y-DIRECTION)

MAINE YANKEE ATOMIC POWER COMPANY

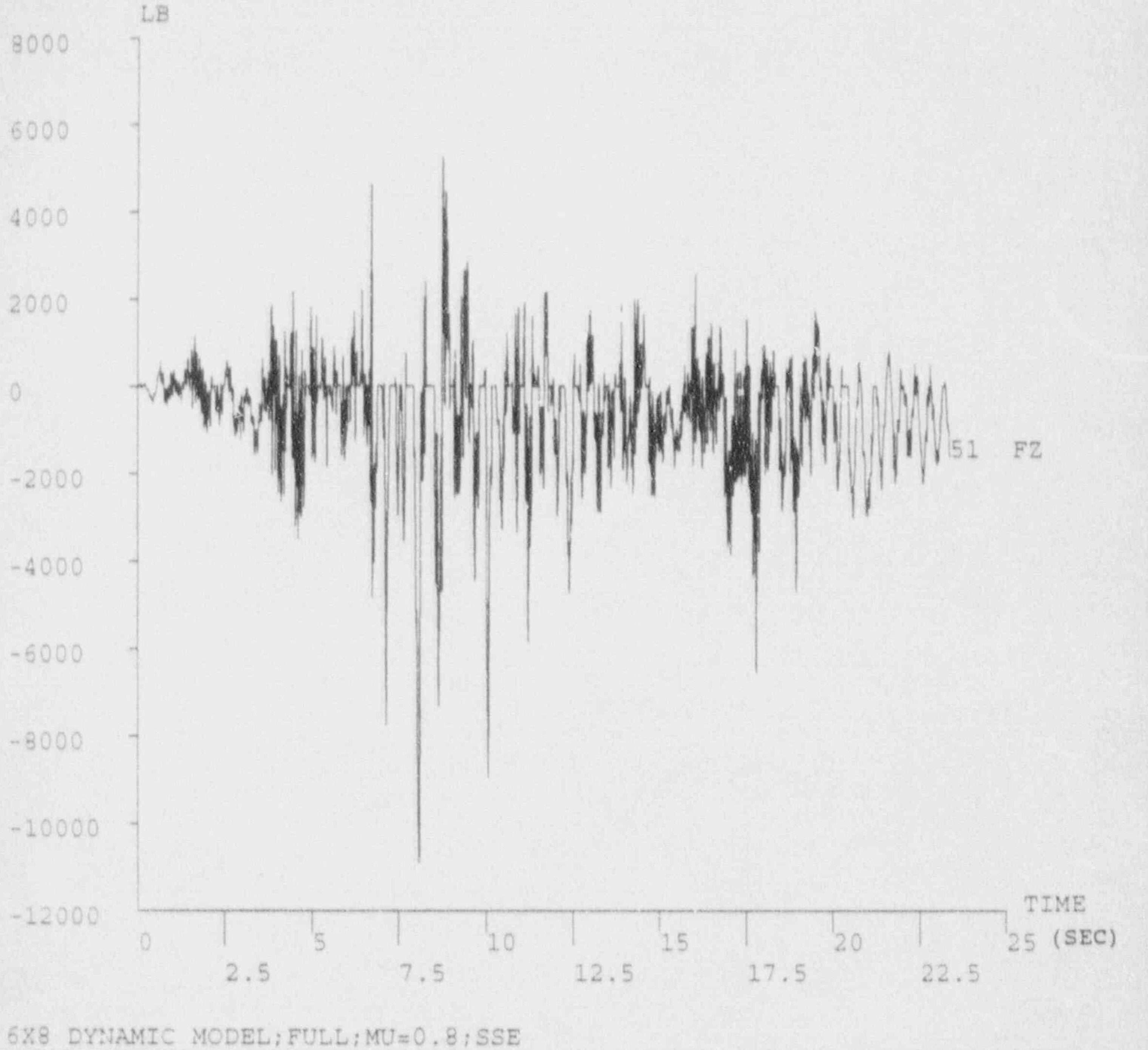

FIGURE 3-22
REGION I SINGLE FOOT
REACTION LOAD (Z-DIRECTION)

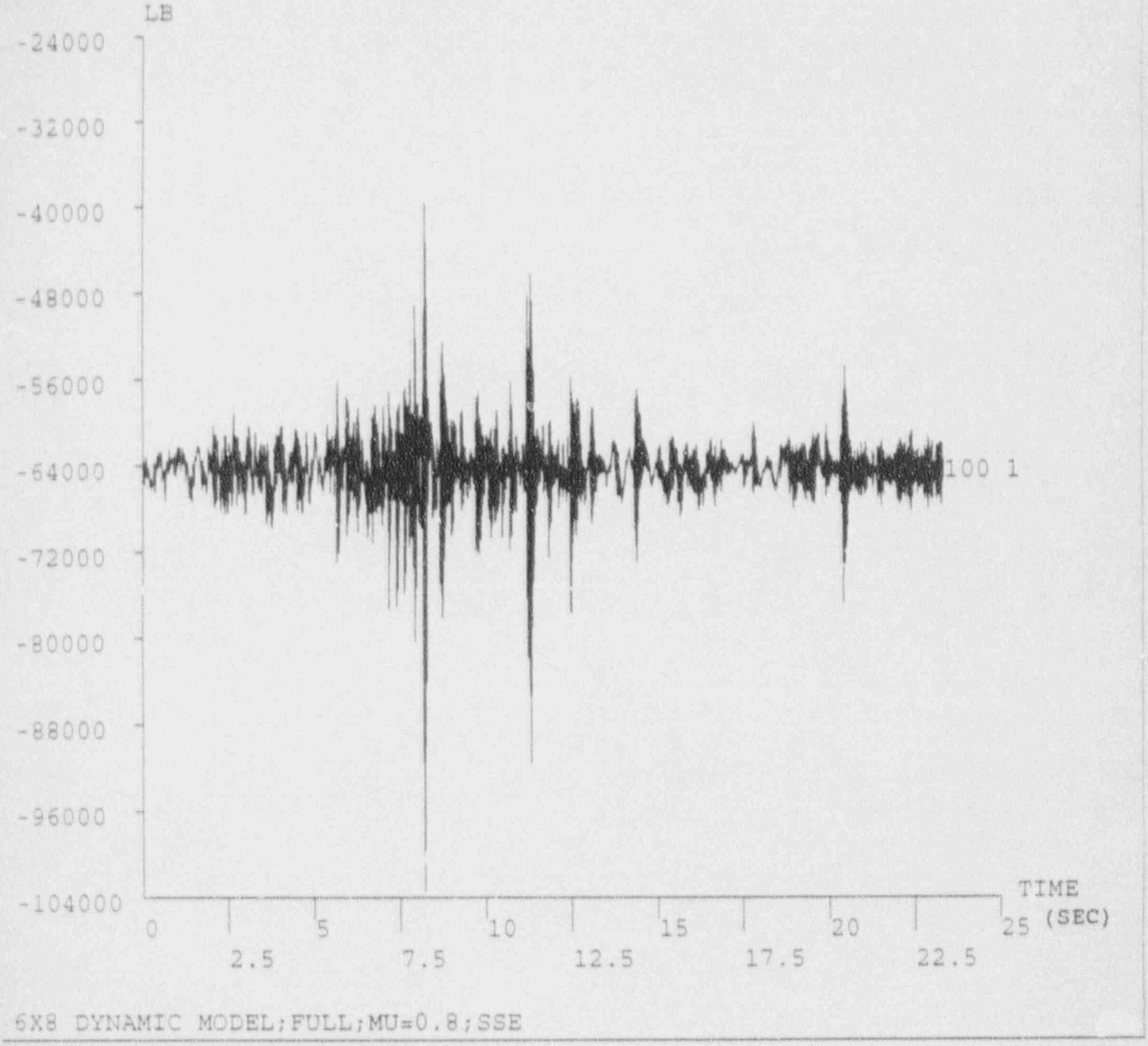

FIGURE 3-23
REGION I FUEL REACTION LOADS

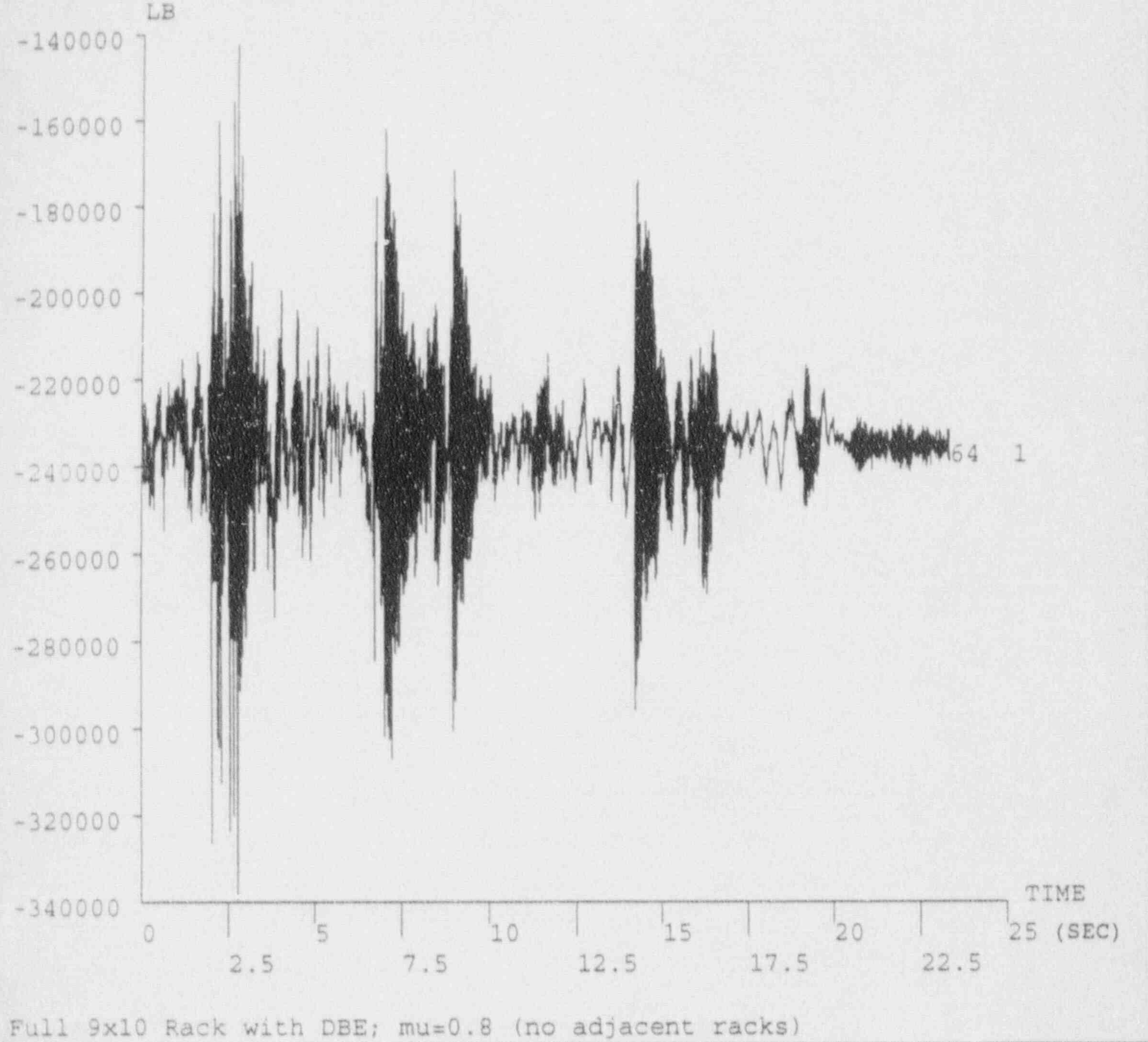

FIGURE 3-24
REGION II FUEL REACTION LOADS

MAINE YANKEE ATOMIC POWER COMPANY

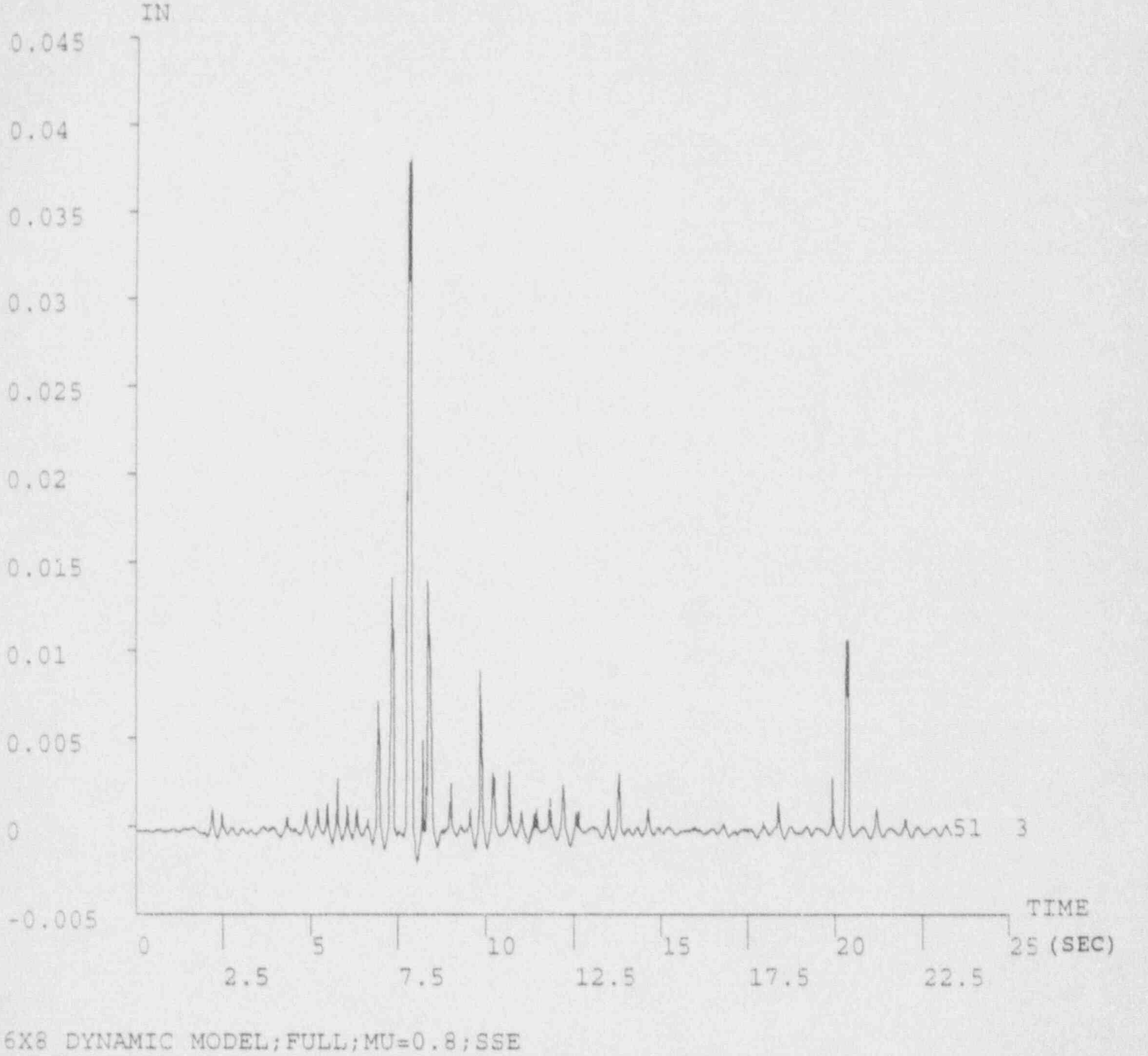

FIGURE 3-25
REGION I INDIVIDUAL
SUPPORT FOOT UPLIFT

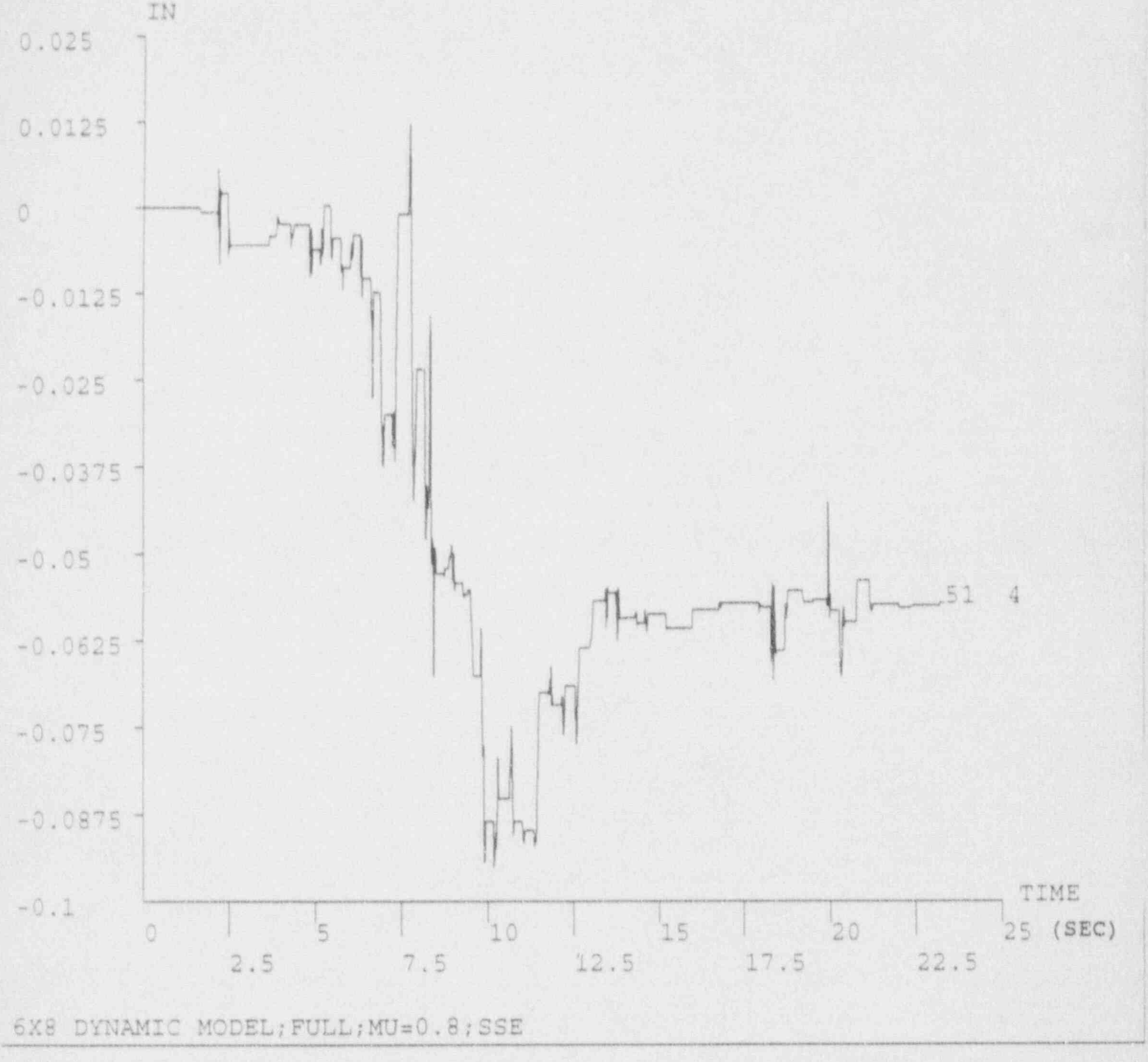

FIGURE 3-26
REGION I INDIVIDUAL SUPPORT FOOT SLIP

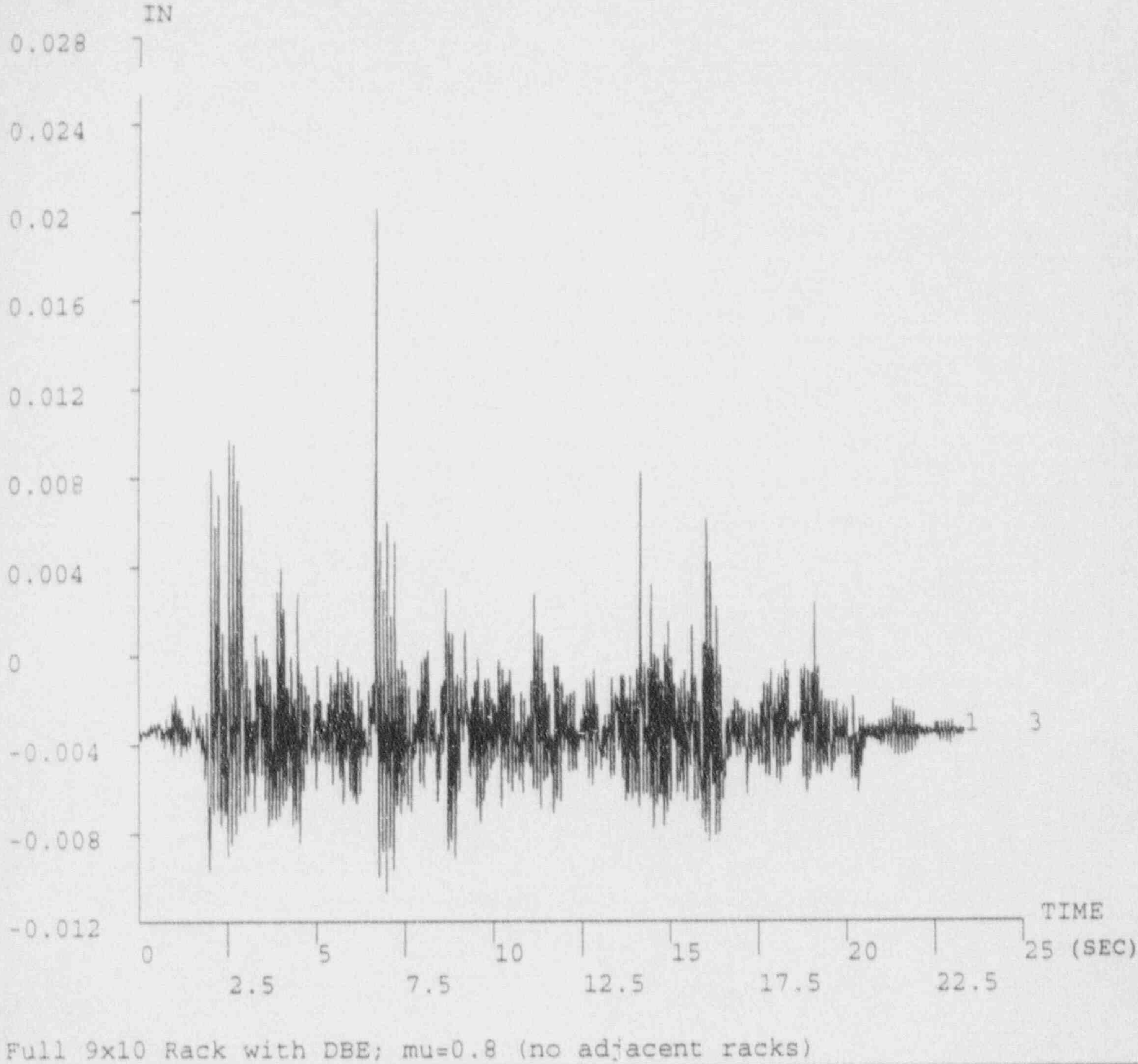

FIGURE 3-27
REGION II INDIVIDUAL
FOOT UPLIFT

MAINE YANKEE ATOMIC POWER COMPANY

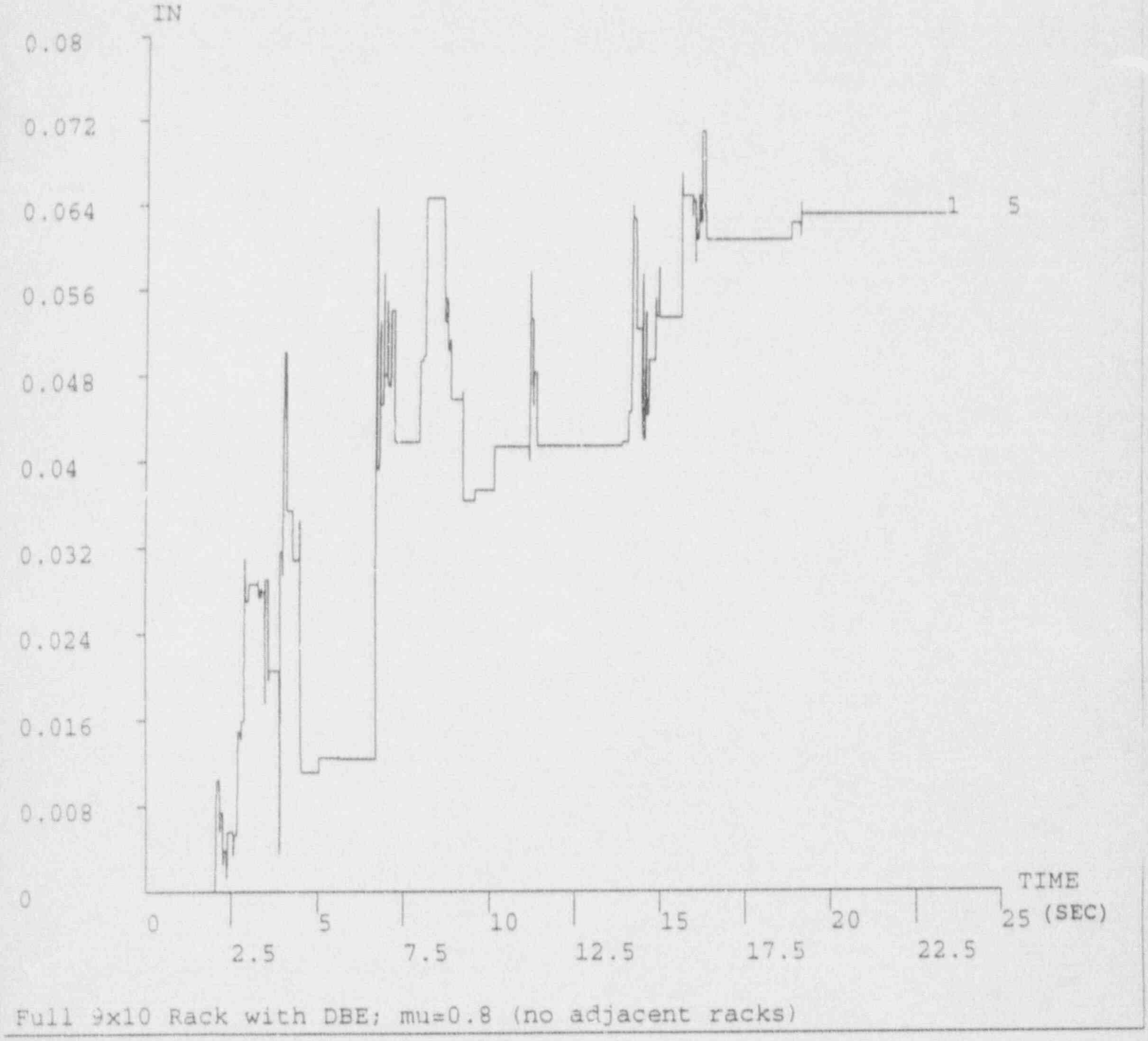

FIGURE 3-28
REGION II INDIVIDUAL
FOOT SLIP

MAINE YANKEE ATOMIC POWER COMPANY

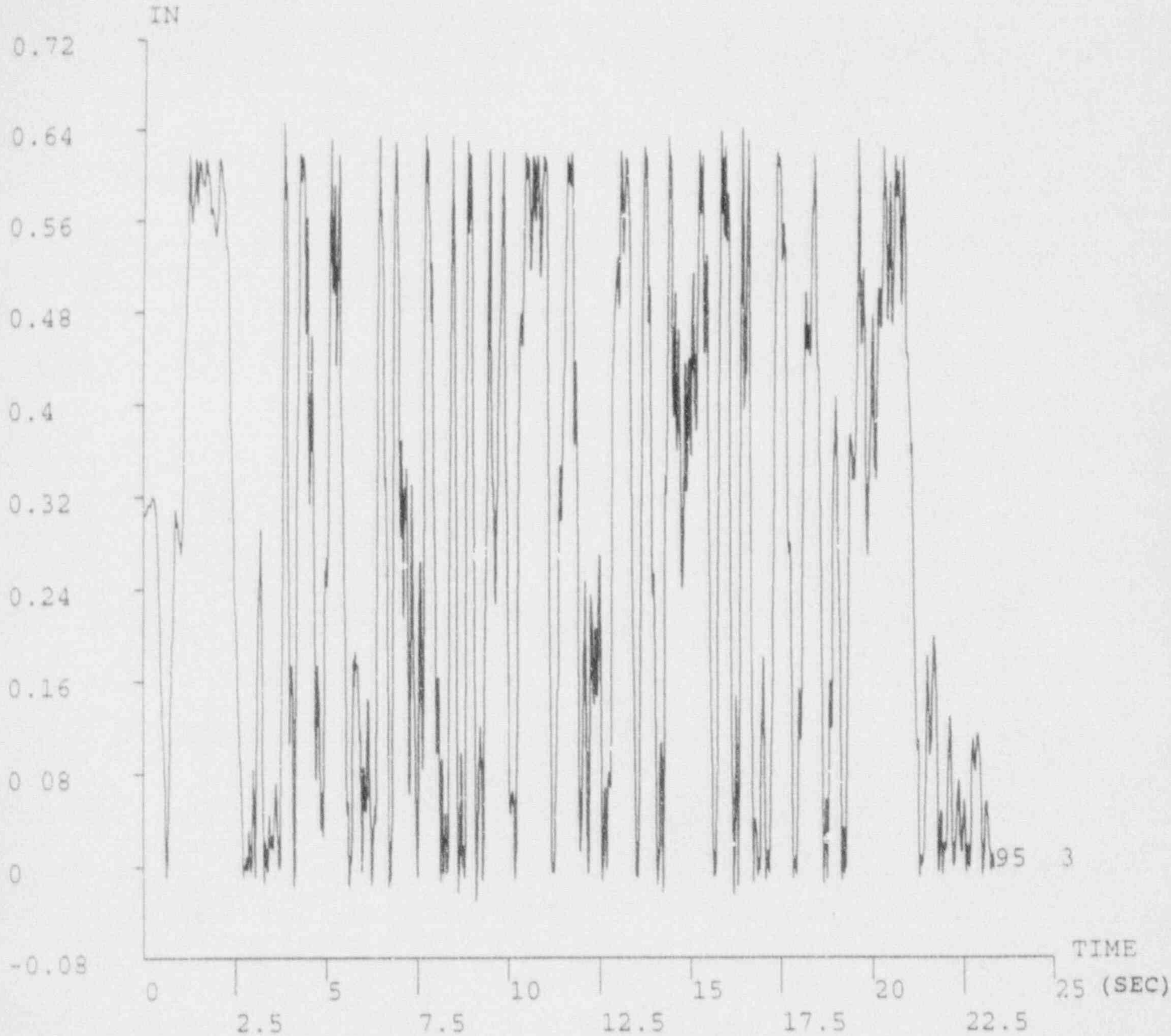

Full 9x10 Rack with DBE; mu=0.8 (no adjacent racks)

FIGURE 3-29
FUEL MOTION WITHIN
STORAGE CELL

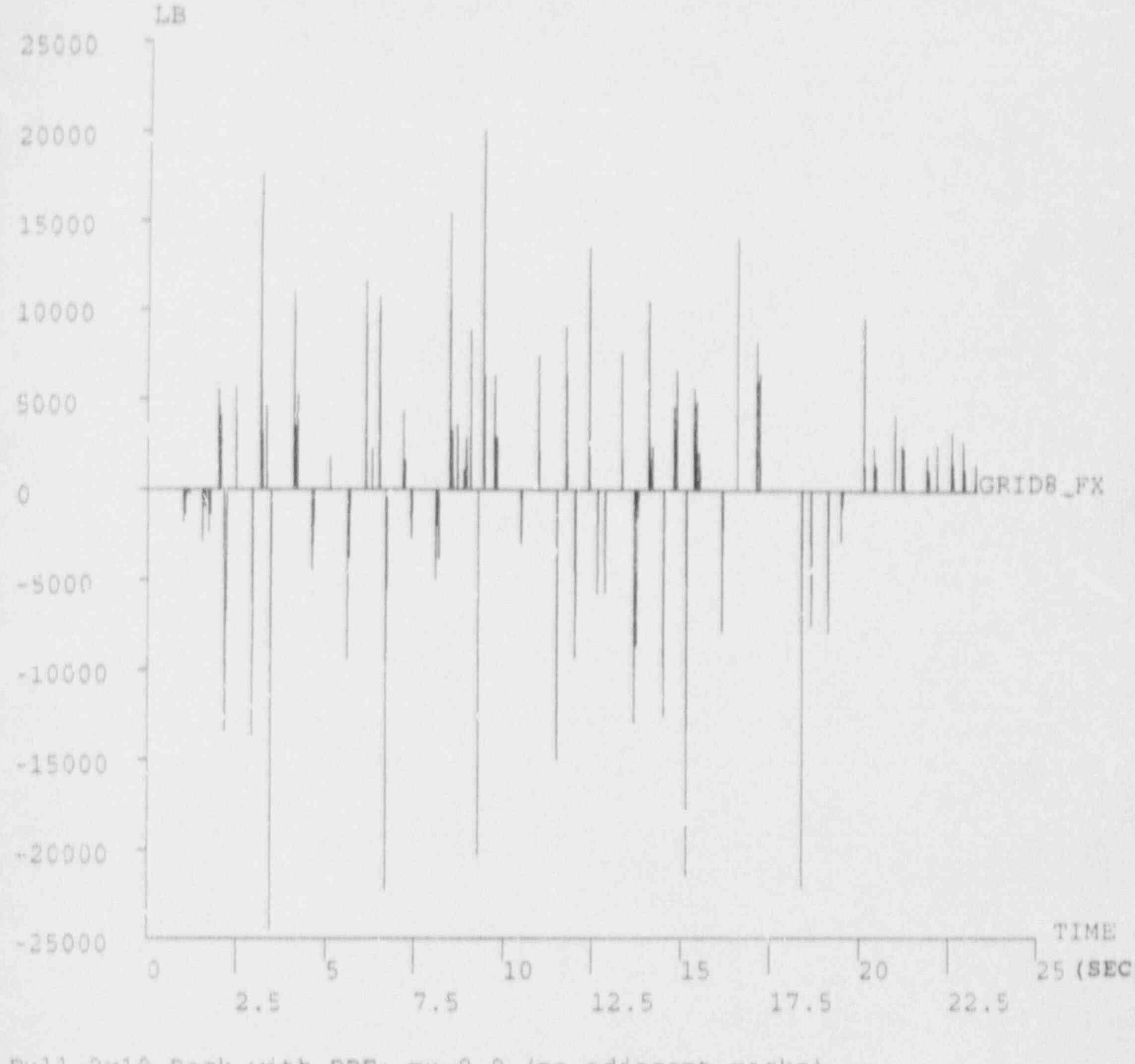

FIGURE 3-30
TOTAL FUEL IMPACT ON STORAGE CELL WALLS

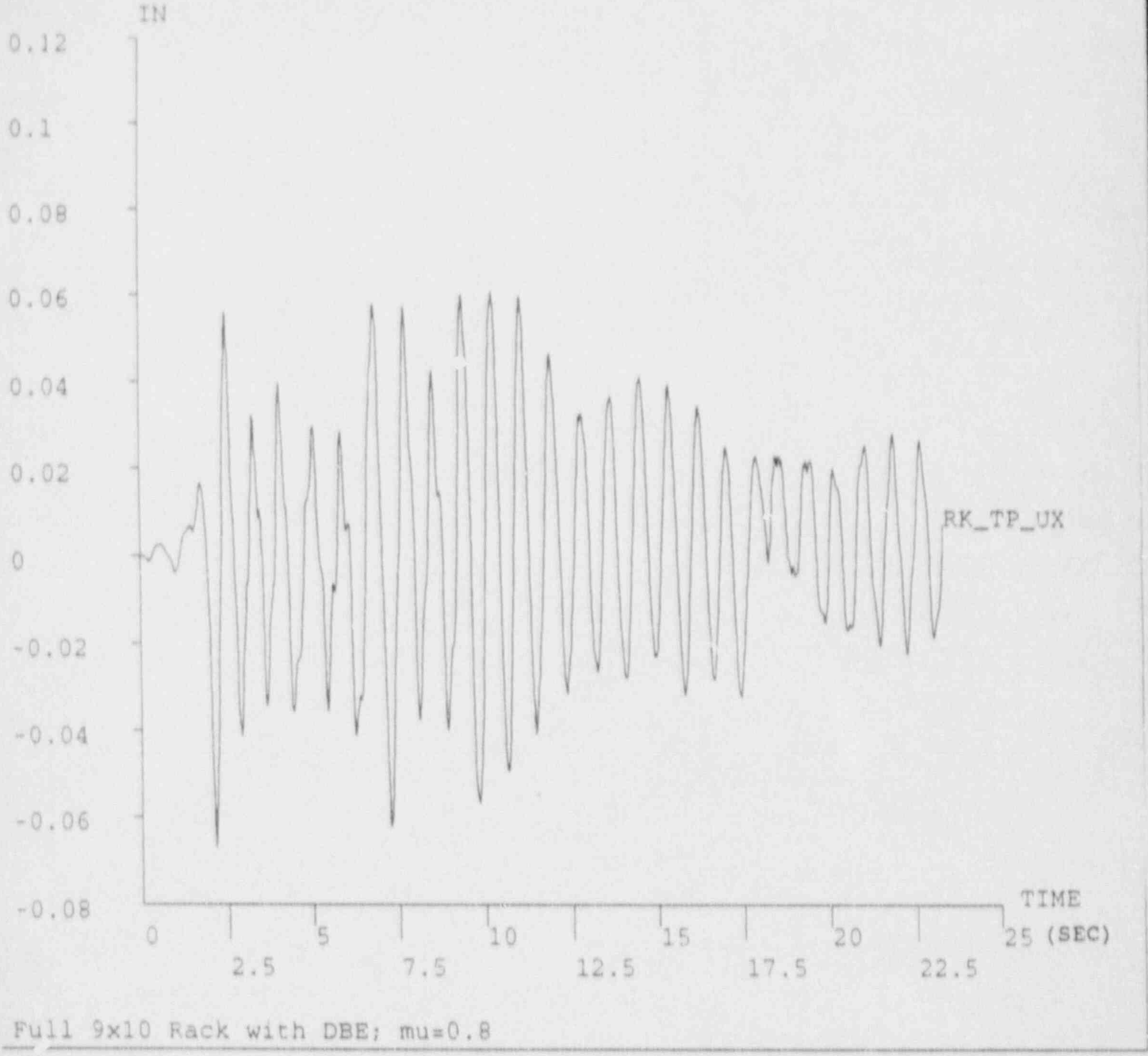

FIGURE 3-31
REGION II RACK X-DIRECTION DISPLACEMENT WITH RACK-RACK HYDRODYNAMIC COUPLING

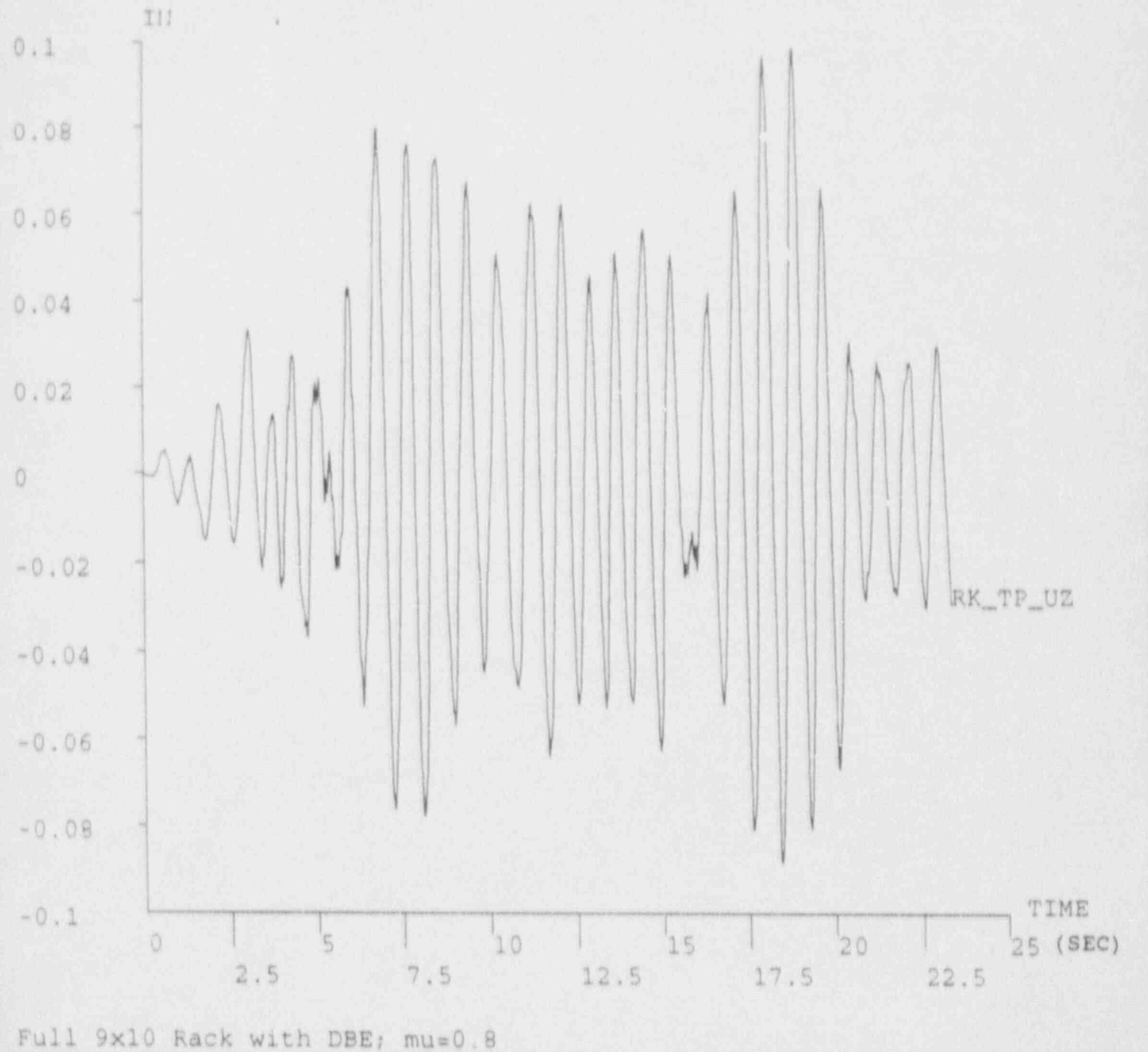

FIGURE 3-32
REGION II RACK Z-DIRECTION DISPLACEMENT WITH RACK-RACK HYDRODYNAMIC COUPLING

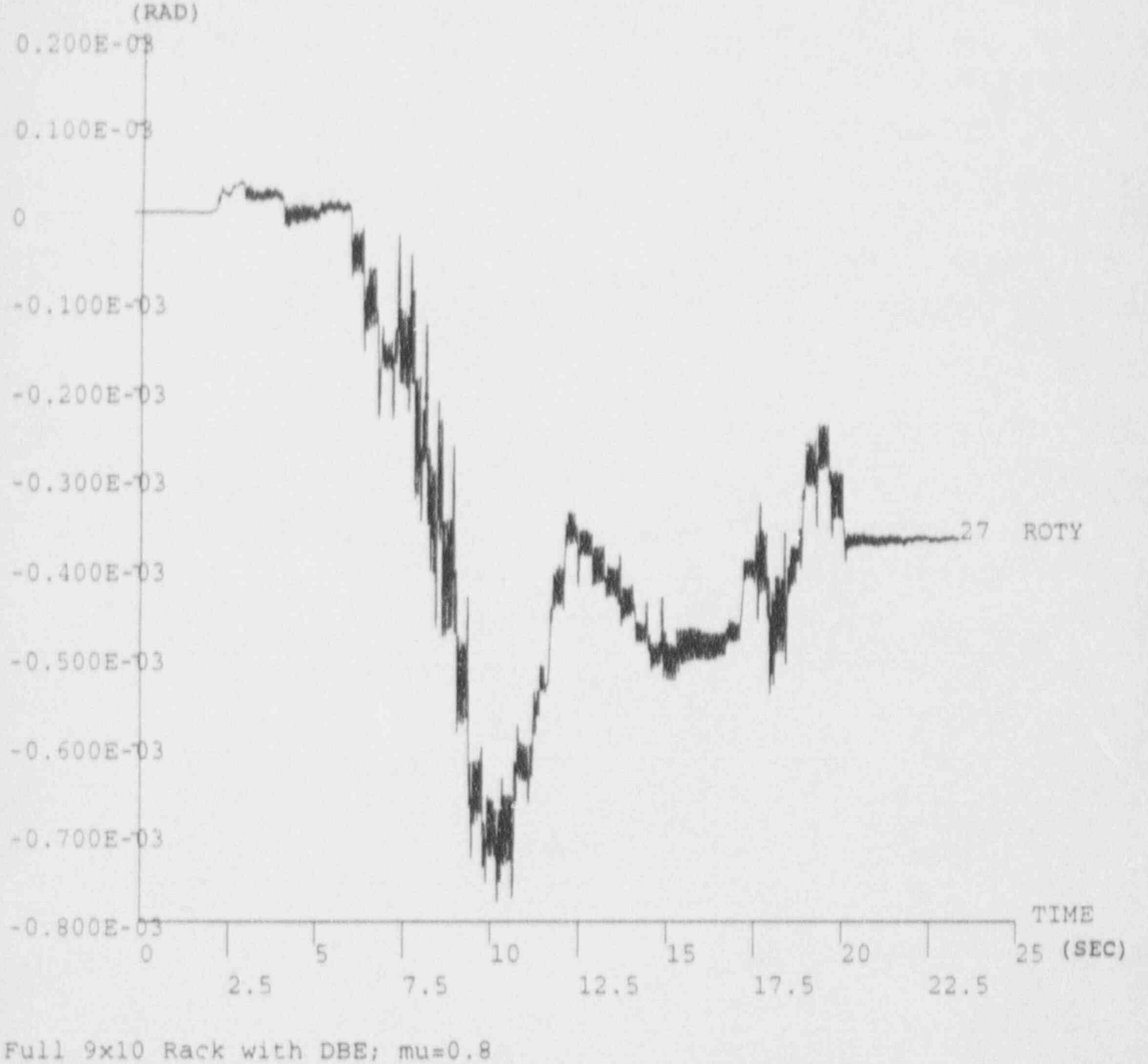

FIGURE 3-33
REGION II RACK ROTATION
WITH RACK-RACK
HYDRODYNAMIC COUPLING

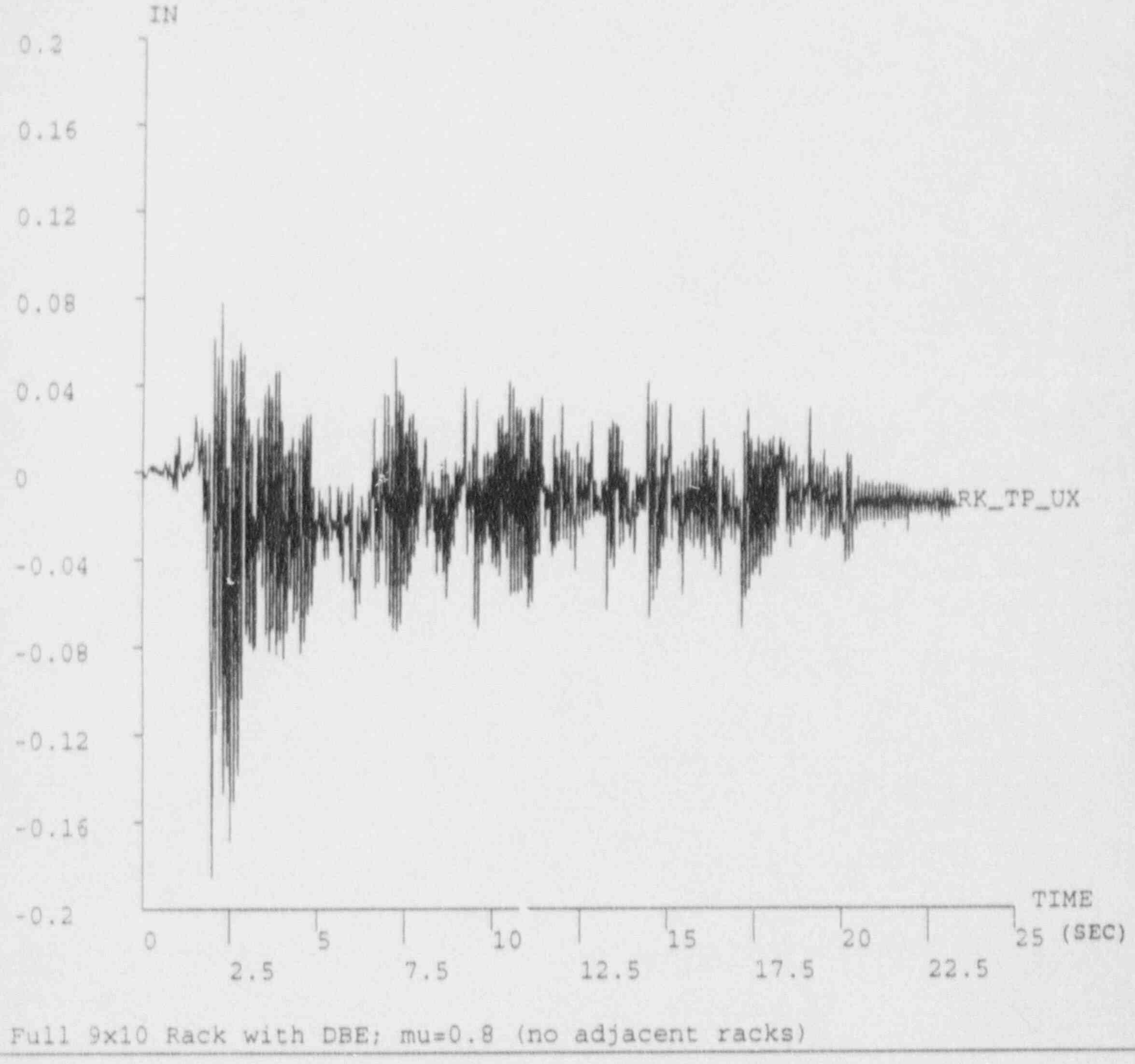

FIGURE 3-34
REGION II RACK X-DIRECTION DISPLACEMENT WITH NO RACK-RACK HYDRODYNAMIC COUPLING

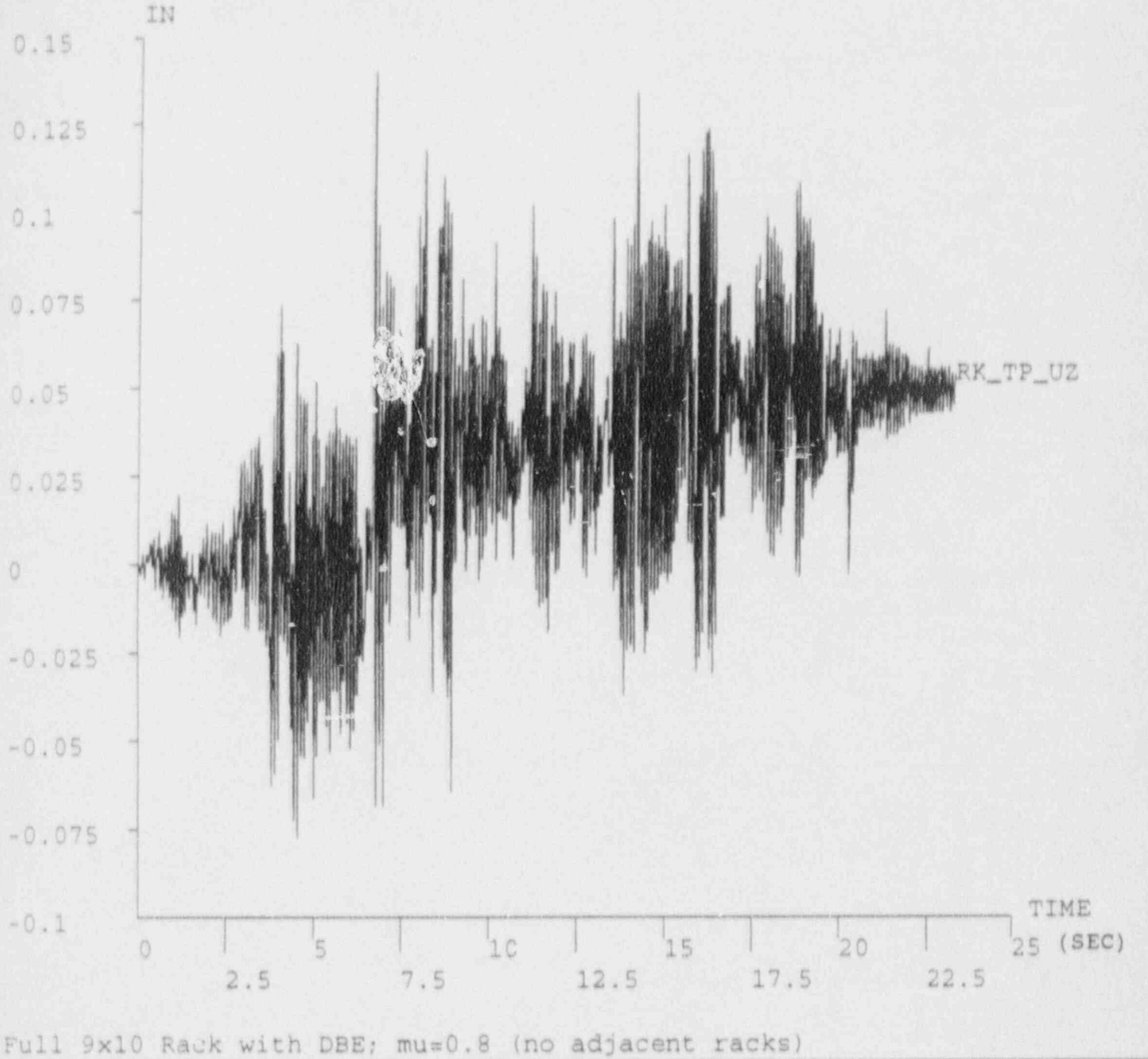

FIGURE 3-35
REGION II RACK Z-DIRECTION DISPLACEMENT WITH NO RACK-RACK HYDRODYNAMIC COUPLING

MAINE YANKEE ATOMIC POWER COMPANY

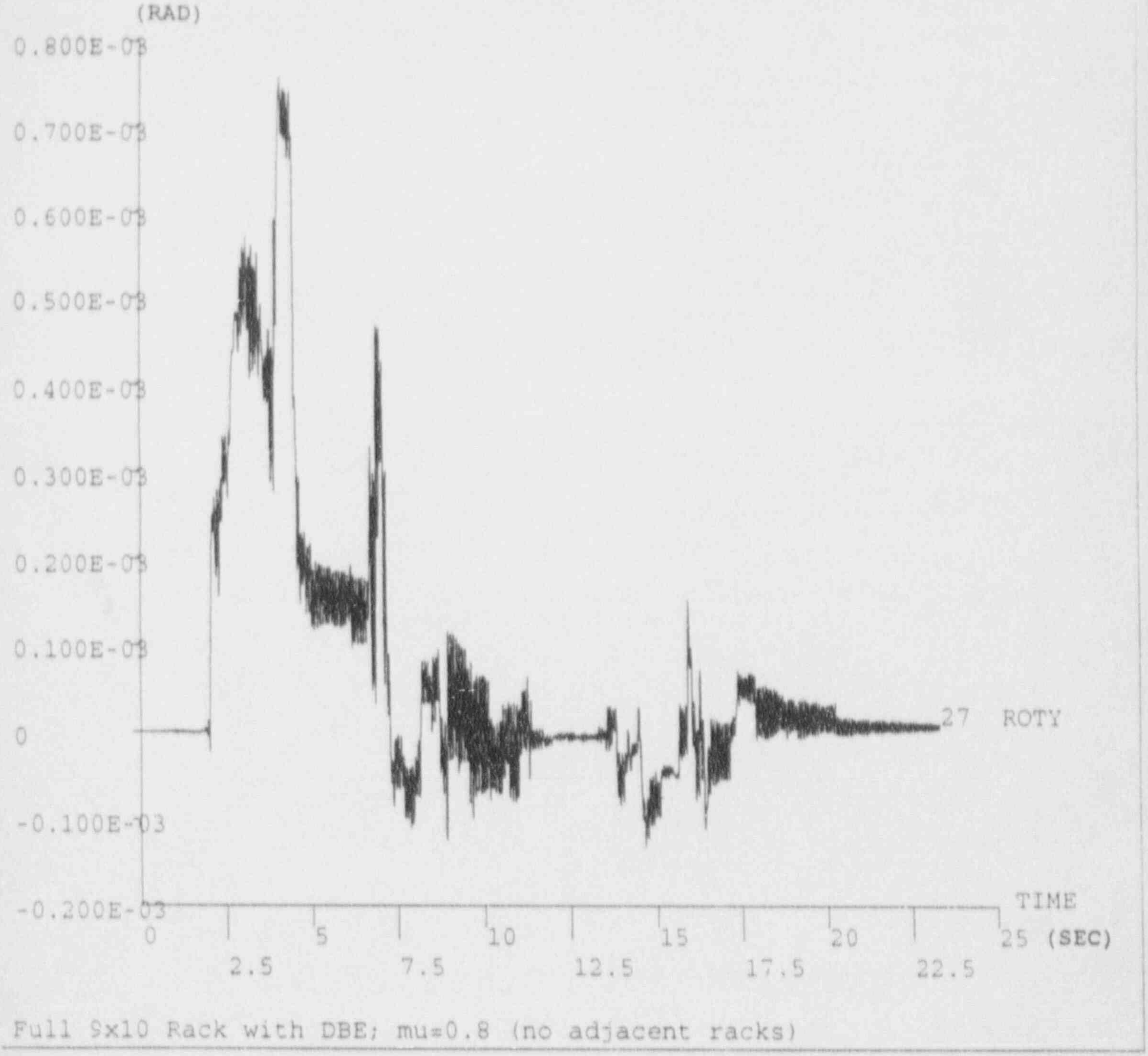

FIGURE 3-36
REGION II RACK ROTATION
WITH NO RACK-RACK
HYDRODYNAMIC COUPLING

MAINE YANKEE ATOMIC POWER COMPANY

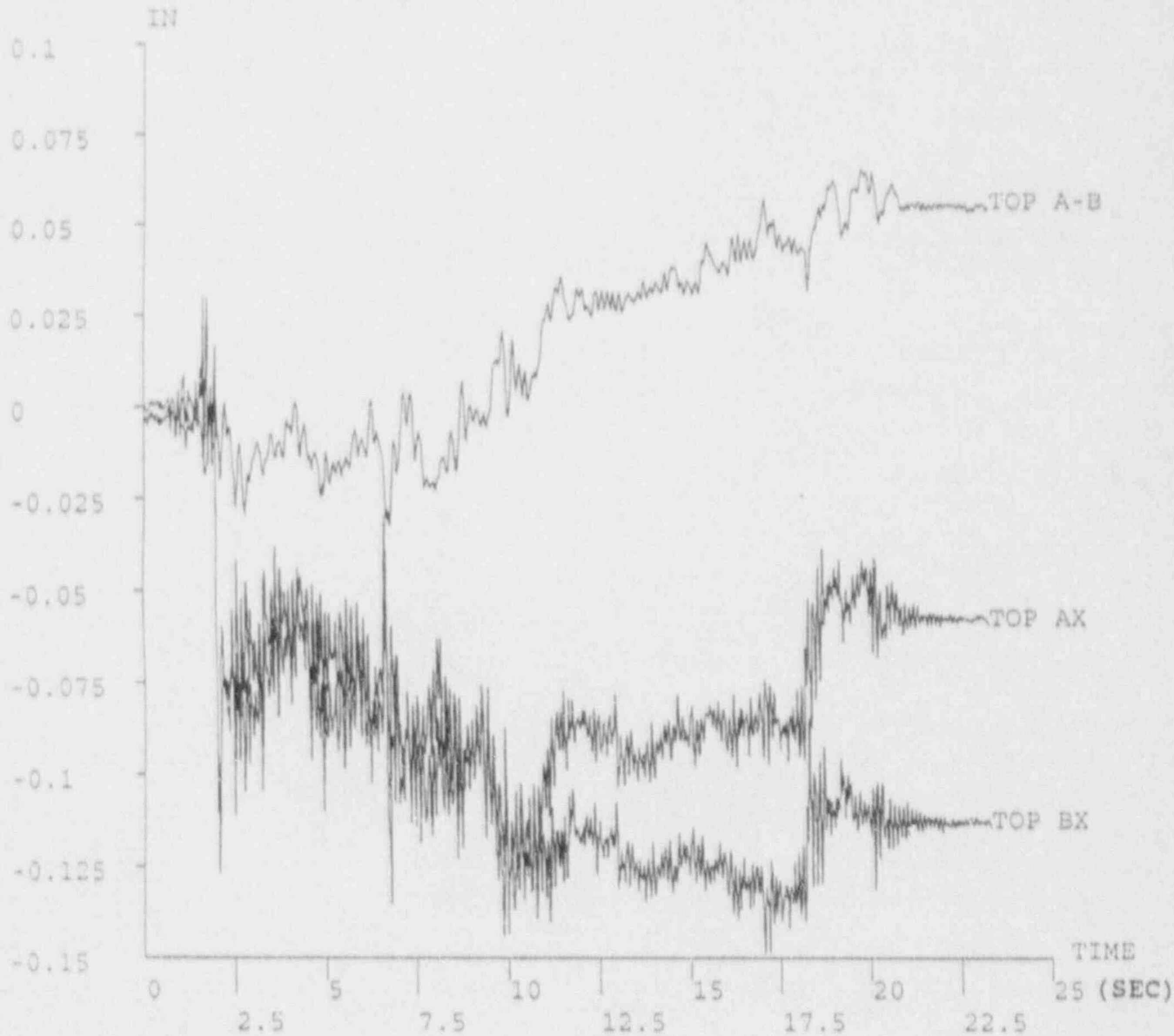

Rack A and B Top Displacements in X; Mu=.2

FIGURE 3-37
MULTIPLE RACK ANALYSIS
MODULE A AND B DISPLACEMENT

MAINE YANKEE ATOMIC POWER COMPANY

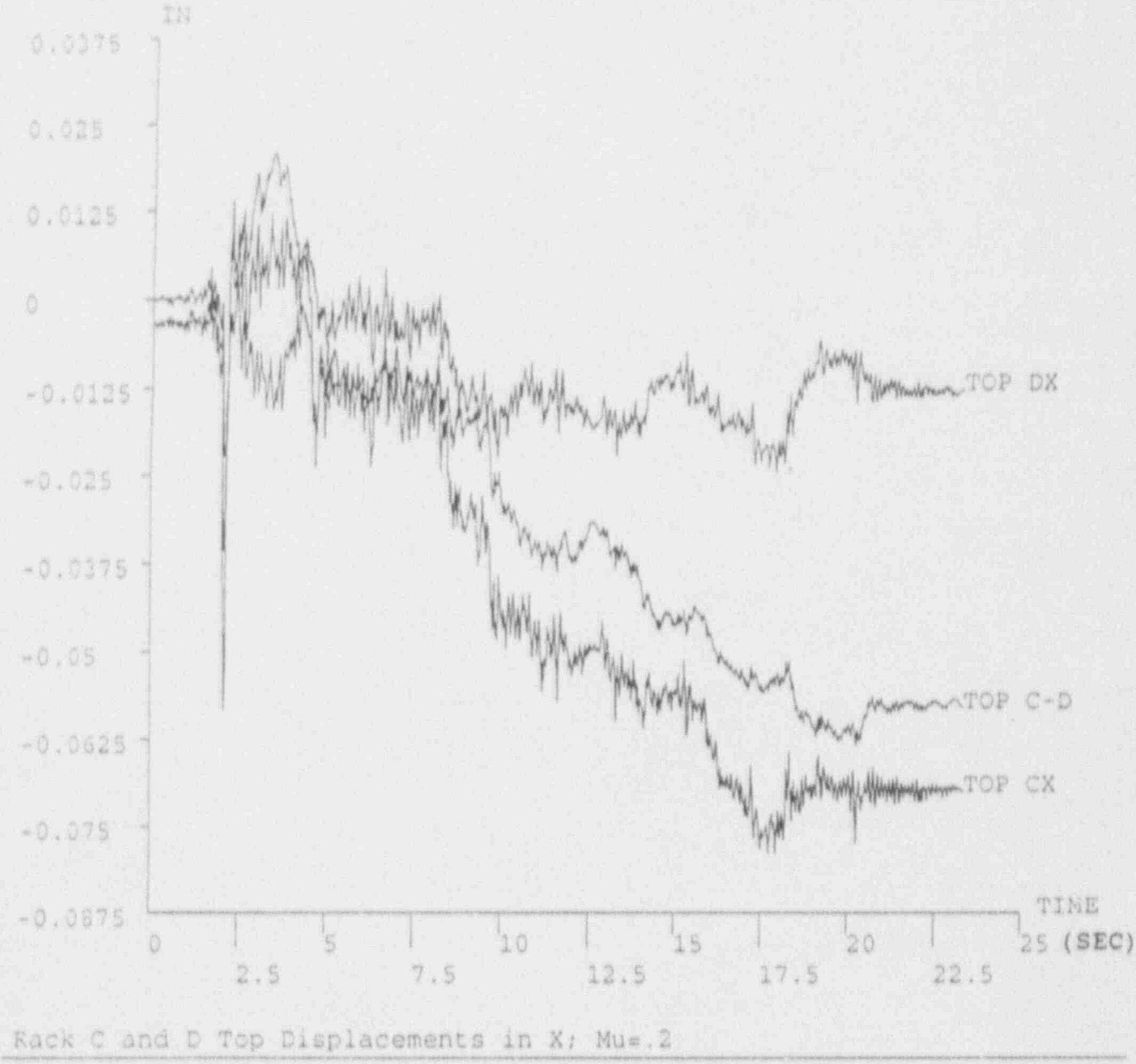

FIGURE 3-38
MULTIPLE RACK ANALYSIS
MODULE C AND D DISPLACEMENT

4.0 FUEL BUILDING

4.1 DESCRIPTION

The Maine Yankee Fuel Building is a nuclear safety-related, Seismic Category I building. The principal function of the Fuel Building is to provide a location for the safe storage of new and spent fuel assemblies. The building houses a new-fuel unloading area, a new-fuel storage vault, a spent fuel pool, the necessary cranes required for the handling of the fuel assemblies and the spent fuel pool support systems. The lower portion of the building is a cast-in-place reinforced concrete structure which supports the structural steel superstructure located above. The spent fuel pool purification system filters and demineralizer are located in shielded cubicles below the fuel unloading area. Shield slabs are removed from the fuel unloading floor to replace expended filter cartridge elements. The Fuel Building arrangement is shown in the Maine Yankee FSAR, Figures 5.2-1 and 5.2-2.

The spent fuel pool is located in the southeast corner of the Fuel Building and abuts the Reactor Containment Building. The spent fuel pool is a stainless steel-lined, rectangular, reinforced concrete box-type structure comprised of a 6-ft thick foundation slab supporting four 6-ft thick walls. These walls extend from 12 ft-6 in. below grade to 26 ft-0 in. above grade. The spent fuel pool foundation slab is supported directly on bedrock. Spent fuel enters the pool from the containment through a fuel transfer tube. Space is provided in the pool to place a spent fuel shipping cask. The pool is serviced by means of the yard crane, as well as a moveable platform with hoist. A new-fuel area adjoins the spent fuel pool and is described in the Maine Yankee FSAR, Section 5.2.

The pool is designed to safely resist the hypothetical earthquake or tornado, as well as the applied loads of the water and fuel. In addition, the steel framing above the pool is designed for earthquake and tornado to prevent it from falling into the pool and damaging fuel assemblies.

4.2 STRUCTURAL ANALYSIS

4.2.1 Description

The reracking will result in an increase in the weight supported by the foundation slab of approximately 18%. The weight increase will be distributed to assure the slab loadings do not exceed design allowables (Ref. 4-1).

4.2.2 Building Analysis

The Fuel Building is designed to resist the hypothetical earthquake or tornado, as well as the applied loads of the water and fuel (Ref. 4-2, Section 5.2.4).

The spent fuel pool is reevaluated incorporating the loadings associated with the new high-density spent fuel storage racks to assure conformance with Seismic Category I design requirements.

The individual loadings on the spent fuel pool structure can be summarized as follows:

(a) Dead weight of the spent fuel pool structure itself and weight from the steel superstructure above.

(b) Dead weight of the spent fuel rack modules and that of the stored fuel.

(c) Weight and corresponding hydrostatic pressures of the contained water mass within the spent fuel pool; on the slab and walls.

(d) Time dependent vertical and horizontal seismic forces transmitted by the spent fuel racks to the slab during either the hypothetical earthquake or the operational basis earthquake (OBE) events.

(e) Time dependent vertical and horizontal seismic inertia forces transmitted by the walls, slab, and contained water mass during either an SSE or an OBE event, as discussed in the Maine Yankee FSAR.

(f) Thermal gradients across the spent fuel pool slab and walls during normal and accident conditions.

(g) Tornado loads due to wind and tornado missiles.

(h) Hydrodynamic loads due to movement of the racks during an earthquake.

Of the above loadings, only items (b), (c), (d), (e), (f), and (h) will change as a result of the new high density fuel rack installation.

As discussed in Section 5.2, reracking of the pool will not change the maximum heat load in the spent fuel pool. Therefore, the maximum design temperature of the spent fuel pool remains the same, and the thermal stresses in the liner and concrete structure due to water temperature are not affected by the proposed storage capacity increase.

The new high density fuel storage racks are designed to be free-standing (i.e., the only direct interface with the building structure is their support points on the foundation slab). Gaps are maintained between the walls and racks during all loading conditions and there is no direct loading of the walls from the racks.

The increased loads transmitted by the rack support feet to the pool foundation slab are computed by a time-history analysis using the site artificial ground time-histories as input (Section 3.2). The maximum impact foot forces from the time-history analysis are used to determine the maximum local bearing stress, punching shear stress, and overall load on the reinforced concrete floor. The overall floor load is obtained by computing the forces transmitted to the slab by the rack feet for one rack and calculating a total for all racks by the square-root-of-the-sum-of-the-squares method (SRSS) due to the random occurrence of the impact forces during a seismic event.

The Maine Yankee spent fuel pool foundation slab is analyzed using manual calculations. The applicable design code for the spent fuel pool reinforced concrete structure is ACI 318-63 (Ref. 4-1), including increases allowed for stresses produced by earthquake loads in combination with other appropriate loads (Ref. 4-2, Section 5.4.2.1). ACI 318-63 is the design code originally used for design of the spent fuel pool and all other safety related, Seismic Category I reinforced concrete structures at Maine Yankee. The allowable stresses for bearing and shear are defined by the criteria in Sections 10.14 and 11.10 of ACI 318-63.

The structure will maintain its structural integrity during the hypothetical earthquake, where the combination of the normal operating loads and the seismic stresses do not exceed 90% of the yield strength. The structure will remain functional during an operational basis earthquake. The structural analyses demonstrate that the structural integrity of the concrete structure is maintained when the spent fuel pool is assumed to be fully loaded with filled high density fuel racks.

Because the foundation slab is a 6-ft thick reinforced concrete slab bearing directly on bedrock, the increased loads produced by the increased rack loads are well within its load carrying capacity.

The new rack configuration causes a change in fuel pool wall loads, due to the racks/fuel assemblies being positioned closer to the walls. The loadings that change are those due to gamma heating (Section 4.2.3) and hydrodynamic pressures caused by the movement of the racks during a seismic event (Section 3.2).

The proposed Maine Yankee spent fuel storage rack replacement program will have no significant affect on the steel liner or 6-ft thick spent fuel pool walls.

MYAPCO is performing confirmatory analyses of the spent fuel pool walls to address all design basis loads, including rack-to-wall hydrodynamic effects associated with the installation of the new racks.

Cask Drop

The new rack configuration does not affect existing cask drop structural considerations since the cask and drop parameters did not change.

Spent Fuel Bundle Drop

The new rack configuration does not affect existing spent fuel bundle drop structural considerations since the fuel bundle handling and drop heights remain the same. Therefore, the previous evaluations of spent fuel bundle drops onto the steel liner and concrete mat remain valid.

Other Items Handled Over the Fuel Pool, Liner, and Foundation Slab

The new rack configuration does not affect existing structural considerations for other items handled over the fuel pool, liner, and foundation slab since the drop parameters remain the same. Thus, previous evaluations for drops of other items onto the steel liner and concrete mat remain valid.

4.2.3 Pool Wall Gamma Heating

The pool wall gamma heating is dependent upon the location of the spent fuel assemblies with respect to the walls. The pool wall gamma heating has been evaluated for the most limiting condition. The resultant heat rate does not impact the structural integrity of the wall.

4.3 SYSTEMS ANALYSIS

4.3.1 HVAC Performance

The Fuel Building HVAC system supplies and heats, as required, 9,000 cfm of outside air. The system exhausts 9,650 cfm; thus, the 650 cfm needed to balance supply and exhaust infiltrates into the building from surrounding areas resulting in a slightly negative pressure inside. The Fuel Building ventilation system outlet is provided with a charcoal filter that is bypassed during normal system operation. The charcoal filter is used during fuel handling operations. The Fuel Building HVAC system is powered from the normal bus.

Clean outdoor air is supplied to clean areas in the radiation control areas of the Fuel Building. Air is exhausted from radiation control areas in greater quantities than supplied so that the general flow of air is from clean or low activity areas to areas of relatively higher activity. The exhausted air is discharged past radiation monitors in the primary vent stack or the service building exhaust.

The Fuel Building HVAC system design remains as described in Reference 4-2. Because the additional spent fuel storage capacity does not affect building heat load or result in additional releases to the Fuel Building atmosphere (Section 7.1), there is no effect on the performance of the Fuel Building HVAC system.

4.3.2 Fuel Pool Cooling System

System Description

The fuel pool reracking does not alter the fuel pool cooling system. The fuel pool cooling system, its components, and interfaces with other plant systems remain as described in Reference 4-2.

The fuel pool cooling system removes the decay heat from spent fuel stored in the fuel pool by circulating the borated pool water through a heat exchanger. Two fuel pool cooling pumps take suction from the fuel pool, circulate the water through a heat exchanger, and return it to the fuel pool below normal water level. Primary component cooling water is used to remove heat from the fuel pool heat exchanger.

The fuel pool cooling system is designed to remove 22.0 MBtu/hr of decay heat while maintaining a fuel pool bulk temperature at or below 154°F. The system is capable of removing the decay heat generated by a full core discharge. Maine Yankee currently controls the spent fuel pool loading rate to ensure that the maximum heat load in the spent fuel pool does not exceed the design heat load, ensuring that the design conditions specified above are not exceeded. Further details on the fuel pool heat load are discussed in Section 5.2.

The fuel pool cooling system provides flange connections to allow the alignment of emergency cooling supplies in the unlikely event that all fuel pool cooling capability is lost.

The fuel pool cooling system also has a purification loop consisting of a pump, two filters, and a demineralizer which may be operated independently of the fuel pool cooling system when the fuel pool temperature is less than 130°F. The purification loop is shared by two other systems each having their own connections to the system. The connections provide a return path to the residual heat removal system and the refueling water storage tank. The purification return line is also used to provide makeup to the fuel pool from the blend tee in the chemical and volume control system.

Evaluation of Fuel Pool Reracking on System Description

The revised thermal-hydraulic analysis of the pool, discussed in detail in Chapter 5 of this report, was performed due to the change in the design geometry of the new fuel racks. The results of the analysis do not pose additional requirements on the fuel pool cooling system, any of the fuel pool cooling system components or operation of the system. This result was expected since the pool heat load design parameters were not changed from the previous design.

4.4 REFERENCES

4-1 Building Code Requirements for Reinforced Concrete, American Concrete Institute, Standard ACI 318-63.

4-2 Maine Yankee Final Safety Analysis Report, Revision 10.

5.0 THERMAL-HYDRAULIC CONSIDERATIONS

5.1 GENERAL DESCRIPTION

This chapter describes the calculations performed to demonstrate that the thermal-hydraulic characteristics of the proposed rack design, coupled with the proposed spent pool rack layout, are adequate to allow sufficient cooling of the spent fuel under normal and postulated accident conditions.

The NRC position on spent fuel pool modification (Ref. 5-1) entitled "OT Position for Review and Acceptance of Spent Fuel Storage and Handling Applications," issued on April 14, 1978 (later amended on January 18, 1979), has been used as a guideline for addressing potential concerns with the thermal-hydraulic aspects of the proposed rack design and pool layout.

Section III of Reference 5-1 identifies specific thermal-hydraulic analyses and acceptance criteria associated with the spent fuel pool addressing the capability of the spent fuel pool cooling system to remove the decay heat load under various core discharge scenarios, the ability of the proposed pool layout and rack design to provide fuel pin and flux trap cooling, and the system response to postulated accident conditions. The thermal-hydraulic analysis methods presented in this section are consistent with those reviewed and approved in the previous Maine Yankee rerack safety evaluation (Ref. 5-2), as well as in licensing submittals for Vermont Yankee (Docket 50-271) and Yankee Rowe (Docket 50-29).

To address the thermal-hydraulic analyses identified in Reference 5-1, this chapter is divided into three sections addressing the pool decay heat load, assembly/fuel pin cooling, and loss of forced pool cooling events. A summary of the analyses described in each section is provided below. Acceptance criteria were developed for each analysis to meet the intent of the NRC position paper and to be consistent with the licensing basis established in the previous Maine Yankee rerack safety evaluation (Ref. 5-2).

Section 5.2, "Spent Fuel Pool Decay Heat Load," describes analyses performed to demonstrate the adequacy of the spent fuel cooling system design performance with the proposed fuel rack layout considering the increase in storage locations from 1476 to 2019. This section provides a description of the analyses performed to address the spent fuel pool and cooling system response to a normal (1/3) core discharge refueling case as well as a full core discharge case.

Section 5.3, "Fuel Assembly/Pin Cooling Analysis," describes analyses performed to demonstrate the adequacy of the spent fuel pool layout and rack hydraulic design characteristics with respect to the coolability of the individual fuel assemblies under normal operating conditions. Thermal-hydraulic evaluations were performed to determine the limiting areas in the spent fuel pool. Specific analyses were performed, using the RETRAN computer code (Ref. 5-3) to conservatively predict the limiting fuel cell coolant conditions to verify that localized boiling will not occur within the spent fuel pool. The limiting cell was then evaluated to determine the peak pin surface, cladding, and fuel pellet temperatures. Analyses were also performed to demonstrate that sufficient cooling flow exists within the flux traps between fuel cells in the Region I racks to preclude boiling due to gamma heating. Cooling of the BORAL™ material via conduction to the pool water was also evaluated.

Section 5.4, "Loss of Forced Pool Circulation," describes analyses performed to evaluate the transient effects on the spent fuel pool and cooling system under postulated accident conditions. Accident conditions include a partial loss of spent fuel pool primary circulation, a complete loss of primary circulation, and a complete loss of spent fuel pool heat exchanger cooling flow. This section also describes alternative methods established for cooling of the spent fuel pool water and providing makeup to the spent fuel pool under postulated accident conditions.

5.2 SPENT FUEL POOL DECAY HEAT LOAD

The spent fuel pool cooling system design is described in the Maine Yankee FSAR, Section 9.8; and in Section 4.3.2 of this report. The spent fuel pool cooling system design parameters are provided in Table 5-1.

This section describes analyses performed to demonstrate the adequacy of the spent fuel cooling system design performance with the proposed fuel rack layout. A description of the method used to ensure that the heat load in the pool will not exceed the design capacity of the spent fuel pool cooling system, considering an increase in storage locations from 1476 to 2019, is provided. Results are provided for the spent fuel pool system response to a normal core discharge refueling case as well as a full core discharge case.

The acceptance criterion established for this analysis is that the heat load in the spent fuel pool cooling system is maintained less than or equal to the licensed basis system design heat load. This ensures that the system components are not subjected to thermal-hydraulic conditions beyond their design specifications.

5.2.1 Spent Fuel Pool Decay Heat Load Calculation

Maine Yankee currently restricts fuel unloading through administrative controls approved in the previous Maine Yankee rerack effort safety evaluation (Ref. 5-2). Fuel movement from the reactor vessel to the spent fuel pool is restricted to a rate which prevents the total decay heat load in the pool from exceeding the spent fuel pool cooling system design heat load. To restrict the heat load on the spent fuel pool cooling system, a fuel discharge schedule is generated prior to each refueling shutdown. The method of developing this discharge schedule, which was approved in the previous Maine Yankee rerack safety evaluation (Ref. 5-2), is described as follows:

1. Each fuel assembly batch residing in the spent fuel pool prior to the discharge is tracked for total burnup and discharge date. Table 5-2 provides the current spent fuel pool assembly inventory as well as projections through the end of license. For each batch, the decay power is projected at the time of the start of the fuel discharge. All decay heat calculations used Branch Technical Position APCSB 9-2, "Residual Decay Energy for Light Water Reactors for Long Term Cooling," Rev. 2, July 1981.

2. Each fuel assembly residing in the vessel is tracked (burnup, relative power), and its decay power is projected as a function of time after shutdown.

3. Based on the sum of the decay power of the assemblies residing in the spent fuel pool prior to the fuel discharge (conservatively assumed constant during refueling) and the time dependent decay power of the assemblies in the vessel to be discharged, a schedule of assembly spent fuel pool loading versus time after shutdown is generated. The rate of discharge is restricted to ensure that the total decay heat load in the spent fuel pool does not exceed the cooling system design heat load.

Use of this discharge schedule ensures that the acceptance criterion for this analysis is met, regardless of the number of fuel cells added to the spent fuel pool by this reracking effort. This ensures that the pool and system components are not subjected to thermal-hydraulic conditions beyond their design specifications. Table 5-1 provides a summary of the spent fuel pool cooling system design conditions, including the peak system heat load and peak pool bulk temperature.

5.2.2 Normal Refueling Core Discharge Scenario

A typical refueling at Maine Yankee involves a normal core discharge into the spent fuel pool. Fuel will be cooled in the reactor vessel for a minimum of 6 days following a shutdown before fuel can be removed from the reactor vessel. Following this time period, the total decay heat level of the fuel to be discharged combined with the existing heat load in the spent fuel pool prior to the fuel discharge is less than the design heat load of the spent fuel pool cooling system. This is verified prior to fuel discharge for each cycle. Thus, under a normal core discharge, cooling fuel in the reactor vessel for 6 days prior to fuel movement is adequate to ensure that the heat load in the spent fuel pool does not exceed the design heat load of the spent fuel pool cooling system. Table 5-1 provides a summary of the peak conditions in the spent fuel pool under a normal core refueling discharge scenario conservatively assuming all the assemblies have been loaded into the pool 6 days after shutdown.

5.2.3 Full Core Discharge Scenario

The decay heat load corresponding to a full core discharge when combined with the existing decay heat load in the spent fuel pool is greater than the design heat load of the spent fuel pool cooling system after 6 days of in-vessel cooling. In the event a full core discharge is required, fuel movement rates will be restricted using the discharge schedule described in Section 5.2.1. Figure 5-1 illustrates the discharge schedule projected for Cycle 13/14 and a schedule for the projected end of plant license (Cycle 23). Table 5-3 provides a summary of the Cycle 13/14 decay heat load in the pool and the projected heat load for the final discharge (Cycle 23), assuming all 2019 spent fuel pool storage locations are filled. The average core operating cycle length was assumed to be 18 months inclusive of outage time. For all future cycles, core power was assumed to be 2700 MW_T.

The use of the discharge schedule limits the total heat load in the pool to ensure that the pool bulk water temperature does not exceed 154°F. To verify that this limit is not exceeded, after the first third of the core is discharged, the pool bulk water temperature is monitored following the insertion of each additional fuel assembly to verify that the limiting pool temperature of 154°F is not exceeded. Should the pool bulk water temperature exceed 154°F, recently discharged fuel will be returned to the reactor vessel until the pool water temperature drops to or below 154°F. This requirement is consistent with the previous Maine Yankee rerack safety evaluation (Ref. 5-2).

5.2.4 Summary/Conclusions

The administrative controls currently in place at Maine Yankee ensure that the design limits of the spent fuel pool cooling system listed in Table 5-1 are not exceeded under a normal and full core discharge scenario. The results of this section demonstrate that as more storage locations become filled, the incremental increase in residual heat load in the pool will result in slightly longer full core off-load times. However, the maximum heat load in the pool will not be increased beyond the spent fuel pool cooling system design conditions.

5.3 FUEL ASSEMBLY/PIN COOLING ANALYSIS

This section describes analyses performed to demonstrate the adequacy of the spent fuel pool layout and rack hydraulic design characteristics with respect to the coolability of the individual fuel assemblies under normal operating conditions. Details on the spent fuel pool layout and rack design are presented in Chapters 1 and 2 of this report.

Thermal-hydraulic evaluations are described that identify the limiting areas in the spent fuel pool. Specific analyses were performed using the RETRAN computer code (Ref. 5-3) to conservatively predict the limiting fuel cell coolant conditions to verify that localized boiling will not occur within the spent fuel pool. The limiting cell was then evaluated to determine the peak pin surface, cladding, and fuel pellet temperatures. Analyses were also performed to demonstrate that sufficient cooling flow exists within the flux traps between fuel cells in the Region I racks to preclude boiling due to gamma heating.

The acceptance criteria established for the analyses performed in this section are as follows:

1. The calculated peak cell coolant exit temperature does not exceed the local saturation temperature of the coolant at the top of the active fuel. This ensures adequate pin cooling while maintaining cell thermal-hydraulic conditions that are consistent with the criticality analysis assumptions (i.e., no voiding).

2. The calculated local peak cladding and fuel pellet temperatures are sufficiently cool to ensure continued long-term integrity.

3. The calculated peak temperature in the flux trap for the Region I racks does not exceed the local saturation temperature at the top of the active fuel. This ensures adequate flux trap cooling while maintaining thermal-hydraulic conditions that are consistent with the criticality analysis assumptions (i.e., no voiding).

A detailed thermal-hydraulic analysis was conducted to ensure that each fuel assembly receives adequate local cooling. The analysis was performed using the RETRAN computer code and is consistent with methods reviewed and approved in previous licensing submittals for Maine Yankee (Ref. 5-2), Vermont Yankee (Docket 50-271), and Yankee Rowe (Docket 50-29).

5.3.1 Limiting Fuel Cell Location Evaluation

The proposed spent fuel pool rack layout is illustrated on Figure 5-2. The proposed layout includes two regions with two different rack designs as described in Chapter 2 of this report. The Region I racks, which are located around the north-east corner of the pool, are available for any assembly burnup and enrichment conditions up to the upper limits defined in Chapter 6. Fuel placed in the Region II racks will be restricted based on the enrichment and burnup limits described in Chapter 6.

The natural circulation cooling patterns in the spent fuel pool are multi-dimensional. Discharged assemblies will heat the coolant within the cell. The resulting lower density fluid rising in these cells will cause water to flow downward through cooler and unheated spots in the spent fuel pool. Thus, areas such as the cask laydown area, the fuel transfer canal, the fuel elevator, the spacing between the racks and the pool walls, the empty fuel storage cells, and even the cells containing relatively low decay powered assemblies become the primary downcomer areas in the pool. A steady-state flow distribution is established when the elevation head and frictional/form pressure losses in the upflow cells match the elevation head and frictional/form pressure losses of the higher density fluid in the downcomer regions.

To evaluate detailed coolant flow to a cell, the spent fuel pool is conservatively reduced to a 2-D model. Credit is taken only for coolant flowing downward between the fuel rack and the wall. This downward flow area will be referred to as the downcomer. No credit is taken for flow available from a third dimension. Flow is then required to traverse the floor until reaching the farthest cell from the wall. Thus, the limiting region can be determined by identifying the cells which a) are farthest away from an available downcomer flow path, and b) draw coolant from a relatively narrow downcomer gap spacing. As illustrated on Figure 5-3, the limiting area is identified near the intersection of Racks L, M, S, and T. Since the potential exists for operators to fill cells from the pool wall on the north side to this area with freshly discharged assemblies, the coolant conditions in these cells are modeled.

5.3.2 RETRAN Fuel Cell Model Description

A 2-D approach is used that selects a single row of storage cells, containing freshly discharged fuel assemblies from the north wall to the most limiting location identified on Figure 5-3. This 2-D modeling approach has been demonstrated to be conservative with respect to a 3-D analysis (Refs. 5-3 and 5-5) and has been approved in previous submittals identified in Section 5.1.

The limiting row of 20 Region II rack cells is illustrated in the RETRAN nodalization diagram, Figure 5-4, which shows all the flow paths assumed in this analysis. Conservative fluid friction and form losses were assumed for all flow paths. As shown on Figure 5-4, credit is taken for downcomer flow only from the space between the rack wall and the north wall. In reality, additional flow would be available from the cask laydown area and the fuel transfer mechanism area as well as from downward flow through nearby cells containing lower powered assemblies.

The following key assumptions were incorporated into the RETRAN model to provide a conservative peak cell exit coolant temperature.

1. Fuel assemblies were assumed to cool in the reactor for 6 days following shutdown prior to the beginning of fuel discharge. Fuel was assumed to be loaded into the cells from the pool wall directly out from the wall to the limiting area. It was assumed that an additional day was required to discharge a sufficient number of fuel assemblies to attain the design system heat load in the pool and to heat the pool bulk temperature to its design condition. Table 5-4 summarizes the assembly power parameters and assumptions, as well as the fuel and the rack dimensional parameters used in the RETRAN model. All decay heat calculations used Branch Technical Position APCSB 9-2.

2. The only downcomer space credited is the downcomer established assuming the minimum spacing between the rack and the pool wall for racks N and EE at the north side of the pool. Flow contributions from the cask laydown area and other adjacent downcomer areas are conservatively neglected.

3. Downcomer flow in the spacing between rack modules is conservatively neglected.

4. The cells are assumed to be filled with fuel assemblies containing a debris resistant inlet spacer grid since the flow resistance of these bundles bounds all other fuel types.

5. No heat transfer between cells is credited.

6. The RETRAN model contains 20 cells in the Region II racks. A parallel model incorporating the Region I rack would contain virtually the same flow resistance, but with one less cell. Thus, the RETRAN model bounds both the Region I and Region II racks.

7. The temperature of the coolant in the downcomer is assumed to be equivalent to the bulk temperature of the spent fuel pool. No credit is taken for coolant returning from the spent fuel pool heat exchanger at a lower temperature.

8. Coolant exiting the cells is assumed to mix completely with the bulk fluid above the racks. It has been demonstrated that stratification does not have a significant effect above the cell exits based on the conclusions of References 5-4 and 5-5.

9. All cells are conservatively assumed to contain a relatively high powered assembly as described in Table 5-4.

5.3.3 Cell Exit Coolant Temperature Results

The analytical results show the peak cell exit temperature to occur in the farthest cell (i.e., 20th cell) away from the pool wall of the row of freshly discharged fuel assemblies. Results of this analysis are summarized in Table 5-5. The maximum outlet temperature for the limiting fuel assembly is well below the saturation temperature at the cell outlet. Since no local boiling has been calculated to occur, the acceptance criterion for the assembly void fraction has been met.

5.3.4 Fuel Pin Temperatures

Having determined the thermal-hydraulic conditions of the limiting fuel cell, this section provides an evaluation of the local conditions of the fuel pins within the limiting cell. Assuming a conservatively high local pin power within the peak assembly, the peak pin surface, cladding, and fuel pellet temperatures are calculated as a function of axial height. Within the reactor core, at the beginning of power operation, the axial power profile is generally in the form of a chopped cosine. However, as the center pellets burn up, the power tends to shift towards the top and the bottom of the core creating a flat axial profile by the end of the cycle. Figure 5-5 illustrates the two design axial power shapes from the Maine Yankee FSAR that were used to calculate the peak pin temperatures.

Given the axial dependent power shape and coolant conditions, the cell and assembly were nodalized axially, and conditions were manually calculated for each axial node using the conduction/convection model of a fuel pin illustrated on Figure 5-6.

The fuel pin temperature distribution is calculated in two parts. First, the temperature from the bulk fluid to the surface of the fuel pellet is calculated. Referring to Figure 5-6, the governing equation for temperatures through the fuel pin to the surface of the fuel pellet is:

$$q = \frac{T_1 - T_2}{\left[\dfrac{\ln(r_2/r_1)}{2\pi k_{He} L}\right]} = \frac{T_2 - T_3}{\left[\dfrac{\ln(r_3/r_2)}{2\pi k_{Zr} L}\right]} = \frac{T_3 - T_4}{\left[\dfrac{\ln(r_4/r_3)}{2\pi k_{ZrO_2} L}\right]} = \frac{T_4 - T_{BULK}}{\left[\dfrac{1}{2\pi r_4 L h}\right]}$$

where:

T_1	UO_2 pellet surface temperature (°F)
T_2	Zr cladding inner surface temperature (°F)
T_3	Zr cladding outer surface temperature (°F)
T_4	ZrO_2 layer outer surface temperature (°F)
T_{BULK}	Coolant bulk temperature (°F)
$r_{1\text{-}4}$	material boundary radii
q	heat generation rate (Btu/hr)
k	thermal conductivity (Btu/hr-ft-°F)
h	convection heat transfer coefficient (Btu/hr-ft^2-°F)
L	length, (ft)

For the pellet temperature distribution, the centerline temperature (assuming a conservatively low constant UO_2 thermal conductivity) is calculated using the following general equation:

$$\frac{d^2T}{dr^2} + \frac{1}{r}\frac{dT}{dr} + \frac{q'''}{k} = 0$$

where:

q''' pellet volumetric power generation rate (Btu/hr-ft^3)

From the above equation, the centerline temperature can be calculated from:

$$T_{CL} = \frac{q''' r_1^2}{4 k_{UO_2}} + T_1$$

Table 5-5 provides a summary of the maximum local pin temperature conditions. From the results of this analysis, the following can be concluded:

1. The peak fuel pin surface temperature is sufficiently cool to prevent the onset of local nucleate boiling. Thus, the conservative acceptance criterion on local boiling continues to be met. Nucleate boiling is not a concern with respect to coolability. However, the presence of local voiding is not consistent with the criticality assumptions.

2. The peak cladding temperature and the peak fuel pellet temperatures are not significantly above the coolant conditions. Thus, the acceptance criterion on fuel pin long term integrity is met.

5.3.5 Flux Trap Cooling

To evaluate the thermal-hydraulic ability of the Region I rack design to maintain cooling of the flux traps between cells, the RETRAN model described in Section 5.3.2 was modified to incorporate flux traps between the cells. The open sided arrangement of the Region I rack design combined with the 1-in. vent holes at the top of each cell provides adequate flow throughout the inter-cell region to remove gamma heat. Calculations were also performed to ensure sufficient cooling via conduction for the BORAL™ material (melting temperature = 1190 °F) and water layered between the cell wall and the stainless steel outer layer described in Chapter 2. Thus, the acceptance criterion on flux trap cooling has been met in that no voiding will occur. This ensures that the assumption of no voiding in the flux trap region in the criticality analysis remains valid.

5.3.6 Blocked Cell Analysis

Using the RETRAN model, an analysis was performed to determine the impact on the pin cooling analysis resulting from a misplaced or dropped fuel assembly laying horizontally across the top of the limiting spent fuel storage cell. Conservatively neglecting flow upwards through the horizontal fuel pins, this event results in a net blockage of the fuel cell exit area by 79%. The results of this analysis, provided in Table 5-5, show that there is no significant increase in the limiting cell coolant exit temperature. This is an expected result given that the additional flow resistance caused by the cell exit blockage is negligible relative to the total resistance for the flow path from the downcomer through the limiting cell.

5.4 LOSS OF FORCED POOL CIRCULATION

The Maine Yankee spent fuel pool cooling system is described in detail in the FSAR, Section 9.8; and in Section 4.3.2 of this report. This section describes analyses performed to evaluate the transient effects on the spent fuel pool and cooling system under postulated accident conditions. Accident conditions include a partial loss of spent fuel pool primary circulation under a normal and full core discharge scenario, a complete loss of primary circulation, and a complete loss of spent fuel pool heat exchanger cooling flow. This section also describes alternative methods established for cooling of the spent fuel pool water and providing makeup to the spent fuel pool under postulated accident conditions.

For a partial loss of primary circulation following a normal core discharge scenario, the acceptance criterion is that the maximum temperature achieved in the pool does not exceed the spent fuel bulk design temperature limit described in Section 5.2. This criterion ensures that the local coolant conditions for this scenario are bounded by the conditions assumed in the pin cooling analysis (Section 5.3).

For a partial loss of primary circulation during a full core discharge scenario, the acceptance criterion is that under design heat load conditions, bulk boiling does not occur in the spent fuel pool. This acceptance criterion is consistent with the previous Maine Yankee safety evaluation (Ref. 5-2).

For a complete loss of circulation and/or heat exchanger cooling during a full core discharge, the acceptance criterion is that sufficient time exists prior to bulk pool boiling to allow for implementation of the alternative methods of cooling.

5.4.1 Loss of One Spent Fuel Pool Cooling Pump

The loss of one spent fuel pool cooling pump during a fuel offload will result in an increase in the pool bulk water temperature and heat exchanger conditions. The system response to this event would be a slow heatup of the spent fuel pool bulk water temperature. Steady-state calculations were performed to determine the peak bulk pool temperature and heat exchanger conditions following a loss of one of the two spent fuel pool cooling pumps during a normal off-load and full core discharge scenario. No credit was taken for heat loss by conduction through the pool walls and floor or for evaporation from the pool surface. The results of these calculations are provided in Table 5-6.

For a loss of one spent fuel pool cooling pump following a normal core discharge, the peak pool bulk water temperature remains below the system design temperature. This ensures that the conditions assumed in Section 5.3 are bounding for this case. Thus, no local boiling would occur for a loss of one pump following a normal core discharge. For a loss of one spent fuel pool cooling pump following a full core discharge, the peak pool bulk temperature remains below the saturation temperature.

5.4.2 Loss of All Forced Circulation Cooling Flow/Total Loss of Spent Fuel Pool Cooling

If all the forced circulation cooling flow to the pool is lost following a full core discharge or for a loss of heat exchanger cooling, the large volume of pool water will provide a heat sink that will allow time for corrective action. The minimum time for the bulk pool water temperature to reach saturation as well as the pool makeup requirements during bulk pool boiling is provided in Table 5-7. These results assume the initial heat load and pool bulk water temperature are at the design conditions listed in Table 5-1, and the initial pool water level is at the minimum level at which the cooling system could operate.

5.4.3 Alternative Methods for Cooling and Makeup

In the event that normal cooling is lost on either the shell or tube side of the pool heat exchanger, backup cooling is available. The plant fire protection system, with two 2500 gpm pumps, can be connected to the pool heat exchanger shell side via two emergency cooling connections (designated ECC on FSAR Figure 9.8-1). Heat exchanger tube side flow is normally provided by two 750 gpm pumps. In the event that one pump is lost, the alternate pump is available to provide flow.

Normal or routine makeup to the spent fuel pool is accomplished via the Chemical and Volume Control System (CVCS). The operator has the option of using any of the following methods:

1. Batch makeup from the refueling water storage tank

2. Batch makeup of demineralized water and/or concentrated boric acid

3. Blended makeup of demineralized water and concentrated boric acid

The valve lineups required to perform any of the above tasks take less than 15 minutes. Each of the above makeup options can provide greater than 150 gpm flow into the spent fuel pool, which is adequate flow to maintain the water inventory.

Additionally, there are at least three primary grade water hose connections in the vicinity of the spent fuel pool. Each of these connections can provide approximately 20 gpm makeup flow to the spent fuel pool via hoses. The combined makeup from this source would be in excess of 60 gpm. Again, this option could be implemented in less than 15 minutes.

In an emergency situation, where normal makeup means were not available, makeup from the fire main system is also available. Using one or more fire hoses, makeup rates in excess of 150 gpm could be accomplished. This makeup flow could be established in less than 20 minutes.

Thus, based on the minimum time to saturation provided in Table 5-7, the above options provide adequate time to establish alternati·e cooling and/or makeup paths to the spent fuel pool.

5.5 REFERENCES

5-1 Letter USNRC to Licensees, "OT Position for Review and Acceptance of Spent Fuel Storage and Handling Applications," April 14, 1978 (amended January 18, 1979).

5-2 Letter USNRC, Robert A. Clark - Chief of Operating Branch Number 3, Division of Licensing to John A. Garrity (MYAPCO), "Safety Evaluation and Environmental Impact Appraisal Regarding Maine Yankee Spent Fuel Storage," June 16, 1982.

5-3 "RETRAN-02 -- A Program for Transient Thermal-Hydraulic Analysis of Complex Fluid Flow Systems," EPRI NP-1850-CCM-A.

5-4 "GFLOW Thermal-Hydraulic Code Volume 1: Spent Fuel Pool Licensing Analysis and Sensitivity Studies," NP-3381-CCM, November 1984.

5-5 C. L. Wheeler, NUREG/CR-5048, PNL-6388, "Review of the Natural Circulation Effect in the Vermont Yankee Spent Fuel Pool," January 1988.

TABLE 5-1

MAINE YANKEE SPENT FUEL POOL COOLING SYSTEM PARAMETERS

Component	Cooling System Design Conditions/ Maximum Conditions for Full Core Discharge	Maximum Conditions for Normal Discharge
System Heat Load (BTU/hr)	22.0×10^6	15.3×10^6
Heat Exchanger Shell Side (PCC) Inlet Temperature (°F)	85	85
Heat Exchanger Shell Side (PCC) Exit Temperature (°F)	137	121
Spent °Fuel Pool Bulk/ Heat Exchanger Tube Side (SFP) Inlet Temperature (°F)	154	134
Heat Exchanger Tube Side (SFP) Exit Temperature (°F)	124	113
Fuel Pool Cooling Pump Flowrate (each - gpm)	750	750

TABLE 5-2

MAINE YANKEE SPENT FUEL POOL ASSEMBLY INVENTORY

Cycle	No. Assy	Cycle Length (MWD/MT)	Cycle Loading (KGU)		Basis of Cycle Length and Burnup
			Design	As-Built	
1	72	10367	81544	81434	Measured
1A	152	4492	83111	83086	Measured
2	70	17365	80885	81027	Measured
3	133	11105	83065	83128	Measured
4	73	10500	81843	81817	Measured
5	73	10799	83034	83008	Measured
6	73	11585	82249	82222	Measured
7	73	12483	81012	80905	Measured
8	73	12504	80528	80232	Measured
9	67	14424	80465	80119	Measured
10	65	12675	81450	81231	Measured
11	73	13786	82354	82385	Measured
12	61	15657	83231	83050	Targeted
13	77	11807	82999	83024	Estimated
14	69	16198	82841	82912	Estimated
15	69	14758	82669	82710	Estimated
16	73	13885	82664	82664	Estimated
17	65	15027	82695	82694	Estimated
18	73	14153	82695	82694	Estimated
19	65	14441	82695	82694	Estimated
20	73	14299	82695	82694	Estimated
21	65	14547	82695	82694	Estimated
22	73	14200	82695	82694	Estimated
23	217	14569	82695	82694	Estimated

TABLE 5-3

PROJECTED REQUIRED DECAY TIMES FOR FULL CORE DISCHARGE

	Projected Cycle 13/14 Discharge	Projected Cycle 23 Discharge
SFP Cooling System Design Heat Load, (Btu/hr)	22.0×10^6	22.0×10^6
SFP Heat Load Prior to Fuel Off-Load, (Btu/hr)	3.4×10^6	4.9×10^6
Available Heat Load for Fuel Off-Load, (Btu/hr)	18.6×10^6	17.1×10^6
Required Cooling Period for Full Core Off-Load, (Days)	19	23

TABLE 5-4

CELL COOLING/PIN COOLING MODEL PARAMETERS

Category	Parameter	Value
RETRAN Model Assembly Power Data	Assembly Type	14 X 14 Debris-resistant
	Assembly Power (MBtu/hr)	64.97
	Assembly Relative Power (F_R)	1.50
	Assembly Burnup (MWD/MTU)	70,000
	Time After Shutdown (days)	7.0
RETRAN Model Rack Dimension Data	Number of Cells Modeled	20
	Cell Flow Area (ft^2)	0.345
	Cell Height (ft)	14.00
	Cell Pitch (in.)	9.085
	Min. Spacing Between Rack and Pool Wall - Downcomer Spacing (in.)	2.875
	Min. Spacing Between Cell Bottom and Floor (in.)	2.5
Pin Cooling Data	Maximum Pin F_R	1.70
	Axial Profile	Fig. 5-5
	Active Fuel Length (in.)	136.25
	Fuel Pellet OD (in.)	0.3765
	Zircaloy Clad OD/Thickness (in.)	0.440/.028
	ZrO_2 Corrosion Layer Thickness (microns)	200

TABLE 5-5

ASSEMBLY COOLING ANALYSIS RESULTS

	Normal Flow Conditions	79% Cell Blockage
Saturation Temperature at Bundle Exit (°F)	236.0	236.0
Peak Cell Exit Temperature (°F)	226.5	226.6
Peak Pin Local Surface Temperature (°F)	237.7	237.8
Peak Pin Local Clad Temperature (°F)	239.1	239.2
Peak Pellet Centerline Temperature (°F)	245.9	246.0

TABLE 5-6

HEAT EXCHANGER CONDITIONS - LOSS OF ONE FUEL POOL COOLING PUMP

Component	Normal Core Discharge		Full Core Discharge	
	Initial Conditions (2 Pumps)	Maximum Conditions (1 Pump Failure)	Initial Conditions (2 Pumps)	Maximum Conditions (1 Pump Failure)
System Heat Load (Btu/hr)	15.3×10^6	15.3×10^6	22.0×10^6	22.0×10^6
Heat Exchanger Shell Side (PCC) Inlet Temperature (°F)	85	85	85	85
Heat Exchanger Shell Side (PCC) Exit Temperature (°F)	121	121	137	137
Spent Fuel Pool Bulk/ Heat Exchanger Tube Side (SFP) Inlet Temperature (°F)	134	150	154	177
Heat Exchanger Tube Side (SFP) Exit Temperature (°F)	113	109	124	116
Fuel Pool Cooling Pump Flowrate (gpm)	1500	750	1500	750

TABLE 5-7

COMPLETE LOSS OF FORCED CIRCULATION/COOLING RESULTS

Event	Limit	Result
Loss of All Forced Circulation - Full Core Discharge Scenario	Minimum initial pool water volume (gal)	3.04×10^5
	Minimum time for bulk pool water temperature to reach saturation (hr)	6.5
	Boil off/make-up rate (gpm)	50

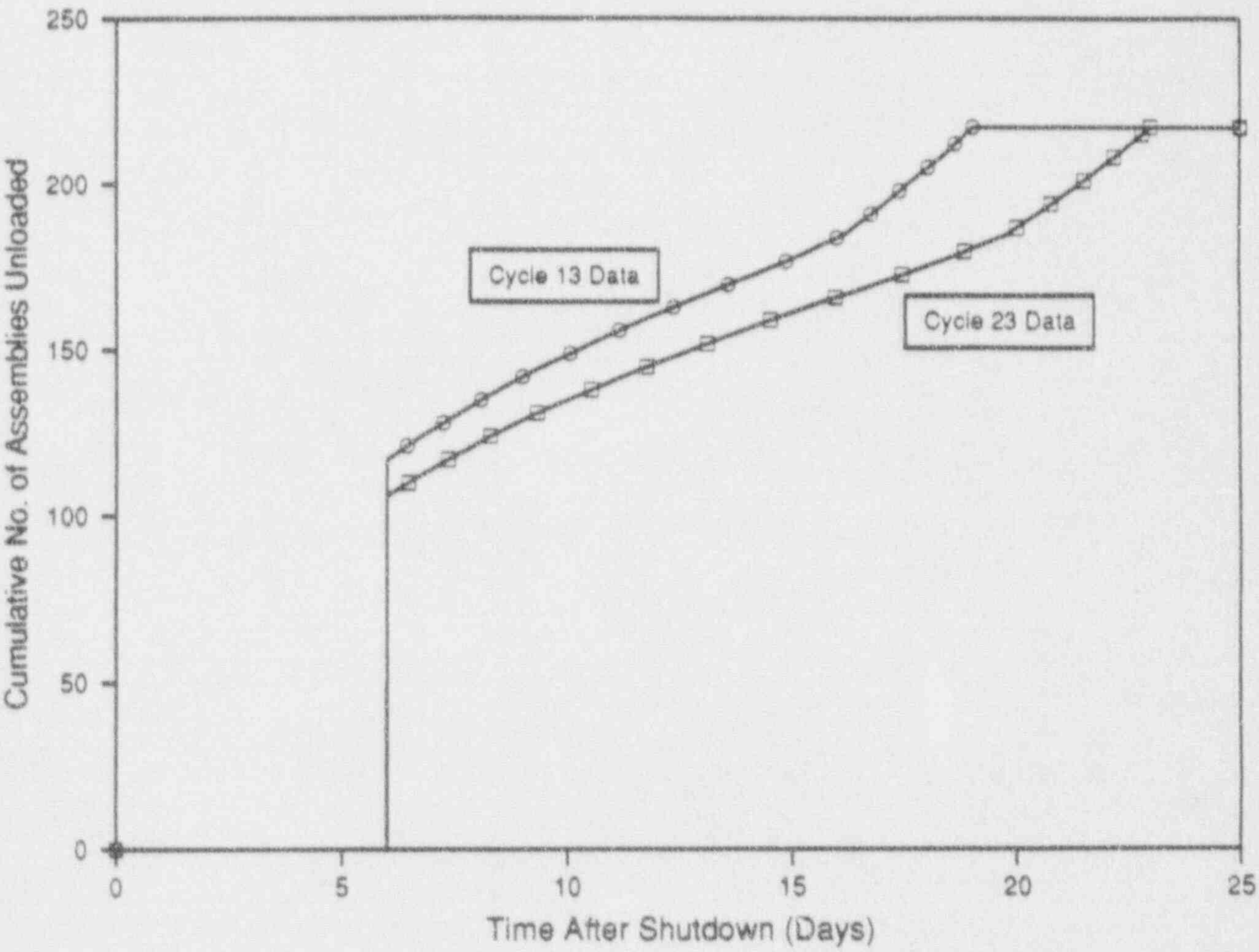

FIGURE 5-1
SPENT FUEL POOL
LOADING SCHEDULES

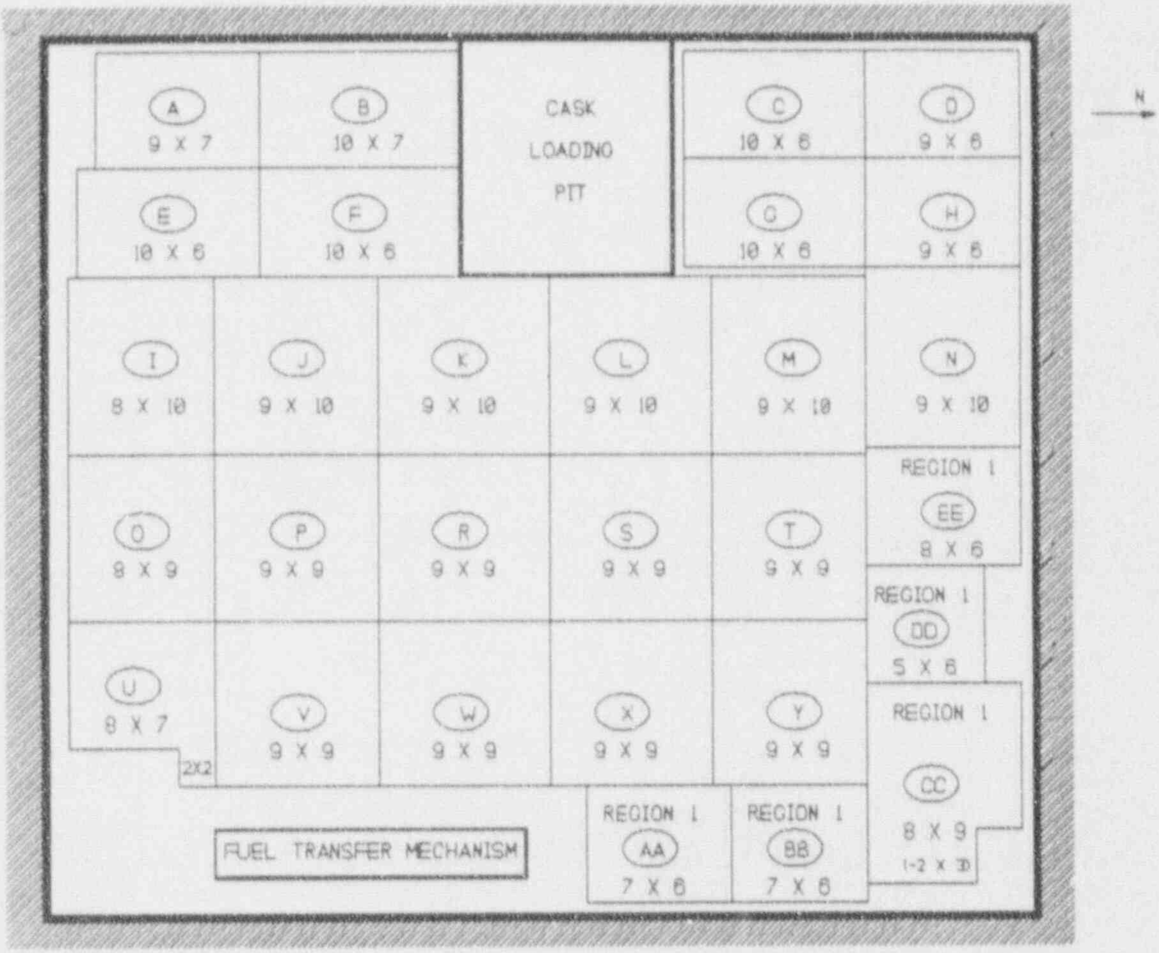

FIGURE 5-2
PROPOSED MAINE YANKEE
SPENT FUEL POOL LAYOUT

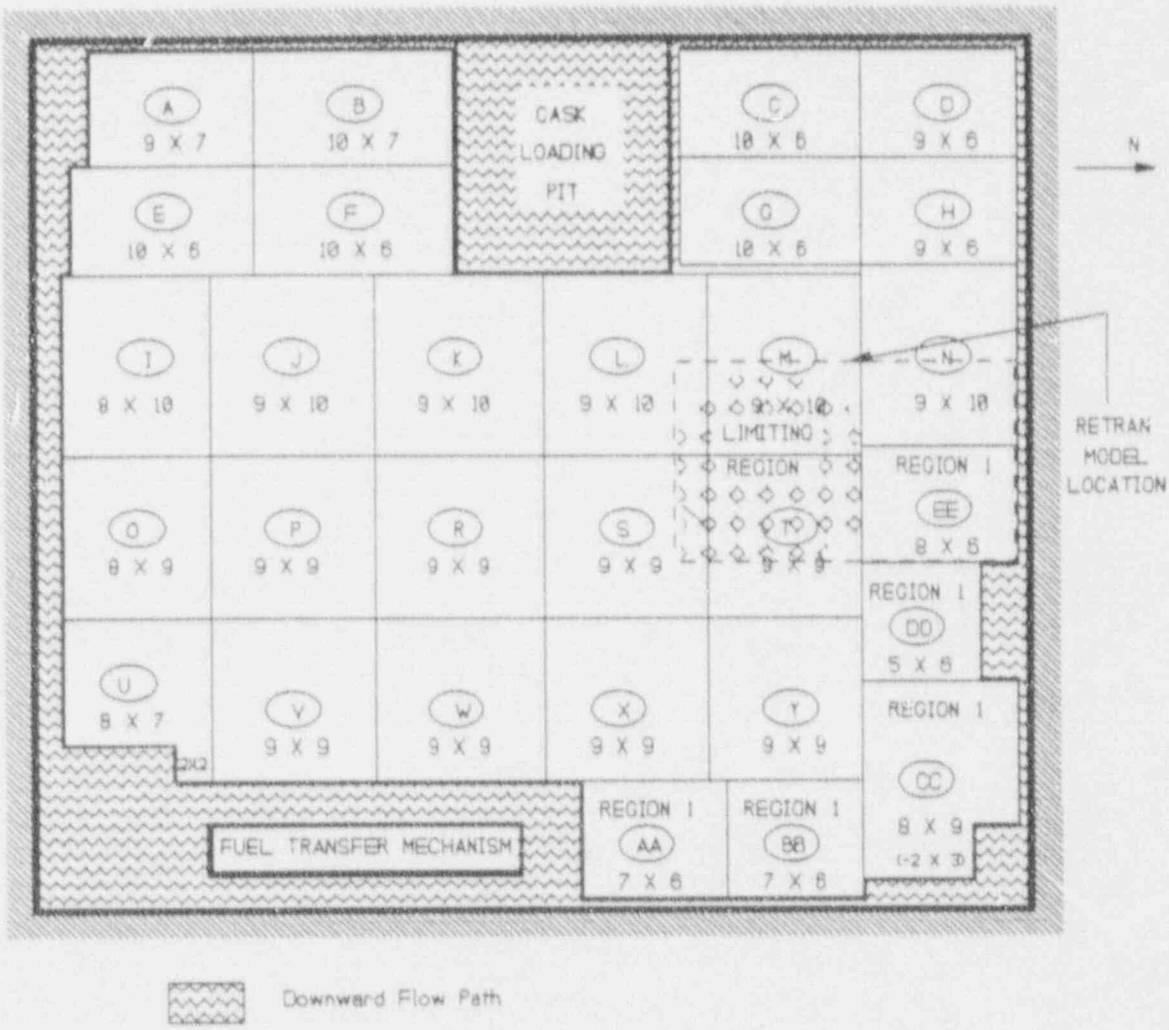

FIGURE 5-3
SPENT FUEL POOL
FLOW LIMITING LOCATIONS

MAINE YANKEE ATOMIC POWER COMPANY

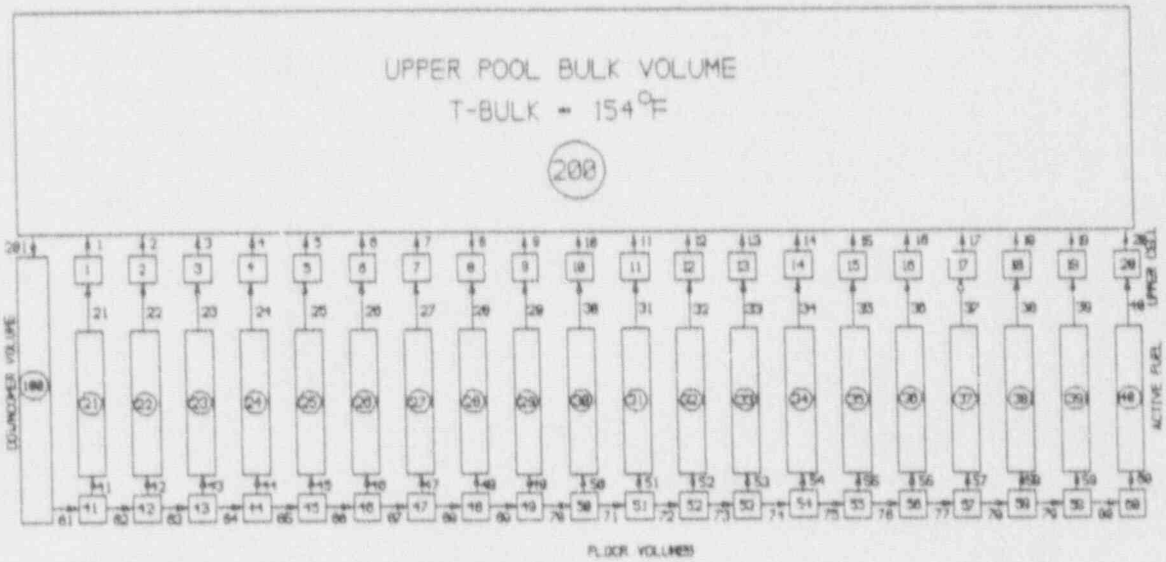

FIGURE 5-4
RETRAN02 MOD5
SPENT FUEL POOL

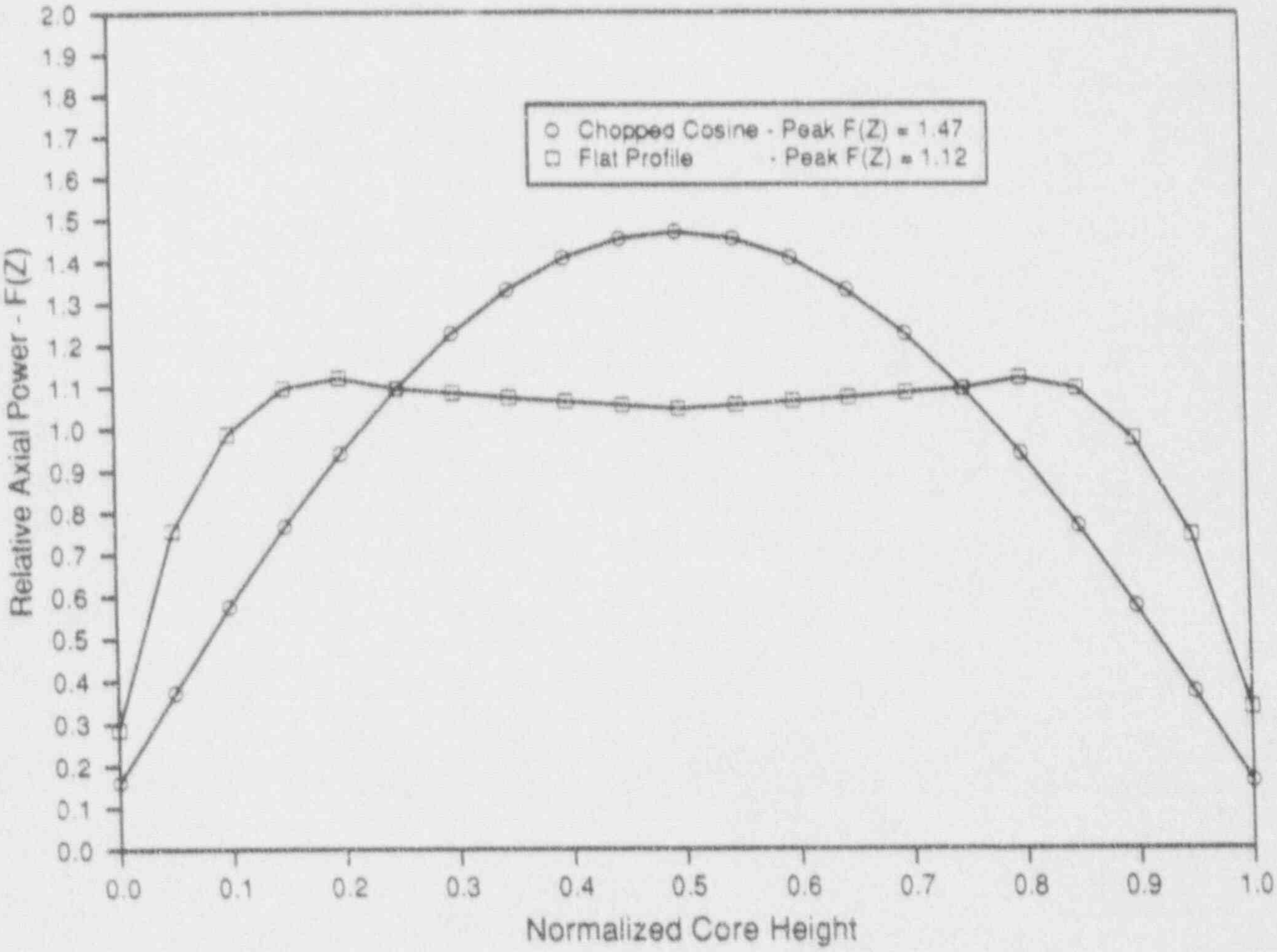

FIGURE 5-5
LIMITING FUEL CELL
AXIAL PROFILE

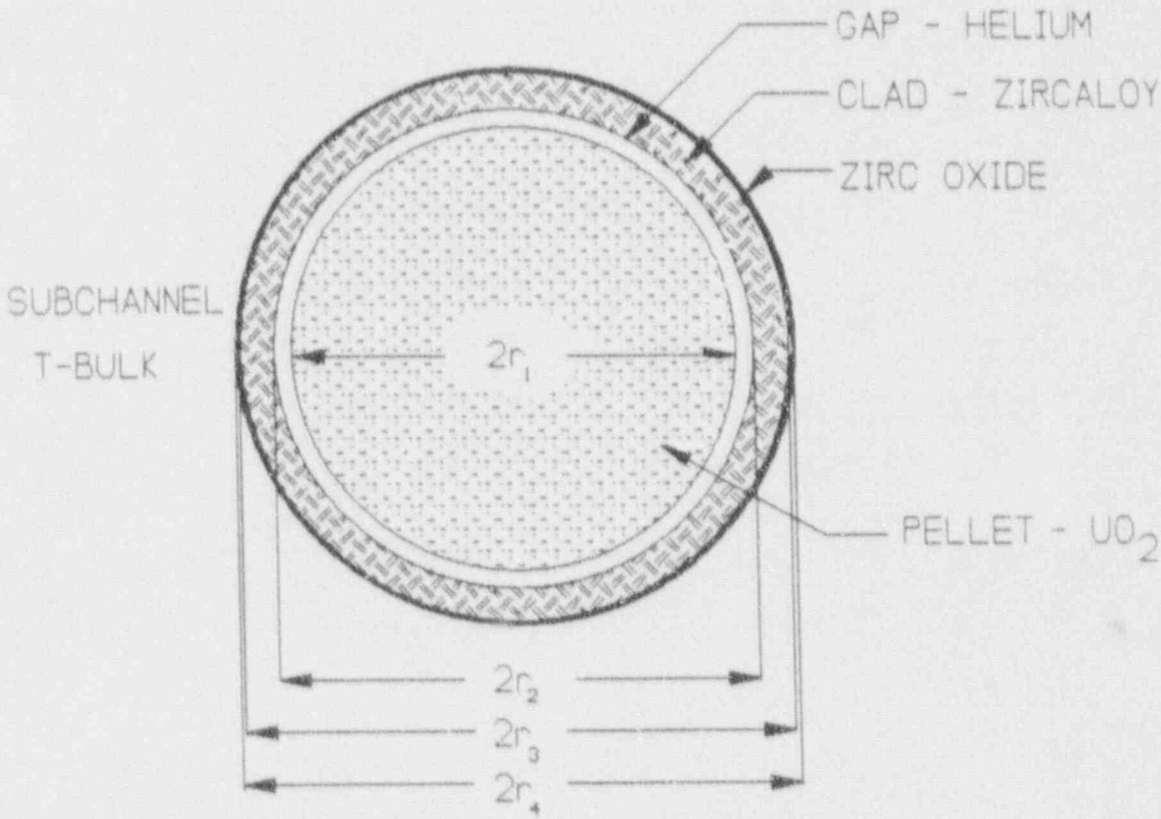

FIGURE 5-6
FUEL PIN CROSS-SECTIONAL CONDUCTION MODEL

6.0 NUCLEAR SAFETY

6.1 CRITICALITY ANALYSIS

6.1.1 Description

The applicable regulations, guides and standards pertaining to criticality safety for spent fuel and new fuel storage include the following:

- General Design Criterion 66 - Prevention of Criticality in Fuel Storage and Handling (note that Maine Yankee is licensed to the interim General Design Criteria issued in 1967).
- NUREG-0800, NRC Standard Review Plan, Section 9.1.2, Spent Fuel Storage and Section 9.1.1, New Fuel Storage.
- ANSI/ANS-57.2-1983, Design Requirements for Spent Fuel Storage Facilities At Nuclear Power Plants, Section 6.4.2.
- ANSI/ANS-57.3-1983, Design Requirements for New Fuel Storage Facilities at LWR Plants, Section 6.2.4.

These guides and standards state that for spent fuel racks the maximum calculated K_{eff}, including margin for uncertainty in calculational method and mechanical tolerances, be less than or equal to 0.95 with a 95% probability at a 95% confidence level. The criticality analysis of the proposed high density spent fuel racks demonstrates that this criteria is satisfied.

In order to assure the true reactivity will always be less than the calculated reactivity, the following conservative assumptions are made in calculating the criticality safety limits for the spent fuel racks:

- Pure, unborated water at 68°F is used in all calculations for non-accident conditions,
- A 2-D infinite array with no radial or axial leakage, and
- Neutron absorption in spacer grids is neglected, i.e. spacer grids are replaced by water.

6.1.2 Methodology

Yankee Atomic Electric Company (YAEC) has developed and validated a combination of criticality safety methods based on KENO-V.a Monte Carlo (Refs. 6-1 and 6-2), CASMO-3 LWR lattice integral transport (Ref. 6-3), PDQ-7 fine mesh diffusion theory (Ref. 6-4) and SIMULATE-3 nodal burnup credit analysis (Refs. 6-5 and 6-6). This permits criticality analysis by several independent methods and allows the flexibility to accommodate various LWR fuel types, fuel storage arrays and criticality safety assumptions. These methods and their applications are described in more detail below.

CASMO-3 is an integral transport lattice code with a hierarchy of energy condensation and spatial detail leading to a seven-group, transmission probability model of the fuel rack unit cell. The 70 micro-group nuclear data is used in all CASMO-3 calculations. CASMO-3 is flexible enough to accommodate up to a 19 x 19 fuel assembly array with storage canister regions, neutron absorber sheets, and water gaps. CASMO-3 can perform transport theory burnup credit analysis. In addition, CASMO-3 produces few-group cross sections for PDQ-7 fine mesh diffusion theory analysis and produces two-group homogenized cross sections for SIMULATE-3 nodal burnup credit criticality analysis on fuel storage arrays. For burnup credit analysis, hot full power fuel lattice depletions are executed and cold zero power restarts in rack geometry are performed.

In the Maine Yankee spent fuel rack analysis, CASMO-3 is used to study rack K_{eff} vs. fresh fuel enrichment, unit cell sensitivity to mechanical tolerances, and rack K_{eff} vs. burnup. Since the results of CASMO-3 calculations are deterministic, the dependance of K_{eff} vs. enrichment is monotonic and smooth. Also, a reactivity change, ΔK, from mechanical tolerances is not overwhelmed by stochastic uncertainty as would be if calculated using a Monte Carlo method.

In the KENO-V.a methodology, the NITAWL-S code prepares a working nuclide library and performs resonance self-shielding for U^{238}. In this analysis, the 123 group data is used in all KENO-V.a calculations. The working nuclide library along with case specific compositions and rack geometry data are input to KENO-V.a. KENO-V.a performs a multi-group, Monte Carlo eigenvalue calculation. The results from the KENO-V.a analysis are K_{eff} vs. generation, fluxes and reaction rates. In this analysis, KENO-V.a is used to verify the CASMO-3 spent fuel rack criticality results.

The PDQ-7 geometric mesh representation makes this code useful for analyzing abnormal configurations. PDQ-7 can analyze large array problems, therefore, it is used in the analysis of accident conditions.

The use of KENO-V.a, CASMO-3 and PDQ-7 for fuel storage criticality analysis has been validated by comparison to 21 B&W fuel storage critical experiments (Refs. 6-7 and 6-8). The methodology bias and uncertainty determined from this validation will be used in the calculation of K_{eff} at a 95/95 probability/confidence level.

In order to address the isotopic and axial burnup distribution issues associated with burnup credit, YAEC has developed and extended its incore methodology to excore fuel storage criticality analysis in fuel storage racks or casks (Ref. 6-9). This methodology is based on the advanced nodal method CASMO-3/TABLES-3/SIMULATE-3 (Refs. 6-3, 6-5, and 6-6) and permits direct coupling of incore reactivity characteristics with excore storage array criticality analysis. To determine axial burnup effects, two dimensional and three dimensional spent fuel rack criticality analyses are performed with SIMULATE-3.

The use of SIMULATE-3 nodal diffusion theory in fuel storage burnup credit criticality analysis has been validated by comparison to reactor critical measurements (Ref. 6-9), measured assembly burnup data (Ref. 6-9), 10 B&W fuel storage critical measurements (Ref. 6-7) and 11 PNL flux trap critical measurements (Ref. 6-10).

The above methodology has been used and approved on previous Maine Yankee spent fuel rack submittals (Refs. 6-11, 6-12, and 6-13).

6.1.3 Fuel Storage Cells

The proposed Maine Yankee spent fuel pool arrangement contains two rack designs designated Region I and Region II. The basic fuel storage cell is shown in Figure 6-1. The Region I rack module comprises an array of fuel storage cells with BORAL™ neutron absorber and a center-to-center spacing of 10.5 in. as can be seen in Figure 6-2. In Region I, criticality control is by the flux trap principle; fast neutrons leaking from stored assemblies are thermalized in the water gap between cells and are then absorbed in the BORAL™ sheets. The nominal rack dimensions and mechanical tolerances that are assumed in the criticality analysis are given in Table 6-1.

The Region II rack module comprises an array of fuel storage cells with BORAL™ neutron absorber arranged in an array of normal cells and virtual cells with a nominal center-to-center spacing of 9.085 in. The normal cell is composed of a stainless steel box with four neutron absorber sheets attached. The virtual cell is derived from combining four normal cells. This arrangement can be seen in Figure 6-3. In Region II, criticality control is from a combination of neutron absorption in the BORAL™ sheets and assembly burnup. The nominal rack dimensions and mechanical tolerances that are assumed in the criticality analysis are also given in Table 6-1. Chapter 2 provides detailed information on construction of the racks.

6.1.4 Analyses and Tolerances

The analysis assumes that standard Maine Yankee 14 x 14 assemblies are used in present and future cycles. Table 6-2 shows the nominal fuel assembly design specifications. No burnable absorber pins or control element assemblies are credited in the fuel storage rack calculations.

In this analysis, CASMO-3 is used to study rack K_{eff} vs. fresh fuel enrichment, unit cell sensitivity to mechanical tolerances, and rack K_{eff} vs. burnup. KENO-V.a is used to verify the nominal K_{eff} values calculated by CASMO-3 and, where necessary, provide a bias to the CASMO-3 calculations.

<u>Analysis Models</u>

The KENO-V.a model of the Maine Yankee spent fuel rack unit cell is an explicit pin by pin model. Reflecting boundary conditions are applied at the sides, top and bottom simulating a two dimensional infinite array. A 123 group working library is created by NITAWL-S for criticality analysis of the racks versus fresh fuel enrichment. Separate resonance calculations are performed for U^{238} at each enrichment with Dancoff factors calculated by CASMO-3. The K_{eff} calculation for each enrichment is calculated with 600 neutrons per generation for 2005 generations, skipping the first five. Thus, each case is a result of 1.2 million histories. For Region I, the KENO-V.a model is a representative cell. For Region II, the KENO-V.a model represents a 2 x 2 array that represents both the normal and virtual cells.

The two dimensional CASMO-3 model of the Maine Yankee spent fuel rack is based on the seven group transmission probability routine, COXY. Reflecting boundary conditions simulating an infinite two dimensional array are implicit in COXY. In the Region I fuel storage rack model, the pin cells representing the fuel assembly are appropriately homogenized square cells surrounded by an explicit inner water gap, steel canister wall, BORAL™ sheets, steel outer wrapper, and flux trap water gap. The model makes use of half diagonal fuel storage symmetry. For Region I, the CASMO-3 model is a representative cell with fresh fuel at an enrichment of 4.5 $^{w}/_{o}$. For Region II, two CASMO-3 models are used. One represents the normal cell and the other represents the virtual cell. CASMO-3 criticality analyses are performed for both cell types with burned fuel at 30 GWD/MTU and the results are averaged to determine the rack K_{eff}. This approach has been verified through KENO-V.a calculations. The KENO-V.a calculated K_{eff} for the normal cell is 0.92113 ± 0.00058, while the KENO-V.a calculated K_{eff} for the virtual cell is 0.92705 ± 0.00056 for an average of 0.92409 ± 0.00057. The actual KENO-V.a calculated K_{eff} for the 2 x 2 array is 0.92289 ± 0.00056. Thus, the averaging technique provides a conservative result.

Sensitivity Analysis

The Region I comparison of CASMO-3 and KENO-V.a fuel storage rack K_{eff} vs. enrichment is plotted on Figure 6-4. Similarly, the Region II comparison of CASMO-3 and KENO-V.a fuel storage rack K_{eff} vs. enrichment at 30 GWD/MTU is plotted on Figure 6-5. In the Region II analysis, the KENO-V.a calculation uses fresh fuel to yield equivalent reactivity in the storage cell. Both sets of calculations are at nominal mechanical dimensions and 68 °F spent fuel pool temperature. The agreement between CASMO-3 and KENO-V.a is very good over the range of enrichment from 3.0 to 5.0 $^{w}/_{o}$ U^{235}. This agreement establishes the validity of the CASMO-3 fuel storage rack model and reactivity at high enrichments.

Calculation of K_{eff} at a 95/95 probability/confidence level requires an evaluation of reactivity effects of the mechanical uncertainties associated with a particular rack and fuel assembly design. CASMO-3 is used to determine the sensitivity of the racks to these mechanical uncertainties. The uncertainties evaluated are center-to-center spacing, thickness of the stainless steel can, can inner dimension, BORAL™ sheath thickness, BORAL™ width, BORAL™ thickness, fuel enrichment and fuel density. The BORAL™ loading is specified as a minimum areal density of 0.020 g/cm^2. Use of this minimum loading in the criticality analysis is conservative. Thus, no sensitivity to BORAL™ loading was performed. The results of the sensitivity analysis for the Region I and Region II Maine Yankee spent fuel racks are presented in Table 6-3.

Eccentric Position

The criticality analysis assumes that the fuel assemblies are located in the center of the storage cells. Since this may not be the case in practice, calculations were made with four fuel assemblies assumed to be in the closest proximity. The change in reactivity due to eccentric position for Region I is -0.00046 ΔK and for Region II is -0.00452 ΔK as calculated by differential PDQ-7 calculations. Thus, the condition with the assemblies located in the center of the storage cell is conservative.

Reactivity Effects of BORAL™ Length

The nominal BORAL™ sheet is 140 ±0.0625 in. in length. This length, including tolerance, covers the entire active fuel length of all past, present and expected future Maine Yankee fuel. Therefore, there is no need to analyze variations in the length of the BORAL™ sheet.

Region II Burnup Axial Effects

In the Region II analysis above, criticality is calculated in two dimensions (2-D) with both CASMO-3 and SIMULATE-3. Usually, 2-D analyses are conservative because axial leakage has a negative effect on reactivity. However, axial burnup/moderator history must be evaluated. SIMULATE-3 is used to analyze these axial effects. Comparison to 2-D calculations is made to determine the axial penalty.

Axial burnup/moderator density history effects have a complicated nonlinear effect on storage array reactivity. At 0 GWD/MTU the effects of axial leakage result in a smaller K_{eff}. As burnup increases, the central regions experience more burnup than the top and bottom of the fuel assembly owing to the buckled shape of the axial power distribution. This leads to more reactive fuel at the bottom and top. Usually, the top is less exposed than the bottom because of slight bottom peaking of the power distribution due to moderator density effects. In addition, the top becomes even more reactive than the bottom with burnup due to the greater buildup of Pu^{239} from moderator density history effects. Generally, when the reactor is at power these effects are not pronounced. But, when core power is reduced to zero and/or coolant temperature is reduced, there can be a strong positive effect in reactivity from the redistribution of flux to the top of the fuel. This effect is especially pronounced in the criticality analysis of spent fuel stored in racks. SIMULATE-3 is used to study the effects of axial burnup/moderator history relative to 2-D analysis. These calculations were performed as a function of enrichment using assembly average exposure and moderator history characteristics of three cycle fuel burnup. The axial penalty as a function of burnup for three different enrichments is provided in Table 6-4. The axial penalty for 4.5 $^{w}/_{o}$ and 30 GWD/MTU is 0.01230 ΔK.

Maximum Fuel Enrichment

The maximum fuel enrichment that can be accommodated by the Region I racks is determined by adding all uncertainties to the nominal K_{eff} values vs. enrichment and then solving for the enrichment at which K_{eff} is at the limit of 0.95.

K_{eff} is calculated at 95/95 probability/confidence level by the following equations:

$$\Delta K_t = \Delta K_{cb} + \sqrt{(\Delta K_c)^2 + (\Delta K_m)^2} \qquad (1)$$

$$K_{95/95} = K_{nom} + \Delta K_t \qquad (2)$$

where:

- K_{nom} — K_{eff} of the nominal configuration,
- ΔK_t — total uncertainty,
- ΔK_{cb} — calculational bias,
- ΔK_c — 95/95 calculational uncertainty, and
- ΔK_m — mechanical uncertainty.

For Region I, the CASMO-3 based fuel storage criticality calculations produces values of ΔK_{cb} = -0.00054 and ΔK_c = +0.00837 (Ref. 6-8). From Table 6-3, the mechanical uncertainty ΔK_m = ±0.00747. Thus, the total uncertainty, ΔK_t, applied to the nominal K_{eff} values is:

$$\Delta K_t = -0.00054 + \sqrt{(0.00837)^2 + (0.00747)^2} = 0.01068 \qquad (3)$$

From Table 6-3, K_{nom} is 0.93164 giving a $K_{95/95}$ of 0.94232. As shown in Figure 6-4, the CASMO-3 calculation for fresh fuel is more conservative than the KENO-V.a calculation, therefore, no KENO bias is applied. For Region I, fresh fuel at 4.5 $^{W}/_{O}$ U^{235} is less than the acceptance criteria of K_{eff}= 0.95 with uncertainties.

For spent fuel racks where credit is taken for burnup, the uncertainty as a function of burnup includes the total uncertainty defined by Equation (1) and a burnup dependent component. In the burnup credit situation, the $K_{95/95}$ is given in the following equation:

$$K_{95/95} = K_{nom} + \Delta K_t + \Delta K_{bu} \tag{4}$$

The burnup dependent component, ΔK_{bu}, accounts for the effect of 2-D vs. 3-D modelling of burnup/moderator history. This effect is a positive contribution to reactivity as a function of burnup. The 2-D to 3-D component accounts for the positive effects of less exposure and high Pu^{239} concentration at the top of a fuel assembly. The 2-D to 3-D penalty is interpolated from Table 6-4 and for 4.5 $^{w}/_{o}$ at 30 GWD/MTU is 0.01230 ΔK.

As with Region I, the Region II CASMO-3 based fuel storage criticality calculations produces ΔK_{cb} = -0.00054 and ΔK_c = +0.00837. From Table 6-3, the mechanical uncertainty ΔK_m = $\pm$0.00607. Thus, the total uncertainty, ΔK_t, applied to the nominal K_{eff} values is:

$$\Delta K_t = -0.00054 + \sqrt{(0.00837)^2 + (0.00607)^2} = 0.00980 \tag{5}$$

From Table 6-3, K_{nom} is 0.91170, as calculated in Equation 5, ΔK_t is 0.00980 and ΔK_{bu} is 0.01230. Combined, they provide a value of 0.93380. However, as shown in Figure 6-5, the CASMO-3 calculation for burned fuel is less conservative than the KENO-V.a calculation. From this analysis a KENO bias of 0.01101 ΔK is applied. This yields a $K_{95/95}$ of 0.94481. This approach is equivalent to applying all uncertainties to the CASMO-3 calculated fuel rack K_{eff} vs. burnup. Therefore, for Region II, burned fuel at 4.5 $^{w}/_{o}$ U^{235} and 30 GWD/MTU is less than the acceptance criteria of K_{eff} = 0.95 with uncertainties.

To obtain a curve of enrichment as a function of burnup, a K_{nom} of 0.91170 for conditions of lower enrichment is determined. Applying the same values of K_{cb}, K_c, K_m and the Region II axial penalty provided in Table 6-3, yields a curve of enrichment as a function of burnup. This curve for the Maine Yankee spent fuel pool is provided in Figure 6-6.

6.2 ACCIDENT SITUATIONS

The postulated accident situations are all of the fuel handling variety. They consist of an assembly dropped on top of the racks, an assembly inadvertently placed adjacent to the sides or corner outside of the racks and a Region I assembly inadvertently placed in a Region II rack. These abnormal situations were analyzed with PDQ-7 with cross section input from CASMO-3. In all cases it was assumed that Region II contained burned fuel of 4.5 $^w/_o$ at 30 GWD/MTU and that Region I contained all fresh fuel at 4.5 $^w/_o$.

6.2.1 Dropped Assembly

An assembly dropped on top of the spent racks is assumed to be laying horizontally on top of the spent fuel racks. In this condition, the dropped assembly is more than 20 in. above the top of the active fuel in the spent fuel racks. However, for this analysis it is assumed that the assembly is touching the top of the active fuel. It is further assumed that the dropped assembly is fresh fuel at 4.5 $^w/_o$. The dropped assembly analysis is performed for both Region I and Region II racks.

6.2.2 Assembly Adjacent to Racks

It is possible to inadvertently place an assembly adjacent to the racks. The side of the Region II storage cells along the outside of a spent fuel rack does not contain a BORAL™ sheet. It is assumed that a fresh fuel assembly of 4.5 $^w/_o$ is placed at the side of the racks. Using these conditions and assumptions, the analysis is performed for both Region I and Region II racks.

6.2.3 Assembly in Corner of Racks

It is possible to inadvertently place an assembly adjacent to the corner on the outside of the racks. The side of the Region II storage cells along the outside of a spent fuel rack does not contain a BORAL™ sheet. It is assumed that the assembly is fresh fuel at 4.5 $^w/_o$. The analysis is performed for a Region I - Region II corner and for a Region II - Region II corner. These are the most limiting corner conditions that exist in the Maine Yankee spent fuel pool.

6.2.4 Misplaced Assembly

For the misplaced assembly, it is assumed that a Region I assembly is placed in a Region II rack. As with the other analyses, it is assumed that the assembly is fresh fuel at 4.5 $^{w}/_{o}$ and is surrounded by spent fuel of 4.5 $^{w}/_{o}$ at 30 GWD/MTU.

6.2.5 Accident Analysis Results

The results of the various fuel handling accidents are presented in Table 6-5. The table shows the increase in reactivity in terms of ΔK as a result of the accident conditions analyzed assuming no boron in the pool water. However, in accident situations, credit is allowed for the presence of soluble boron in the pool water. The typical Maine Yankee refueling concentration of soluble boron is 1500 ppm and the spent fuel pool is required to be at or above the same concentration. Table 6-5 shows the decrease in reactivity in terms of ΔK associated with the addition of 1500 ppm compared to the unborated condition. Also shown in Table 6-5 is the equivalent boron concentration required to offset the various accident conditions. Based on the most reactive condition, a boron concentration of 663 ppm is the maximum concentration required to cover any of the accident situations analyzed. The boron concentration of 663 ppm will keep the K_{eff} less than the acceptance criteria of 0.95 under accident conditions.

6.3 OTHER SITUATIONS ANALYZED

6.3.1 Effects of Pool Temperature

The analysis of the spent fuel racks is analyzed at a conservative 68°F. To verify this conservatism, the effects of pool temperature were analyzed with CASMO-3 over a range from 68°F to 212°F. The results, shown in Table 6-6, indicate that 68°F is indeed conservative.

6.3.2 Region I to Region II Interface

In the criticality analysis, Region I and Region II were analyzed separately. Since the racks will be in close proximity, the effect at the interface is evaluated. PDQ-7 calculations were performed with fresh fuel in Region I and 4.5 $^{w}/_{o}$ U^{235} at 30 GWD/MTU in Region II. This condition produced a K_{eff} of 0.93806 including uncertainty.

6.4 REFERENCES

6-1 R. M. Westfall, L. M. Petrie, N. M. Greene, and J. L. Lucius, ORNL/NUREG/CSD-2/V2, "NITAWL-S: SCALE System Module for Performing Resonance Shielding and Working Library Production," October 1981.

6-2 L. M. Petrie and N. F. Landers, ORNL/NUREG/CSD-2/V1/R2, "KENO-V.a, An Improved Monte Carlo Criticality Program with Supergrouping," December 1984.

6-3 M. Edenius and B. Forssen, STUDSVIK/NFA-89/3, "CASMO-3, A Fuel Assembly Burnup Program," User's Manual, January 1991.

6-4 B. M. Rothleder, EPRI/ARMP Documentation,"PDQ-7/HARMONY User's Manual," March 31, 1983.

6-5 K. S. Smith, STUDSVIK/SOA-92/03, "TABLES-3, Library Preparation Code for SIMULATE-3," April 1992.

6-6 K. S. Smith and J. T. Cronin, STUDSVIK/SOA-92/01, "SIMULATE-3 Advanced Three Dimensional Two Group Reactor Analysis Code," April 1992.

6-7 N. M. Baldwin, G. S. Hoovler, R. L. Eng, and F. G. Welfare, BAW-1484-7, "Critical Experiments Supporting Close Proximity Water Storage of Power Reactor Fuel," July 1979.

6-8 S. Van Volkinburg and R. C. Paulson, YAEC-1862, "Validation of the YAEC Spent Fuel Criticality Methodology Using Workstations," April 1993.

6-9 D. G. Napolitano and D. G. Adli, "Burnup Credit Using Advanced Nodal Techniques," Sandia/EPRI Report, May 1990.

6-10 S. R. Bierman, PNL-6205, "Criticality Experiments to Provide Benchmark Data on Neutron Flux Traps," June 1988.

6-11 Letter USNRC, Robert A. Clark to John H. Garrity, "Safety Evaluation and Environmental Impact Appraisal Regarding Maine Yankee Spent Fuel Storage," NMY 82-117, June 16, 1982.

6-12 Letter USNRC, Carl Stahle to J. B. Randazza, NMY 88-085, June 23, 1988.

6-13 Letter USNRC, E. H. Trottier to C. D. Frizzle, "Issuance of Amendment No. 133 to Facility Operating License No. DPR-36 - Maine Yankee Atomic Power Station (TAC No. M83029)," NMY 92-074, September 3, 1992.

TABLE 6-1

NOMINAL DIMENSIONS AND TOLERANCE

Parameter	Region I	Region II
Center-to-Center Spacing, in.	10.50 ± 0.050	9.085 ± 0.050
Can Thickness, in.	0.0747 ± 0.004	
BORAL™ Sheath Thickness, in.	0.032 ± 0.004	
BORAL™ Areal Density, B^{10} g/cm^2	0.020 minimum	
BORAL™ Width, in.	7.75 ± 0.0625	
BORAL™ Length, in.	140 ± 0.0625	
BORAL™ Thickness, in.	0.075 ± 0.004	
Fuel Density tolerance, g/cm^3	± 0.13	
Fuel Enrichment tolerance, $^w/_o$	± 0.05	

TABLE 6-2

FUEL ASSEMBLY NOMINAL DESIGN SPECIFICATIONS

Fuel Rod Data	
Outside Diameter, in.	0.440
Cladding Thickness, in.	0.028
Cladding Inside Diameter, in.	0.384
Cladding Material	Zr-4
Pellet Density, % T.D.	95.25
Stack Density, g UO_2/cc	10.1072
Pellet Diameter, in.	0.3765
Fuel Assembly Data	
Fuel Rod Array	14 x 14
Number of Fuel Rods	176
Fuel Rod Pitch, in.	0.580
CEA Guide Tube Outside Diameter, in. Inside Diameter, in. Material	 1.115 1.035 Zr-4

TABLE 6-3

SUMMARY OF CRITICALITY ANALYSES

	Region I	Region II
Design Burnup at 4.5 $^{w}/_{o}$ GWD/MTU	0	30
Temperature for Analysis, °F	68	68
Nominal Configuration, K_{nom}	0.93164	0.91170
Calculational Bias, ΔK_{cb}	-0.00054	-0.00054
Uncertainties		
Center-to-Center Spacing	± 0.00424	± 0.00136
Can Thickness	± 0.00104	± 0.00067
Can Inner Dimension	± 0.00527	± 0.00272
BORAL™ Sheath Thickness	± 0.00044	± 0.00067
BORAL™ Density	*	*
BORAL™ Width	± 0.00075	± 0.00108
BORAL™ Thickness	± 0.00157	± 0.00266
Fuel Density	± 0.00144	± 0.00190
Fuel Enrichment	± 0.00190	± 0.00386
Mechanical Uncertainty, ΔK_m	±0.00747	±0.00607
Calculational Uncertainty, ΔK_c	+0.00837	+0.00837
Total Uncertainty, ΔK_t	+0.01068	+0.00980
Allowance for Burnup, ΔK_{bu}	N/A	+0.01230
KENO-V.a Bias	0.0	+0.01101
$K_{95/95}$	0.94232	0.94481

* Minimum value of BORAL™ areal density was used in the criticality analyses.

TABLE 6-4

AXIAL BURNUP/MODERATOR HISTORY EFFECTS

3.0 $^{w}/_{o}$ Fuel			
Burnup (GWD/MTU)	SIMULATE-3 K_{eff}		ΔK (3-D)-(2-D)
	2-D	3-D	
0	1.04598	1.04320	-0.00278
5.404	0.99449	0.98787	-0.00662
10.730	0.94607	0.94201	-0.00406
14.634	0.91109	0.90979	-0.00130
19.276	0.87014	0.87532	+0.00518
24.785	0.82454	0.83933	+0.01479
30.057	0.78047	0.80159	+0.02112
4.0 $^{w}/_{o}$ Fuel			
Burnup (GWD/MTU)	SIMULATE-3 K_{eff}		ΔK (3-D)-(2-D)
	2-D	3-D	
0	1.11484	1.11188	-0.00296
4.403	1.07480	1.06791	-0.00689
10.380	1.02576	1.01907	-0.00669
14.552	0.99294	0.98869	-0.00425
19.681	0.95310	0.95458	+0.00148
23.993	0.92097	0.92886	+0.00789
30.201	0.87312	0.88871	+0.01559

TABLE 6-4 (CONT)

AXIAL BURNUP/MODERATOR HISTORY EFFECTS

4.5 $^{w}/_{o}$ Fuel			
Burnup (GWD/MTU)	SIMULATE-3 K_{eff}		ΔK (3-D)-(2-D)
	2-D	3-D	
0	1.14063	1.13760	-0.00303
4.569	1.10030	1.09333	-0.00697
9.366	1.06288	1.05490	-0.00798
15.080	1.02041	1.01545	-0.00496
20.435	0.98143	0.98170	+0.00027
24.988	0.94926	0.95580	+0.00654
29.393	0.91738	0.92909	+0.01167
35.690	0.87062	0.88884	+0.01822

TABLE 6-5

SUMMARY OF ACCIDENT ANALYSES

Condition	ΔK with No Boron	ΔK with 1500 ppm Boron	Equivalent* Boron (ppm)
Dropped Assembly			
Region I	+0.06324	-0.21352	318
Region II	+0.07192	-0.21720	362
Assembly Adjacent			
Region I	+0.09209	-0.22863	460
Region II	+0.08315	-0.22106	422
Assembly in Corner			
Region I - Region II	+0.11782	-0.28455	607
Region II - Region II	+0.11921	-0.22323	663
Misplaced Assembly	+0.03357	-0.16935	241

* This is the boron concentration which is required to offset the reactivity increase for the accident condition analyzed ($K_{eff} \leq 0.95$).

TABLE 6-6

EFFECT OF TEMPERATURE ON REACTIVITY

	Incremental Change, ΔK	
Pool Temp (°F)	Region I	Region II
68	0.00000	0.00000
80	-0.00071	-0.00070
100	-0.00200	-0.00215
120	-0.00344	-0.00389
212	-0.01156	-0.01471

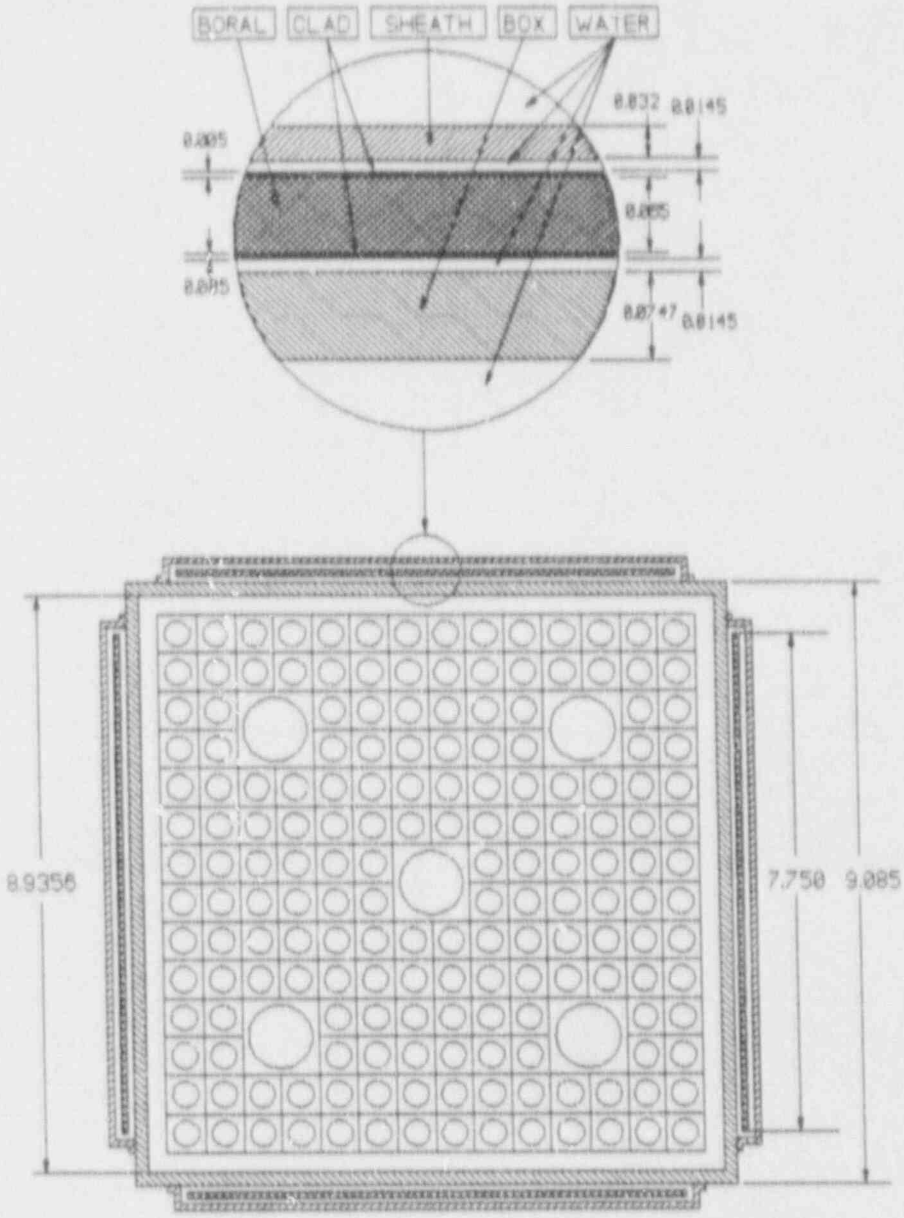

FIGURE 6-1
BASIC FUEL STORAGE CELL

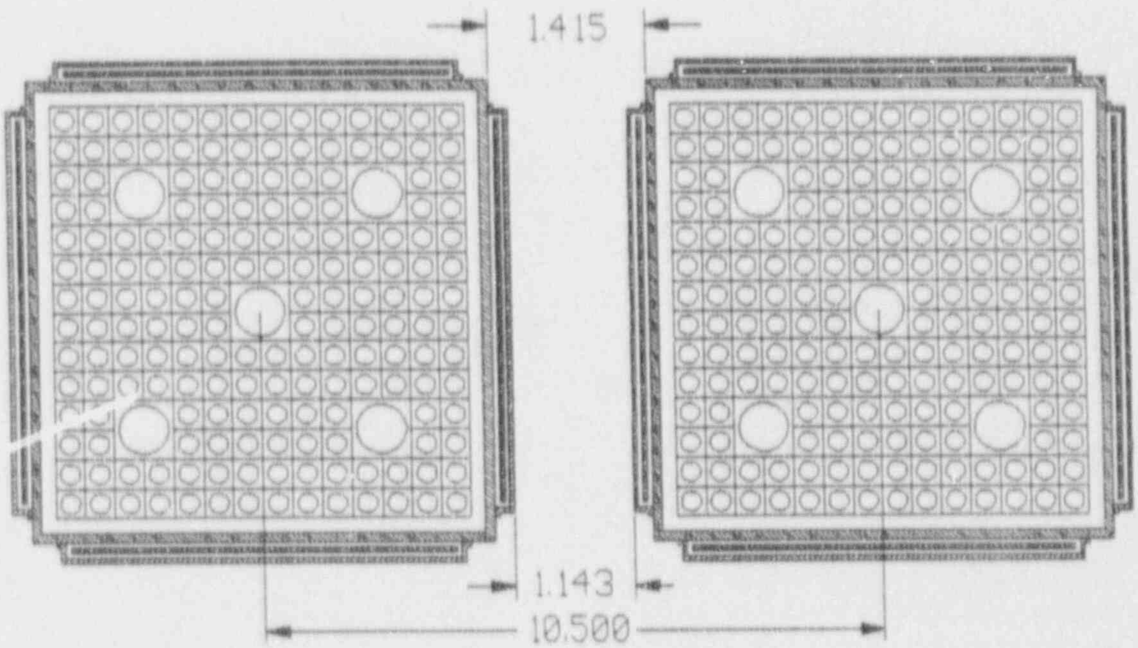

FIGURE 6-2
REGION I CONFIGURATION

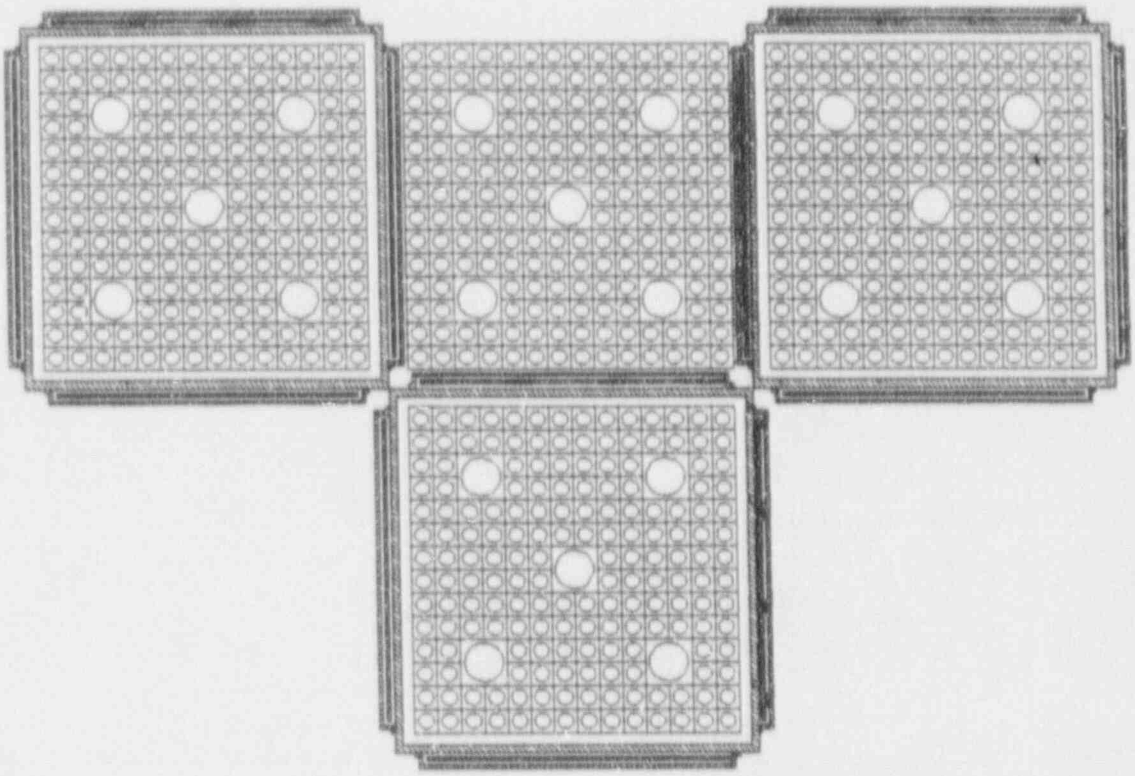

FIGURE 6-3
REGION II CONFIGURATION

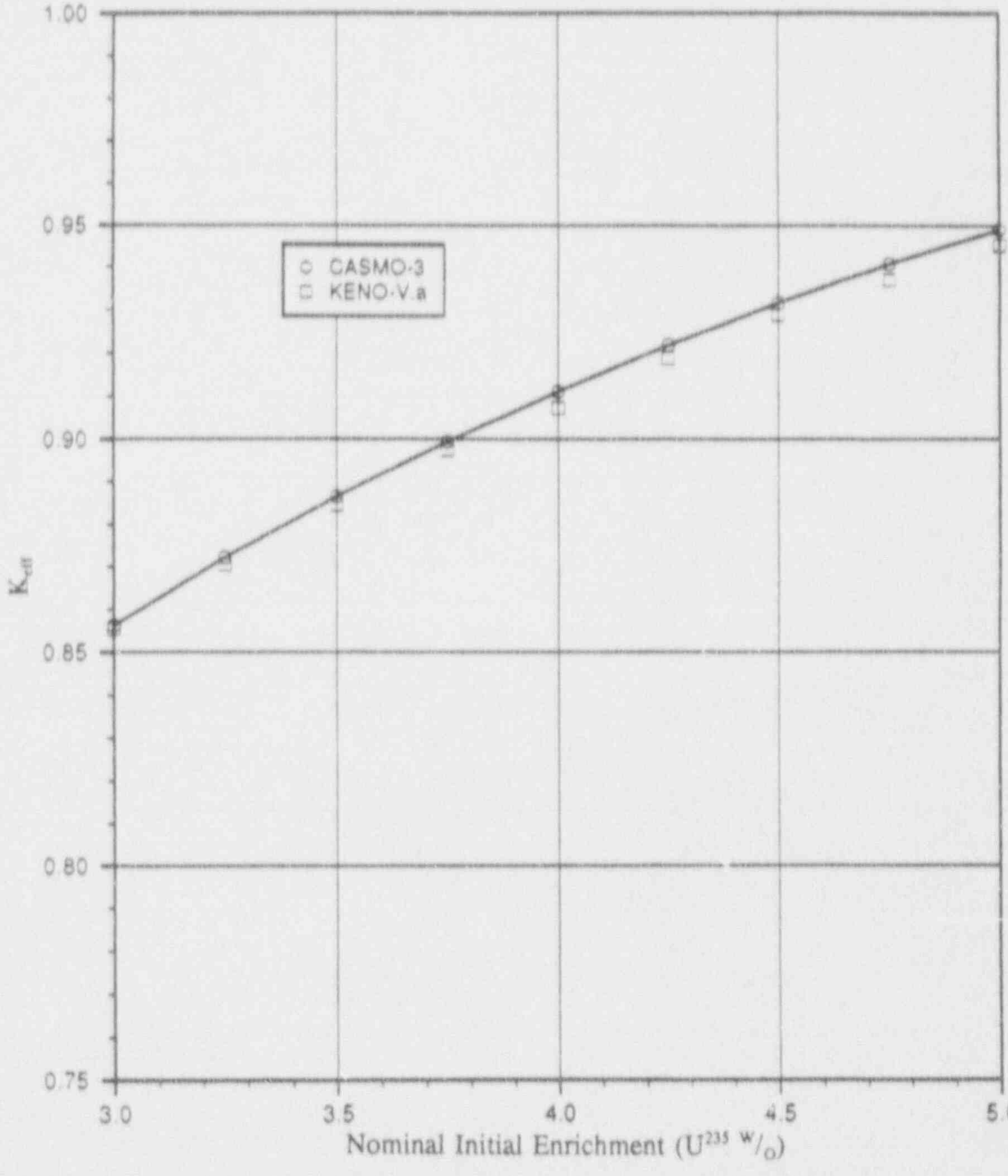

FIGURE 6-4
REGION I CASMO-3/KENO-V.a
COMPARISON

MAINE YANKEE ATOMIC POWER COMPANY

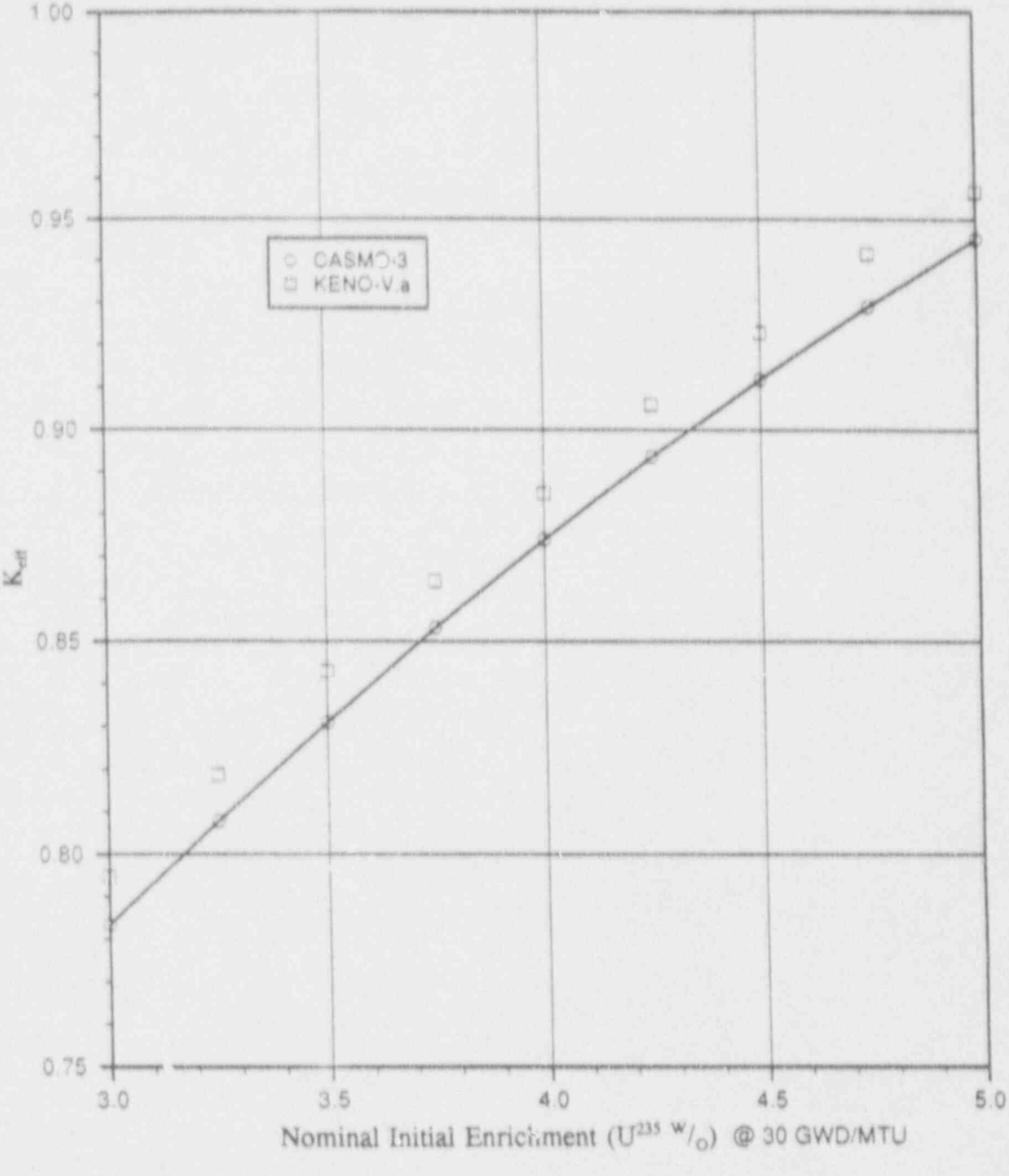

FIGURE 6-5
REGION II CASMO-3/KENO-V.a
COMPARISON

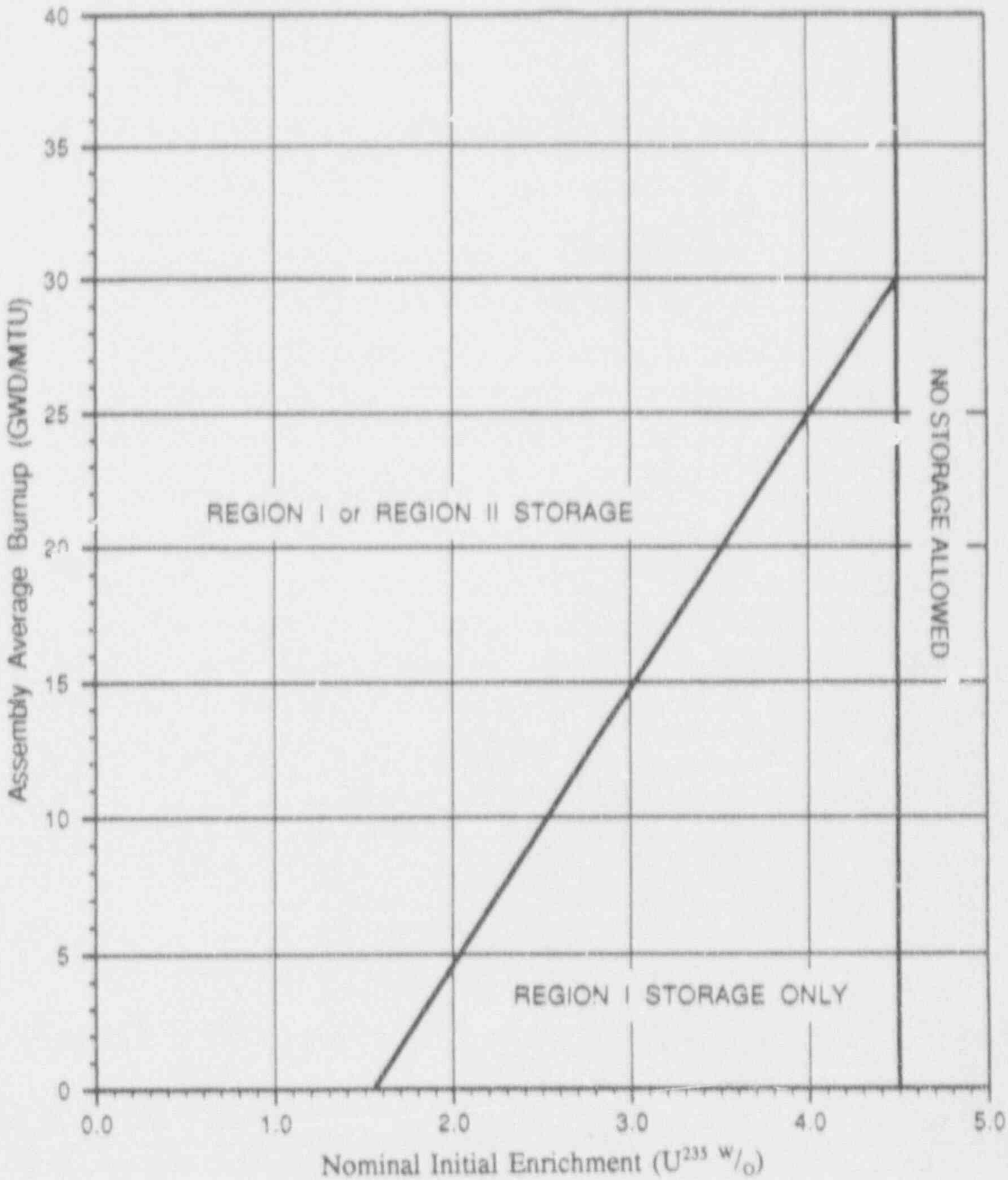

FIGURE 6-6
MAINE YANKEE SPENT FUEL POOL
ASSEMBLY PLACEMENT LIMITATIONS

7.0 RADIOLOGICAL SAFETY

7.1 EFFECT OF RERACKING ON NORMAL OPERATIONS AND ACCIDENT EVALUATIONS

7.1.1 Fuel Assembly Accidents

The Maine Yankee design basis fuel handling accident is the drop of a spent fuel assembly in the spent fuel pool. Since the reracking causes no changes in the fuel design or in the fuel handling procedures, and the new rack is designed to withstand the impact of a dropped fuel assembly, and all stored assemblies are recessed in the rack (such that only one assembly can be impacted by a straight downward drop), it is concluded that no additional fuel rods beyond that currently assumed in the licensing basis will be damaged due to reracking. Additionally, since neither the fuel design nor the refueling frequency has changed, the source term activities associated with the spent fuel are not impacted. Therefore, the fuel handling accident analysis in the current licensing basis is unchanged.

The current Maine Yankee Technical Specifications do not allow spent fuel shipping cask movement over the spent fuel storage pool. Shipping cask movement over the pool, including appropriate operational limitations, is not part of this reracking amendment submittal and will be developed when spent fuel shipment becomes a reality.

7.1.2 Fuel Building Radiation Zones

The Radiation Zones in the Fuel Building will not be affected by the spent fuel pool reracking.

The depth of water covering the stored spent fuel assemblies has not changed as a result of reracking, and the additional fuel assemblies in the spent fuel pool will have a negligible affect on the dose rates in the area above the fuel pool due to their long decay time. Currently, the spent fuel pool has the capacity to store 1476 spent fuel assemblies. This storage capacity is sufficient to provide storage for one full core plus spent fuel resulting from 17 refuelings, i.e., the oldest fuel will have decayed for at least 18 years, assuming refueling one-third of the core occurs every 12 months. This is a conservative assumption and covers any future use of extended burn-up fuel which increases the refueling cycle to 18 months. The reracking allows room for an additional 543 assemblies. The dose rate contribution from fuel that has decayed for 18 years or more as compared to the contribution from fresh spent fuel is insignificant.

Additionally, operating experience has shown that the area radiation dose rates near the surface of the fuel pool originate primarily from the radionuclides in the pool water. The major source of this activity is the reactor coolant that enters the fuel pool during refueling periods, and not the spent fuel. Since there is no change in the reactor coolant activity and volume or the frequency of refueling periods, the radiation zone in the area near the pool surface will not be impacted.

The dose rate through the walls of the spent fuel pool has been evaluated to account for the outer storage locations being closer to the walls. The spent fuel pool has a minimum wall thickness of about 6 ft and the increase in dose rate in the adjacent areas is minimal. Consequently, there is no impact on the radiation zone designations of areas adjacent to the fuel pool. For further detail, see Section 7.1.5.

7.1.3 Annual Radioactive Waste Generation

The annual rate of radioactive waste generation will not be impacted by an increased spent fuel storage capacity. As discussed above, the major source of the activity collected on the spent fuel pool purification system filters and demineralizer originates from the reactor coolant that enters the spent fuel pool during refueling and not due to any leakage of radioactivity from the stored spent fuel into the pool water. Therefore, since reracking does not change the pool concentrations, and the frequency of refueling remains the same, the rate of buildup of activity on the filters and demineralizer will not be impacted. As discussed above, any additional activity due to the added spent fuel capacity will be insignificant since the additional storage space is being used to house spent fuel assemblies that have decayed for more than 18 years.

7.1.4 Airborne Activity

Operating experience has shown that the primary contributor of airborne activity in the Fuel Building atmosphere is the tritium that is released from the fuel pool. As discussed before, since there is no change in the reactor coolant concentration, the concentration of tritium in the spent fuel pool water will also remain the same. Consequently, since the temperature of the fuel pool that is maintained by the fuel pool cooling system remains the same as before reracking, and there is no change in the fuel pool area ventilation system, the evaporation rate of tritium from the spent fuel pool remains unchanged. Therefore, neither the airborne activity in the Fuel Building nor the radioactive effluent releases will change.

7.1.5 Radiation Doses

Operator Dose - Resin Handling

The increase in fuel pool activity due to increased fuel pool storage in the spent fuel pool is expected to be negligible as discussed in Section 7.1.3. In addition, since the total resin handling time will remain the same, the dose to the operators from resin handling actions is not expected to increase.

Control Room Dose

The control room doses presented in the current licensing basis analysis due to a fuel handling accident are conservatively calculated assuming that the damaged spent fuel assembly is the most radioactive assembly from the core with the least possible decay time. As discussed in Section 7.1.1, a fuel handling accident following the reracking will not result in any additional fuel damage than that specified in the current licensing basis analysis. Therefore, the estimated doses in control room will not be impacted due to fuel pool reracking.

The normal operating doses in the control room subsequent to reracking will remain the same as the prereracking operating doses. As indicated in Section 7.1.4, the airborne activity released from the fuel building will remain the same. Consequently, the resulting control room airborne concentrations will remain unchanged.

Site Boundary Dose

For the same reasons as stated for the control room dose impact evaluation, the site boundary doses due to a fuel handling accident will not be impacted due to reracking.

Similarly, the normal operating offsite doses will not be impacted by the reracking.

Dose Rate

The impact of the reracking on the dose rates in the vicinity of the spent fuel pool and the support systems, i.e., spent fuel pool cooling and cleanup systems, will be negligible. As the additional capacity is for the storage of older fuel, and the depth of water over the spent fuel is not changed, the dose rate at the surface of the spent fuel pool will remain the same. Because the new rack design allows the spent fuel assemblies in the outer rows to be closer to the walls, the dose rate through the walls of the spent fuel pool has been evaluated. The calculated dose rates in the areas adjacent to the spent fuel pool walls due to the storage of spent fuel are well within the Radiation Zone II limits (2.5 mr/hr) for Fuel Building passageways in general.

7.2 RADIATION PROTECTION DURING RERACKING OPERATIONS

7.2.1 Introduction

Planning for the Maine Yankee spent fuel pool reracking project is in accordance with the station's commitment to the as low as reasonably achievable (ALARA) policy. mprehensive radiological controls will be implemented as part of the overall program to ensure personnel doses are maintained ALARA. The combination of radiological surveys, routine radiochemical analyses, and an extensive contamination control protocol will provide the adequate technical bases for program implementation.

The Radiation Protection Department will define the content of the spent fuel pool. A program of sampling, sample analysis, and results evaluation in conjunction with direct radiation measurements is designed to provide added measures of assurance toward the goal of personnel safety and the control of any radioactive waste generated during reracking operations.

The data obtained from the characterization effort will be used to generate appropriate documentation governing contamination control techniques, decontamination equipment and effective radioactive waste processing. The actual physical and radiological characteristics of the material in the spent fuel pool will affect both the procedures and methodology used for the decontamination of equipment and radioactive waste classification of material removed from the spent fuel pool.

7.2.2 Spent Fuel Pool Radiological Characterization

Purpose

The radiological characterization of the spent fuel pool is intended to provide sufficient technical data concerning the radiological environment within the spent fuel pool to ensure that adequate planning can be performed to incorporate the necessary surveys, decontamination of the area and equipment, and controls for the various stages of the reracking operation, including radioactive waste processing, packaging, shipping, and disposal of radioactive waste materials.

Objectives

Specific objectives have been identified to provide a complete and accurate representation of the radiological content of the spent fuel pool. These objectives include the following:

1. Identify radionuclide types and concentrations as well as preparing dose profiles for personnel exposed to in-pool components.

2. Determine contaminants and concentrations in the spent fuel pool water.

3. Determine the radiological characteristics of spent fuel pool sediment.

4. Provide preliminary 10CFR61 waste stream characteristics and analyses for specific classification.

Application of Information

The information obtained from the radiological characterization of the spent fuel pool will be applied for use within the standard Radiation Protection Program currently in place. It is not anticipated that the Radiation Protection Program will need to be modified for the reracking project.

Information relating to problems identified by the industry (e.g., NRC, EPRI, INPO, other utilities) will be reviewed and pertinent requirements followed during the reracking. Examples of this information may be found in NRC Information Notices 90-08, 90-33, 90-44, and 90-47.

Selection of Instrumentation

The quantitative results obtained from the radiological characterization of the spent fuel pool will help to determine the adequacy of the instrumentation intended for use during reracking operations. Standard instrumentation for underwater surveys, air sampling, and normal surveys will be used in conjunction with direct monitoring equipment for surfaces and materials outside the pool.

A temporary area radiation monitoring system will be installed to monitor gamma radiation levels in the spent fuel pool area. Continuous air monitors (CAMs) will be utilized, as appropriate, to support specific activities that could generate airborne radioactivity. These will be used to augment the normal radiation and contamination surveys of the area that will be performed during work.

Dosimetry

All personnel in the work area will be required to wear personnel monitoring devices in accordance with station procedures. Such devices will, as a minimum, consist of a thermoluminescent dosimeter (TLD) and a pocket ion chamber (PIC).

During specific work evolutions, additional personnel monitoring devices such as extremity dosimetry or multiple whole body badges may be required. Supplemental dosimetry will be specified in the radiological work packages and/or on the Radiation Work Permit (RWP) for the specific task.

The calibration of special dosimetry devices will be appropriate for the anticipated work environment. This calibration will be in accordance with station procedures.

7.2.3 ALARA Program

Preplanning Efforts

Preplanning of the various work tasks is considered as the single most important ALARA initiative. This aspect of the ALARA program is intended to provide the assurance that personnel exposures are minimized. The preplanning effort is a major contributor to the success of the overall ALARA program since the amount of forethought and engineering controls that are incorporated into the specific work tasks will ensure adherence to the principle of ALARA.

Preplanning involves representation from each major discipline of the project team. The ALARA motivated preplanning efforts include, but are not limited to, the following:

1. The philosophy of remote technology use will be used in the planning for all underwater work on a task specific basis. In all cases, parallel planning will occur such that as a last resort, the use of divers will not hamper the safety, ALARA considerations, or schedule of work as planned. Installation techniques, equipment for use, and work sequencing are being chosen accordingly.

2. Job planning includes consideration for the repositioning of spent fuel to support the dose minimization/ALARA effort.

3. Both preinstallation and installation decontamination efforts are planned to minimize the potential for fuel fragment and hot particle exposure. These efforts

are also expected to minimize the general area dose rates consistent with the principle of ALARA.

4. Appropriate training of personnel will be conducted to ensure compliance with station procedures. Personnel will be trained for the specific tasks to be performed during reracking.

5. As during routine operations, work evolutions in and around the spent fuel pool will be controlled and monitored by Radiation Control personnel at all times.

ALARA Job Reviews

ALARA job reviews will be formally established such that both pre-job and post-job reviews will be performed by Radiation Protection personnel. ALARA reviews will help to prescribe the various job specific Radiation Protection requirements for incorporation into the RWP. Such information as man-rem estimates, stay time limitations, the use of specifically prescribed engineering controls, and mock-up training shall be covered in the ALARA review. All pre- and post- job reviews will be performed in accordance with station procedures. Pre- and post- job meetings will be mandatory for those personnel involved in the various segments of work evolution. Workers, their supervision and the Radiation Protection technician responsible for job coverage will meet with the Maine Yankee ALARA representative to review the ALARA considerations and any additional information helpful to performing work in a safe and dose-conscious manner.

Key Performance Indicators

Key performance indicators will be formally established for use during spent fuel pool work evolutions. The Radiation Protection organization will track these indicators, trending results and routinely identifying these trends to management. The indicators include but are not limited to the following:

1. Personnel contaminations.

2. SFP area contamination levels and total building area in ft^2 that is contaminated to those levels.

3. Gross activity in the spent fuel pool water.

4. Dose rate at the surface of the spent fuel pool water at poolside.

7.2.4 Training

Personnel will be trained and qualified in accordance with station procedures prior to performing work within the spent fuel pool and associated areas. Task specific training will be provided for all personnel. For each remote operation (e.g., vacuuming, lift rig engagement), personnel will be specifically trained and qualified on the tools and procedures.

7.2.5 Work Controls

Radiation Protection work controls during remote operations in and around the spent fuel pool shall be delineated in the radiological work packages, ALARA reviews, and job specific Radiation Work Permits (RWPs). The documents described will cover each major radiological task evolution.

These work controls shall be applied in addition to any procedural requirements.

7.2.6 Radiation and Contamination Surveys

The types and frequencies of radiological surveys will be performed in accordance with approved Maine Yankee procedures. Normal Radiation Protection job coverage will dictate that both radiation and contamination surveys be performed, as a minimum, before a work evolution and after its completion. Contamination surveys will also be performed as the work progresses. During work in which the potential for high radiation levels exists, local radiation dose rates may be taken during job performance and will be supplemented with data from local continuous monitoring stations.

7.2.7 Contamination Control

As with other principle elements of radiological controls, contamination control practices will be delineated within the radiological work package and the ALARA review. The areas in which work will be on-going will be considered potential Hot Particle Zones and activities will be controlled in accordance with station procedures.

The Radiation Protection staff will closely monitor and control all aspects of the work to ensure personnel exposures are maintained ALARA.

7.2.8 Decontamination Efforts

Decontamination efforts will be on-going during the entire work evolution to maintain adequate contamination control in the areas surrounding the spent fuel pool and the remainder of the building. Specific decontamination requirements will be described in the radiological work package and will also be contained in the RWP covering decontamination. Periodic updates will be used to adjust the methodology used for decontamination if unexpected conditions are encountered during any phase of operations.

All equipment and other items removed from the water will be appropriately decontaminated. Tools and equipment will be removed from the spent fuel pool in accordance with approved procedures. Additional decontamination will be performed, as required, in preparation for packaging and shipment. Specially selected areas designed to handle potentially contaminated items from within the spent fuel pool will be established for such decontamination.

7.2.9 Radwaste Generation/Disposal During Reracking

Small increases in activity on the filters and demineralizers may occur during the installation of the new racks due to the more frequent fuel shuffling and underwater hydrolazing of the old racks during removal.

Section 9.5 discusses decontamination, packaging, and disposal of existing racks. The estimated volume of radwaste resulting from this project is discussed in Section 9.5.6.

Disposal and transportation of radwaste materials will be performed in accordance with applicable government regulations including 10CFR71 and 49CFR173. Material and equipment used for reracking and any radioactive waste hardware or solid material generated will be decontaminated and/or packaged appropriately for shipment. The 10CFR61 waste characterization analyses will be performed to determine burial classification and packaging requirements.

7.2.10 Anticipated Radiation Exposure During Reracking

The radiation exposure estimates are made based on the anticipated installation plan. They include the expected fuel transfers, the use of remote tools and the onsite decontamination, cleanup and packaging of the old storage racks. Current spent fuel pool radioactivity levels were used in calculating these exposures. The types of activities anticipated and the projected man-rem estimates are summarized in Table 7-1. The total occupational exposure for the remote reracking operation is estimated to be 4 to 6 man-rem. This value is the estimate of the expected accumulated dose and represents the maximum or upper boundary conditions. As a comparison, some previous personnel man-rem exposures are listed for previous reracking projects.

Location	Year Completed	Crew Size	Installation Method	Man-Rem Total
Millstone	1988	10	Diving & remote	10.016
St. Lucie	1988	15	Diving	2.61
LaSalle	1989	15	Diving	13.02*
Indian Point 2	1990	15	Remote	2.94
Indian Point 3	1990	15	Remote	2.39
San Onofre	1991	23**	Remote	6.96

* Project extended by 50% due to delays by owner.
** Average personnel loading.

TABLE 7-1

ESTIMATED RADIATION DOSES FOR CONSTRUCTION ACTIVITIES

Item Description	Dose (rem)
Shuffle Fuel	0.20
Install/Test/Remove Temporary Gantry Crane	0.13
Rack Removal and Installation (including the following) 1. Lifting fixture installation & removal 2. Monitoring lifting/rigging activities 3. Hydrolase/vacuum rack 4. Vacuum path/work area before and after work 5. Install floor plates 6. Elevation survey 7. Install, level, and torque new rack	2.50
Drag Test New Racks	0.30
Prepare Racks and Other Radwaste for Shipment Offsite	0.88
Miscellaneous (including mobilization and demobilization)	0.65
Total Dose (rem)	4.66

Assumptions

1. Values are based on the anticipated construction approach where the in-pool work is accomplished by remote methods only.

2. The current measured radionuclide concentrations in the spent fuel pool water remain constant throughout the work.

3. All values are estimates of the expected cumulative dose and represent the maximum or upper boundary conditions.

8.0 FUEL RACK FABRICATION

The new racks will be manufactured by General Dynamics/Electric Boat Division (GD/EB) at their Quonset Point Rhode Island manufacturing facility.

The spent fuel racks will be assembled in modules to fill the Maine Yankee storage pool providing the maximum number of storage locations. The configuration and quantities of rack modules for Region I and Region II are discussed in Chapter 2.

The rack module design information will be input to computer numerically controlled (CNC) Wiedemann multi-tool, plasma assisted turret punch presses. The CNC presses are used to precision cut each rack part from sheets of stainless steel. These presses are bi-axial and have an accuracy to 0.001 in. on material up to 3/8-in. thick, ensuring very accurate component nesting, cutting, and punching. The Wiedemann cuts the stainless steel plate, automatically punches the flow holes, and marks bend data onto the plate.

A CNC brake, using computer set positioning, stops and dies, accurately folds the cell half-sections, and forms the neutron absorber cover plates, the completion channels for virtual cells, and base structure components.

Semi-automatic gas metal arc welding (GMAW) will be utilized to assemble the cell elements and rack modules. Horizontal welding has proven to be the most efficient and error-free process and will be utilized, to the maximum extent possible, with the cell element fabrication and rack module assembly fixtures.

All manufacturing is controlled by formal configuration management controlled work authorizations. This process ensures that the shop personnel have the correct technical data to manufacture the rack modules.

ASME certified welding procedures are controlled by Welding Technique Sheets that have been developed specifically for the rack module fabrication. Welders are trained and certified to weld the stainless steel materials.

8.1 REGION I RACK MODULE

The rack module fabrication sequence for Region I includes parallel component nesting, cutting, forming, machining, and sub-assembly of the adjustable feet, rack base structure elements, cell element half sections, neutron absorber cover plates, cell element spacer support structures, and rack module banding.

The cell element half-sections will be full-length welded along two opposite corners, utilizing a fabrication fixture to ensure consistent holding to the design alignment tolerances. The fixture can be rotated while holding the cell half-sections to bring the opposite corner up to be welded. The neutron absorber material, BORAL™, will be accurately positioned on an exterior side of the cell and contained in place by a 24-gage (0.032-in. thick) ASTM A240 Type 304L stainless steel cover. The cover is intermittently welded to the cell by 1/2-in. long welds, 6 in. on center around the periphery of the cover. The top end of the cover is tapered into the cell wall to eliminate abrupt edges. This process is repeated three times, installing neutron absorber and a cover plate on all four cell exterior walls.

The cell elements have an automatically punched, 1-in. hole centered at the top of each side above the neutron absorber to ensure sufficient flow under all conditions. The base structure has an automatically cut 4-in. hole positioned at the center of each cell element base, also, to ensure sufficient flow under all conditions.

The rack modules will be assembled in the axis-horizontal position utilizing an assembly fixture to accurately position each cell element and maintain alignment. The rack module will be assembled row by row incrementally introducing base structure components and intermediate and top cell element spacer support structural components. This axis-horizontal assembly methodology will ensure consistently holding to the design alignment tolerances and afford the maximum extent of horizontal welding while providing the maximum access to each weld location. The outside tie bars and the adjustable feet will be installed on each module prior to removing it from the module assembly fixture. A typical Region I rack module is depicted on Figure 8-1.

A full-size Region I prototype rack module has been manufactured to verify the fabrication and assembly processes. This Region I prototype rack module includes four cells in a 2 x 2 configuration. Each storage location has been successfully drag tested with the test device that will be used to test the production rack modules at GD/EB.

8.2 REGION II RACK MODULE

The rack module fabrication sequence for Region II is very similar to that for Region I. It includes parallel component nesting, cutting, forming, machining, and sub-assembly of the adjustable feet, rack base structure elements, cell element half sections, virtual cell completion walls, neutron absorber cover plates, cell top structure, and rack module banding.

The cell elements for Region II are similar to those for Region I with differences on the top and bottom for attaching the integrating structure. The Region II cell elements will be fabricated utilizing the same fabrication processes and sequence as for the Region I cell elements. The rack modules will be assembled in the axis-horizontal position utilizing an assembly fixture to accurately position each cell element and maintain alignment. The rack module will be assembled row by row incrementally introducing base and cell top tie bars and welding the interfacing cell corners. The pieces that complete the outside virtual cells will also be introduced into the rack module assembly around the outer perimeter. This axis-horizontal assembly methodology will ensure consistently holding to the design alignment tolerances and afford the maximum extent of horizontal welding while providing the maximum access to each weld location. The outside banding of the rack module and the adjustable feet will be installed on each module prior to removing it from the module assembly fixture. Cleats will be added to the tops of the cell walls perpendicular to the cell top tie bars to strengthen the cell wall lead-in edge.

A typical Region II rack module is depicted on Figure 8-2.

A full-size Region II prototype rack module has been manufactured to verify the fabrication and assembly processes. This Region II prototype rack module includes nine cells in a 3 x 3 configuration. This includes five fuel storage locations made by cell elements and four storage locations made by virtual cells. Each fuel storage location has been successfully drag tested with the test device that will be used to test the production rack modules at GD/EB.

8.3 FABRICATION AND CONSTRUCTION PRACTICES

The following fabrication and construction practices will be utilized as appropriate in the fabrication of the racks:

ASME	Boiler and Pressure Vessel Codes Sections II, III, Div. I, V, and IX
ASTM	Annual Book of ASTM Standards
ASTM B-240	Specification for Heat-Resisting Chromium and Chromium-Nickel Stainless Steal Plate, Sheet, and Strips for Pressure Vessels
ANSI Y14.5	Dimensioning and Tolerancing (1973)
ANSI N45.2.1	Cleaning of Fluid Systems and associated Components During Construction of Nuclear Power Plants (1973)
ANSI N45.2	Quality Assurance Program Requirements for Nuclear Power Plants (1977)
SNT-TC-1A	Personnel Qualifications and Certification in Non-Destructive Testing (1975)
ANSI N45.2.2	Packaging, Shipping, Receiving, Storage and Handling of Items for Nuclear Power Plants (1972)
ANSI/ASME NQA-1	Quality Assurance Program Requirements for Nuclear Facilities

8.4 FABRICATION AND CONSTRUCTION MATERIALS

All rack structural material is ASTM A240 304L stainless steel. The material is primarily thin plate, ranging from 0.032 in. to 0.5 in.

Nuclear quality control (NQC) personnel will review all purchase orders to ensure that the full scope of the technical ordering data and related quality assurance (QA) provisions are properly and completely passed down to the subcontractor and that such subcontractors have a QA program appropriate for their degree of involvement in a nuclear services contract. This is required by the in-place Nuclear Services Quality Assurance Manual and Nuclear Services Standards. NQC personnel have final approval of material subcontractor selection for QA attributes. NQC personnel have on-site subcontractor audits of their QA practices as deemed necessary. Upon receipt of the material, the NQC personnel inspect the material and documentation for compliance with all QA attributes.

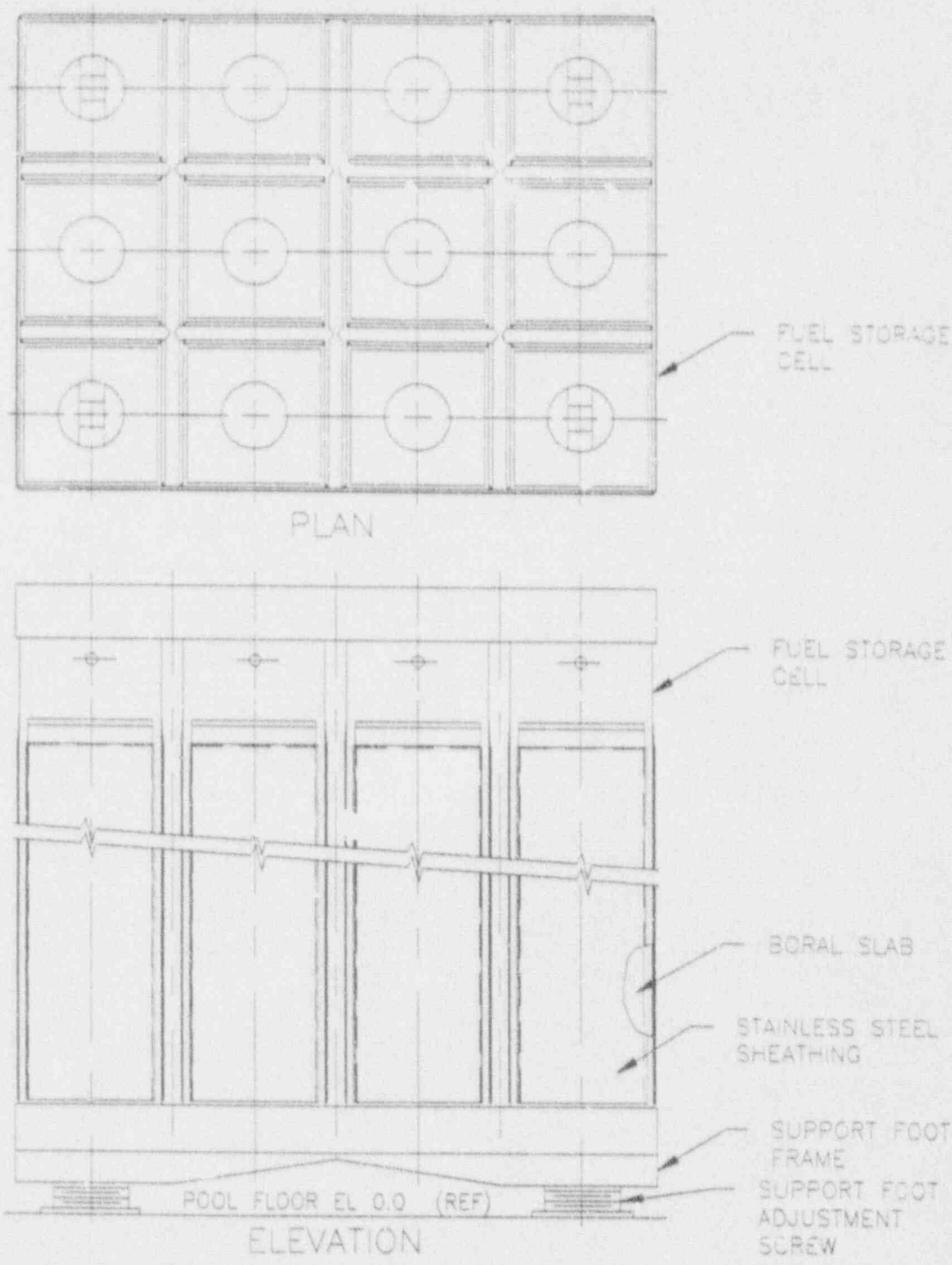

FIGURE 8-1
TYPICAL REGION I RACK MODULE

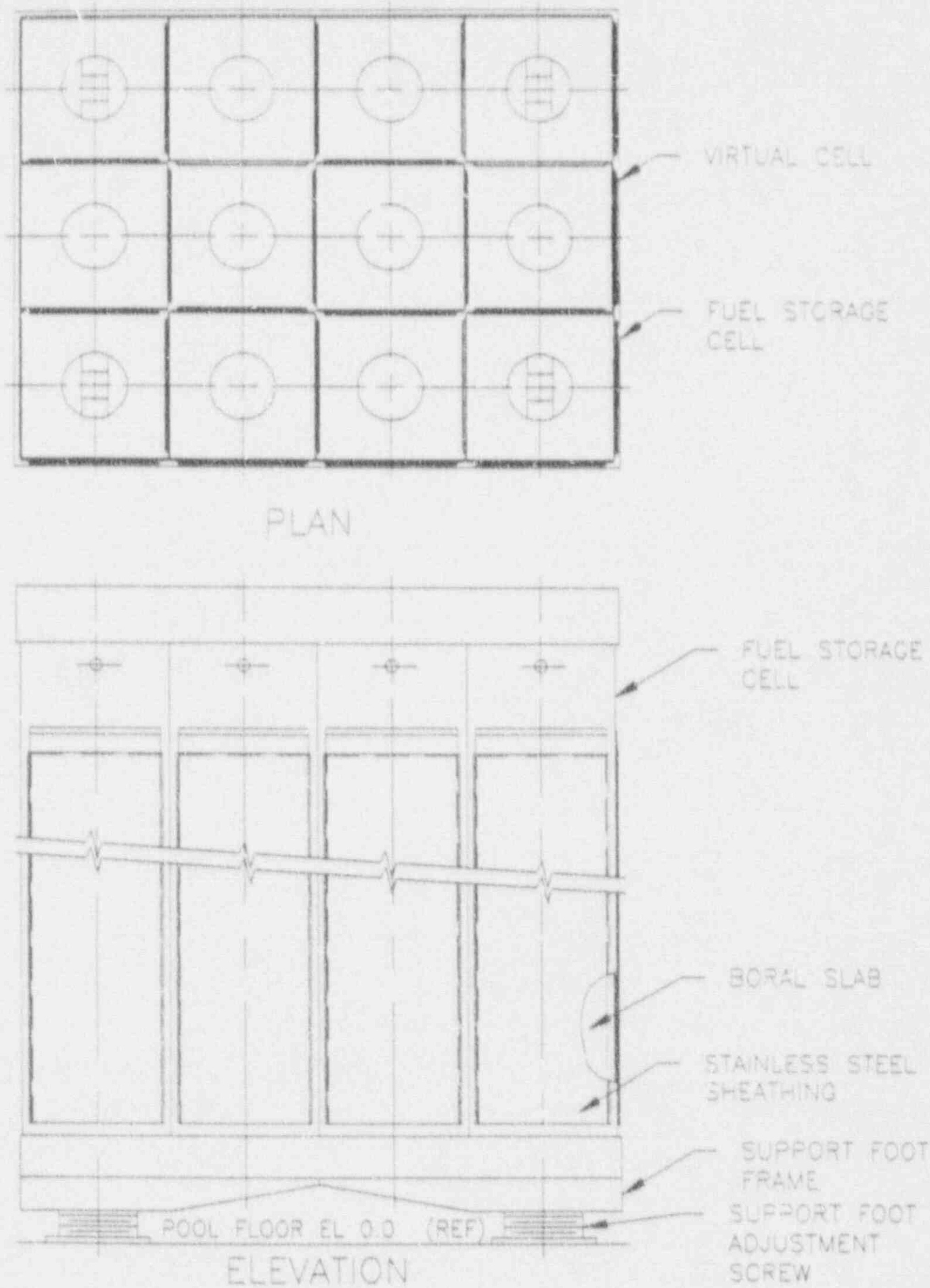

FIGURE 8-2
TYPICAL REGION II
RACK MODULE

9.0 INSTALLATION AND REMOVAL OPERATIONS

The spent fuel pool is 37-ft wide by 41-ft long by 38-ft deep, and is located in the south end of the fuel building adjacent to the reactor containment. The pool is constructed of reinforced concrete with a wall and floor lining of 1/4-in. thick stainless steel. A fuel transfer tube connects the fuel pool at the south end with the refueling cavity located in the containment. Welds in the liner are backed up by test channels which are piped to the fuel building sump. The fuel pool is protected from being drained down by a rupture of any pipe normally connected to the pool by a siphon breaker. An area is provided in the fuel pool for inspection of fuel assemblies, and room is also provided for the spent fuel cask.

The Maine Yankee spent fuel pool will have approximately 1204 fuel assemblies stored in 26 racks at the proposed time of reracking in May 1995. As there are a total of 1476 storage locations currently licensed for fuel storage, there will remain 272 empty locations at the proposed time of reracking. This empty space will provide a satisfactory number of unoccupied cells to permit the necessary fuel shuffling to remove existing storage racks and replace them with empty high density racks.

In order to update the pool as-built information to the precision required for high density rack positioning, and to accurately determine pool wall characteristics for verification of the expected rack-to-wall clearances, an acoustical dimensioning pool survey has been performed. The results of this survey refined and confirmed measurements critical to both the rack arrangement and installation sequence.

Two significant efforts for the reracking project which will be completed by Maine Yankee prior to the high density rack installation are as follows:

a. Thorough cleaning of the spent fuel pool. Additional cleaning will be performed for those areas underneath the existing storage racks as they are replaced during the installation of new racks.

b. Overhaul and refurbishment of the 125/20 ton Whiting yard crane.

The above preparations add a significant measure of reliability to the intended installation operations and contribute to maintaining radiation exposure as low as reasonably achievable (ALARA) during the reracking.

The existing storage racks are of six different sizes and weights, and are arranged as shown on Figure 9-1. The maximum dry weight of an existing rack is 22,400 lb.

The proposed high density racks will provide a total of 2019 storage locations, of which 228 are Region I and 1791 are Region II. These racks will provide locations for the safe, controlled storage of an additional 543 spent fuel assemblies as shown on Figure 9-2. A general description of the proposed high density racks is presented in Chapter 2. The maximum dry weight of a new rack is 13,000 lb.

The reracking operation is a sequenced, repeated series of phases. Each phase consists of six repetitive steps ultimately resulting in the removal of existing racks and the installation of the new high density racks. The number of phases is directly proportional to the number of empty storage locations and the rack module sizes. That is, the fewer number of empty locations the greater the number of phases required to accomplish the replacement. With the present schedule for reracking in the summer of 1995, the expected minimum number of empty locations is satisfactory.

The steps repeated in each phase are:

1. Shuffle fuel out of the existing racks identified for immediate removal,

2. Remove existing empty rack,

3. Vacuum clean newly exposed pool area,

4. Install pre-leveled new high density rack,

5. Precision level the new rack, and

6. Free-path test each fuel storage location for acceptability.

The actual sequence for the existing rack removal and new rack installation is determined by available clearances between racks, the number of phase dependent empty locations and the maintenance of a safe load path. Except in the cask loading pit, existing racks and new racks will be lifted less than 12 in. above the fuel pool floor while moving along this safe load path. Thus, no empty racks will pass over racks containing fuel assemblies.

9.1 LIFTING AND POSITIONING OF RACKS

All equipment designs and operations involving heavy lifts and the use of heavy lift equipment are governed by the guidance contained in NUREG-0612, NUREG-0554, ANSI 14.6, and the Maine Yankee Control of Heavy Loads Program.

In order to effect the reracking, all parts of the spent fuel pool must be accessible by the heavy lift equipment. Because Maine Yankee's 125/20 ton Whiting yard crane is limited to servicing the cask pit area only, a temporary heavy lift system for the other areas of the spent fuel pool will be utilized as in the previous reracking at the plant.

Although the 125/20 ton yard crane will be overhauled and refurbished, its use will be limited to 24% of its capacity, or 30 tons, to provide additional margin of safety during the reracking process and to ensure compliance with NUREG-0554 and NUREG-0612.

The temporary heavy lift system is depicted on Figures 9-3 and 9-4, and is composed of the following:

1. BRAND's temporary gantry crane; a double-reeved, electric hoist designed specifically for reracking operations which incorporates multiple, duplicate safety devices as well as two completely independent motors, gearboxes, and brakes.

2. A two-beam, motorized bridge to span the spent fuel pool from east to west, enabling the positioning of the temporary gantry crane in the north/south directions.

3. A motorized trolley, upon which the temporary gantry crane traverses the pool in the east/west direction, which itself travels on the bridge.

4. A single-failure-proof lift rig assembly which is adaptable to lifting both the existing and the new fuel racks and can be engaged remotely.

This reracking lift system, designed and qualified to NUREG-0554, NUREG-0612, and ANSI 14.6 criteria, enables heavy lift accessibility to all parts of the spent fuel pool and also prevents the plant's 125/20 ton yard crane from becoming contaminated through submersion in the spent fuel pool. At the completion of the reracking, all of the temporary equipment will be removed from the [illegible] after any required decontamination as discussed in Section 7.2.8.

The design of the temporary gantry crane incorpcrates "fail-safe" operation of electrical components. That is, upon loss of power:

1. Both brakes fail to the "engaged" position, thus instantly preventing further movement, and

2. All control circuit breakers reset to a neutral position such that, upon re-energizing the hoist, control breakers are in a predetermined, "safe start" position.

The specifications for the temporary gantry crane and its associated bridge and trolley system are:

Temporary Gantry Crane

Capacity:	20 tons NUREG-0612 useable; ANSI 14.6, 60 ton test
Height of Lift:	50 ft available
Hoist Speed:	Two speed, 6/2 fpm
Hoist Brakes [2]:	AC disc type plus regenerative braking
Hoist Motors [2]:	10/3.3 HP, Squirrel Cage, TENV, 60 min., Class F insulation.
Hoist Gearboxes [2]:	Totally enclosed parallel cycloidal type
Power Supply:	460 VAC-3ϕ-60A
Control Circuit:	110 VAC fused
Hook Block:	6 sheaves
Limit Switches [4]:	Dual circuit uppers and lowers
Operator Station:	Pushbutton station suspended from hoist
Bumpers:	Rubber
Hoist Drums [2]:	Fabricated steel with machined grooves
Hoist Housing:	Fabricated steel
Hoist Reeving:	Double 6 part [12 parts]
Hoist Weight:	10,500 lb

Bridge and Trolley

Rated Capacity:	20 tons NUREG-0612; ANSI 14.6, 60 ton test
Span:	38 ft
Power:	460 VAC-3ϕ-60A
Bridge Speed:	20/6 fpm
Trolley Speed:	20/6 fpm

Rack Lift Rig Assembly

Although the dual purpose lift rig, depicted on Figure 9-7, is designed specifically for the Maine Yankee reracking project, it utilizes the same design principles and technology as used in spent fuel pool rerackings previously approved by NRC. The dual function of the lift rig is in the rack attachment point. The rack lifting assembly will be able to remove the existing racks (top of rack attachment) and install the new racks (bottom of rack attachment). The common strength member for both methods is the cruciform, independent, double beam lifting assembly. This lift rig assembly is designed to meet all NUREG-0554 and NUREG-0612 requirements.

A sampling of previous uses of the three aforementioned methods is depicted below:

a. Independent Cruciform Beams

San Onofre	(1990)	Removal and installation
LaSalle	(1989)	Installation

b. Top of Rack Attachment

Davis-Besse	(1981)	Installation
Arkansas Nuclear One	(1984)	Installation and removal
Millstone 2	(1987)	Removal

c. Bottom of Rack Attachment

St. Lucie	(1988)	Installation and removal
LaSalle	(1989)	Installation
Indian Point 2	(1990)	Installation and removal
San Onofre	(1990)	Removal and installation

9.2 RACK MOVEMENT SCENARIO

The following is a description of the sequence used for removal of the existing racks from the spent fuel pool and how the Maine Yankee 125/20 ton yard crane and temporary gantry crane are used in combination. This description is an illustration and not a procedure; numerous quality assurance and ALARA steps have been omitted for clarity.

1. Stage fuel transfer bridge in safe parking zone to avoid contact with temporary gantry crane.

2. Configure/adjust the lifting rig for the existing rack removal task.

3. Position temporary gantry crane, via its bridge and trolley, directly over rack to be removed.

4. Assemble existing rack lift rig and attach to temporary gantry crane.

5. Lower lift rig and attach to rack.

6. Lift rack approximately 6 in. above the pool floor.

7. Laterally move rack, via safe load path, to the cask pit.

8. Stage rack in the cask pit and disengage gantry crane.

9. Engage the 125 ton yard crane's sister hook with temporary hoists' lifting adapter and lift to a height of 1 ft.

10. Stage the bridge rails to the side to clear a load path for the exiting rack.

11. Lower the temporary gantry crane's hook block and again remotely engage it to the rack lift rig.

12. Raise the rack to the minimum height position necessary to clear the pool wall and obstructions. Underwater hydrolazing would be commenced in parallel with the raising of the rack and associated lifting gear. Allow the rack to drip dry.

13. Transfer the dry rack to decontamination pad area.

14. While suspended within a foot of the floor, place the shipping bag on the rack.

15. Position bagged rack on downender, remove lift rig and downend.

16. Attach horizontal lifting slings to downended rack.

17. Attach horizontal lift slings to downended rack and lift rack from decontamination pad area to awaiting special container and flatbed truck for shipping.

18. Return temporary gantry crane to bridge and position it for the next lift. This sequence, and its reverse for installation, will be interrupted several times in order to remove the bridge halves so that they will not interfere with fuel shuffling.

The existing racks will be shipped in accordance with 10CFR71 and 49CFR171-178, via the use of special shipping containers and transportation, to an approved processing facility for decontamination and volume reduction. Babcock and Wilcox, Environmental Services Division (B&W-ESD), will accomplish the decontamination processing.

9.3 INSTALLATION AND TEST DEVICES

A Drag Test Module, Up-Ending Fixture, Lifting Fixture, and Fuel Rack Height Adjustment Tool will be used in the transportation and installation of new racks. These devices are shown on Figures 9-5, 9-6, 9-7, and 9-8, respectively.

The Drag Test Module will be used to drag test each rack module at Maine Yankee prior to installation in the pool to ensure that they were not damaged during transportation and again after their installation into the pool has been completed. The Up-Ending fixture will allow the rack modules, transported in an axis-horizontal position, to be rotated to an axis-vertical position, while properly supporting the module, prior to the site drag test. The Lifting Fixture will provide the interface between the rack and the lifting device; evenly spreading the load for a safe operation. The Fuel Rack Height Adjustment Tool will allow for the remote adjusting of the adjustable foot in the unloaded condition from above the pool.

9.4 SAFETY PRECAUTIONS

In line with the entire project's "defense-in-depth" approach to NUREG-0612, the following is a list of additional safety measures which will be implemented during reracking operations:

1. The 125/20 ton yard crane will be tested operationally in accordance with the existing Maine Yankee Control of Heavy Loads Program. The in-place inspection and maintenance of the temporary gantry crane will be conducted in accordance with the guidelines of Section 5.1.1 of NUREG-0612 and tested in the following manner:

   a. An operational test will be conducted in accordance with the provisions of paragraph 2-2.2.1 of ANSI B30.2-1976 at the factory prior to shipment, at the site prior to installation and over the spent fuel pool prior to the initial rise. These tests include hoisting and lowering tests, trolley and bridge travel, and testing of limit switches.

   b. A full performance test will be performed using the maximum critical load of 25 tons at the factory in accordance with Section 8.2 of NUREG-0554 and Section 2-2.2.2 of ANSI B30.2, 1976.

   c. A rated load test of 60 tons will be conducted in accordance with paragraph 5.2.1 of ANSI 14.6-1978 at the factory prior to installation.

   Note: No load tests will be conducted over the spent fuel pool or other safety-related equipment.

2. All special lifting devices, including ancillary equipment (e.g., slings, shackles, padeyes, etc.) will comply with the following:

   a. Meet the provisions of Guideline 4 of Section 5.1.1 of NUREG-0612. The old and new rack lifting rigs will comply with the requirements of ANSI 14.6-1978, and

   b. Be tested, inspected, maintained, and repaired in compliance with NUREG-0612, Section 5.3, "Testing to Verify Continuing Compliance" and Section 5.4, "Maintenance and Repair," and ANSI N14.6-1978, "American National Standard for Special Lifting Devices for Shipping

Containers Weighing 10,000 Pounds (4,500 kg) or More for Nuclear Materials."

3. When lifting racks, a load cell, attached in series with the load, will be monitored for expected weight readings.

4. All rack lifts will incorporate a 5 minute hold at a height of 6 in. or less prior to continued raising or lateral movement.

5. The racks will be lifted no more than 12 in. above the fuel pool floor during movement toward the cask pit area.

6. The vertical lifting rate for the racks will not exceed 6 ft per minute.

7. The lateral movement rate for the racks will not exceed 6 ft per minute.

8. A minimum distance of 1 in. will be maintained during rack lateral movements between racks and between racks and walls. Only during final precision positioning will the minimum be encroached.

9. Safe load paths have been developed for all rack movements. No racks will be transported over any spent fuel.

10. Heavy lift equipment and safe load paths have been developed for all temporary gantry crane bridge installation and removal operations.

11. The upending and downending of the rack modules will be accomplished in an area away from and not overlapping any safety related components.

12. Personnel involved in the reracking operation will have completed required training in the use of heavy lift and upending/downending equipment. This training will specifically address the exact rigging, loads and methods used for the Maine Yankee reracking project.

13. A minimum of 22 ft of water above irradiated fuel assemblies seated within the rack cells will be maintained throughout the reracking process.

14. No fuel handling operations will be conducted when the yard crane roll-up door to the spent fuel pool is open.

9.5 EXISTING RACK DISPOSAL

9.5.1 Packaging and Shipping

The fuel racks will be hydrolased and dried prior to packaging and shipment to B&W-ESD. The contractor will deliver the sea van containers and bags to the Maine Yankee facility. Slings will be pre-positioned in the bags that receive the racks which must then be closed around the racks with the slings pulled through the bags to allow for lifting the bag and rack at the decontamination facility. The packaged racks will then be shipped to the B&W-ESD facility using standard radiological material shipping procedures.

9.5.2 Unloading and Staging (at B&W-ESD)

The bagged racks will be lifted out of the shipping containers and moved into the B&W-ESD spent fuel building for further processing. Decontamination facility personnel will arrange the racks in a fashion to facilitate the timely and safe unwrapping and processing of the materials in the large work area.

9.5.3 Cutting and Dismantling (at B&W-ESD)

The racks and other materials will be cut into sections that will allow for the effective decontamination and surveying of the pieces. The primary means of cutting stainless steel items will be with the plasma arc torch.

9.5.4 Decontamination (at B&W-ESD)

The BORAL™ sheets will be cleaned with a Hot-Chemical Dip method. This methodology has proven to be the most successful means of removing the contamination from aluminum-type materials. The cleaning of the stainless steel materials will be conducted with abrasive steel shot blasting as the primary means of decontamination.

9.5.5 Surveying of Materials After Cleaning (at B&W-ESD)

The materials that have been decontaminated will be surveyed. The pieces to be surveyed are placed on a conveyor and sent through a shielded array of three Bismuth Germanium detectors. The readout of the detectors is fed through a computerized network that identifies to the trained operator exactly where and to what level any remaining contamination exists. The system takes the uncertainty and the inefficiency of manual frisking out of the cycle. Additionally, the shielded detectors are much more sensitive than hand-held devices.

9.5.6 Final Disposal

Clean materials are released for scrap. Any nonclearance material will be sent to a licensed low level radioactive waste melt facility for further use as contaminated shielding or may be disposed of in an approved licensed low level radioactive waste facility.

The estimated volume of radwaste resulting from this project is 415 cu ft. This represents more than a 97% volume reduction when compared to the volume of the racks and BORAL™ inserts (16,045 cu ft) scheduled to be processed.

MAINE YANKEE ATOMIC POWER COMPANY

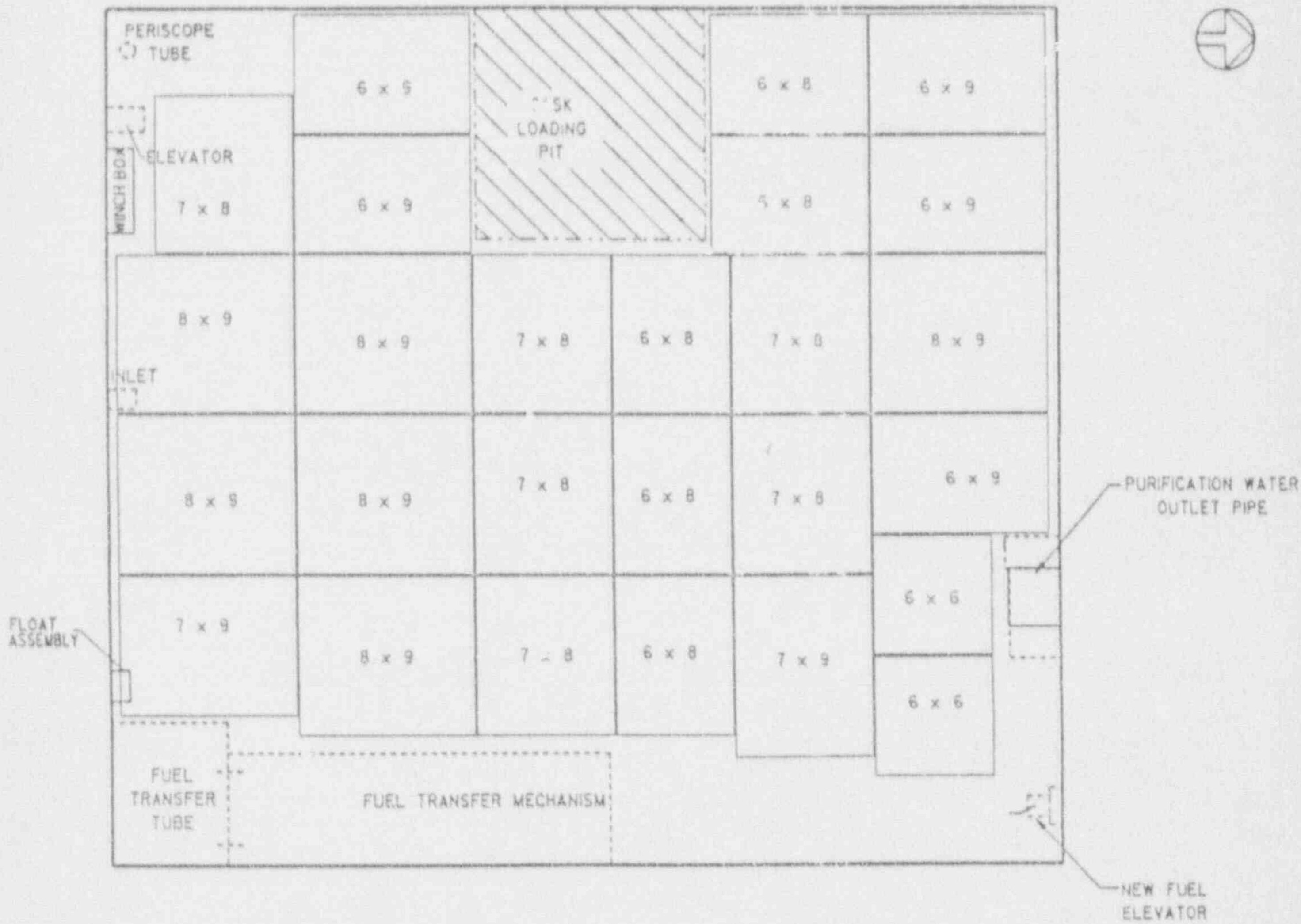

FIGURE 9-1
EXISTING SPENT FUEL POOL ARRANGEMENT

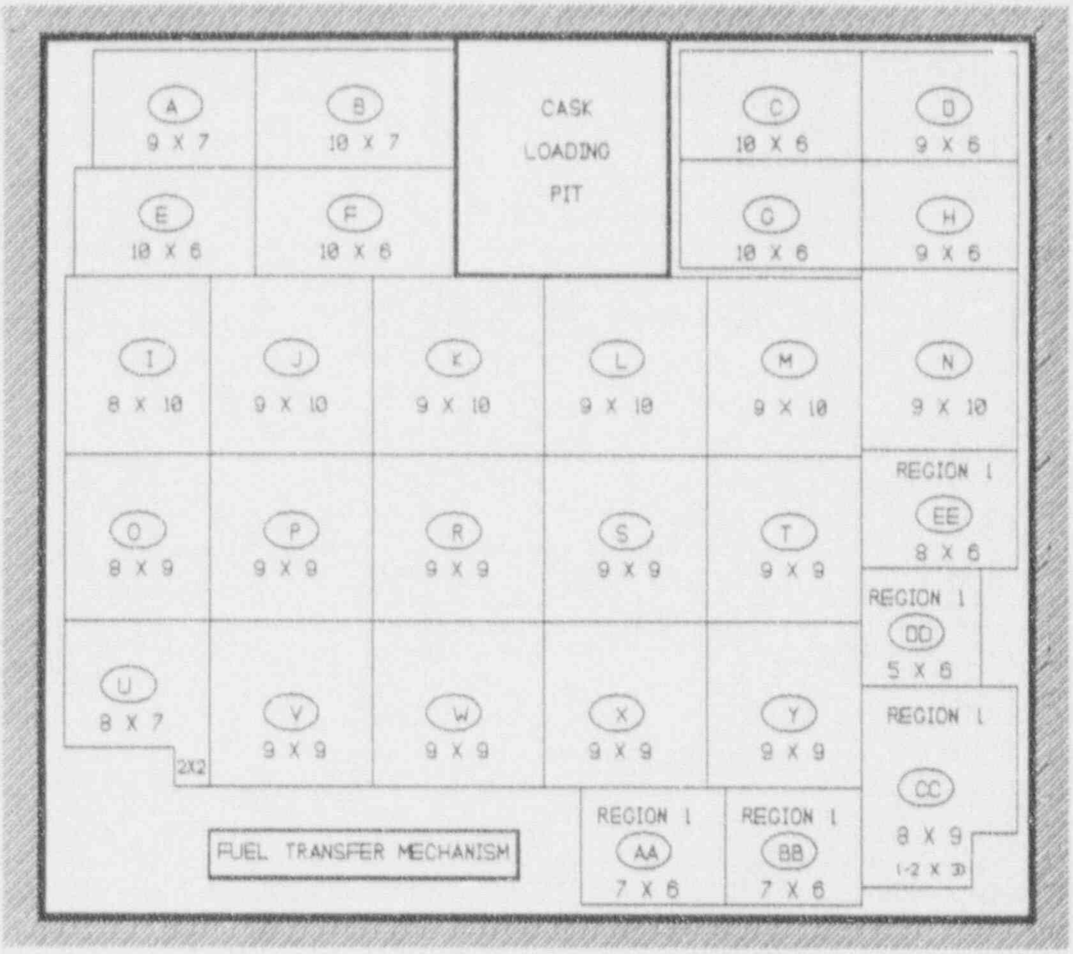

FIGURE 9-2
PROPOSED SPENT FUEL POOL ARRANGEMENT

MAINE YANKEE ATOMIC POWER COMPANY

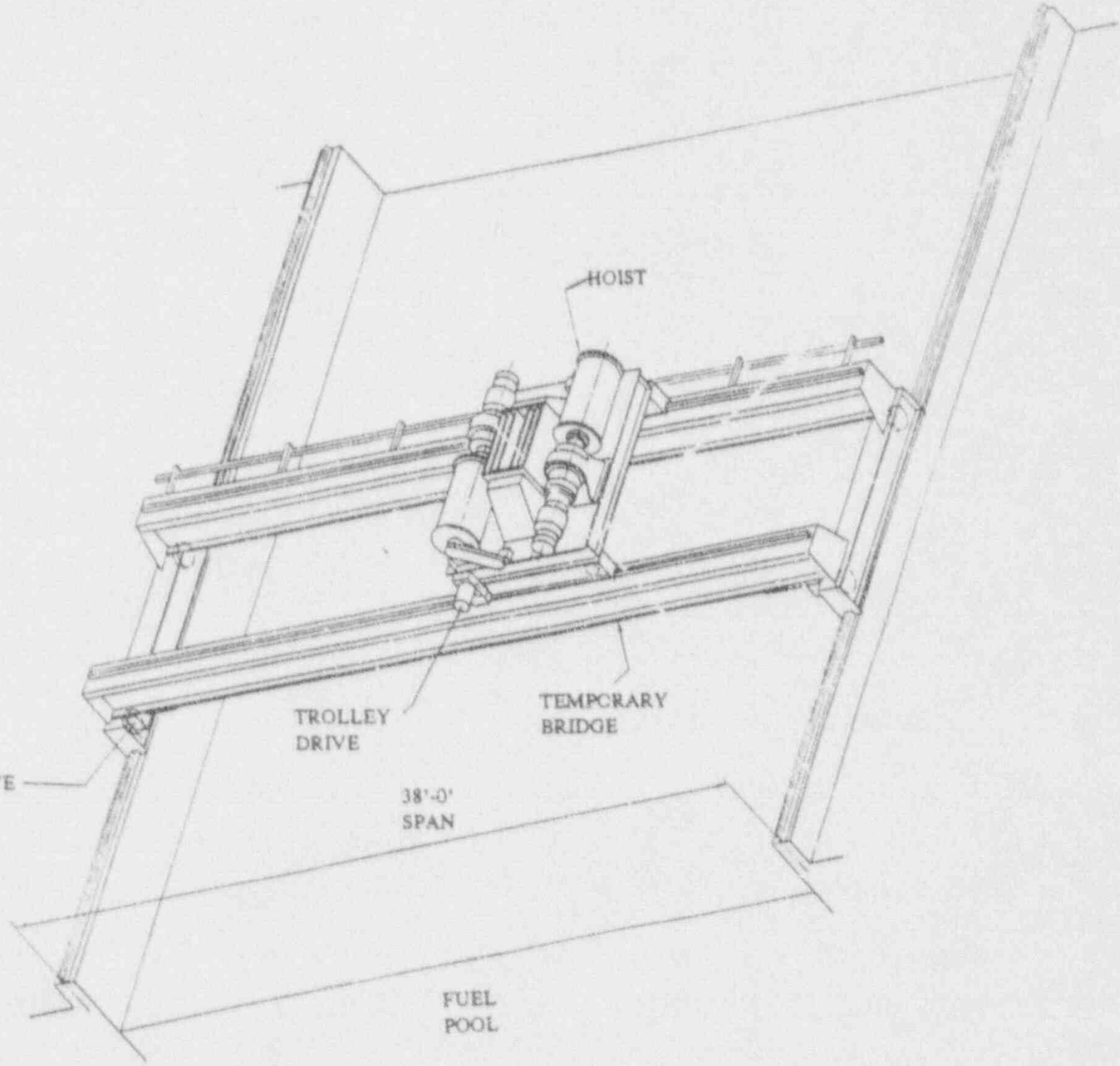

FIGURE 9-3
TEMPORARY HEAVY LIFT SYSTEM

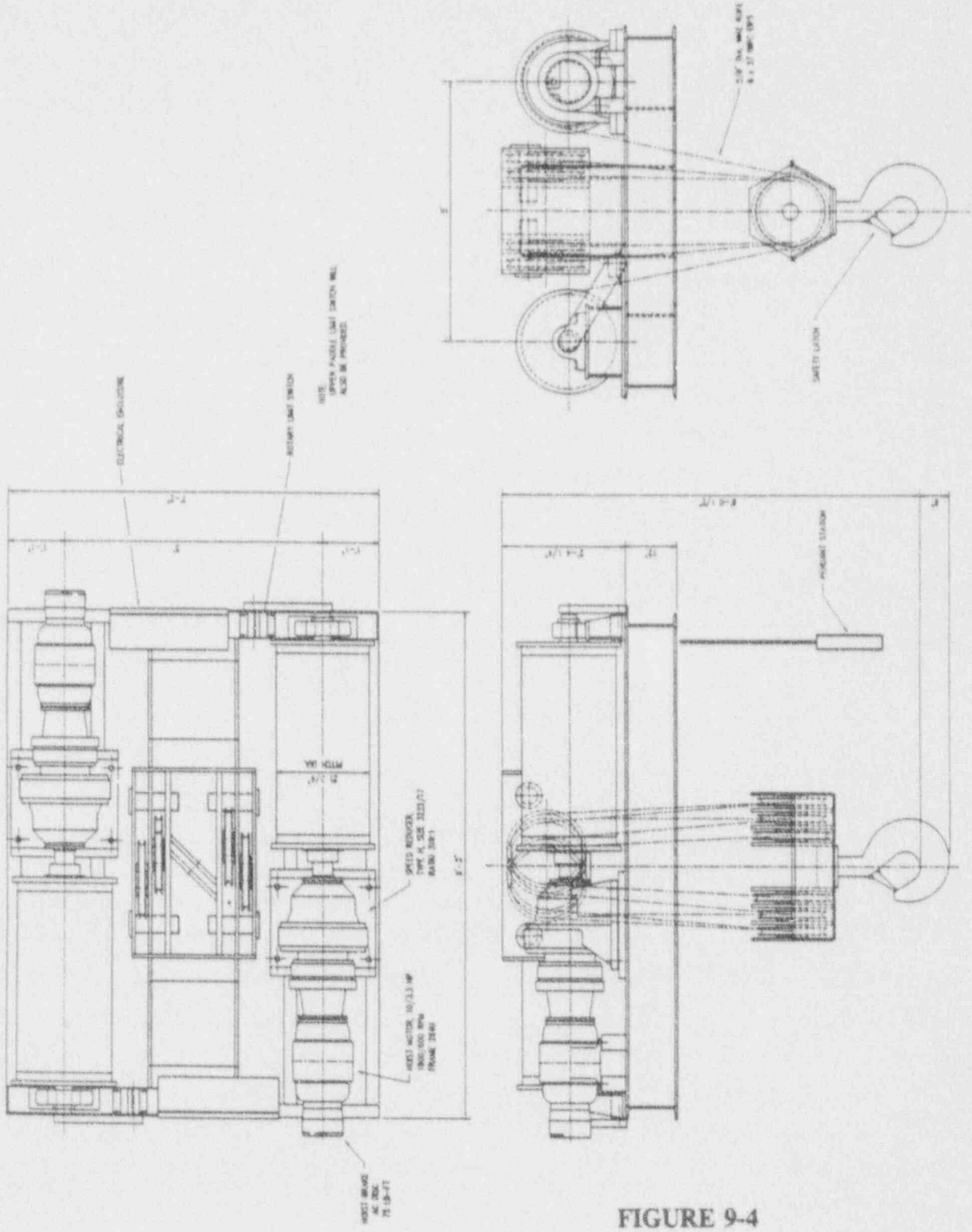

FIGURE 9-4
TEMPORARY GANTRY CRANE

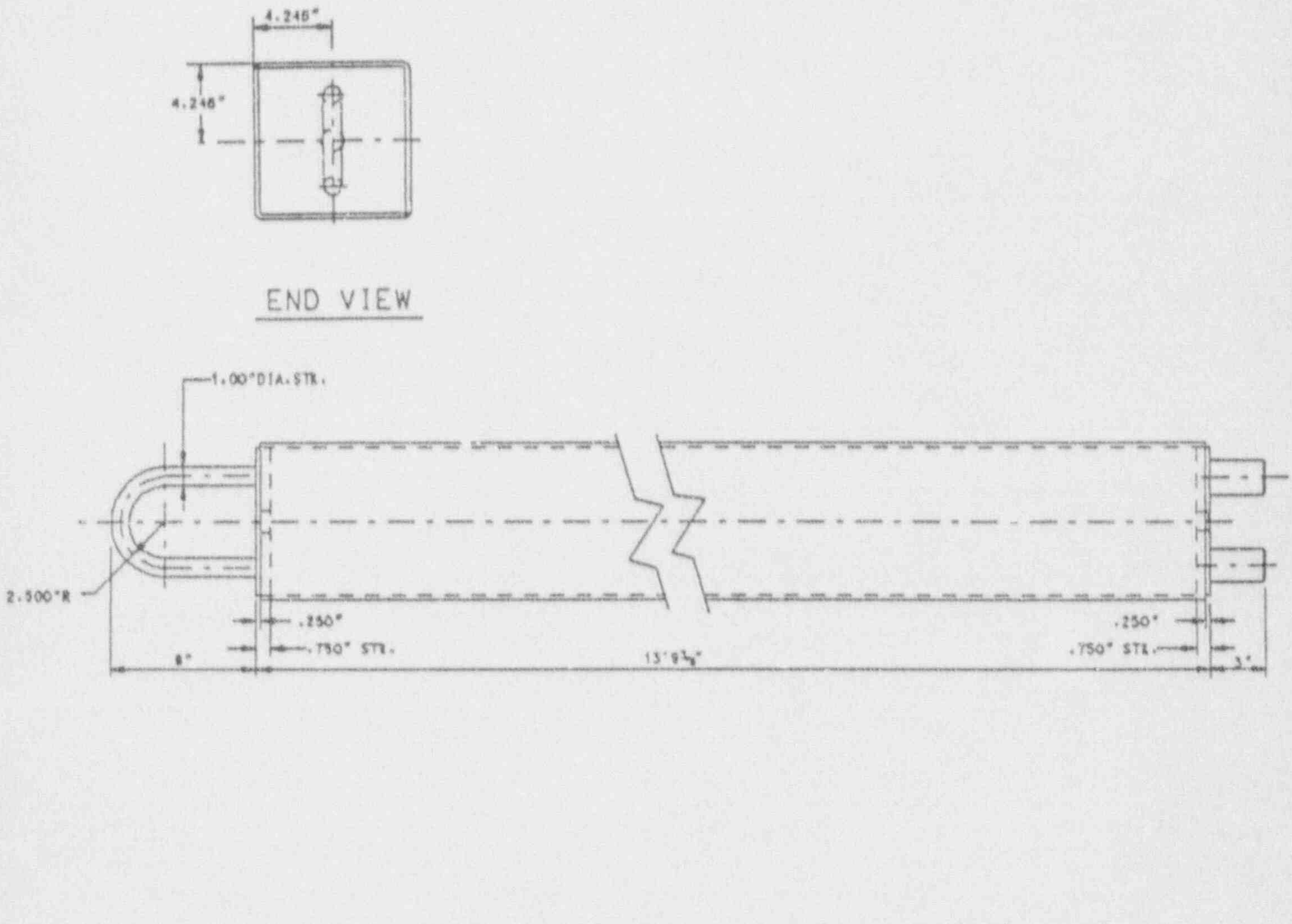

FIGURE 9-5
DRAG TEST MODULE

MAINE YANKEE ATOMIC POWER COMPANY

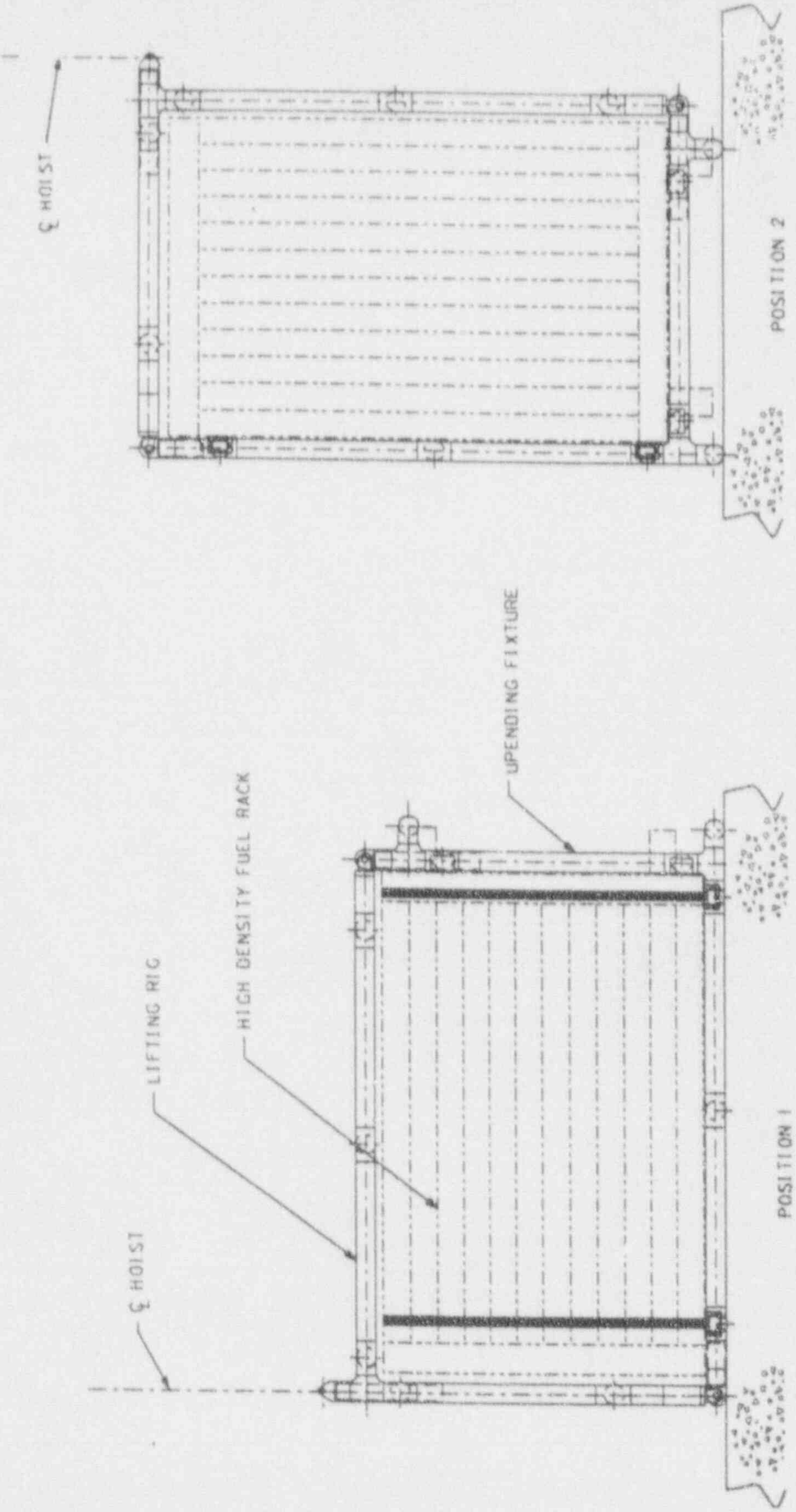

FIGURE 9-6
UP-ENDING FIXTURE

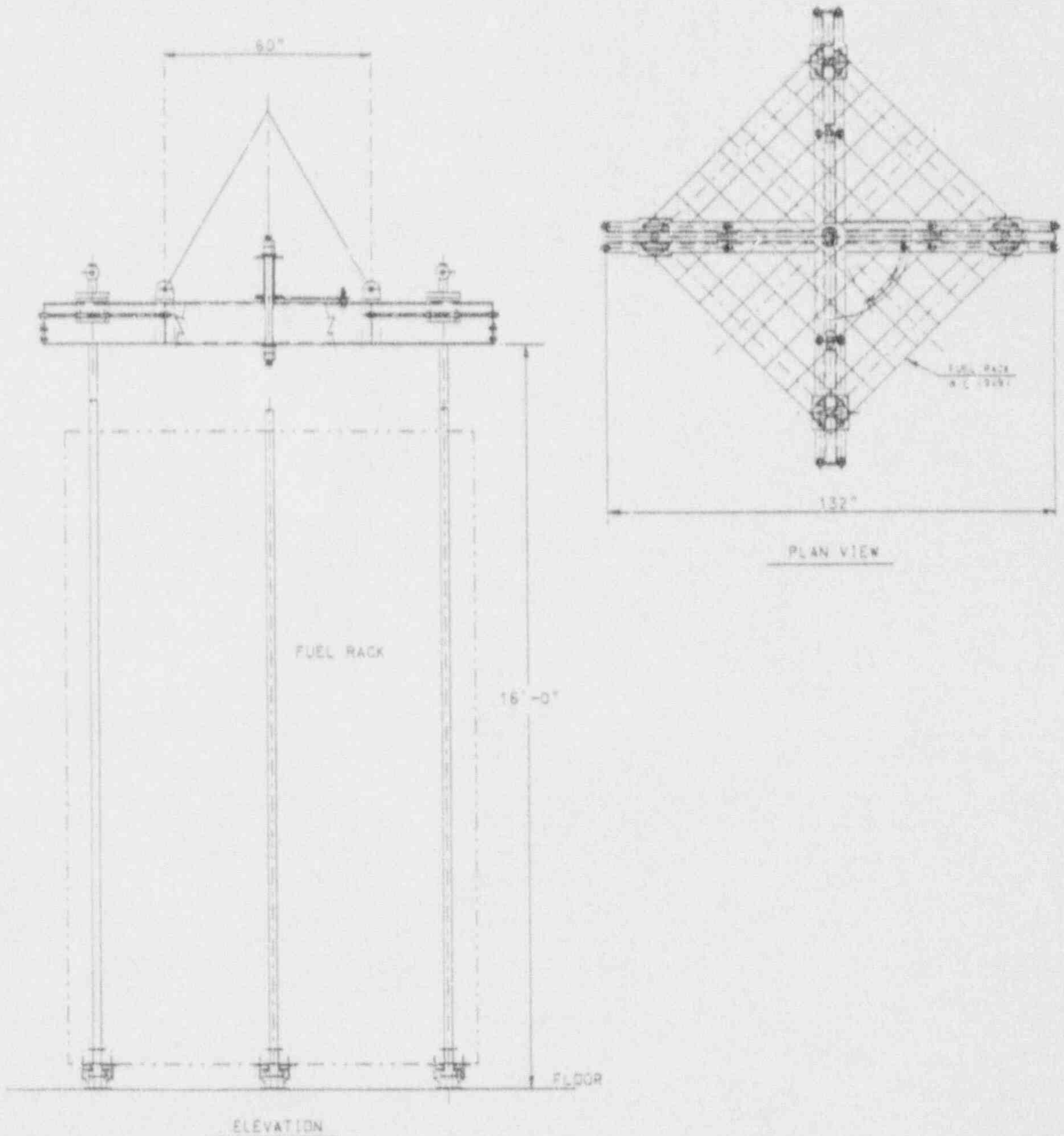

FIGURE 9-7
LIFTING FIXTURE

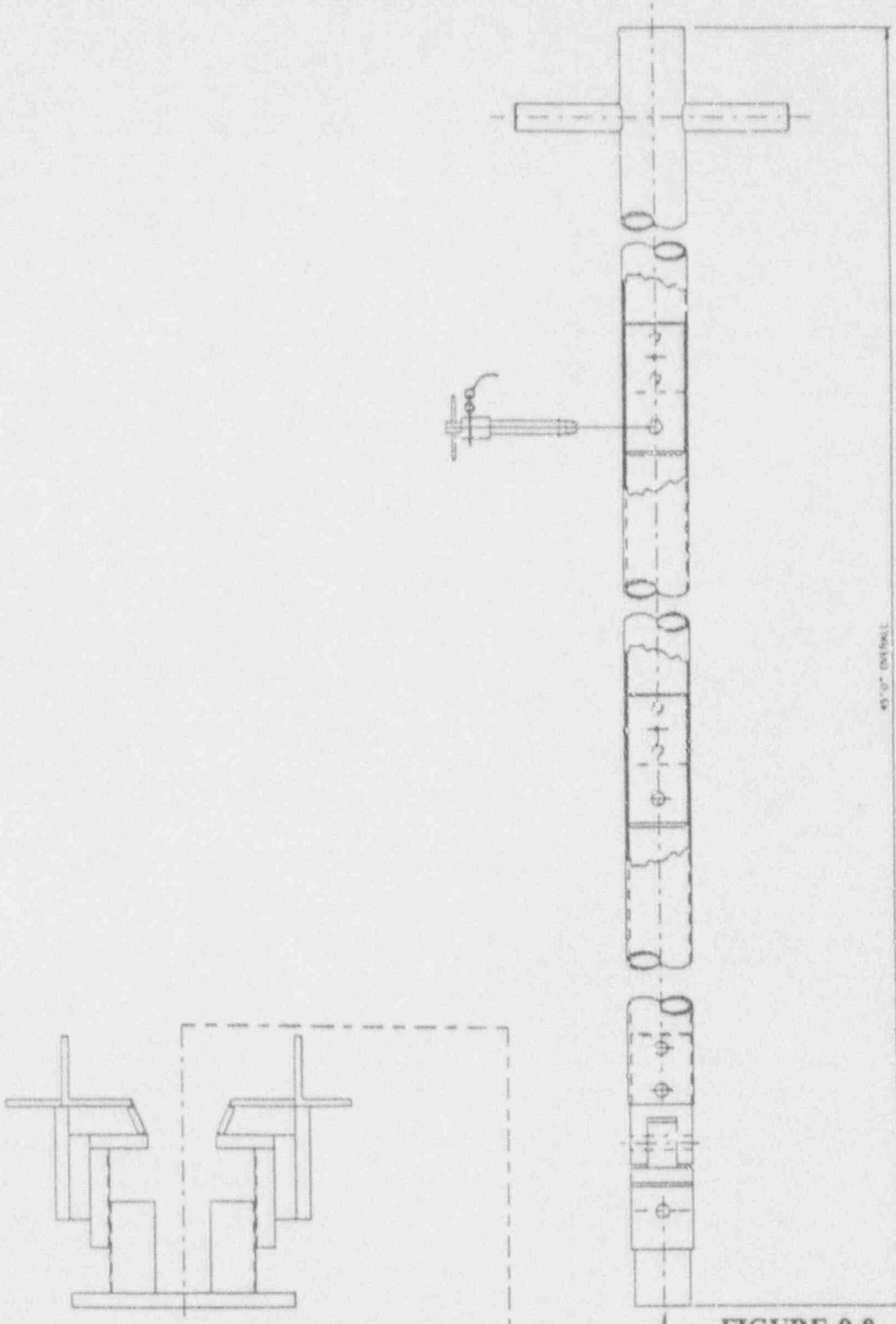

FIGURE 9-8
FUEL RACK HEIGHT ADJUSTMENT TOOL

10.0 ACCIDENT ANALYSIS

Accidents are evaluated in this report to determine the adequacy of the new high-density spent fuel storage racks to perform their function of safe long-term storage of the spent fuel and to determine the suitability of the Maine Yankee plant systems, structures, and components to accommodate the increased inventory of spent fuel.

The accidents currently addressed in the Maine Yankee licensing basis that involve the spent fuel storage racks are as follows:

- Fuel Handling (i.e., impact of dropping a spent fuel assembly)
- Thermal-Hydraulics (i.e., partial loss of spent fuel pool cooling system circulation flow and complete loss of circulation flow and/or cooling)
- Criticality (i.e., spent fuel assembly drop in the spent fuel pool on the racks or placing an assembly alongside the racks)
- Construction (i.e., removal of existing racks and installation of the new racks)

Analysis of these potential accidents demonstrates that the consequences remain within the current licensing basis for Maine Yankee. The new high-density spent fuel storage racks create no additional accident scenarios.

Chapter 3 presents the analysis of heavy loads dropped on the racks, and Chapter 4 discusses dropping such loads on the spent fuel pit structure. The potential radiological consequences of these accidents are discussed in Chapter 7. The consequences of these events are encompassed by the current Maine Yankee licensing basis.

Thermal-hydraulic analysis of accident conditions are discussed in Chapter 5. The results indicate that the fuel assemblies do not exceed the allowable pin temperatures and no fuel failures will result from storage of spent fuel in the new racks.

Criticality accidents are analyzed in Chapter 6. The results of the criticality analysis indicate that the accident scenarios do not cause the K_{eff} to exceed 0.95.

Accidents during the heavy handling operations in the Fuel Building while installing the new racks are precluded since the guidelines of NUREG-0612 and the Maine Yankee Control of Heavy Loads Program will be followed. All load handling will follow clearly established safe load paths. The temporary gantry crane, its associated bridge and trolley system, as well as the associated lifting device, are designed to meet the criteria of NUREG-0612.

11.0 IN-SERVICE SURVEILLANCE PROGRAM

11.1 GENERAL

The In-Service Surveillance Program will provide confirmation of the integrity of the BORAL™ over the 40-year design life of the spent fuel racks. To ensure that the surveillance test samples perform in the same manner as the full-size neutron absorber panels used in the racks, the Maine Yankee Surveillance Program will rely on full size BORAL™ panels. The program is designed to provide exposure test data in a shortened time span where 1 year of testing is equivalent to 4 to 5 years of normal fuel storage time. This is accomplished by placing freshly discharged fuel adjacent to the surveillance samples at each refueling. At 1, 3, 5, and 10 years, a surveillance sample will be removed. The sample will be subjected to the tests described in Section 11.2.3.

11.2 BORAL™ PANEL TESTING

11.2.1 Description

BORAL™ panel testing will be performed on components identical to those in the actual racks bearing full length BORAL™ panels. This will eliminate any question of test sample reliability. Each test sample will consist of a full length BORAL™ panel mounted on a stainless steel plate and covered with the standard stainless steel sheath used in the fuel racks. The total number of test samples in the program will be six. These test samples will be located along the north side of Region I rack module DD (see Figure 1-2).

11.2.2 Benchmark Data

Six surveillance panels will be set aside during production of the BORAL™ panels for benchmark testing. These samples will be taken from the production run at equal intervals to give a representative group of test samples. Benchmark data will be established by performing all the tests described in the next section on these surveillance samples. The results of these benchmark tests will be recorded and sent with the samples to Maine Yankee.

11.2.3 Testing

One sample panel will be removed for testing as discussed in Section 11.1. Upon removal from the spent fuel pool, the test panel will be subjected to the following test program:

1. Measurement of Assembly

   Thickness measurements will be made every 6 in. along the length. The measurements will be made at the edge, middle, and edge, and include the sheath, panel, and plate wall.

2. BORAL™ Panel Measurements

   The BORAL™ panel will be removed from the assembly, and the thickness measurements will be repeated as defined above. In addition, visual examination will be performed along selected locations of the BORAL™ panel using a 5 X magnification, and abnormalities will be recorded.

3. Destructive Examination

   The surveillance sample will be cut up to fit a standard shipping container and sent to an appropriate laboratory for final destructive examination. The tests to be performed will include the following (the location of samples for testing will be the middle of the panel):

   1. Neutron Radiography

   2. Neutron Attenuation

   3. Hardness Testing

   4. Chemical Analysis

These results will be compared to the benchmark data identified in Section 11.2.2.

11 2.4 Acceptance Criteria

The measurements before and after testing should agree within the measurement uncertainty range, typically $\pm$ 10% except for the neutron attenuation that should be within $\pm$ 3%.

12.0 QUALITY ASSURANCE

Maine Yankee Atomic Power Company (MYAPCO), as the licensee, is responsible for the overall management plan for project quality. MYAPCO's Quality Assurance (QA) Department, assisted by Yankee Atomic Electric Company's (YAEC) Vendor QA Group, will act as independent partners with Brand Utility Services, Inc. (BRAND) in the QA supervision and program oversight.

Within these roles, MYAPCO and YAEC will conduct performance-based audits and surveillances to assure that the entire project, from the design of the new racks through the disposal of the old racks, meets 10CFR50, Appendix B requirements and the requirements imposed by the codes and standards specified in this report.

The MYAPCO Reracking Management Plan for Project Quality is a project oriented "canopy" plan which outlines the specific quality related organizational interfaces and the individual scopes and procedures of the interfacing organizations. Figure 12-1 is a graphic representation of these interfaces.

12.1 BRAND UTILITY SERVICES, INC.

For the Maine Yankee rerack project, Brand Utility Services, Inc. (BRAND), the prime contractor, will have overall QA responsibility for all services and materials supplied to MYAPCO. BRAND, as an approved vendor of MYAPCO, will in turn impose the requirements of 10CFR50, Appendix B and the codes and standards specified in this report on its vendors.

BRAND is responsible for ensuring that the QA programs of vendors are qualified and approved in accordance with 10CFR50, Appendix B, and that these programs are being appropriately and adequately implemented for the Maine Yankee reracking project.

BRAND performs a second function as the installer in this reracking project. As the installer, BRAND will remove old racks and install new racks, prepare old racks for shipment and disposal, and provide a complete documentation package relating to the completed project. The BRAND QA Program is designed to meet the requirements of 10CFR50, Appendix B; ANSI/ASME NQA-1; and the intent of ANSI N45.2. This program also has provisions for the responsibilities under 10CFR21. The BRAND QA Program for the Maine Yankee reracking project will specify the procedures from the BRAND QA Program to be implemented during this project.

12.2 STONE AND WEBSTER ENGINEERING CORPORATION

12.2.1 Nuclear Quality Assurance Program (SWSQAP 1-74)

Stone & Webster Engineering Corporation (SWEC), as subcontractor to BRAND, is the Maine Yankee reracking project designer, engineer, and licensing support coordinator. The SWEC Nuclear QA Program (SWSQAP 1-74) applies to all activities performed by SWEC affecting quality. The program complies with 10CFR50, Appendix B and quality related NRC Regulatory Guides, and has been approved by the NRC for use in a full range of activities, including design, licensing, procurement, construction, startup, and preoperational testing. SWEC's program has been evaluated and approved by audit in accordance with ANSI N45.2.12, BRAND's QA Manual Section 18, and BRAND's Quality Procedure 07.02 (Supplier Evaluation and Approval Procedure). The SWEC program also requires the following:

a. Procedures that are consistent with program commitments are to be used. SWEC has corporate procedures in place that implement the requirements of SWSQAP.

b. Each project is to describe the scope of work with special attention given to exceptions or additions to SWSQAP requirements, responsibilities, and interfaces with other organizations. A Project Quality Assurance Plan is used to document these requirements.

12.2.2 Project Quality Assurance Plan

The SWEC Project Quality Assurance Plan (QA Plan) for the Maine Yankee spent fuel rack design and licensing project describes the specific portions of SWSQAP that apply to the project's scope of work. It also identifies the procedures that will be used to implement the project's scope of work and requirements.

12.2.3 Surveillances

During design and engineering activities MYAPCO, YAEC, and BRAND QA will perform audits and surveillances, as applicable, at the working locations to verify effective implementation of design engineering, and inspection procedures.

12.3 GENERAL DYNAMICS/ELECTRIC BOAT DIVISION

General Dynamics/Electric Boat Division (GD/EB), in its capacity as the spent fuel rack fabricator, will work in accordance with its own approved QA program. GD/EB's program has been evaluated and approved by audit in accordance with ANSI N45.2.12, BRAND's QA Manual Section 18, and BRAND's Quality Procedure 07.02 (Supplier Evaluation and Approval Procedure).

During fabrication, MYAPCO, YAEC, and BRAND QA organizations will perform surveillance inspections at the Quonset Point Facility to verify effective implementation of the fabrication and inspection procedures.

12.3.1 Quality Assurance Program Implementation

GD/EB maintains a QA Program to ensure that the quality of products produced anywhere within the organization meets all internal quality related directives and customer contract requirements. The Nuclear Services QA (NSQA) program that applies to this work meets the criteria of 10CFR21; 10CFR50, Appendix B; and ANSI/ASME NQA-1. The QA Program ensures that the finished products produced at all division locations and facilities comply with all applicable quality requirements.

GD/EB maintains a Nuclear Services QA (NSQA) Manual that embodies all of the requirements of these governing documents and establishes the top level QA Program requirements for nuclear services programs at GD/EB.

The NSQA Manual requires that, when a nuclear services project begins, three project-specific QA documents are written. The first is a Project Control Document (PCD) that defines all of the QA requirements for that specific project. The PCD implements all of the 10CFR21, 10CFR50, and ANSI/ASME NQA-1 requirements, identifies all of the defining technical documentation, identifies any project-specific requirements, and lists all existing applicable procedures and/or process instructions. The second is a QA Plan that describes in detail the processes that will be followed to ensure that the requirements identified in the PCD are met. The third is the Engineered Inspection Plan that identifies all of the inspections or tests that are to be performed, their acceptance/rejection criteria, and when they must be performed during the fabrication process.

Each of these three documents may identify the need for project-specific procedures and/or instructions to be developed and validated or certified. In the case of spent fuel rack fabrication, the Drag Test Inspection Procedure is a example of a project-specific procedure to be developed.

The hierarchy of the GD/EB fabrication QA documentation is depicted on Figure 12-2.

12.3.2 Inspection

The qualifications of the GD/EB non-destructive test personnel meet or exceed the requirements specified in SNT-TC-1A. Inspection personnel are qualified to ANSI N45.2.

GD/EB maintains a QA program that utilizes a mixture of trades-person performed "verifications" and QA personnel performed "inspections." This is important to maintain full trade accountability for the quality of the rack modules.

NQC personnel develop an Engineered Inspection Plan that extracts all of the quality attributes from the manufacturing drawings. They add quality attributes based on experience gained in similar fabrication efforts to ensure that the quality of the finished product meets or exceeds those on the manufacturing plan. Some welding is verified in-process by the tradesperson making the weld, and some welding will be inspected by QA personnel. QA personnel reserve the authority to conduct random welding audits and adjust the verification/inspection equation based on the results of these random audits.

BRAND will coordinate the development of appropriate check and hold points through the liaison with SWEC and GD/EB. The resulting fabrication QA plan will then be approved by MYAPCO prior to fabrication by GD/EB.

12.4 YANKEE ATOMIC ELECTRIC COMPANY

Yankee Atomic Electric Company (YAEC) will provide QA support services to Maine Yankee as directed by MYAPCO. These services will include vendor audits and vendor surveillances of BRAND and sub-tier vendors. YAEC QA services will be provided in accordance with the YAEC Operational QA Manual, YOQAP-1-A. Engineering services provided by YAEC to MYAPCO for this project will likewise conform to YOQAP-1-A.

MAINE YANKEE ATOMIC POWER COMPANY

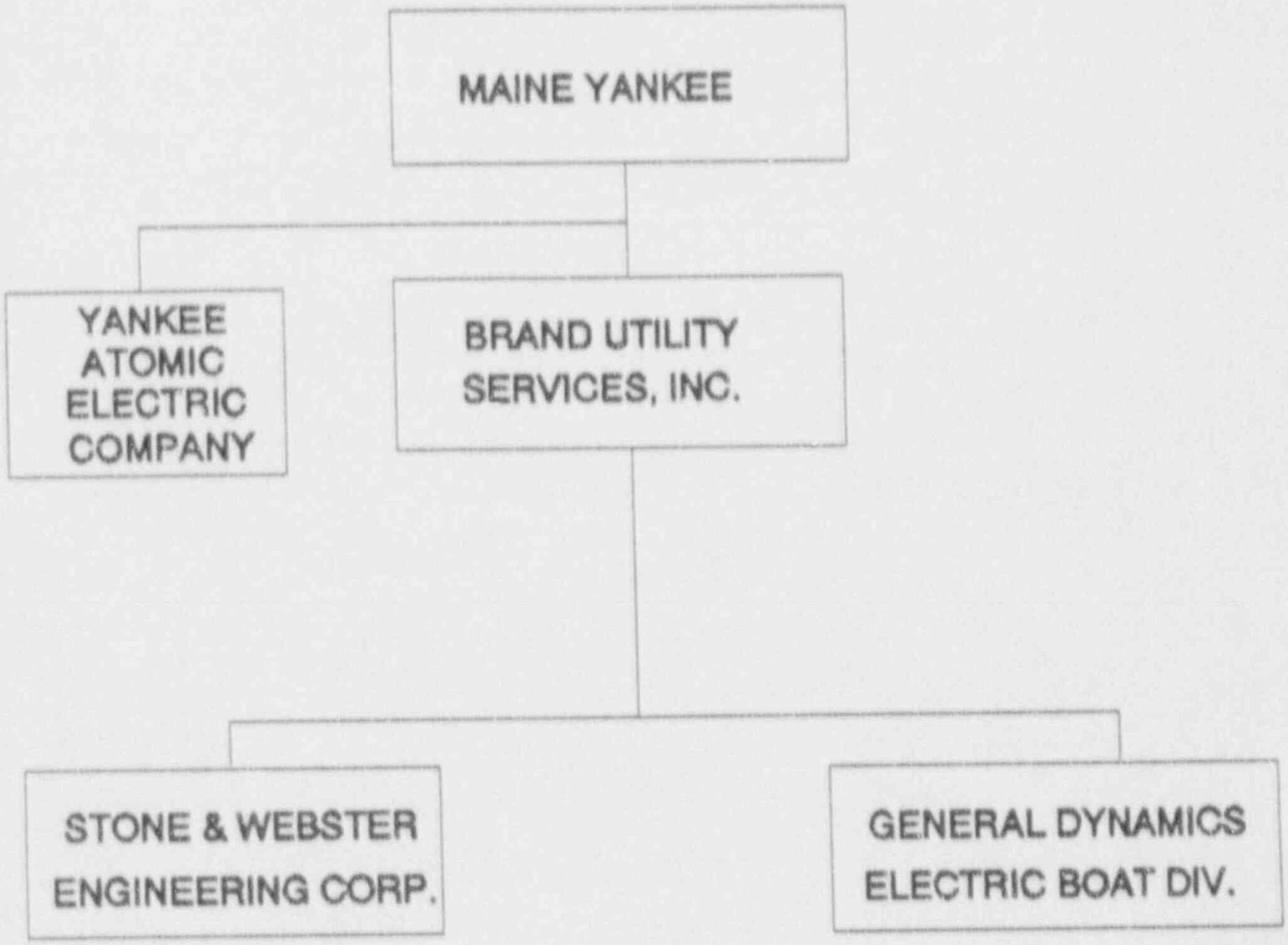

FIGURE 12-1
QUALITY ASSURANCE
ORGANIZATION

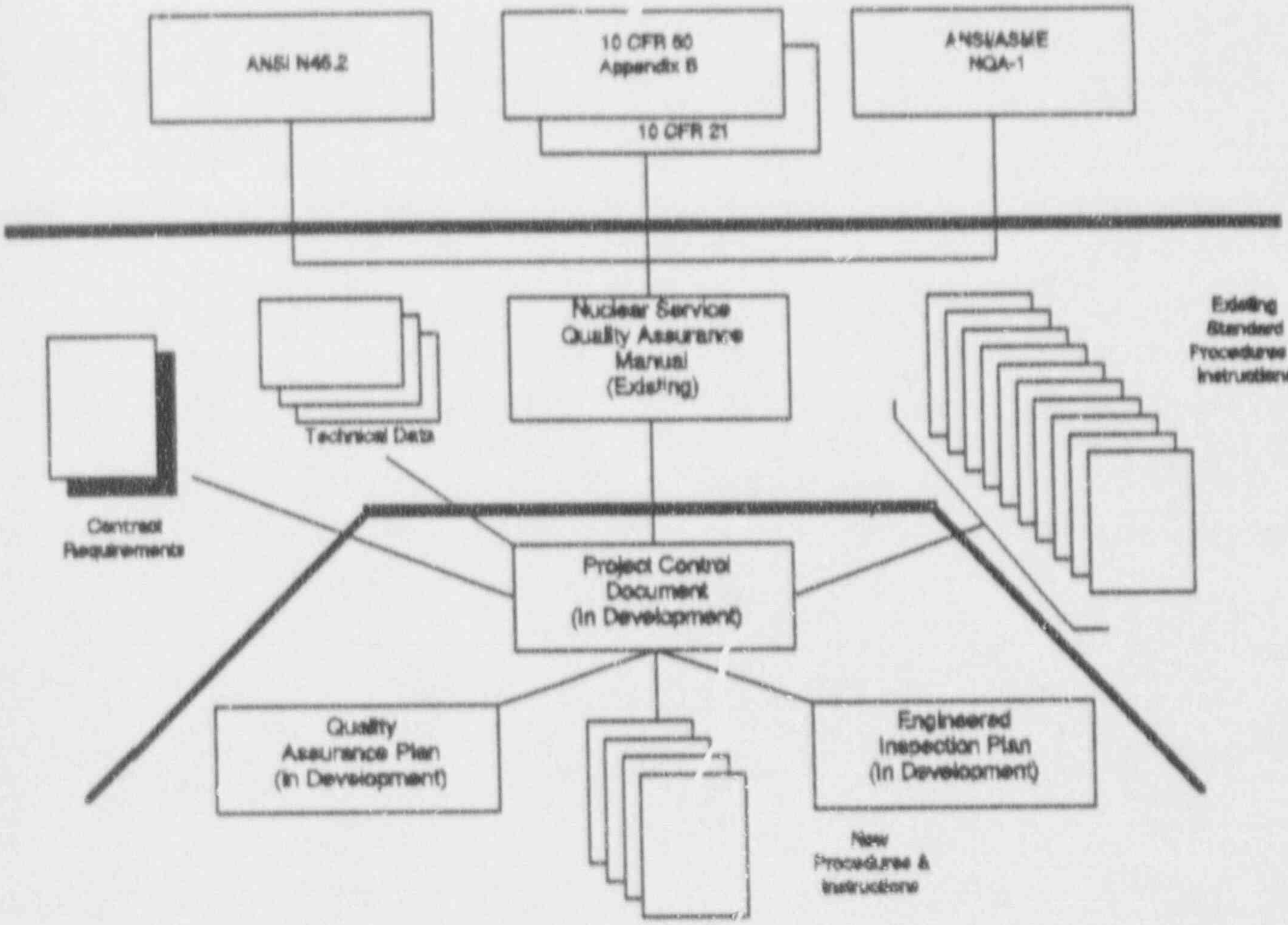

FIGURE 12-2
FABRICATION QA PROGRAM
DOCUMENTATION

13.0 ENVIRONMENTAL ASSESSMENT

Based on the following environmental assessment for the proposed reracking of the Maine Yankee spent fuel storage pool, MYAPCO has concluded that the proposed spent fuel storage capacity increase will result in no significant impact on the environment.

13.1 NEED FOR INCREASED STORAGE CAPACITY

The current licensed storage capacity of the Maine Yankee spent fuel pool is 1476 fuel assemblies. Chapter 5 of this report discusses the anticipated refueling schedule and the expected number of fuel assemblies to be transferred into the spent fuel pool at each refueling. Without the increased storage capacity provided by approval of this submittal, Maine Yankee will no longer have the capacity to conduct a reloading of the reactor core beyond 1999.

The Maine Yankee spent fuel pool is expected to contain approximately 1204 spent fuel assemblies at the proposed time of reracking in May 1995.

Based on the proposed increased storage capacity to 2019 spent fuel assemblies, the estimated date that the Maine Yankee spent fuel storage racks would be filled is as discussed in Chapter 1.

Spent fuel will be shipped offsite for final disposition under an existing contract with the U.S. Department of Energy (DOE) pursuant to the Nuclear Waste Policy Act of 1982. Although the contract specifies the start of DOE acceptance of spent fuel in 1998, the Federal facility is not expected to be available prior to the year 2010.

13.2 ALTERNATIVES

Maine Yankee has considered and evaluated various alternatives to the proposed increase in spent fuel storage capacity at the plant. The storage of spent fuel at Maine Yankee is an interim solution until a Federal repository, currently expected to be available in 2010, is established to accept spent fuel assemblies in accordance with the Nuclear Waste Policy Act of 1982 (Public Law 97-425). When Maine Yankee was originally designed, commercial reprocessing of spent fuel was expected, in large part, to minimize onsite spent fuel storage capacity requirements. Commercial reprocessing of spent fuel has not developed and is, therefore, not a currently available option to minimize storage capacity.

In 1979, the NRC issued a final "Generic Environmental Impact Statement on Handling and Storage of Spent Light Water Reactor Power Reactor Fuel" (Ref. 13-1) that analyzed alternatives for the handling and interim storage of spent fuel as well as the possible restriction or termination of the generation of spent fuel. One alternative considered in detail in Reference 13-1 is the expansion of onsite spent fuel storage capacity by modifying existing spent fuel pools. Since there are several variations in storage designs and limitations, Reference 13-1 recommends that an evaluation of other alternatives be done on a case-by-case basis.

MYAPCO has identified alternative spent fuel storage methods currently utilized by the nuclear industry and evaluated their application at Maine Yankee. These alternative spent fuel storage methods include the following:

a. High density racks in existing spent fuel pool

b. Fuel rod consolidation in existing racks

c. Construction of new spent fuel pool

d. Dry cask spent fuel storage

The above alternatives were considered with respect to environmental impact, operational impact, and technical feasibility. Each alternative is addressed below:

a. <u>High Density Racks in Existing Spent Fuel Pool</u>

Since the existing spent fuel storage racks are of a high density storage design, exercising this option requires the use of a more efficient spent fuel storage rack. Such racks have been installed and used for spent fuel storage at other utilities.

Spent fuel pool reracking, in general, has been used extensively by other utilities and, in particular, twice before at Maine Yankee.

There are several advantages to this option. The application of new high density spent fuel storage racks does not require any modification to the plant site or the surrounding environment. Additionally, the location and method of storage of spent fuel assemblies will not change from current practice. Therefore, there is no need to transport spent fuel assemblies outside the spent fuel pool. A significant advantage of this option is that there are no onsite construction activities and, therefore, no attendant environmental, operational, or infrastructure concerns. The existing spent fuel pool support systems (i.e., cooling and purification systems, building ventilation systems, etc.) can continue to be used without modification.

Therefore, the use of high density spent fuel storage racks as proposed in this report is determined to have no significant impact on the environment. The environmental assessment, as defined by the NRC, of the use of the existing high density spent fuel storage racks may be found in Reference 13-2.

b. <u>Fuel Rod Consolidation in Existing Racks</u>

An additional option in expanding the storage capacity of the spent fuel pool is to utilize the process of fuel assembly consolidation. Consolidation is comprised of removing the individual fuel rods from multiple assemblies to a compact configuration. The resultant empty fuel assembly structure (end plates, grids, etc.) is then compacted to reduce storage volume requirements.

The consolidation process, as currently licensed at Maine Yankee for demonstration purposes, is a technically feasible option for expanding storage capacity. This process is essentially identical to that used in the past to recover damaged spent fuel assemblies. Because the consolidation of fuel assemblies occurs within the confines of the spent fuel pool, the impact of the process is limited to the existing Fuel Building and associated systems and thus is deemed to have no significant impact on the environment. However, implementation of fuel rod consolidation at Maine Yankee will require the long-term dedication of manpower and equipment resources outside of the normal operational requirements of the plant. The use of these resources will require modifications to the operational and associated infrastructure of the plant.

Previously, the consolidation process has been evaluated with respect to its environmental impact by the NRC (Ref. 13-2) and found to have no significant impact.

c. Construction of New Spent Fuel Facilities

Additional storage capacity may be developed on the Maine Yankee site with the construction and operation of a new spent fuel pool. Such a facility would operate completely independently from the existing fuel storage facility.

In assessing this option, it is noted that completion of such a facility to meet the additional storage capacity needs within the available time may be possible, but the capital costs appear prohibitive in comparison to the other alternatives. Construction of a Seismic Category I structure onsite would require additional site investigations to ensure no adverse environmental impacts during construction and/or operation. A new structure would require additional land use commitment as well as additional mechanical, electrical, and ventilation systems. These new systems would require changes to the existing infrastructure and would necessitate additional costs for operation, security, and training. Additional staff and equipment associated with operating and maintenance would be required as well as training, radioactive waste management, health physics, security, and fire protection.

Although evaluated to have potentially no significant environmental impact, the use of a newly constructed spent fuel pool is not currently an attractive acceptable alternative to expanding the existing spent fuel storage capacity.

d. Dry Cask Spent Fuel Storage

The use of dry casks in expanding the existing spent fuel storage capacity has been evaluated for use at the Maine Yankee site. Fuel storage utilizing dry casks necessitates the removal of spent fuel from the spent fuel pool via the use of a cask and the placement of that cask in an independently controlled spent fuel facility outside of the Fuel Building.

In reviewing the application of dry storage casks at the Maine Yankee site, it is noted that findings of no significant environmental impact (Ref. 13-3) have been issued for the generic use of certain casks, as contingent on the bounding of site specific environmental parameters by cask design parameters. Therefore, it is concluded that there would be no significant environmental impact associated with the use of a dry storage cask at Maine Yankee.

The use of dry cask spent fuel storage would necessitate the placement of an independent spent fuel storage facility at the Maine Yankee site. In addition to land use commitments, construction and operation of this facility would require resources from Maine Yankee in the areas of mechanical systems, electrical systems, security, and radiation protection. Additionally, the implementation of this alternative would require changes to the existing plant infrastructure and would necessitate additional costs for operations, radiation protection, security and training. The consequences of this new facility are outlined under option (c) (Construction of a New Spent Fuel Pool).

The use of dry casks to augment the existing spent fuel storage at Maine Yankee, is determined to have no significant environmental impact.

Based on evaluations of currently available storage options, Maine Yankee has concluded that there are several alternatives available for safely increasing the number of spent fuel assemblies stored at the plant, each of which presents no significant environmental impact. However, following due consideration, Maine Yankee has selected a reracking of the spent fuel pool for the third time in light of the company's and the nuclear industry's extensive prior successful experience with this technology.

13.3 RESOURCES COMMITTED

Reracking of the Maine Yankee spent fuel pool will not result in any additional commitments of water or air resources. The old racks will be packaged and shipped offsite, and decontaminated for treatment prior to either release or disposal at a low-level waste facility. This will result in the generation of approximately 415 ft^3 of radioactive waste volume. The onsite land area currently committed to spent fuel storage will be more efficiently utilized while safely increasing the density of spent fuel storage. The materials used for new rack fabrication are discussed in Chapter 2. The use of these materials will not foreclose available alternatives, as associated with other licensing actions, that are designed to alleviate shortages of spent fuel storage capacity.

13.4 REFERENCES

13-1 "Generic Environmental Impact Statement on Handling and Storage of Spent Light Water Reactor Power Reactor Fuel," USNRC, 1979.

13-2 Letter, NRC to Maine Yankee, "Safety Evaluation and Environmental Impact Appraisal Regarding Maine Yankee Spent Fuel Storage." June 16, 1982.

13-3 Federal Register, Volume 55, No. 138, pages 29181 through 29195, July 18, 1990.

APPENDIX A

ANSYS® DESCRIPTION AND BENCHMARKING

A.0 ANSYS® DESCRIPTION AND BENCHMARKING

Structural and mechanical analyses utilize the ANSYS® code. This is a general purpose structural analysis system for the design and analysis of engineering problems using finite element modeling techniques.

Analysis capabilities include static and dynamic; elastic, plastic, creep, and swelling; buckling; small and large displacements; steady state and transient heat transfer; and fluid flow.

The wave-front (or frontal) direct solution method for the system of simultaneous equations developed by the matrix displacement method is used.

Input consists of geometric data, material constants, element properties, boundary conditions, applied loads, and control options.

Analysis results can be printed and/or plotted on a hard copy device or graphics terminals. Post processing of the results can be performed if necessary.

A.1 INTRODUCTION

The ANSYS® computer program is a large-scale general purpose finite element program which may be used for solving several classes of engineering analyses. The analysis capabilities of ANSYS® include the ability to solve static and dynamic structural analyses, steady-state and transient heat transfer problems, mode-frequency and buckling eigenvalue problems, static or time-varying magnetic analyses, and various types of field and coupled-field applications. The program contains many special features which allow nonlinearities or secondary effects to be included in the solution, such as plasticity, hyperelasticity, creep, swelling, large deflections, stress stiffening, temperature dependency, material anisotropy, and radiation. As ANSYS® has been developed, other special capabilities, such as substructuring, submodeling, random vibration, kinetostatics, kinetodynamics, free convection fluid analysis, acoustics, magnetics, piezoelectrics, coupled-field analysis and design optimization have been added to the program. These capabilities contribute further to making ANSYS® a multi-purpose analysis tool for varied engineering disciplines.

The ANSYS® program has been in commercial use since 1970, and has been used extensively in the aerospace, automotive, construction, electronic, energy services, manufacturing, nuclear, plastics, oil, and steel industries. In addition, many consulting firms and hundreds of universities use ANSYS® for analysis, research, and educational use. ANSYS® is recognized worldwide as one of the most widely used and capable programs of its type.

A.2 PROGRAM OVERVIEW

The ANSYS® element library contains more than 50 elements for static and dynamic analyses, over 20 for heat transfer analyses, and includes several magnetic, field, and special purpose elements. This variety of elements allows the ANSYS® program to analyze two- and three-dimensional frame structures, piping systems, two-dimensional plane and axisymmetric solids, three-dimensional solids, flat plates, axisymmetric and three-dimensional shells and nonlinear problems including gaps (interfaces) and cables.

The input data for an ANSYS® analysis are prepared using preprocessors. The general preprocessor (PREP7) contains powerful solid modeling and mesh generation capabilities, and is also used to define all other analysis data (geometric properties (real constants), material properties, constraints, loads, etc.), with the benefit of database definition and manipulation of analysis data. Parametric input, user files, macros and extensive on-line documentation are also available, providing more tools and flexibility for the analyst to define the problem. Extensive graphics capability is available throughout the ANSYS® program, including isometric, perspective, section. Edge, and hidden-line displays of three-dimensional structures, x-y graphs of input quantities and results, and contour displays of solution results. A load-history preprocessor (PREP6) is available for creating transient or sequential loading and boundary conditions.

A graphics-based user interface is available throughout the program, to guide new users through the learning process and provide more experienced users with on-line access to context-sensitive command information, usage notes, procedural information, and reference material including diagrams.

The analysis results are reviewed using postprocessors, which have the ability to display distorted geometries, stress contours, safety factor contours, potential field (thermal, magnetic, fluid) contours, mode shapes, time history graphs, and stress-strain curves. The postprocessors can also be used for algebraic operations, database manipulations, differentiation, and integration of calculated results. Root-sum-square operations may be performed on seismic modal results. Response spectra may be generated from dynamic analysis results. Results from various loading modes may be combined for harmonically loaded axisymmetric structures.

A.3 PROGRAM VERIFICATION

ANSYS® is continuously being verified by the developers (Swanson Analysis Systems, Inc.) as new capabilities are added to the program. The verification of the ANSYS® program is conducted in accordance with written procedures that form a part of an overall Quality Assurance program at Swanson Analysis Systems, Inc. (SASI). The test cases listed later in this Appendix represent comparisons of ANSYS®-calculated solutions with known theoretical solutions, experimental results, or other independently-calculated solutions.

KEY TO ANALYSIS TYPES AND ELEMENT NAMES

KAN Value	Analysis Type
0	STATIC ANALYSIS
1	EIGENVALUE BUCKLING
2	MODAL ANALYSIS
3	FULL HARMONIC RESPONSE ANALYSIS
4	NONLINEAR TRANSIENT DYNAMIC ANALYSIS
5	LINEAR TRANSIENT DYNAMIC ANALYSIS
6	REDUCED HARMONIC RESPONSE ANALYSIS
7	SUBSTRUCTURE (SUPERELEMENT) ANALYSIS
-1	THERMAL AND POTENTIAL FIELD ANALYSIS

ANSYS® Element Designation (STIF)	Element Name
1	2-D SPAR
2	2-D 6-NODE TRIANGULAR SOLID
3	2-D ELASTIC BEAM
4	3-D ELASTIC BEAM
5	3-D MULTI-FIELD SOLID
6	SURFACE EFFECT ELEMENT
7	JOINT ELEMENT
8	3-D SPAR
10	TENSION-ONLY OR COMPRESSION--ONLY SPAR
12	2-D INTERFACE
13	2-D MULTI-FIELD SOLID
14	SPRING-DAMPER
15	2-D THERMAL-FLUID SOLID
16	ELASTIC STRAIGHT PIPE
17	ELASTIC PIPE TEE
18	ELASTIC CURVED PIPE (ELBOW)
20	PLASTIC STRAIGHT PIPE
21	GENERALIZED MASS
23	2-D PLASTIC BEAM

KEY TO ANALYSIS TYPES AND ELEMENT NAMES (Cont)

(STIF)	Element Name
24	3-D THIN-WALLED PLASTIC BEAM
25	AXISYMMETRIC STRUCTURAL SOLID WITH NONAXISYMMETRIC LOADING
26	2-D CONTACT SURFACE ELEMENT
27	STIFFNESS, DAMPING, OR MASS MATRIX
30	3-D ISOPARAMETRIC ACOUSTIC FLUID
31	RADIATION LINK
32	2-D HEAT CONDUCTING BAR
33	3-D HEAT CONDUCTING BAR
34	CONVECTION LINK
35	2-D 6-NODE TRIANGULAR THERMAL SOLID
37	CONTROL ELEMENT
38	DYNAMIC FLUID COUPLING
39	NONLINEAR FORCE-DEFLECTION ELEMENT
40	COMBINATION ELEMENT
41	MEMBRANE SHELL
42	2-D ISOPARAMETRIC SOLID
43	PLASTIC QUADRILATERAL SHELL
44	3-D TAPERED UNSYMMETRIC BEAM
45	3-D ISOPARAMETRIC SOLID
46	8-NODE LAYERED SOLID
50	SUPERELEMENT (OR SUBSTRUCTURE)
51	PLASTIC AXISYMMETRIC CONICAL SHELL
52	3-D INTERFACE
54	2-D TAPERED UNSYMMETRIC BEAM
55	2-D ISOPARAMETRIC THERMAL SOLID
57	ISOPARAMETRIC QUADRILATERAL THERMAL SHELL
59	IMMERSED PIPE/CABLE
60	PLASTIC CURVED PIPE (ELBOW)
61	AXISYMMETRIC CONICAL SHELL WITH NONAXISYMMETRIC LOADING
63	ELASTIC QUADRILATERAL SHELL
64	3-D ANISOTROPIC SOLID
65	3-D REINFORCED CONCRETE SOLID
66	TRANSIENT THERMAL-FLOW PIPE
67	2-D THERMAL-ELECTRIC SOLID

KEY TO ANALYSIS TYPES AND ELEMENT NAMES (Cont)

(STIF)	Element Name
68	THERMAL-ELECTRIC LINE ELEMENT
69	3-D THERMAL-ELECTRIC SOLID
70	ISOPARAMETRIC THERMAL SOLID
71	LUMPED THERMAL MASS WITH VARIABLE HEAT GENERATION
75	AXISYMMETRIC THERMAL SOLID WITH NONAXISYMMETRIC LOADING
77	2-D 8-NODE ISOPARAMETRIC THERMAL SOLID
78	8-NODE AXISYMMETRIC THERMAL SOLID WITH NONAXISYM. LOADING
79	2-D FLUID ELEMENT
80	3-D FLUID ELEMENT
81	AXISYMMETRIC FLUID ELEMENT WITH NONAXISYMMETRIC LOADING
82	2-D 8-NODE ISOPARAMETRIC SOLID
83	8-NODE AXISYMMETRIC STRUCTURAL SOLID WITH NONAXISYM. LOADING
84	2-D HYPERELASTIC SOLID
85	CRACK TIP SOLID
86	3-D HYPERELASTIC SOLID
87	3-D 10-NODE TETRAHEDRAL THERMAL SOLID
90	20-NODE ISOPARAMETRIC THERMAL SOLID
91	8-NODE LAYERED SHELL
92	3-D 10-NODE TETRAHEDRAL SOLID
93	8-NODE ISOPARAMETRIC SHELL
95	20-NODE ISOPARAMETRIC SOLID
97	20-NODE ISOPARAMETRIC MAGNETIC-THERMAL-ELECTRIC SOLID
98	TETRAHEDRAL MULTI-FIELD SOLID
99	8-NODE LAYERED SHELL

TITLES INDEXED BY TEST CASE NUMBER

This index lists test case titles in numerical order, indicating the ANSYS® product(s) that are capable of performing the test and a brief status of the test changes, if any. The product key is to be interpreted as:

Product Key	Meaning
F	The full ANSYS® program is required to perform the test.
L	ANSYS®-PC/LINEAR can perform this test.
S	ANSYS®-PC/SOLID is required for test preprocessing.
T	ANSYS®-PC/THERMAL can perform this test.
O	ANSYS®-PC/OPT is required for this test.

Note that the full ANSYS® program can perform any of the tests. Tests marked "L,S" can be performed without PC/SOLID if the modeling is done by direct node and element generation. Tests marked L(MS) could be performed with PC/LINEAR if the test is restructured to use the mode superposition method of dynamic analysis.

TITLES INDEXED BY TEST CASE NUMBER

Test No.	Product Key	Test Changes	Title
Section A			
1	L		Statically Indeterminate Reaction Force Analysis
2	L		Beam Stresses and Deflections
3	L		Thermally Loaded Support Structure
4	L		Deflection of a Hinged Support
5	L	C	Laterally Loaded Tapered Support Structure
6	F	F200,T5	Pinched Cylinder
7	F	C	Plastic Compression of a Pipe Assembly
8	L,S	N,T7	Parametric Calculation of Point-to-Point Distances
9	F	N,T7	Large Lateral Deflection of Unequal Stiffness Springs
10	L		Bending of a Tee-Shaped Beam
11	F		Residual Stress Problem
12	L		Combined Bending and Torsion
13	L		Cylindrical Shell Under Pressure
14	F		Large Deflection Eccentric Compression of a Slender Column
15	L,S		Bending of a Circular Plate Using Axisymmetric Shell Elements
16	L		Bending of a Solid Beam (Plane Elements)
17	L		Bending of a Solid Beam (Solid Elements)
18	L		Out-Of-Plane Bending of a Curved Bar
19	L		End Supported (Propped) Cantilever Under Gravity Loading
20	F		Cylindrical Membrane Under Pressure
21	L		Tie Rod with Lateral Loading
22	L		Small Deflection of a Belleville Spring
23	L,S		Thermal Stresses in a Plate
24	F		Plastic Hinge in a Rectangular Beam
25	L,S	C	Stresses in a Long Cylinder
26	F	N,T25	Large Deflection of a Cantilever
27	L	C	Thermal Expansion to Close a Gap
28	T	N,T27	Transient Heat Transfer in an Infinite Slab
29	F		Friction on a Support Block
30	L,S		Pin-Jointed Support Truss
31	F		Cable Supporting Hanging Loads
32	L,T	C	Thermal Stresses in a Long Cylinder
33	F	N,T32	Transient Thermal Stress in a Cylinder

TITLES INDEXED BY TEST CASE NUMBER (Cont)

Test No.	Product Key	Test Changes	Title
34	L	C	Bending of a Tapered Plate (Beam)
35	F	F190,T34	Bimetallic Layered Cantilever Plate with Thermal Loading
36	L		Limit Moment Analysis
37	L		Elongation of a Solid Bar
38	F	C	Plastic Loading of a Thick-Walled Cylinder Under Pressure
39	L		Bending of Circular Plate with a Center Hole
40	F		Large Deflection and Rotation of a Beam Pinned at One End
41	L	C	Small Deflection, of a Rigid Beam
42	F	F201,T41	Barrel Vault Roof Under Self Weight
43	F		Bending of an Axisymmetric Thick Pipe Under Gravity Loading
44	F		Bending of an Axisymmetric Thin Pipe Under Gravity Loading
45	L		Natural Frequency of a Spring-Mass System
46	L		Natural Frequency of a Cantilevered Mass
[illegible]	L		Torsional Frequency of a Suspended Disk
[illegible]	L		Natural Frequency of a Motor Generator
49	L		Fundamental Frequency of a Bar-Mass System
50	L,S		Fundamental Frequency of a Simply Supported Beam
51	L		Natural Frequencies of a Cantilever Beam
52	L		Automobile Suspension System Vibration
53	F	C	Vibration of a String Under Tension
54	F	N,T53	Vibration of a Rotating Cantilever Blade
55	L	C	Vibration of a Stretched Circular Membrane
56	F	C,T55	Hyperelastic Thick Cylinder Under Internal Pressure
57	L	C	Torsional Frequencies of a Drill Pipe
58	S,T	F198,T57	Centerline Temperature of a Heat Generating Wire
59	L	C	Lateral Vibration of an Axially Loaded Bar
60	F	F199,T59	Natural Frequency of a Cross-Ply Laminated Spherical Shell
61	L,S		Longitudinal Vibration of a Free-Free Rod
62	L,S	C	Vibration of a Wedge
63	F	F203,T62	Static Hertz Contact Problem
64	F		Thermal Expansion to Close a Gap at a Rigid Surface
65	F		Transient Response of a Ball Impacting a Flexible Surface
66	L,S		Vibration of a Flat Plate

TITLES INDEXED BY TEST CASE NUMBER (Cont)

Test No.	Product Key	Test Changes	Title
67	F	C	Radial Vibrations of a Circular Ring from an Axisymmetric Model
68	L	F197,T67	PSD Response of a Two DOF Spring-Mass System
69	L		Seismic Response
70	L,S		Seismic Response of a Beam Structure
71	F		Transient Response of a Spring-Mass-Damper System
72	F		Logarithmic Decrement
73	F		Free Vibration with Coulomb Damping
74	F		Transient Response to an Impulsive Excitation
75	F		Transient Response to a Step Excitation
76	L(MS)	N, T77	Harmonic Response of a Guitar String
77	L(MS)	C	Trans. Resp. to a Constant Force with Finite Rise Time
78	F	N, T77	Transverse Shear Stresses in a Cantilever Beam-
79	L(MS)		Transient Response of a Bilinear Spring Assembly
80	F		Plastic Response to a Suddenly Applied Constant Force
81	F	C	Transient Response of a Drop Container
82	F	N,T81	Simply Supported Laminated Plate Under Pressure
83	F		Impact of a Block on a Spring Scale
84	L(MS)		Displacement Propagation Along a Bar with Free Ends
85	L(MS)		Transient Displacements in a Suddenly Stopped Moving Bar
86	L(MS)		Harmonic Response of a Dynamic System
87	F		Equivalent Structural Damping
88	F		Response of an Eccentric Weight Exciter
89	L		Natural Frequencies of a Two-Mass-Spring System
90	L(MS)		Harmonic Response of a Two-Mass-Spring System
91	F		Large Rotation of a Swinging Pendulum
92	T		Insulated Wall Temperature
93	T		Temperature Dependent Conductivity
94	T		Heat Generating Plate
95	T	C	Heat Transfer from a Cooling Spine
96	S,T	F196,T95	Temperature Distribution in a Short Solid Cylinder
97	T		Temperature Distribution along a Straight Fin

TITLES INDEXED BY TEST CASE NUMBER (Cont)

Test No.	Product Key	Test Changes	Title
98	T		Temperature Distribution along a Tapered Fin
99	T		Temperature Distribution in a Trapezoidal Fin
100	T		Heat Conduction Across a Chimney Section
101	T		Temperature Distribution in a Short Solid Cylinder
102	T		Cylinder with Temperature Dependent Conductivity
103	T	C	Thin Plate with Central Heat Source
104	S,T	N,T103	Liquid-Solid Phase Change
105	T		Heat Generating Coil with Temperature Dependent Conductivity
106	T		Radiant Energy Emission
107	T		Thermocouple Radiation
108	F		Temperature Gradient Across a Solid Cylinder
109	T		Temperature Response of a Suddenly Cooled Wire
110	T		Transient Temperature Distribution in a Slab
111	T		Cooling of a Spherical Body
112	T		Cooling of a Spherical Body
113	S,T		Transient Temperature Distribution in an Orthotropic Metal Bar
114	S,T		Temperature Response to a Linearly Rising Surface Temperature
115	S,T		Thermal Response of a Heat Generating Slab
116	T		Heat Conducting Plate with Sudden Cooling
117	T		Electric Current Rowing in a Network
118	T	C	Centerline Temperature of a Heat Generating Wire
119	T	C	Centerline Temperature of an Electrical Wire
120	S,T	N,T118	Microstrip Transmission Line Capacitance
121	F	N,T119	Flow Through a Pipe with Uniform Heat Flux
122	F		Pressure Drop in a Turbulent Flowing Fluid
123	F		Laminar Flow in a Piping System
124	F		Discharge of Water from a Reservoir
125	F		Radiation Heat Transfer Between Concentric Cylinders
126	F		Heat Transferred to a Flowing Fluid
127	L		Buckling of a Bar with Hinged Ends (Line Elements)

TITLES INDEXED BY TEST CASE NUMBER (Cont)

Test No.	Product Key	Test Changes	Title
128	L		Buckling of a Bar with Hinged Ends (Area Elements)
129	F		Numerical Differentiation and Integration
130	F		Fourier Series Generation for a Saw Tooth Wave
131	L		Acceleration of a Rotating Crane Boom
132	F		Stress Relaxation of a Tightened Bolt due to Creep
133	F		Motion of a Rod due to Irradiation Induced Creep
134	F		Plastic Bending of a Clamped I-Beam
135	L		Bending of a Beam on an Elastic Foundation
136	F		Large Deflection of a Buckled Bar (The Elastica)
137	F		Large Deflection of a Circular Membrane
138	F		Large Deflection Bending of a Circular Plate
139	F		Bending of a Long Uniformly Loaded Rectangular Plate
140	F		Stretching, Twisting and Bending of a Long Solid Shaft
141	L,S	C	Diametral Compression of a Disk
142	F	F195,T141	Stress Concentration at a Hole in a Plate
143	F		Fracture Mechanics Stress Intensity for a Crack in a Finite Width Plate
144	F	N,D	Bending of a Composite Beam
145	F		Stretching of an Orthotropic Solid
146	F		Bending of a Reinforced Concrete Beam
147	F		Bending of a Curved Thick Beam
148	F		Bending of a Parabolic Beam
149	F		Rotation of a Tank of Fluid
150	F		Acceleration of a Tank of Fluid
151	F		Nonaxisymmetric Vibration of a Circular Plate
152	F		Nonaxisymmetric Vibration of a Stretched Circular Membrane (Using Harmonic Elements)
153	F		Nonaxisymmetric Vibration of a Stretched Circular Membrane (Using Cyclic Symmetry)
154	F	C	Vibration of a Fluid Coupling
155	L,O,S	F191,T154	Shape Optimization of a Cantilever Beam
156	F	C	Natural Frequency of a Nonlinear Spring-Mass System
157	L,O	F192,T156	Optimization of a Frame Structure

TITLES INDEXED BY TEST CASE NUMBER (Cont)

Test No.	Product Key	Test Changes	Title
158	F		Motion of a Bobbing Buoy
159	F		Temperature Controlled Heater
160	F	N,D	Solid Cylinder with Harmonic Temperature Load
161	F		Heat Flow From an Insulated Pipe
162	F		Cooling of a Circular Fin of Rectangular Profile
163	S,T		Groundwater Seepage (Permeability Analogy)
164	T		Drying of a Thick Wooden Slab (Diffusion Analogy)
165	F		Current-Carrying Ferromagnetic Conductor
166	F		Long Cylinder in a Sinusoidal Magnetic Field
167	F		Transient Eddy Currents in a Semi-Infinite Solid
168	F		Magnetic Field in a Nonferrous Solenoid
169	F	C	Permanent Magnet Circuit with an Air Gap
170	F	N,T169	Magnetic Field from a Square Current Loop
171	F		Permanent Magnet Circuit with an Elastic Keeper
172	F		Stress Analysis of a Long, Thick, Isotropic Solenoid
173	F		Centerline Temperature of an Electrical Wire
174	F		Bimetallic Beam under Thermal Load
175	F		Natural Frequency of a Piezoelectric Transducer
176	F		Frequency Response of Electrical Input Admittance for a Piezoelectric Transducer
177	F		Natural Frequency of a Submerged Ring
178	F		Plane Poiseuille Flow
179	F		Dynamic Double Rotation of a Jointed Beam
180	L,S		Bending of a Curved Beam
181	L,S		Natural Frequency of a Flat Circular Plate with a Clamped Edge
182	L,S		Transient Response of a Spring-Mass System
183	L,S		Harmonic Response of a Spring-Mass System
184	F	C	Straight Cantilever Beam
185	F	N,T184	AC Analysis of a Slot Embedded Conductor
186	F	N,T184	Transient Analysis of a Slot Embedded Conductor
187	F	C	Bending of a Curved Beam
188	F	N,T187	Force Calculation on a Current Carrying Conductor

TITLES INDEXED BY TEST CASE NUMBER (Cont)

Test Product No. Key	Test Changes	Title
Section B		
C1	N	Clamped Plate Under Uniformly-Distributed Load
C2	N	Elliptic Membrane Under a Uniformly-Distributed Load
C3	N	Barrel Vault Roof Under Self Weight
C4	N	Simply Supported Thin Annular Plate
C5	N	Simply Supported Solid Square Plate
C6	N	Two-Dimensional Heat Transfer With Convection
C7	N	One-Dimensional Transient Heat Transfer with Convection
D1	N	Straight Cantilever Beam Under Unit Load
D2	N	Barrel Vault Roof Under Self Weight
D3	N	Free-free Vibration of a Solid Beam

The following 15 Test Cases (from the 4.3 VM) were moved or combined.

(old 189)	T187	Curved Beam (Multi-field Tetrahedrons)
(old 190)	T35	Bimetallic Layered Cantilever Plate with Thermal Loading
(old 191)	T155	Shape Optimization of a Cantilever Beam
(old 192)	T157	Optimization of a Frame Structure
(old 193)	T56	Hyperelastic Thick Cylinder Under Internal Pressure (2-D)
(old 194)	T56	Hyperelastic Thick Cylinder Under Internal Pressure (3-D)
(old 195)	T142	Stress Concentration at a Hole in a Plate (Submodeling)
(old 196)	T96	Temperature Distribution in a Short Solid Cylinder
(old 197)	T68	PSD Response of a Two DOF Spring-Mass System
(old 198)	T58	Centerline Temperature of a Heat Generating Wire
(old 199)	T60	Natural Frequency of a Cross-Ply Laminated Spherical Shell
(old 200)	T6	Pinched Cylinder
(old 201)	T42	Barrel Vault Roof Under Self Weight
(old 202)	T38	Plastic Thick-Walled Cylinder Under Internal Pressure
(old 203)	T63	Static Hertz Contact Problem

The following is a partial list of other publications verifying the ANSYS® program:

"Symposium on Engineering Computer Software - Verification, Qualification, Certification," from presentations at the ASME First National Congress on Pressure Vessels and Piping, San Francisco, California, May 1971. Published by ASME, New York, 1971.

"Thermal Structural Analysis Programs - A Survey and Evaluation," from presentations at the Third Annual Pressure Vessels and Piping Conference, and the 27th Annual Petroleum-Mechanical Engineering Conference, New Orleans, LA, September 1972. Published by ASME, New York, 1972.

"Pressure Vessels and Piping 1972 Computer Programs Verification - An Aid to Developers and Users," sponsored by the Committee on Computer Technology, Pressure Vessel and Piping Divn., ASME. Published by ASME, New York, 1972.

"Three Dimensional Continuum Computer Programs for Structural Analysis," from presentations at the Winter Annual Meeting of the American Society of Mechanical Engineers, New York, NY, November 1972. Published by ASME, New York, 1972.

Reimers, Carl, "Evaluation of Three Dimensional Structural Analysis Capabilities," Report No. 8716-01 (13) ER, Aerojet Manufacturing Company, Fullerton, CA, 1973.

"Guidelines and Procedures for Design of Nuclear System Components at Elevated Temperatures," RDT Standard F9-5T, Published by the Division of Reactor R&D, A.E.C., Oak Ridge National Laboratory, March 1974.

"Structural Mechanics Computer Programs - Surveys, Assessments, and Availability," edited by W. Pilkey, et al., Univ. Press of Virginia, Charlottesville, 1974, Pps. 15, 63, 116, 140, 146, 153, 219, 266, 533, 687, etc.

Yamada, Y., "Verification and Qualification Activities in Japan of Inelastic Analysis Computer Program," ASME Paper 76-PVP-44, PVP Conference, Mexico City, Mexico, September 1976.

"Comparison of a Finite Element and a Finite Difference Computer Code in Heat Transfer Calculation," C.T. Hsu, ASME Paper 79-PVP-63 PVP Conference, San Francisco, CA, June 1979.

Dietrich, D.E., "Verification of a General Purpose finite Element Code used in the Public Domain," presented at the 3rd National Congress on P.V.P. Technology, San Francisco, CA, 1979.

Jones, J.W., "3-D Stress Analysis," Machine Design, Aug. 10, 1972, pp. 84-89.

"Application of the ANSYS® Finite Element Code to the Analysis of Pressure Vessel Component, Vol. 1 and Vol. 2 by S.B. Bennett, et. al., published by Westinghouse Electric Corp., Lester, PA, 1973.

Slot, T., and Branca, T.R., "On the Determination of Effective Elastic-Plastic Properties for the Equivalent Solid Plate Analysis of Tube Sheets," ASME Paper No. 74-PVP-18.

Dietrich, D.E., "Three Dimensional Inelastic Analyses of a Shell Appurtenance per Section III - Appendix F," PVP: Analysis and Computers, edited by I.S. Tuba, et al., June 1974.

Thompson, G.U. and Rauschenplot, H.C., "Closure Analysis Using Self Energizing, Double Conical Gaskets," PVP Analysis and Computers, edited by I.S. Tuba, et al., June 1974.

Maruyama, T., Ishizaki,T. and Yokouchi, Y., "Parametric Study of the Elastic Plastic - Creep Deformation of Thick Cylinder and Program Verification," ASME Paper 76-PVP-43, PVP Conference, Mexico City, Mexico, September 1976.

Clinard, J.A., McKinley, D.A., Kroenke, W.C., Sartory, W.K., "Verification by Comparison of Independent Computer Program Solutions," Pressure Vessels and Piping Computer Program Evaluation and Qualification, edited by D.E. Dietrich, September 1977.

Rusin, T.M., Leeschutte, D.G., Coughlin, J.M., "Application of the Finite Element Method in the Development of Improved Railroad Car Wheel Design," ASME Paper No. 78-WA/RT-5.

Slack, N., "Computing the Fatigue Strength and Field Life of Shovel Loader Axle Shafts Using Finite Element, Off-Highway Vehicle Meeting and Exposition MECCA, Milwaukee, S.A.E., Inc., September 10-13, 1979.

Macdonald, B.D., "Correlation of Structural Steel Fractures Involving Massive Plasticity," Elastic-Plastic Fracture. ASTM STP 668, J. D. Landes, J. A. Begley, and G. A. Clarke, Eds., American Society for Testing and Materials, 1979, pp. 663-673.

Macdonald, Bruce D., "Moment Connections Weakened by Laminations," Journal of the Structural Division, ASCE, Vol. 105, No. ST8. Proc. Paper 14776, August 1979, pp. 1605-1619.

Elfmann, W., Heeschen, U., Muller, G., "Nonlinear, Dynamic, Plastic Component-Support Analysis," Transactions of the 5th Intern. Conf. on Structural Mechanics in Reactor Technology, Berlin, Germany, Materials Modeling and Inelastic Analysis of Metal Structures, Vol. L, August 13-17, 1979.